

Alma Mater Studiorum – Università di Bologna

DOTTORATO DI RICERCA IN  
Scienze Biochimiche e Biotecnologiche

Ciclo XXVIII

**Settore Concorsuale di afferenza: ING-IND/25**

**Settore Scientifico disciplinare: 09/D3**

BIOCONVERSION OF AGRO-FOOD WASTES INTO BIOFUELS AND BIO-  
BASED CHEMICALS

**Presentata da: Dr. Luca Longanesi**

**Coordinatore Dottorato**  
Chiar.mo Prof  
Santi Mario Spampinato

**Relatore**  
Chiar.mo Prof Davide Pinelli

**Correlatore**  
Dr. Dario Frascari

## ABSTRACT

---

Biorefineries represent the main key for the future world economic strategy. A plethora of biofuel and bio – based chemicals can be produced from different types of feedstocks, through different bioprocess, closely interlinked with each other. Moreover, the exploitation of agro industrial by – products, correspond today to one of the most challenging aspect in the developing of more sustainable biorefinery systems. In this work, different biorefineries strategies were used in order to produce different fuels and chemicals from agro – industrial by product, focusing in particularly on microbial fermentation processes. Mixed consortia and pure culture of *Thermotoga neapolitana* were used to produce biomethane (through anaerobic digestion) and biohydrogen, respectively from grape pomace and milk whey. Due to the lignocellulosic nature of this by products, white and red grape pomaces in the anaerobic digestion process were tested alone, or in co – digestion, in batch, fed – batch and continuous tests in a 29 L CSTR bioreactor, in a partnership between our department and different private companies. Furthermore, inhibition experiments were performed in order to better characterize the biochemical process and to evaluate the effect of, oxygen, acetic acid and lignocellulosic derived compounds to the biomethanization process. Besides that, the possibility to enrich this biorefinery to produce 1 – propanol from the mixture of VFAs originated in the first steps of AD was evaluated. Bio – H<sub>2</sub> tests (in the framework of the national “Bio – Hydro” Project) were performed with milk whey alone or in co – digestion with molasses both in a 116 ml microcosms – scale, both in a 19 L SPCSTR reactor, coupled to a membrane module separation system, to enrich the hydrogen purity. Milk whey was also investigated as only carbon source for the production of succinic acid, one of the Top 12 building block according to the U.S.A Department of Energy, using *Actinobacillus succinogenes* pure culture in a collaborative project between our department and the Flemish Institute For Technological Research. Besides batch and continuous fermentations, different aspects were studied, as an innovative procedure for a biofilm fermentation in 1 L PFR – type reactor, and the possibility to couple the fermenter to an innovative electrodialysis plant, used as ISPR (*In Situ Product Recovery*) technique without cell retention steps in between.

## KEYWORDS

---

Biorefinery, Reactor Set – Up, Anaerobic Digestion (AD), Biomethane, Agro – Industrial Wastes, Batch, Fed – Batch, Continuous, Continuous Stirred Tank Reactor (CSTR), Mixed Consortia, Acclimatization, Inhibition, Biohydrogen, *Thermotoga neapolitana*, Membrane, Co – Feeding, Bioalcohol, 1 – Propanol, Succinic Acid (S.A.), Electrodialysis, Limiting Current Density (LCD), In Situ Product Recovery (ISPR), Biofilm, Plug Flow Reactor (PFR), Monod Model

# TABLE OF CONTENTS

---

<b>1</b>	<b>INTRODUCTION</b>	<b>8</b>
1.1	Environmental issues.....	8
1.1.1	GHGs emission .....	8
1.1.2	Fossil fuel depletion .....	13
1.1.3	Human overpopulation.....	17
1.1.4	Wastes and food losses.....	20
1.2	Biorefinery and Green Chemistry .....	23
1.2.1	Concepts and principles .....	23
1.2.2	Waste-to-Energy (WTE) and Circular Economy (CE) .....	24
1.2.3	Legislation and perspectives .....	28
1.3	Renewable Energy: A necessity.....	31
1.4	Biorefineries: Inside a deep view .....	35
1.4.1	Types, classification and complexity .....	36
1.4.2	Industrial-scale bioprocesses.....	41
1.4.3	Funding opportunity.....	48
1.5	Lignocellulosic biomass: from waste to biochemical conversion.....	49
1.5.1	Composition .....	49
1.5.2	Pretreatments.....	52
1.5.3	Biocatalytic valorization .....	55
1.6	Bioconversion into biofuels and bio-based chemicals .....	58



<b>2</b>	<b>AIM OF THIS WORK</b>	<b>62</b>
<b>3</b>	<b>STATE OF THE ART</b>	<b>65</b>
3.1	Bio – Hydrogen .....	65
3.2	Anaerobic digestion and Bio - Methane.....	68
3.3	Alcohol production: 1 - propanol .....	73
3.4	Succinic acid production .....	78
<b>4</b>	<b>MATERIALS AND METHODS</b>	<b>84</b>
4.1	Wastes supplying.....	84
4.1.1	Wastes collection.....	84
4.1.2	Physico – chemical characterization of the collected wastes .....	85
4.2	Strain/consortia acquisition and stock preparation.....	87
4.3	H <sub>2</sub> project.....	91
4.3.1	Bioreactor set - up .....	91
4.3.2	Bioreactor membrane coupled test.....	94
4.3.3	Microcosm Co-Feeding experiments .....	96
4.4	CH <sub>4</sub> project.....	97
4.4.1	Bioreactor set-up .....	97
4.4.2	Red grape pomace digestion with “DICAM” inoculum. Batch, - fed batch and continuous bioreactor tests.....	100
4.4.3	White pomace digestion with “DICAM” inoculum. BioMethane Potential (BMP) microcosms test.....	105
4.4.4	Microcosms inhibition tests with “DICAM” inoculum .....	107
4.4.5	Microcosms co-digestion of grape pomace with other by-products with “SEBIGAS” inoculum .....	110
4.5	Propanol project .....	113
4.5.1	Screening and acclimatization of the consortia.....	113
4.5.2	Production tests .....	116
4.6	Succinic acid project (VITO) .....	118
4.6.1	Bioreactor & Electrodialysis plants set - up.....	118
4.6.2	Reactor batch experiments .....	122
4.6.3	Electrodialysis optimization: LCD determination.....	125

4.6.4 Electrodialysis tests with synthetic and real broth .....	126
4.6.5 Fermenter – ED coupled test.....	127
4.7 Succinic acid project (DICAM) .....	129
4.7.1 Bioreactor set - up .....	129
4.7.2 Carrier screening .....	132
4.7.3 Kinetic parameters estimation: lactose and milk whey tests .....	135
4.7.4 Bioprocess scale – up in 1 L plant.....	136
4.8 Principal analytical techniques.....	139
4.8.1 DNA extraction and PCR - DGGE .....	139
4.8.2 HPLC & GC .....	141
4.8.3 Total solids (TS) and volatile solids (VS) determination.....	143
4.8.4 Biomass determination: Lowry’s method .....	144
4.8.5 Chemicals .....	147
<b>5 RESULTS AND DISCUSSION</b>	<b>148</b>
5.1 Bio – H <sub>2</sub> project.....	148
5.1.1 Integrated bioreactor – membrane experiment.....	148
5.1.2 Co – feeding tests .....	152
5.2 Bio – CH <sub>4</sub> project: Anaerobic digestion.....	156
5.2.1 Batch, fed – batch and continuous bioreactor test.....	156
5.2.2 White pomace BMP experiment .....	179
5.2.3 Inhibition assays .....	182
5.2.4 Co – digestion results .....	195
5.3 Bio – Propanol production: Screening results .....	201
5.4 Succinic acid – VITO results .....	216
5.4.1 Batch results with CSTR reactor: lactose VS milk whey.....	216
5.4.2 Electrodialysis outcomes: LCD and parameters determination .....	223
5.4.3 ED results with synthetic broth .....	229
5.4.4 ED results with real broth.....	235
5.4.5 Integrated test .....	240
5.5 Succinic acid – DICAM results.....	245
5.5.1 Choosing the best carrier: screening and statistical evaluations .....	246

5.5.2	Poraver ® or Glaxstone ®? Monod model with lactose .....	252
5.5.3	Monod model with milk whey .....	258
5.5.4	Biofilm plant: preliminary results with repeated batch tests .....	263
<b>6</b>	<b>CONCLUSIONS</b>	<b>271</b>
<b>7</b>	<b>APPENDIX</b>	<b>283</b>
<b>8</b>	<b>REFERENCES</b>	<b>293</b>
<b>9</b>	<b>LIST OF ABBREVIATIONS</b>	<b>312</b>
<b>10</b>	<b>ACKNOWLEDGEMENTS</b>	<b>315</b>

# 1 INTRODUCTION

---

In a famous report to the United Nation in October 1987 named ““Sustainable Development”. Our Common Future”, the World Commission on Environment and Development (WCED), described the sustainability concept as “development that meets the needs of the present without compromising the ability of future generations to meet their own needs” (United Nations, 1987).

Then, the first principle of the Rio Declaration signed by the United Nation Environmental Program (UNEP) in the framework of the Conference on Environment and Development held in Rio de Janeiro on June 1992, affirms that “*Human beings are at the center of concerns for sustainable development. They are entitled to a healthy and productive life in harmony with nature.*” (United Nation, 1992), Still nowadays, these documents indicate the objectives for a sustainable developments and the principles to fulfil this goal.

## 1.1 ENVIRONMENTAL ISSUES

### 1.1.1 GHGs emission

Considering the global CO<sub>2</sub> emission (Figure 1), a biorefinery approach seems essential for the developing of a more sustainable economy.

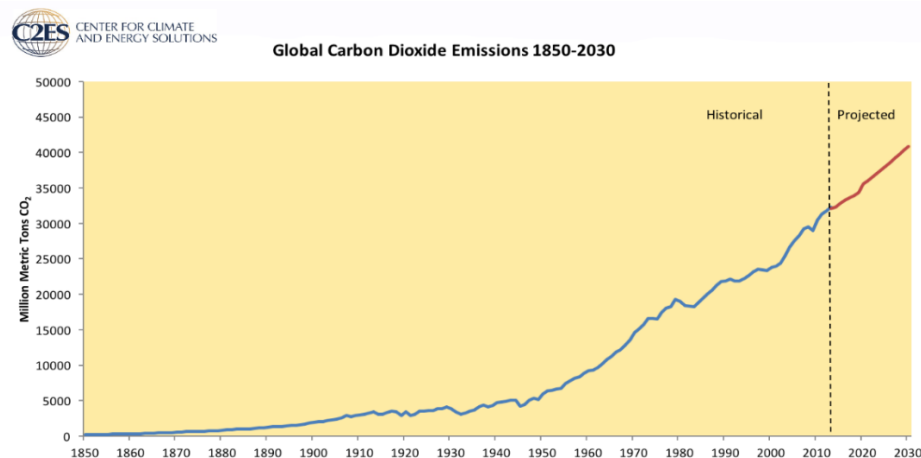


**Figure 1.1:** CO<sub>2</sub> emission history and perspective. Sources: Carbon Dioxide Information Analysis Centre, Oak Ridge National Laboratory (2015), and International Energy Agency, World Energy Outlook (2015)

Global emissions of carbon dioxide stood at 32.3 million metric tons in 2015, and before 2030 (according to IEA data) will reach the 40 million of metric tons of CO<sub>2</sub> in the atmosphere (International Energy Agency, 2013). Taking a deep insight into GHGs (Greenhouse gases) global emission in 2014, is evident that carbon dioxide represents the most abundant part (76%) of the total anthropogenic gas emission, but also other GHGs like CH<sub>4</sub>, N<sub>2</sub>O and different type of fluorinated gas (like hydrofluorocarbons (HFCs), perfluorocarbons (PFCs), and sulfur hexafluoride (SF<sub>6</sub>)) emitted from industrial processes and refrigeration systems, contributes for the 24% of the total. Figure 1.2 shows in detail this trend (Intergovernmental Panel on Climate Change, 2014).

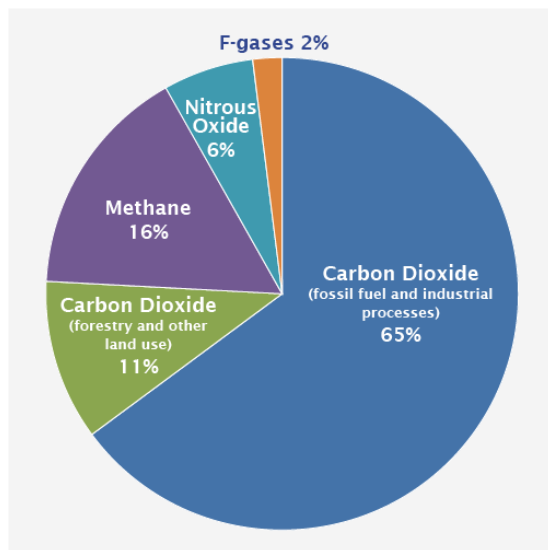


**Figure 1.2:**

*Global GHG emissions from 2010 to 2014 (Intergovernmental Panel on Climate Change, 2014)*

To aggravate the situation, the Intergovernmental Panel on Climate Change (IPCC) estimate that certain greenhouse gases (GHGs) are more effective on global warming than other. Based on data obtained from U.S. Global Change Research Program, assessing a Global Warming Potential (GWP) = 1 for CO<sub>2</sub>, methane has a GWP more than 20 times higher than CO<sub>2</sub> on a 100-year time scale. Moreover, nitrous oxide (N<sub>2</sub>O) and CFCs gas have respectively a GWP 300 times and 6000 higher respect to CO<sub>2</sub> potential on a 100-year timescale, and higher residence time in atmosphere respect to CH<sub>4</sub> and CO<sub>2</sub> (Melillo, 2014).

In the same study is also reported the partial contribution of each global process on climate alteration, expressed as Radioactive Force (W/m<sup>2</sup>). This index is a measure of the influence of a particular factor

on the net change in Earth's energy balance. A positive radiative forcing tends to warm the surface of the planet, while a negative forcing tends to cool the surface (Environmental Protection Agency, 2014). As is shown in figure 1.3, carbon dioxide emitted from anthropogenic activities is presently the largest climate forcing agent (note that natural forces, like volcanic eruptions for example, produces a net change approximately near 0, due to the net balance of biogenic carbon flux).

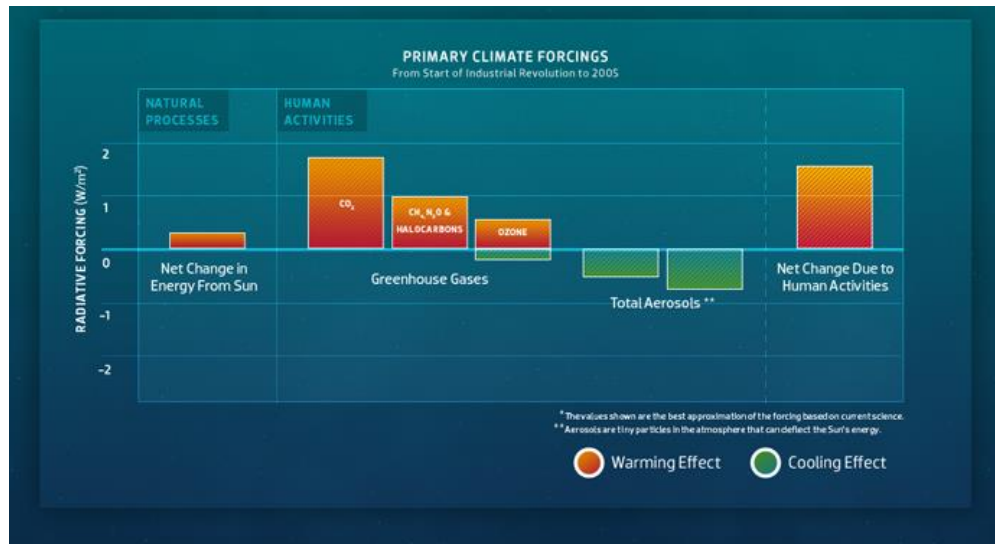


**Figure 1.3:** Contribution to the radioactive force index of each global process. (Environmental Protection Agency, 2014)

Also CFCs gas and ozone-derived complex (like ozone oxides), contributes to the global warming, but not like anthropogenic carbon dioxide emissions. A side-effect of the burning of fossil fuel that release CO<sub>2</sub> is the formation of aerosol particles. Aerosols are tiny particles in the atmosphere composed by water, ice, ash, mineral dust, or acidic droplets, that deflect the sun's energy having a cooling effects. Anyway, these particles contribute to the global air pollution, as reported in many literature studies (S. Matthias-Maser, 1995), (Andrew D. Maynard, 2005).

This graph reports a clear evidence that human activities are responsible for most of the recent global warming (as shown in the last graph bar on the right), and justify the society effort in the reduction of CO<sub>2</sub> emissions.

Going deeply inside to the causes of CO<sub>2</sub> increasing in the atmosphere due to human activities, it's possible to divide the carbon dioxide emission by activity sector (figure 1.4).

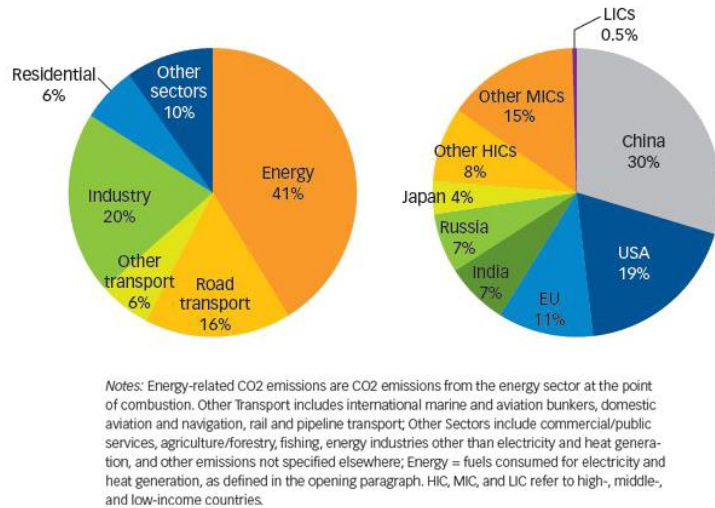


**Figure 1. 4:**

*Global CO<sub>2</sub> emission divided by sectors and geographic regions in 2013 (International Energy Agency, 2015)*

From this repartition, is evident that the cumulative emission from energy related compound, transport, industry and residential sectors results in 90% of total carbon dioxide release. Burning of fossil fuel is the principal cause of CO<sub>2</sub> production in these activities, with China, in particularly, but also U.S.A, as the large polluting countries. For these reason, in the last 2015 Paris Climate Conference - COP21, U.S.A, together with China and other 193 countries, signed a formal document where in the article 2 is affirmed the “urgent need to reduce greenhouse gases emission by 2020 consistent with holding the increase in the global average temperature to well below 2 °C, pursuing efforts to limit the temperature increase to 1.5 °C” (Paris Climate Conference, 2015).

Moreover, the burning process, produces low-size particles called “particulate matter” (PM) extremely dangerous for human health. The Environmental Protection Agency in its website defines PM “a complex mixture of extremely small particles and liquid droplets. Particle pollution is made up of a number of components, including acids (such as nitrates and sulfates), organic chemicals, metals, and soil or dust particles”. (Environmental Protection Agency, 1987). Sources of those particles include all types of combustion activities (motor vehicles, power plants, wood burning, etc.) and all the industrial processes that requiring fossil fuel combustion. Moreover, the size of these particles is

directly related to their potential for causing health problems. PM 10 are particles with diameter not less than 10  $\mu\text{m}$ , but the PM 2.5, are the most dangerous for human population. Due to the small diameters, indeed, those particles can pass through the throat and nose and enter the lungs, causing serious health concerns. Regarding this aspect, the Environmental Protection Agency, in collaboration with the World Health Organization agency, published in 2012, a comprehensive document where is reviewed and assessed the numerous studies relevant the health effects of PM published in peer – reviewed journal until 2009. In this publication are screened more than 120 articles, regarding epidemiologic and toxicology consequences to short and long term exposure to PM10 and PM 2.5 (Environmental and Protection Agency, World Health Organization, 2012).

Current limit of PM 2.5, established by the European Union with the air quality directive of 2008, are no more than 25  $\mu\text{g}/\text{m}^3$  based on 3 years average data for PM 2.5. The PM 10 daily mean value, instead, may not exceed 50  $\mu\text{g}/\text{m}^3$  more than 35 times in a year and the PM 10 annual mean value may not exceed 40  $\mu\text{g}/\text{m}^3$  (European Union, 50 / 2008).

In June 2015, NASA satellite data, designs a PM 2.5 global pollution map, based on the average data of the last three years (figure 1.5). From this graph, it's easy to understand the global concern about this big public health issues, in particularly in China, North Africa and North America, middle East and Europe. (Van Donkelaar, 2015).

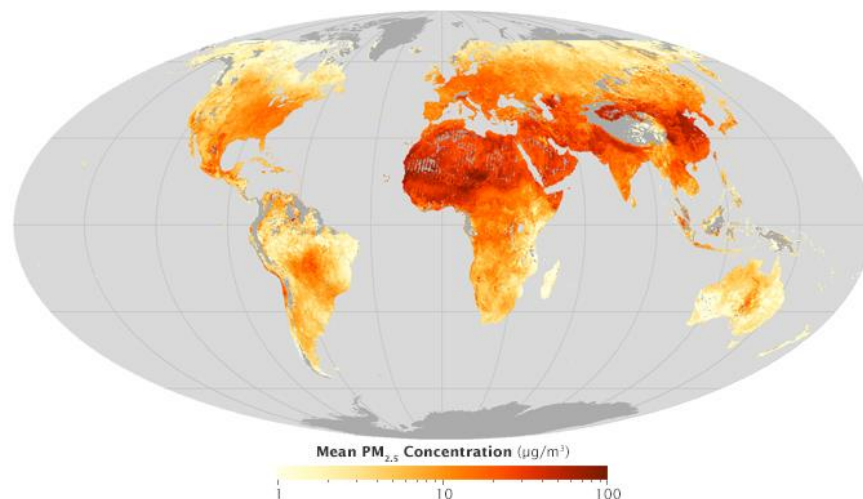


**Figure 1.5:** PM 2.5 distribution in June 2015 ( $\mu\text{g}/\text{m}^3$ ) according to NASA (Van Donkelaar, 2015)



### *1.1.2 Fossil fuel depletion*

Another main driver for the establishment of a bioeconomy is the fossil fuel limitation.

Fossil fuels are hydrocarbons generally defined by International Energy Agency like “fuels obtained by carbonization of organic matter” (International Energy Agency, 2009).

There are three primary types of fossil fuel: crude oil, coal and natural gas, and all of them are formed during the Carboniferous period of Paleozoic era (360 – 286 million of years ago) from the decomposition of organic matter under anaerobic condition and extreme temperature and pressure conditions.

- ✓ Crude oil is the most exploited fossil fuel, and its formation derived principally from the high – pressure and high – temperature carbonization of zooplankton and algae settled to the sea or at the lakes bottom. This process caused the organic matter to change, first into a waxy material known as kerogen, and then with more heat into liquid and gaseous hydrocarbons via a process known as “catagenesis” (B.P. Tissot, 1985) (Braun & Burnham, 1993).

When crude oil is extracted by oil well, is formed by a mixture of numerous type of hydrocarbons, (gaseous, liquid, or solid, depending on subsurface conditions and on the phase diagram of the petroleum mixture), (Hyne, 2001). In average, the principal types are alkanes (30%), cycloalkanes (up to 50%) and various aromatic hydrocarbons like asphaltene-types (15%), with trace amounts of metals such as iron, nickel, copper and vanadium (depending from the extraction site).

- ✓ Coal is another type of carbon – based, solid, black colored and rock-like fossil fuel, usually with higher amount of sulphur. Its formation involves the carbonization of forestry residues in Paleozoic era. There are three main types of coal: anthracite, bituminous coal and lignite, depending on the carbon content, presence of impurities, and the intrinsic highest calorific content (MJ/kg), (Taylor, Taylor, & Krings, 2009). Anthracite is the harder and purest material, with the highest carbon content, and between 26 to 33 MJ/kg of intrinsic calorific content. Bituminous coal and lignite have lower carbon quantity and less calorific content, respectively 24 – 34 MJ/kg and 10 – 20 MJ/kg. These value are derived from a lower pressure applied during the

carbonization of the organic matters. This leads to a poorer quality coal (World Coal Institute, 2013).

- ✓ Natural gas, is the only gaseous fossil fuel. Is primarily composed by methane with varying amounts of other higher alkanes, and sometimes a small percentage of carbon dioxide, nitrogen, and/or hydrogen sulfide. Natural gas formation is strongly related to crude oil formation; the only difference is the profundity at which the carbonization process occurs (Overview of Natural Gas, 2012).

An important distinction needs to be made between resources and reserves. This distinction reflects how the fossil fuels will be brought to the market. Resources are those volumes that have yet to be fully characterized, or that present technical difficulties or are costly to extract. Reserves are those volumes that are expected to be produced economically using today's technology (International Energy Agency, 2013).

In the figures 1.6, 1.7 and 1.8 are reported the globally proven reserves of each fossil fuel, according to the last IEA report in 2013 "Resources to Reserves":

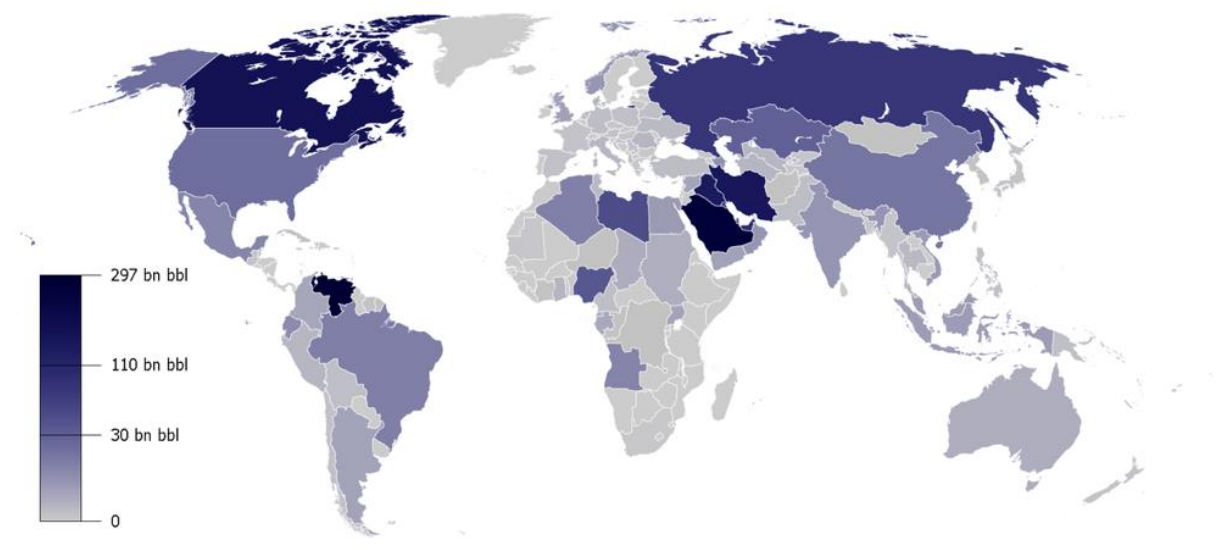


**Figure 1.6:** Proven crude oil reserves in billions of barrel (bn bbl), according to International Energy Agency in 2013

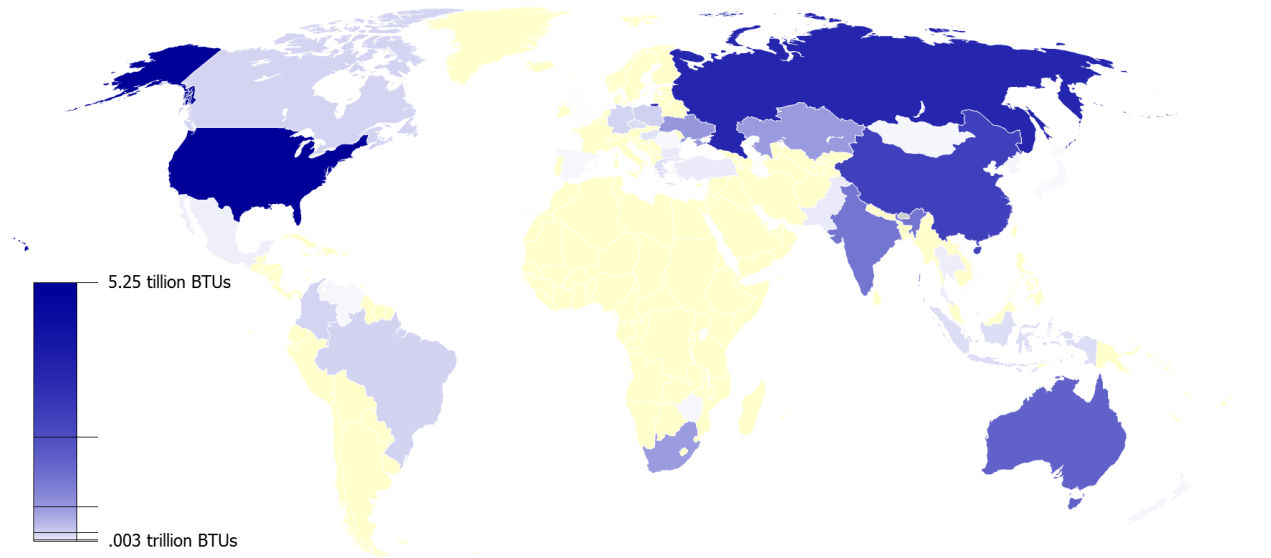


**Figure 1.7:** Proven coal reserves in British Thermal Units (BTUs), according to International Energy Agency in 2013

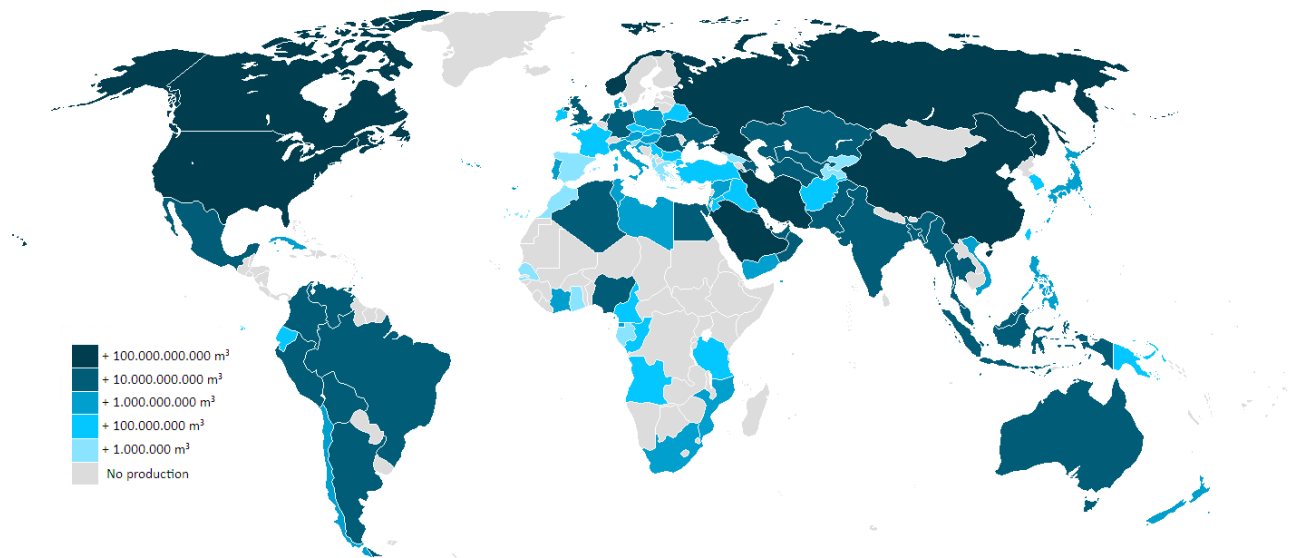


**Figure 1.8:** Proven natural gas reserves in cubic meters ( $m^3$ ), according to International Energy Agency in 2013

According to the same report, currently, fossil fuel meets 80% of total global energy. In 2035, the GED (Global Energy Request) is expected to rise by 40%, with stable fossil fuel contribution (75%). In this report is also assessed the production-perspective expressed in years, divided between crude oil, natural gas, and coal for both reserves and resources (figure 1.9) (International Energy Agency, 2013).

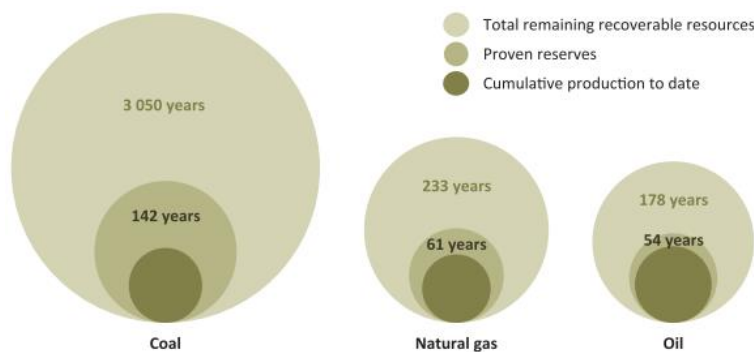


**Figure 1.9:** Number of years of production based on estimated production rates in 2013 between reserve and expected resources (International Energy Agency, 2013).

Up to now, proven world resources and reserves of crude oil are estimated to be around 1.3 trillion of equivalent oil barrels (“boe”), with remaining recoverable oil resources representing about 2.7 trillion barrels, leading in 178 years of continuous production at 2013 rates. Coal and natural gas resources are instead more available, with resources for respective of 1.4 and 3.6 trillion of boe and an expected production for 233 and 3050 years respectively (International Energy Agency, 2013).

Moreover, in the same document, the International Energy Agency presented three scenarios with energy projections to 2035: Current Policies Scenario, the New Policies Scenario and the 450 Scenario.

- *Current Policies Scenario* assumes no change in government policies and measures.
- *New Policies Scenario* assumes new measures have been introduced to implement broad policy commitments, including national pledges to reduce greenhouse gas emissions (GHGs) and, in some countries, plans to phase out fossil fuel energy subsidies.
- *450 Scenario* aimed at limiting the increase in the future global temperature to 2 °C, which assumes that GHG concentrations can be stabilized in the atmosphere at a level of 450 parts-per-million carbon dioxide-equivalent (ppm CO<sub>2</sub> -eq), as established by COP 21 conference in Paris.

In any case, the energy global demand is expected to 14870 Mtoe (Mega tons of oil equivalent) in the 450 scenario, or in the worst case, to more than 18500 Mtoe maintaining the current policies scenario (figure 1.10).

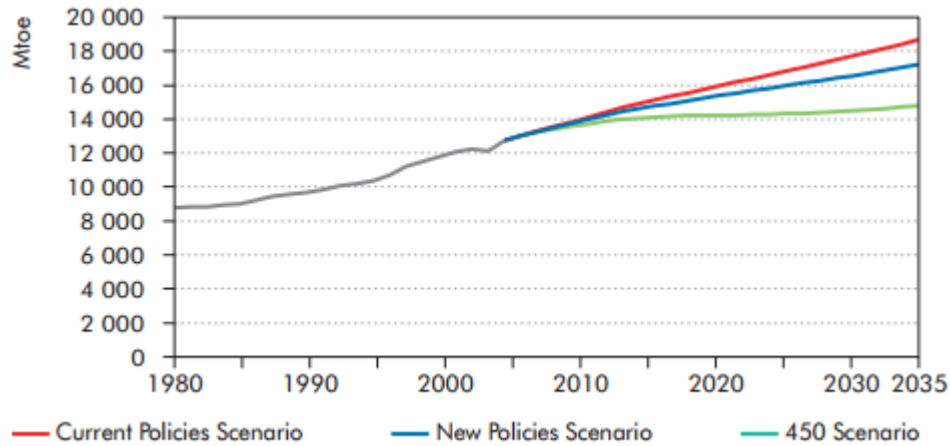


**Figure 1.10:** Global demand for primary energy to 2035 in Mtoe, by scenario

Besides these data, due to the intrinsic difficulties in continuously reviewing the current trend of fossil fuel depletion, a lot of articles in peer – reviewed journal are published with frequency on this topic (N. Abas, 2015), (Mikael Hööka, 2013), (Nick A. Owen, 2010).

### 1.1.3 Human overpopulation

According to the last world population prospect of July 2015, published by The Department of Economic and Social Affairs of the United Nations, the world population reached 7.3 billion in July 2015. Moreover, 60% of the global population lives in Asia (4.4 billion), and 16% in Africa (1.2 billion), resulting in more than 75% of the world population. China (1.4 billion) and India (1.3 billion) remain the two largest countries of the world, both with more than 1 billion people, representing 19 and 18 per cent of the world’s population, respectively. The forecast regarding the future are clear.

Major area	Population (millions)			
	2015	2030	2050	2100
World .....	7 349	8 501	9 725	11 213
Africa .....	1 186	1 679	2 478	4 387
Asia .....	4 393	4 923	5 267	4 889
Europe .....	738	734	707	646
Latin America and the Caribbean .....	634	721	784	721
Northern America .....	358	396	433	500
Oceania .....	39	47	57	71

**Table 1.1:** Population of the World and Major Areas, Until 2100, According to The Medium-Variant Projection (United Nations, Department of Economic and Social Affairs, Population Division, 2015)

Currently, the world population continues to grow though more slowly than in the recent past. Ten years ago, world population was growing by 1.24% per year. Today, it is growing by 1.18% per year, or approximately an additional 83 million people annually. The world population is projected to increase by more than one billion people within the next 15 years, reaching 8.5 billion in 2030, and to increase further to 9.7 billion in 2050 and 11.2 billion by 2100. (see table 1.1). As expected, more than half of global population growth between now and 2050 is expected to occur in Africa (United Nations, Department of Economic and Social Affairs, Population Division, 2015).

Until 2000, historic evidences demonstrate a strict correlation between growth population and total energy required.

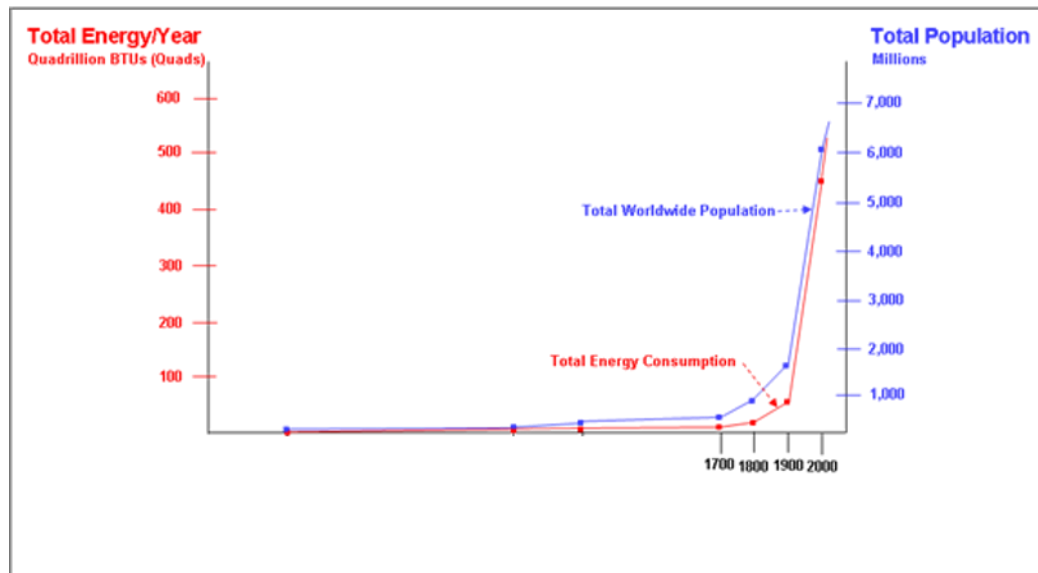


**Figure 1.11:** Historic Global Energy Consumption (expressed in Quadrillions of BTU required) and Population Growth (expressed in millions). (U.S. Census Bureau, 2012)

This trend is obviously related to the increasing of human activities, in particularly from the middle of 1900 (where the slope of the previous graph dramatically increases). Looking deeper into the Census Bureau document, there is also a common trend between the energy consumed (“per capita”) expressed in gigajoule (GJ), and the CO<sub>2</sub> emissions (“per capita”) expressed in metric tons/year (figure 1.12).

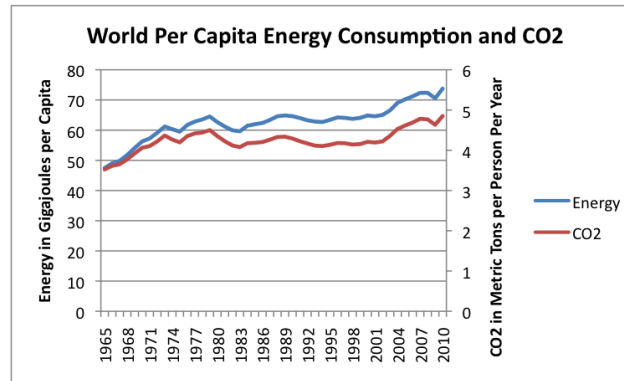


**Figure 1.12:** Relationship between energy consumption “per capita” and CO<sub>2</sub> emissions (U.S. Census Bureau, 2012)

There are evident, then, the causes of this increase. In these years, indeed, there was a huge increment of fossil fuel consumption to sustain the growth during the 3<sup>o</sup> industrial revolution period.

It’s difficult to make a forecast on the future development. There are no precise studies in literature, only in the Annual Energy Outlook with Projection to 2040, prepared by the U.S. Energy Information Administration (EIA) in April 2015, is reported that “the future path of crude oil and natural gas in U.S.A. can vary substantially, depending on assumptions about the size of global and domestic resources, demand for petroleum products and natural gas (particularly in non-Organization for Economic Cooperation and Development (non-OECD) countries), levels of production, and supplies of other fuels” (U.S. Energy Information Administration, 2015). Anyhow, in the same 2001 report, the EIA made a prevision of the global energy requirements (including renewables and nuclear) from 2001 to 2025 divided by each fossil fuel, considering the population growth index and the energy consumption according to 2001 rates (figure 1.13).

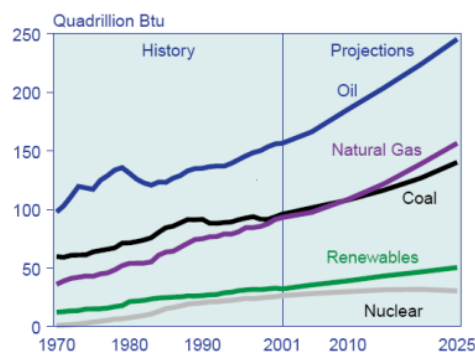


**Figure 1.13:** Projection of the requirement of fossil fuel, renewable and nuclear energy considering the population increasing rate, and the global energy consumption in 2001, according to a stationary scenario. (United States Energy Information Administration, 2001)

### 1.1.4 Wastes and food losses

Waste, as all knows, is another global issues. According to authoritative Chambers 21st Century Dictionary, waste is defined as an unwanted or discarded materials ‘rejected as useless, unneeded or excess to requirements’ (Mairi Robinson, 1999).

Providing data on the global amount of waste production is not easy, due to the limited indication (especially in developing country) and low accuracy of the existing reports. Anyway, the Global Waste Management Outlook edited yearly by the United Nations Environment Program, assess that in 2014, the “order of magnitude” of production of Municipal Solid Waste (MSW) states between 7 and 10 billion of tons per annum. Moreover, MSW fraction represents more than 80% of global waste production across the world. Besides that, in high-income level country, c.ca 70% of total MSW are made by food waste (34%), paper (24%) and plastics residues (11%). In addition to this, figure 1.14 shows the global perspective until 2100 regarding the MSW production. It’s evident that, especially in South Asia and Sub – Saharan Africa regions, there will be a huge increase (United Nations Environment Programme, 2015).

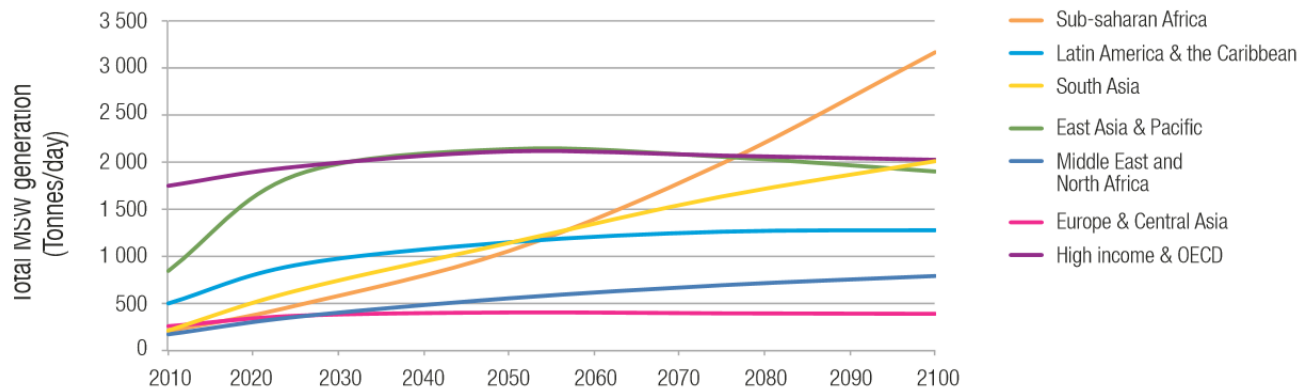


**Figure 1.14:** Global MSW production until 2100, divided by regions, in tons/day (United Nations Environment Programme, 2015).

As I told before, more than 30% of total MSW are represented by food scraps. According to the last report of Food and Agriculture Organization (FAO), it’s possible to define three different type or food-related dispersion: food losses, food waste and food wastage (FAO, 2014)



- ✓ Losses: a decrease in mass (dry matter) or nutritional value (quality) of food that was originally intended for human consumption. These losses are mainly caused by inefficiencies in the food supply chains, such as poor infrastructure and logistics, lack of technology, insufficient skills, knowledge and management, capacity of supply chain actors, and lack of access to markets.
- ✓ Waste: food appropriate for human consumption being discarded, whether or not after it is kept beyond its expiry date.
- ✓ Wastage: any food lost by deterioration or waste. Thus, the term “wastage” encompasses both food loss and food waste.

In the same report is also estimated that c.ca 1/3 of total food production for human consumption is lost, corresponding to 1.3 billion of tons per year (United Nation, 2011). This is absolutely not acceptable in a world where 850 million people are undernourished (12.5% of the entire global population) (FAO, 2012). Here there is a summary of the key facts regarding carbon, water and hectare footprint to produce lost food, underlined in the last FAO report:

- ❖ Food wastage's carbon footprint is estimated at 3.3 billion tons of CO<sub>2</sub> equivalent of GHG released into the atmosphere per year.
- ❖ The total volume of water used each year to produce food that is lost or wasted (250km<sup>3</sup>) is equivalent to the annual flow of Russia's Volga River, or three times the volume of Lake Geneva.
- ❖ Similarly, 1.4 billion hectares of land (28% of the world's agricultural area) is used annually to produce food that is lost or wasted.

Moreover, an enormous percentage of the total edible food wastage is loss during harvest, storage, handling and transportation process (e.g. more than 80% of roots, tubers, fruits, vegetables and fish, are lost before retailing (Gustavsson, 2011)).

Concluding, the global food wastage, produces an economical loss of USD 1 trillion each year.

FAO, also, estimated that the global food production must increase by 60% by 2050 in order to meet the demands of the growing world population. It is absolutely evident that this trend is no more sustainable.

Besides these data shown in these chapters, multiple factors like recent policy instability in the OPEC countries, the fluctuating of oil price and the non-equal distribution of fossil resources, requires a strong turnaround from petroleum-based economy to an environmental-friendly one. To do that, is required a deep shift in our economy vision, towards a greener society, in a long-term vision of carbon footprint reduction.

Green chemistry and biorefinery are two fundamental concepts helping our society to reach a new and environment-friendly development. These approaches are conceptually based on the valorization of natural resources for the creation of a sustainable future.

## 1.2 BIOREFINERY AND GREEN CHEMISTRY

### *1.2.1 Concepts and principles*

Besides several definitions of biorefinery, the International Energy Agency (IEA), identified a biorefinery as an “industrial facility (or network of facilities) that cover an extensive range of combined technologies aiming to full sustainable transformation of biomass into their building blocks, with the concomitant production of biofuel, energy, chemicals and material, preferably of added-value” ([www.siadeb.org](http://www.siadeb.org)). Most recently, with the “Task 42 for Biorefining” the IEA updated the previous concept of biorefinery, delineating a biorefinery like a “sustainable process conversion of biomass into a spectrum of marketable product and energy” (Jungmeier G, 2013).

Both of them, depicts a biorefinery as a comprehensive technology towards the biomass conversion, leading to a whole portfolio of valuable products (Ana R.C. Morais, 2013). This concept is pretty similar to the traditional refinery definition, where the raw materials are converted to fuel and chemicals for our everyday lives through chemical and polluting procedures. The most important differences are the utilization of renewable resources as input, and a defined biochemical route for the conversion of substrate in final products.

To accomplish these needs, science developed many less-energy and less-waste generation technologies (Ana R.C. Morais, 2013), however new studies and new investments are needed for a complete switch between petroleum based compound to natural resources input. Indeed, the ultimate goal in sustainability must be to emulate the nature, by harnessing the sun’s energy for the production of chemicals and energy, using inly water and carbon dioxide (Sheldon R. A., 2014).

One of the principle instrument of our society to fulfill the biorefinery purpose, is the green chemistry.

As defined by P.T. Anastas and J.C. Warner, green chemistry “efficiently utilizes raw materials (preferably renewables), eliminates wastes, and avoid the use of toxic/hazardous solvents and reagents in the manufacture and application of chemical products” (P.T. Anastas, 1998).

The concept of green chemistry doesn't involve any economic aspects typical of biorefinery. In fact, it's only a technological resource to reach the objective of a sustainable development.

It's possible to categorize the biorefinery process through a green chemistry typical instrument, introduced in the early 1990s: The E – factor. This value is defined as the amount of waste produced ( $\text{Kg}_{\text{waste}}/\text{Kg}_{\text{product}}$ ) in the whole process. Moreover, in this contest, is considered as waste everything that is not the final product, excluding water (Sheldon R. , 2008).

In the production of biofuel and bio-based chemicals, the E- factor dramatically increases from bulk and platform molecules to fine and pharmaceutical. For this reason, is mandatory an integrated approach between policy institution, big industrial company and university system, to define a unique strategy for the developing of a circular economy based system. For example, E-factor has been widely adopted as a useful metric to quick assessing the environmental footprint of a manufacturing process. Pharmaceutical company made a lot of efforts to develop a more environmental process; Pfizer scientist published a guide to green reagents and solvent used in 2008 (K. Alfonsi, 2008), and GSK recently described a guide used to rank commonly used reagents in 15 different types of transformation, commonly used in pharmaceutical operations (J. P. Adams, 2013).

To simultaneously solve the dilemma of global energy demand, GHGs emission and fossil fuel limitation, related to a constant increase of energy requirement and world populations, it's evident that biorefinery and green chemistry principles needs to be connected to a more global effort toward recycling principles. It's possible to summarize them in two fundamental strategies: Waste to Energy (WTE) and Circular Economy (CE) reviewed in the next chapter.

### *1.2.2 Waste-to-Energy (WTE) and Circular Economy (CE)*

Providing a global plan towards a greener society is as much difficult as necessary. Environmental friendly development requires a sustainable supply of clean and affordable renewable energy sources that do not cause negative societal impacts. (Richa Kothari, 2010). United Nation, in

according to the principal international organizations proposed a plan that integrates WTE technologies and CE. As defined in the previous chapter, the increasing of waste production from now to 2100 (MSW, and food losses especially), in particularly in Africa and Asia, imposes a deep re-thinking in waste management and food supply chain.

Typical examples of WTE technologies are thermo-chemical treatments, like direct combustion or co-combustion (Helmut Rechberger, 2010), pyrolysis or gasification (Astrup & Bilitewski, 2011), or more recently biochemical procedures like biogas production (bioCH<sub>4</sub>, bioH<sub>2</sub>), fuel cell technologies or other fermentation-related processes, deeply reviewed in this dissertation.

WTE concept is enhanced and implemented in a more global Circular Economy (CE) strategy defined in the EU Action Plan for the Circular Economy document released by EU in 2015. This plan establishes a concrete and ambitious program of actions, with measures from production, consumption and waste management. The proposed actions will contribute to "closing the loop" of product lifecycles through greater recycling and re-use, and bring benefits for both the environment and the economy.

But how can be defined circular economy? The best way to explain what a circular economy is, is to compare it to our current linear economy so called “take, make and dispose” (Ness, 2008), as depicted in figure 1.15

### Where we are coming from: The linear economy and waste management

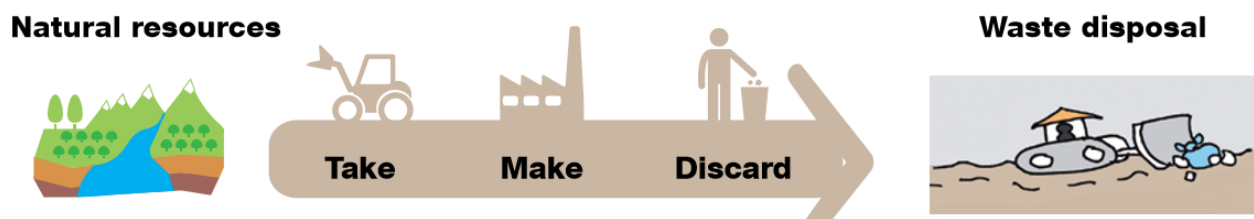


*Figure 1.15: “Take, Make and Dispose” linear economy (United Nations Environment Programme, 2015).*

As demonstrated before, this system is no more sustainable, and a more environmental-friendly concept needs to be developed. It's possible to define 6 principles on which circular economy is based, regarding materials, energy, ecosystem, value, health and society:

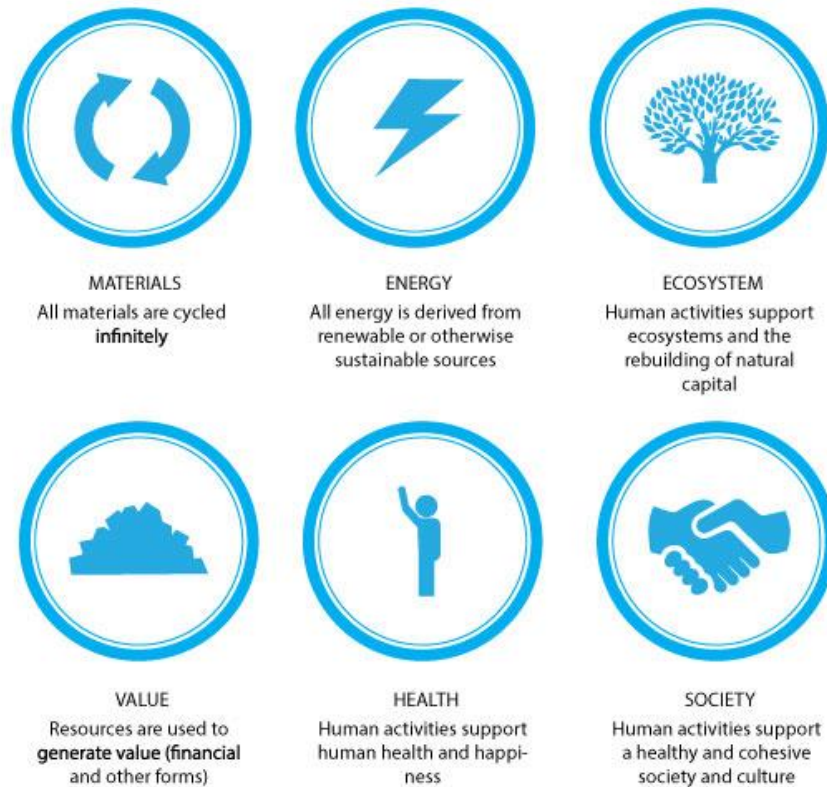


*Figure 1.16: Key principle of circular economy (EllenMcCarthur Foundation, 2013)*

The results of the application of these 6 principles is a closed economy where both technical and biological cycles are closed and different “feedback loops” are defined at different levels.

## Where we need to get to: Resource management within a circular economy

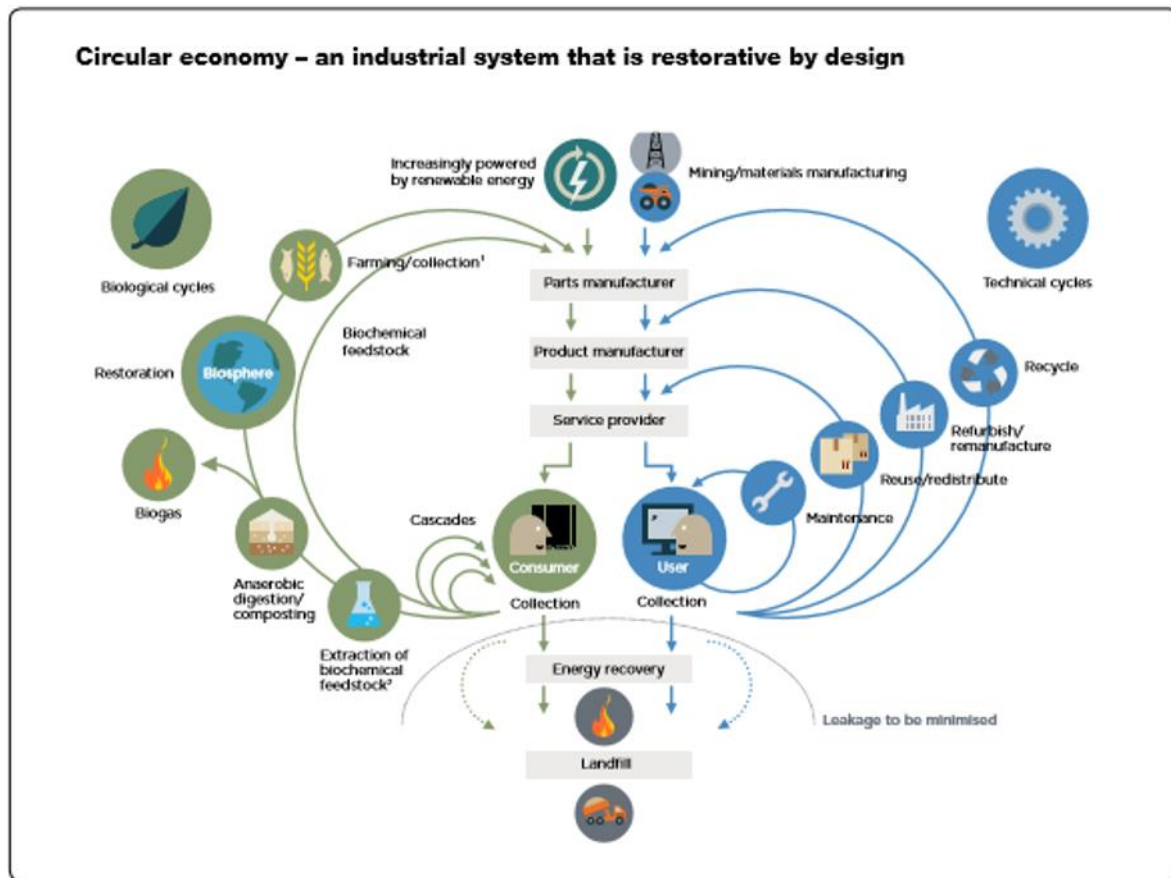


*Figure 1.17: Closed Circular Economy scheme (EllenMcCarthur Foundation, 2013)*

A large number of peer reviewed studies are made regarding theoretical and practical application of circular economy, most of them in China (N.U., 2005), (Andersen, 2006), (Zhijun, 2007), (Biwei Sua A. H., 2013), (Yong Geng, 2008), (John A. Mathews, 2011). In this country, indeed, are largely diffuse, environmental, social and health problems, connected to the rapid industrial development. The concept of circular economy traces back to the middle of XX century (DW Pearce, 1990); from that moment, more than 250 articles (case studies, reviews, scientific reports, etc.) are published worldwide (Ghisellini, 2015).

Circular economy mainly emerges in the literature through three main “concepts”, so called 3R's principles: Reduction, Reuse and Recycle (Preston, 2012), (Lett, 2014), (Biwei Sua A. H., 2013), (Sakai, 2011). The Reduction principle aims to minimize the input of primary energy, raw materials and waste through the improvement of efficiency in production (so called eco-efficiency) and

consumption processes (introducing better technologies, or more compact and lightweight products, simplified packaging, more efficient household appliances, a simpler lifestyle, etc.) (Ghisellini, 2015). The Reuse principle refers to “any operation by which products or components that are not waste are used again for the same purpose for which they were conceived” (European Union, 2008). The Recycle principle refers to “any recovery operation by which waste materials are reprocessed into products, materials or substances whether for the original or other purposes” (European Union, 2008). CE and WTE concepts promote a more appropriate and environmentally sound use of resources aimed at the implementation of a greener economy, characterized by a new business model and innovative employment opportunities, as well as by improved wellbeing and evident impacts on equity within and among generations (Stahel, 2010), (EllenMcCarthur Foundation, 2013).

### *1.2.3 Legislation and perspectives*

As it clearly reported in the previous paragraph, Circular Economy is one of the pillar of the United Nation strategy in the next future. A lot of efforts are made to establish a global and unique action to reach a complete shift from “take, make and dispose” principle to a circular model.

In this contest it’s important to review briefly what European Union has done since 2012 regarding the Circular Economy policy.

In January 2012, indeed, a fundamental document from EU was released entitled “Towards the Circular Economy: Economic and business rationale for an accelerated transition”. This report, commissioned by the Ellen MacArthur Foundation, was the first of its kind to consider and concretely develop an economical and business opportunity for the transition to a circular economy model. In this report was accurately detailed the benefits across the whole EU, using case-studies and economy-wide analysis. For example, it defines that the commercial subset of the whole EU manufacturing sector could reach up to \$630 billion of net materials cost saving towards 2025 (Ellen MacArthur Foundation, 2012).



It's globally accepted that this document was the first concrete building block in the transition from linear to circular model.

In 2014, European Union announced a united documents called “The 2014 Proposal on Waste Review”. In this text, all the previous different directive for different type of wastes were united in one proposal, like The Waste Framework Directive (European Commission, 2008), The Packaging and Packaging Waste Directive (European Commission, 1994), the Landfill Directive (European Commission, 1999), the Batteries Directive (European Commission, 2006), the End-of-life Vehicles Directive (European Commission, 2000), and the WEEE Directive (European Commission, 2012).

Immediately thereafter, in July 2015, the Commission announced the intention to withdraw the 2014 proposal on Waste Review and to replace it with a new, more ambitious proposal to promote the circular economy, called “The 2015 Circular Economy Package”, because the previous policy had a rather exclusive focus on waste management, without appropriately exploring synergies with other aspects of circular economy.

The concrete proposals can be summarized as follow (European Commission, 2015):

- ✓ A common EU target for recycling 65% of municipal waste by 2030;
- ✓ A common EU target for recycling 75% of packaging waste by 2030;
- ✓ A binding landfill target to reduce landfill to maximum of 10% of all waste by 2030;
- ✓ A ban on landfilling of separately collected waste;
- ✓ Promotion of economic instruments to discourage landfilling;
- ✓ Concrete measures to promote re-use and stimulate industrial symbiosis - turning one industry's by-product into another industry's raw material;
- ✓ Economic incentives for producers to put greener products on the market and support recovery and recycling schemes.

In the last Global Waste Management Outlook, published by UNEP in 2015 (United Nations Environment Programme, 2015), are reported the preliminary results and the trend from 1990 to 2020 regarding the municipal solid wastes for landfilling and recycling (figure 1.18). The results show a decreasing in landfill from more than 80% to 50% probably in 2020, and an increasing in recycling

up to 50% from less than 15% in 1990. These results are encouraging but are not enough. To respect the EU directive, must be increased the recycling percentage, but moreover highly reduce the quantity of landfilling.

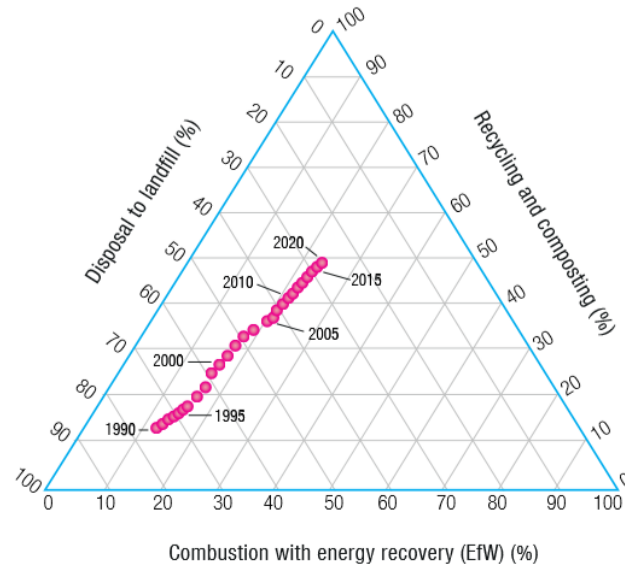


**Figure 1.18:** Results overview and future trends of landfilling, recycling and energy recovery according to Bartl, 2014











### 1.3 RENEWABLE ENERGY: A NECESSITY

As extensively reviewed until now, fossil fuel reserves are running out, global warming is becoming a sad reality, waste production is increasing, and the continuous population growth requires more and more energy to sustain the economy. (Stéphane Octave, 2009).

In this situation, the only solution seems to be a deep shift towards the renewable sources of energy to create the basis for an economically-sustainable development.

In 2015, two global reports, the “Global Trends in Renewable Energy Investment Report” (GTR), and the “Renewables Global Status Report” (GSR), assesses the state-of-the-art regarding all the aspects of the renewable energy. The first report is published by published by UNEP at the end of the year (United Nation Environment Program, 2015), the second one by REN21, the Renewable Energy Policy Network for the 21st Century, a global renewable energy multi-stakeholder policy network that provides international leadership for the rapid transition to renewable energy. (REN 21 - Renewable Energy Policy Network for the 21st Century, 2015).

In table 1.2 is reported a complete trend of global investments, overall energy production divided by sector, and number of country with specific national policies toward renewables energy from 2004 to 2014:

		START 2004 <sup>1</sup>	2013	2014
<b>INVESTMENT</b>				
New investment (annual) in renewable power and fuels <sup>2</sup>	billion USD	45	232	270
<b>POWER</b>				
Renewable power capacity (total, not including hydro)	GW	85	560	657
Renewable power capacity (total, including hydro)	GW	800	1,578	1,712
 Hydropower capacity (total) <sup>3</sup>	GW	715	1,018	1,055
 Bio-power capacity	GW	<36	88	93
 Bio-power generation	TWh	227	396	433
 Geothermal power capacity	GW	8.9	12.1	12.8
 Solar PV capacity (total)	GW	2.6	138	177
 Concentrating solar thermal power (total)	GW	0.4	3.4	4.4
 Wind power capacity (total)	GW	48	319	370
<b>HEAT</b>				
 Solar hot water capacity (total) <sup>4</sup>	GW <sub>th</sub>	86	373	406
<b>TRANSPORT</b>				
 Ethanol production (annual)	billion litres	28.5	87.8	94
 Biodiesel production (annual)	billion litres	2.4	26.3	29.7
<b>POLICIES</b>				
Countries with policy targets	#	48	144	164
States/provinces/countries with feed-in policies	#	34	106	108
States/provinces/countries with RPS/quota policies	#	11	99	98
Countries with tendering/ public competitive bidding <sup>5</sup>	#	n/a	55	60
Countries with heat obligation/mandate	#	n/a	19	21
States/provinces/countries with biofuels mandates <sup>6</sup>	#	10	63	64

<sup>1</sup> Capacity data are as of the beginning of 2004; other data, such as investment and biofuels production, cover the full year. Numbers are estimates, based on best available information.

<sup>2</sup> Investment data are from Bloomberg New Energy Finance and include all biomass, geothermal, and wind generation projects of more than 1 MW; all hydro projects of between 1 and 50 MW; all solar power projects, with those less than 1 MW estimated separately and referred to as small-scale projects or small distributed capacity; all ocean energy projects; and all biofuel projects with an annual production capacity of 1 million litres or more.

<sup>3</sup> The GSR 2014 reported a global total of 1,000 GW of hydropower capacity at the end of 2013; this figure has been revised upwards. Hydropower data do not include pumped storage capacity. For more information, see Methodological Notes, page 243.

<sup>4</sup> Solar hot water capacity data include water collectors only. The number for 2014 is a preliminary estimate.

<sup>5</sup> Data for tendering/public competitive bidding reflect the number of countries that had held tenders at any time up to the year in question, but not necessarily during that year.

<sup>6</sup> Biofuel policies include policies listed both under the biofuels obligation/mandate column in Table 3 (Renewable Energy Support Policies) and in Reference Table R18 (National and State/Provincial Biofuel Blend Mandates).

**Note:** All values are rounded to whole numbers except for numbers <15, and biofuels, which are rounded to one decimal point. Policy data for 2014 include all countries identified as of early 2015.

**Table 1.2:** Trend of the investments in global energy production and number of country with renewables energy policies from 2004 towards 2014 (REN 21 - Renewable Energy Policy Network for the 21st Century, 2015).

The most important data shows that in only ten years, the new investments (in billions of dollars) in renewable power and fuels passes from 45 to 270 billion of dollars (6 times higher), demonstrating the results of a common strategy for the establishment of circular economy.

China saw by far the biggest renewable energy investments in 2014 — a record \$83.3 billion, up 39% from 2013. The US was second at \$38.3 billion, up 7% on the year but well below its all-time high reached in 2011. Third came Japan, at \$35.7 billion, 10% higher than in 2013 and its biggest total ever. Additional to China, in the developing countries Brazil (\$7.6 billion), India (\$7.4 billion) and South Africa (\$5.5 billion) were all in the top 10 of investing countries while more than \$1 billion was invested in Indonesia, Chile, Mexico, Kenya and Turkey (United Nation Environment Program, 2015). In 2014, solar compartment was the largest recipient, with a total investment in China and Japan of \$74.9 billion, followed by biofuels at \$610 million. The same trend is reflected in the following graph, that compare the global investment in renewable energies only in 2014 (figure 1.19).

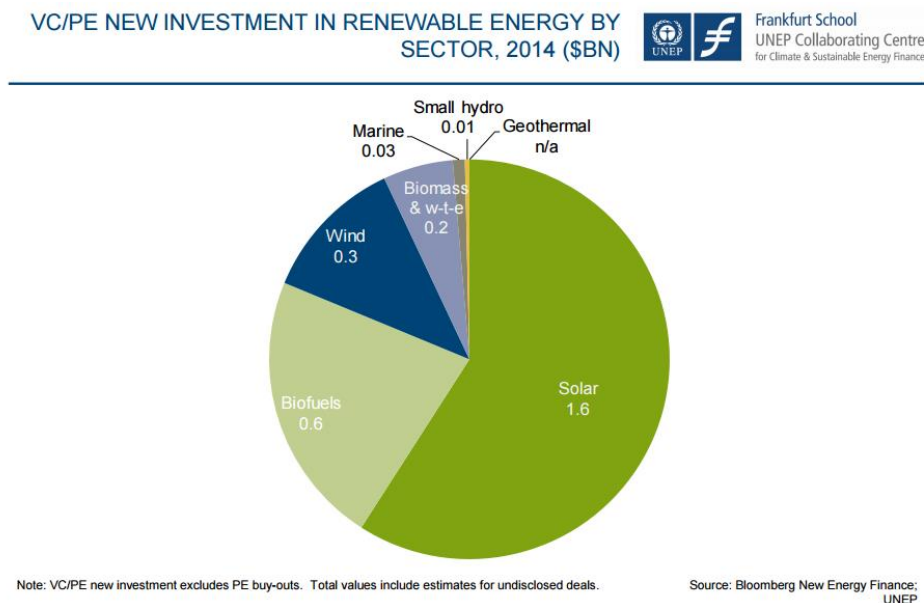


**Figure 1.19:** Global investment in renewable energy in 2014 in billions of dollars (REN 21 - Renewable Energy Policy Network for the 21st Century, 2015)

After the approval of the “2015 Circular Economy Package”, there will be an inversion of the trend. Although the predominant investment in the solar compart in 2014, the expected funding in 2022 for biofuel plants and researches (according to Clean Edge, Inc.) will overtake the funding expected for solar programs, as demonstrated in figure 1.20.

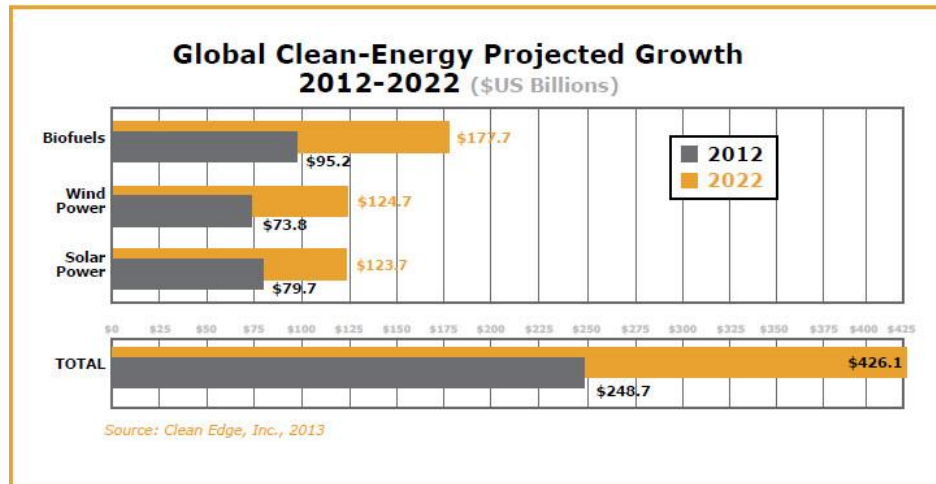


**Figure 1.20:** Expected investment in solar, wind and biofuel compartment in the period 2012-2022 (\$UD billions) (Clean Edge, Inc, 2013)

From this point of view is clear that the valorization of the organic matter parts of the MSW (that represents one of the most predominant part of the entire waste production) for the production of biofuel and bio-based chemicals with a biorefinery approach, can represent, in the immediate future, a fundamental contribution for the circular economy.

## 1.4 BIOREFINERIES: INSIDE A DEEP VIEW

As reported previously, IEA Bioenergy Task 42 has developed the following definition for biorefinery:

*“Biorefinery is the sustainable processing of biomass into a spectrum of marketable products and energy”* (Jungmeier G, 2013).

The biorefinery approach is based on the use of carbon molecules extracted from renewable sources, to substitute carbons from oil and gas (B. Kamm, 2004). The feedstock can include trees, energy crops (switchgrass), agricultural products such as grain and waste products such as municipal waste. It may use one or many feedstock and may use different types of conversion technologies as biochemical, thermochemical or both. Moreover, biorefineries exploit all of the elements of biomass, recycling secondary products and wastes into valuable products or fuel for the biorefinery plant. From this point of view, the approach is the same of a petroleum refinery, however there is a big difference. Biorefineries are based on the use of renewable materials as a feedstock whereas petroleum refineries are based on the use of fossil fuels. As depicted in figure 1.21, it's possible to imagine a biorefinery as a closed loop where biomass is converted to a family of building blocks and subsequently in final products as materials, fuels and fine chemicals. These products are then recycled, closing the loops, and re-converted again in biomass.

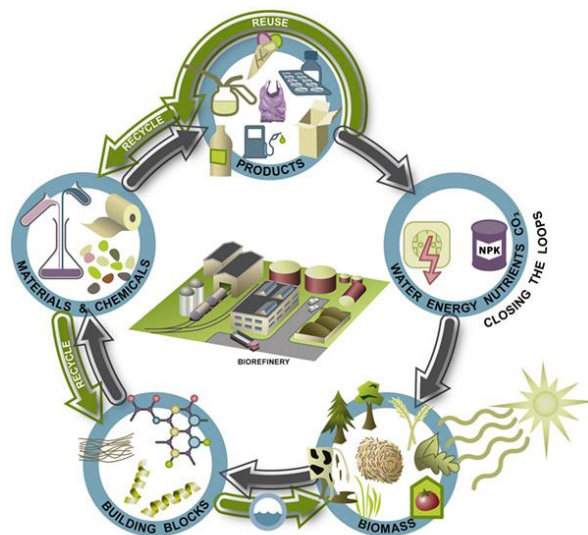


**Figure 1.21:** Biorefinery approach (BRIDGES, 2013)

One of the best advantages of the biorefinery is the versatility. Different types of biomasses can be converted, with different type of bio-thermochemical processes, in different types of fuels, chemicals and materials, maximizing the intrinsic value of a feedstock. This concept is clearly exemplified in the official classification of different types of biorefineries made by IEA in the Task 42 for Biorefining (IEA, 2014).

#### *1.4.1 Types, classification and complexity*

Until 2015, when the circular economy package document was signed by EU countries, many attempts to classify the biorefinery types were made in literature (Kamm B., 2005), (Ree van R, 2007). Moreover, these classifications were made for single types of specific biorefineries set-up, like “liquid phase catalytic processing biorefinery” or “forestry biorefinery, without a complete and unique categorization set. Depending on which parameters are considered, different categories can be made, but this classification criterion is not homogeneous. Some of these systems refer to the type of feedstock (e.g., lignocellulosic feedstock biorefinery, marine biorefinery and others), while others focus on the technologies involved (e.g., thermochemical, conventional and two-platform concept biorefinery) (Francesco Cherubini, 2009). Again, is possible to use only a part of the feedstock, (e.g. lignocellulosic residues) or the entire whole crop. Moreover, there will be some ambiguous classifications. For example, if the carbohydrate fraction of a lignocellulosic feedstock is used to produce cellulose and xylose, the system is classified as a lignocellulosic feedstock biorefinery; but can also be classified as a forest-based biorefinery and, if the lignin fraction is pyrolyzed, the same biorefinery is also suitable for classification as a two platform concept biorefinery (Francesco Cherubini, 2009). For this reason, a comprehensive approach in the biorefinery classification is needed. This classification needs to be flexible to include present and future’s features, but also fixed and not-ambiguous, to permit to the big stakeholders the accessibility to the market.

The basic idea developed by Cherubini et.al. adopted by EU in the framework of Task 42 for Biorefinery, is based on 4 principal common main features of all biorefineries (importance order list).



1. Platforms
2. Products
3. Feedstocks
4. Processes

All these features are common because a biorefinery can be defined as a conversion process from feedstock to products, through different platforms and different processes. All these characteristics can be divided in sub-categories, as reported in table 1.3

Platforms	Products	Feedstocks	Processes (selected)
<b>I.) C5 sugars</b>	<b>I.) Energy products</b>	<b>I.) Dedicated crops</b>	<b>I.) Thermochemical</b>
	I.1) Biodiesel	I.1) Oil crops	I.1) Combustion
<b>II.) C6 sugars</b>	I.2) Bioethanol	I.2) Sugar crops	I.2) Gasification
	I.3) Biomethane	I.3) Starch crops	I.3) Hydrothermal upgrading
<b>III.) Oils</b>	I.4) Synthetic biofuels	I.4) Lignocellulosic crops	I.4) Pyrolysis
	I.6) Electricity and heat	I.5) Grasses	I.5) Supercritical
<b>IV.) Biogas</b>		I.6) Marine biomass	<b>II.) Biochemical</b>
	<b>II.) Material products</b>		II.1) Fermentation
<b>V.) Syngas</b>	II.1) Food	<b>II.) Residues</b>	II.2) Anaerobic digestion
	II.2) Animal feed	II.1) Lignocellulosic residues	II.3) Aerobic conversion
			II.4) Enzymatic processes
<b>VI.) Hydrogen</b>	II.3) Fertilizer	II.2) Oil based residues	<b>III.) Chemical processes</b>
	II.4) Glycerin	II.3) Organic residues & others	III.1) Catalytic processes
<b>VII.) Organic juice</b>	II.5) Biomaterials		III.2) Pulping
	II.6) Chemicals and building blocks		III.3) Esterification
<b>VIII.) Pyrolytic liquid</b>	II.7) Polymers and resins		III.4) Hydrogenation
	II.8) Biohydrogen		III.5) Hydrolysis
<b>IX) Lignin</b>			III.6) Methanisation
			III.7) Steam reforming
<b>X) Electricity and heat</b>			III.8) Water electrolysis
			III.9) Water gas shift
			<b>IV.) Mechanical/physical</b>
			IV.1) Extraction
			IV.2) Fiber separation
			IV.3) Mechanical fractionation

**Table 1.3:** Features (and relative sub-groups) used in proposed categorization approach (Francesco Cherubini, 2009)

*Platforms* are the main pillars of this biorefinery classification. They are intermediate compounds that links raw materials with final products. This concept is the same of petroleum-based biorefinery,

where fossil fuels are fractionated in a broad spectrum of different molecules which are therefore converted into final products.

*Products* can be clumsily divided into energy and materials. The energy compound is comprehensive of different type of fuels (biodiesel, bioCH<sub>4</sub> or bioethanol), energy or heat, that are internal re-used in the biorefinery, sold to the grid or, better, upgraded to a more valuable fine chemical. Materials products are primarily biomaterials (like bio-plastics as PLA or PHA), lubricants, fine chemicals or building blocks (like aromatics, amino acids, xylitol, polyols, succinic-, lactic- levulinic- and itaconic acid, phenols, furan dicarboxylic acid, furfural and so on), fibers and resin (Francesco Cherubini, 2009). In this contest is important to define also the market targets; in fact, a product can be used both in energy and product sector (e.g. hydrogen for fuel cells application or hydrogen as chemical catalyst).

*Feedstocks* are defined as the raw materials converted to marketable products. It's possible to sub-categorize them in "dedicated" and "residues", and both of them can come from different sectors, as agriculture, aquaculture, forestry or industries and household residues. Mostly the dedicated feedstocks are marine biomass (algae or seaweed), plants (sugar or starch) or plants-derived materials (grass silage, immature cereals or plant shoots). It's evident that these feedstocks create a social and ethic issue due to the competition with food. For this reason, a lot of attention is paid to the residues-based biorefinery, which involves the utilization of forestry and agriculture residues (e.g. lignocellulosic or manure) or municipal residues (e.g. oil waste or MSW).

*Processes* are the technical part of a biorefinery. They transform the feedstocks in products using one or more platforms. It's evident that this parameter is the key for the flexibility of a biorefinery. Combinations of different processes using the same feedstocks can result in an increase of social and environmental value of the process itself. For example, during the conversion of a lignocellulosic feedstock to bioethanol, the lignin residues (biochemical process), the lignin residues can be combusted (thermochemical process) to obtain heat. It's possible to define four types of processes (with a lot of sub-categories, depending of the technology involved). Mechanical/physical (e.g., pressing, pre-treatment, milling, separation, distillation), which do not change the chemical structure

of the biomass components, but they only perform a size reduction or a separation of feedstock components. Biochemical (e.g., anaerobic digestion, aerobic and anaerobic fermentation, enzymatic conversion), which occur at mild conditions (lower temperature and pressure) using microorganisms or enzymes. Chemical processes (e.g., hydrolysis, transesterification, hydrogenation, oxidation, pulping), where a chemical change in the substrate occurs. Thermochemical (e.g., pyrolysis, gasification, hydrothermal upgrading, combustion), where feedstock undergoes extreme conditions (high temperature and/or pressure, with or without a catalytic mean) (Francesco Cherubini, 2009).

In addition to a unique classification, the industrial market and the big companies needs an index to evaluates the process complexity. For example, some simple biorefinery uses one feedstock to produce two or three products with current available commercial technologies. However, other biorefinery are sometimes very complex using many different feedstocks to coproduce a broad spectrum of different products using technologies that still need to become commercial in the upcoming years (Ashok Pandey, 2015). A fixed and simple-use index is needed to embrace all of these different concepts. This index, called BCI (Biorefinery Complexity Index) is introduced by EU in the Task 42 of Circular Economy Package in 2015, and is based on the Nelson's complexity index was developed by Wilbur L. Nelson, to determine the petroleum based biorefinery complexity. That index assigns a complexity factor to each major piece of refinery equipment based on its complexity and cost in comparison to crude distillation, which is assigned a complexity factor of 1.0. The complexity of each piece of refinery equipment is then calculated by multiplying its complexity factor by its throughput ratio as a percentage of crude distillation capacity. Adding up the complexity values assigned to each piece of equipment, including crude distillation, determines a refinery's complexity (Nelson, 1960). Based on this index, the BCI is a summary of the complexity factor called "Technology Readiness Level (TRL)" assigned on a singular feature (Platform, Product, Feedstock and Process) from 1 to 9. BCI is expressed by a unique profile:  $\sum BCI (TRL_{Platforms}/TRL_{Feedstocks}/TRL_{Products}/TRL_{Processes})$ . For example, 8 (1/1/3/3) is a biorefinery with BCI = 8 where from one feedstock are produced three different products through one platform and three processes (Ashok Pandey, 2015).

Summarizing all of these concepts, we can graphically schematize a biorefinery as in figure 1.22

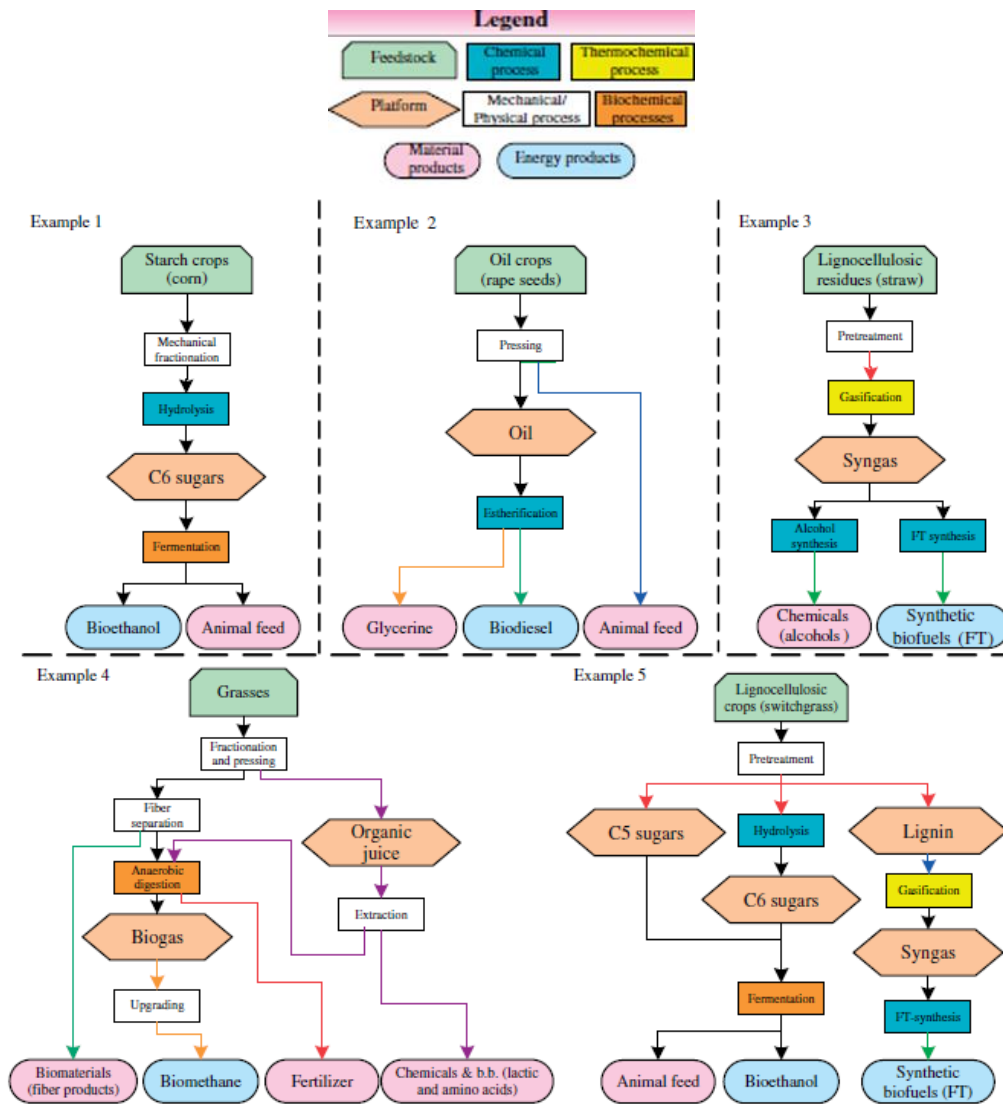


**Figure 1.22:** Scheme for the classification of biorefinery systems (Ashok Pandey, 2015).

Where example 1 is a 7 (1/1/2/3) biorefinery with one C-6 sugars platform, one starch crop feedstock, two products as bioethanol and animal feed and three processes like mechanical fractionating, hydrolysis and fermentation. Using the same approach example 2 is a 7 (1/1/3/2) biorefinery, example 3 is a 8 (1/1/2/4) biorefinery, and examples 3 and 4 are respectively a 12 (2/1/4/5) and 13 (4/1/3/5) biorefineries.

In task 42 of the European Package For Circular Economy, is depicted a biorefinery network where all the existing biorefinery approaches are linked each other using these categorization (figure 1.23).

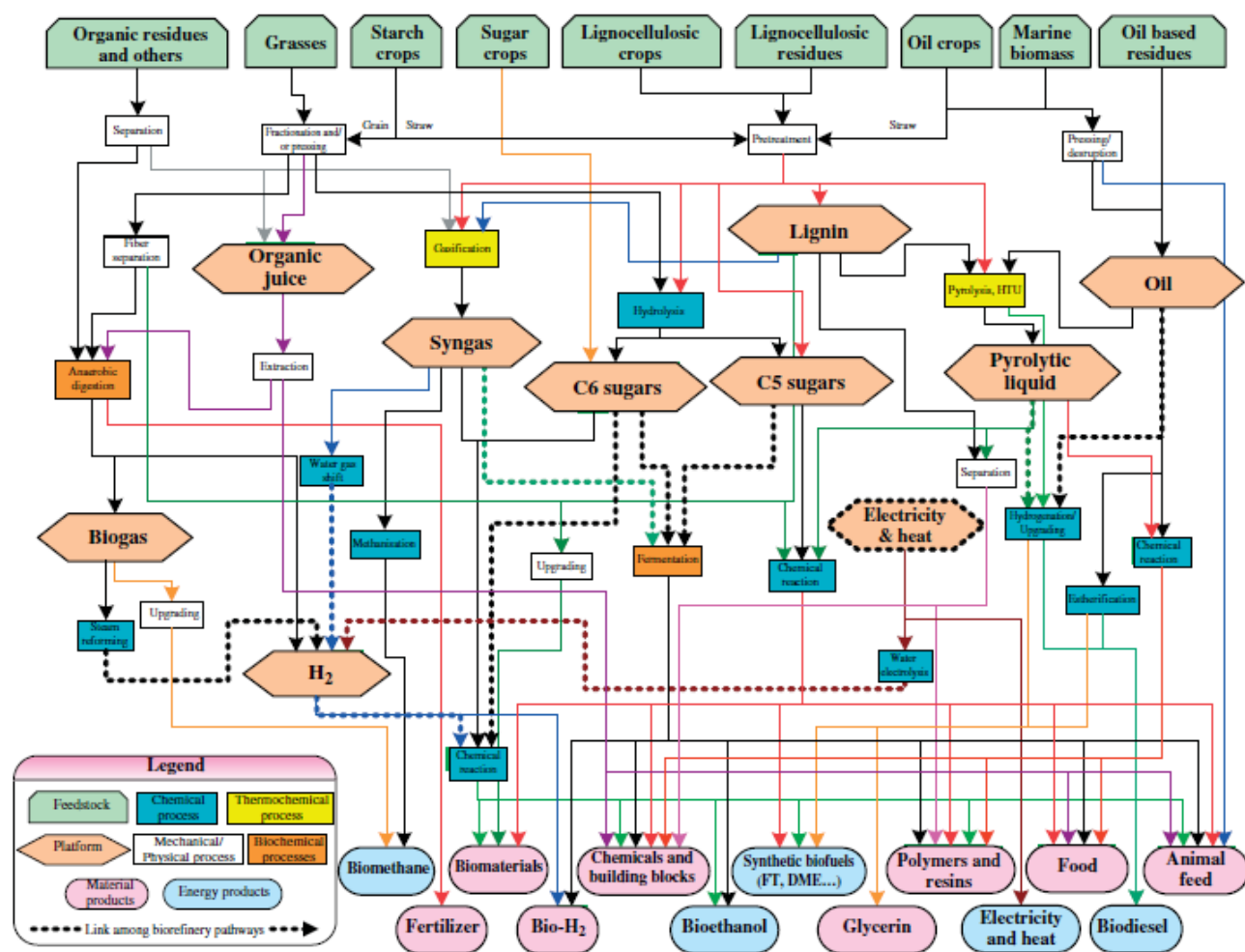


**Figure 1.23:** Biorefinery network where the individual biorefinery systems are combined. Dotted lines represents the link between different biorefineries (Ashok Pandey, 2015).

### 1.4.2 Industrial-scale bioprocesses

In this section are briefly reviewed the most consolidated biorefinery processes currently on industrial scale.

#### ALGAE BIOREFINERY

Macro and micro algae are cultivated since XVIII century in China, Japan and Mexico for food purposes (Milledge JJ., 2011). In the early 1950s, as a result of searching for new fuels and food alternative to address increase in world population, research on algae was broadly initiated, mostly with *Chlorella vulgaris* and *Arthrospira platensis* as microalgae. More recently, also cyanobacteria,

like *Scenedesmus* and *Pediastrum* genre are cultivated for their CO<sub>2</sub> fixation pathway (Ashok Pandey, 2015). Besides their conventional applications (food in particularly for Asian cousin and Agar production), algae are used for the production of polyunsaturated fatty acids (PUFAs) like ω-3 fatty acid, or a broad spectrum of compound used in cosmetic and medical sector (e.g. squalene) and different types of pigment (e.g. carotenoids) used as colorant in food industries. A lot of company are currently producing these products like Martek in U.S.A for PUFAs or BASF regarding the pigment productions (Milledge JJ., 2011), (C. Curtain, 2000).

Nowadays, the most promising biorefinery application of algae biomass is the exploitation of algal oil for the production of FAMES (fatty acid methyl esters) like biodiesel, an alternative to conventional fuels. Algal oils are composed of saturated and unsaturated fatty acids with 12–22 carbon atoms with chain lengths and degree of unsaturation depending on species (Tornabene TG, Benemann JR, 1985). Synthesis of FAME is performed by transesterification of algal oil and a short chain alcohol (usually methanol) in the presence of a catalyst (usually KOH or NaOH).

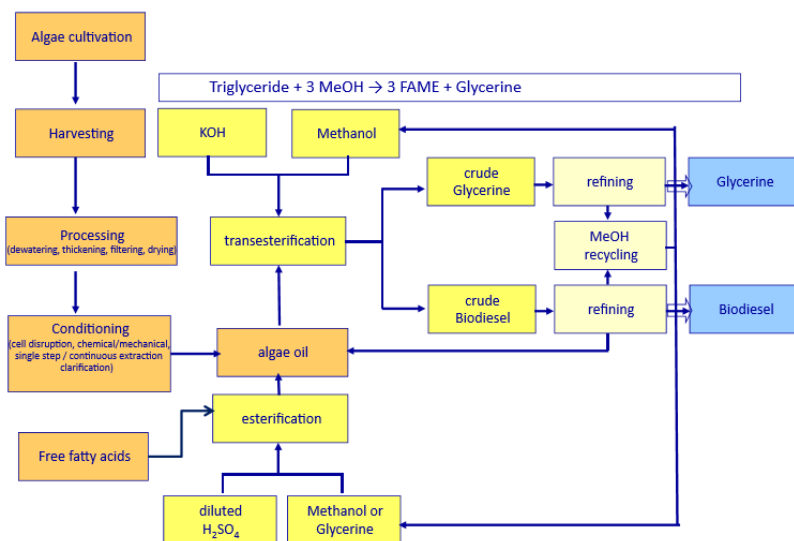


**Figure 1.24:** Algal biodiesel pathway (Höfer R, Bigorra J., 2008).

In this process methanol is continuously recycled and crude glycerine (remained from transesterification reaction) is further processed and refined for the production of glycerine, to make soap, for example. A lot of companies, (e.g. Solazyme) adopted this process using metabolic tools to

engineering microalgae strains to develop a cost-effective and sustainable algal oil production to boost biodiesel production.

### PULP MILLS BIOREFINERY

In the paper production via “Kraft” process a lot of residues are produced. Thus, a modern pulp mill that is capable of green manufacturing of this by-product can be considered as a rather sophisticated biorefinery (Alén R, 2011). In the first part of the process, small diameters wood chips are produced. In this phase, bark residues are formed, and a lot of process can be made to valorize this lignocellulosic by-product, as described in the “lignocellulosic biorefinery” section. Then, the chips are pre-heated with steam and treated with a strong alkaline solution (sodium hydroxide and sodium sulphide, generally) in the first stage of Kraft process, to extract pulp fibers (pure cellulose fibers) from wood, removing lignin. This phase produces a mixture of compounds called “black liquor”, formed by aqueous solution of lignin, hemicellulose and chemical sulphite-rich compounds. After that, the pulp mill is further washed, bleached and processed to obtain fine paper (Biermann, Christopher J, 1993). Approximately 7 tons of black liquor are produced in the manufacture of one ton of pulp, so this represents the major waste of the whole Kraft process, together with the bark in the pre-treatment stage. Until now the black liquor was burned to obtain steam and energy for the process itself (Benefits of Black Liquor Gasification, 2003). The biorefinery ideas is clearly expressed in figure 1.25:

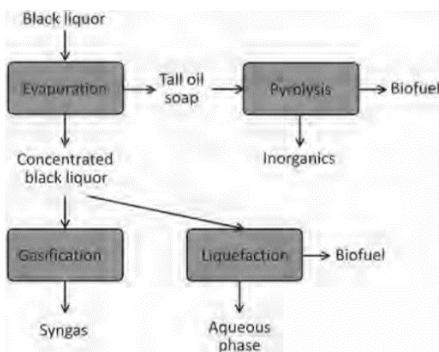


**Figure 1.25:** Biorefinery possibilities of black liquor residues in Kraft process (Ashok Pandey, 2015).

The black liquor can be evaporated, obtaining a solid mixture of tall oil and turpentine used in ink, soap and perfume industries (Ghezzaz H, 2012). This vegetable oils can be also fast pyrolyzed and used for the production of new generation biofuels (mainly biodiesel) (Arpiainen V., 2001). Moreover, the concentrated black liquor can be directly gasified to obtain syngas for further fermentation or energy production, or liquefied to obtain pure lignin and short chain carboxylates. The lignin can be used (together with bark residues in a lignocellulosic biorefinery), and short chain carboxylates can be the intermediate for biofuel production by fermentation processes. A black liquor gasification technology is currently under operation in a 3 MW pilot plant at Chemrec's test facility in Piteå, (Sweden) (Alén R, 2011).

#### LIGNOCELLULOSIC AND SUGAR/STARCH BASED BIOREFINERIES

These biorefineries are strictly linked together, and a lot of processes are dependent by each other. In the lignocellulosic biorefinery, woody-based energy crops residues are cleaned, pre-treated (to improve accessibility of sugars for subsequent processing) and then broken down into its primary constituents (cellulose, hemicellulose and lignin) through biochemical or chemical routes.

Cellulose and hemicellulose can be converted in sugar monomers (C5/C6 based) and further fermented in the sugar/starch biorefinery in a lot of different marketable compounds, instead lignin (due to its tightly composition) is combusted, gasified or pyrolyzed to obtain syngas and energy. More recently, lot of literature studies are made on the valorization of lignin residues, because this is a key-issue for an economically viable lignocellulosic biorefinery (Jyri-Pekka Mikkola, 2010). An example is the biotechnological route to depolymerize the lignin polymer in ferulic acid for the production of vanillin (B Bartolome, 1997).

In figure 1.26 it's clear the correlation between these two biorefinery approaches. In the first part, the lignocellulosic biorefinery provides the conversion of the wood residues in cellulose, hemicellulose and lignin, with the further conversion of lignin in heat, building block (e.g. ferulic acid) or syngas. The second part represents the sugar/starch biorefinery where cellulose and hemicellulose are transformed via fermentation in a plethora of different compounds.



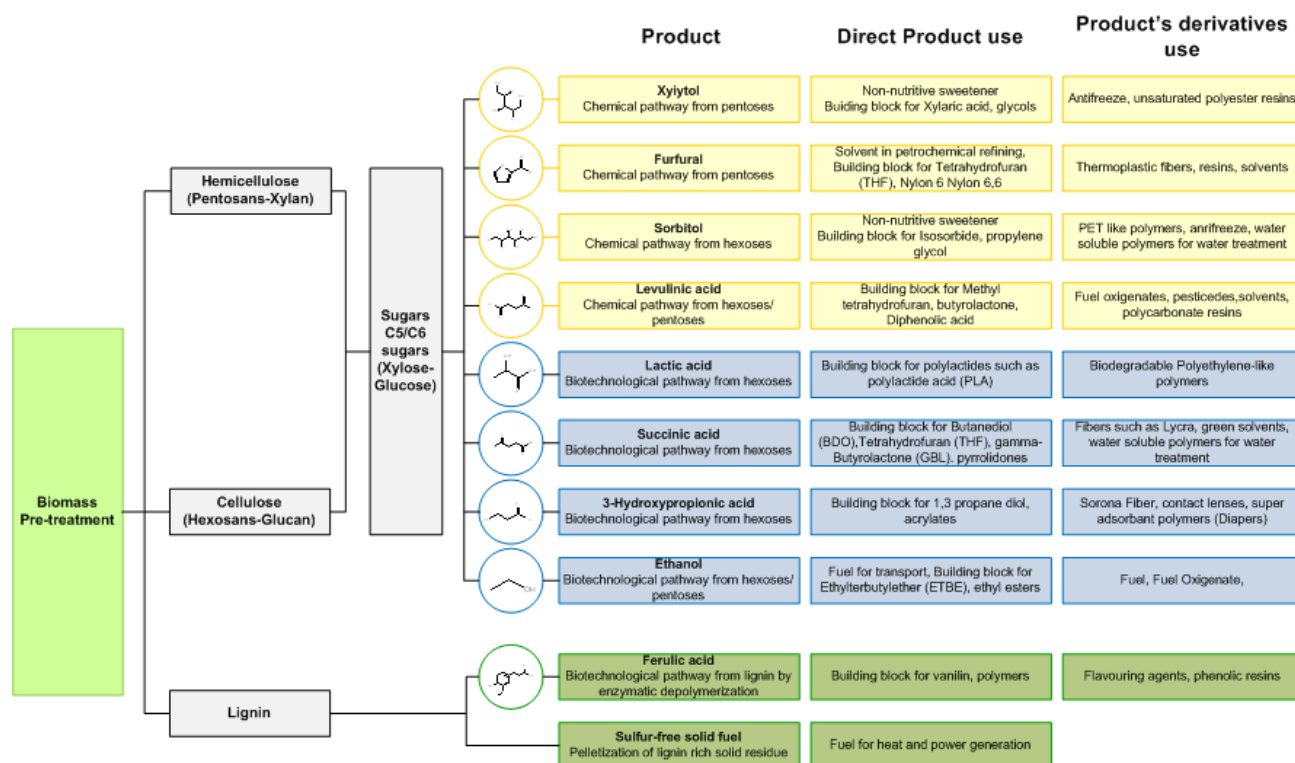


**Figure 1.26:** Integration between lignocellulosic and sugar/starch biorefineries (Alén R, 2011).

A lot of wood based crops like wheat straw, rice straw, rice hulls, nut hulls, barley straw, olive stones and wood residues (e.g. bark residues for the pulp mill industries) can enter in these integrated biorefinery. As demonstrated in the previous figure, a lot of compound can be produced via sugar/starch biorefinery, mainly with fermentation processes.

## OIL BIOREFINERY

In the field of the production of vegetable oils for human feed but also for cosmetic and detergents, industries are starting their transition in order to increase its contribution to the bio-based economy. Vegetable oils, in fact, are mainly extracted from soybeans, the palm fruit (pulp oil and palm kernel oil), rapeseed, sunflower, cottonseed, groundnuts, coconuts, olives, flax, and castor seed (Hill K, 2009). Those crops are rich in different types of fatty acids, saturated (e.g. myristic, palmitic, stearic), monounsaturated (palmitoleic, oleic), and also polyunsaturated (omega 3 in particularly). Based on

the reactions occurred on the carboxy – group, or on the fatty chain, figure 1.27 shows a large number of compounds and further modification of triglycerides biorefinery.

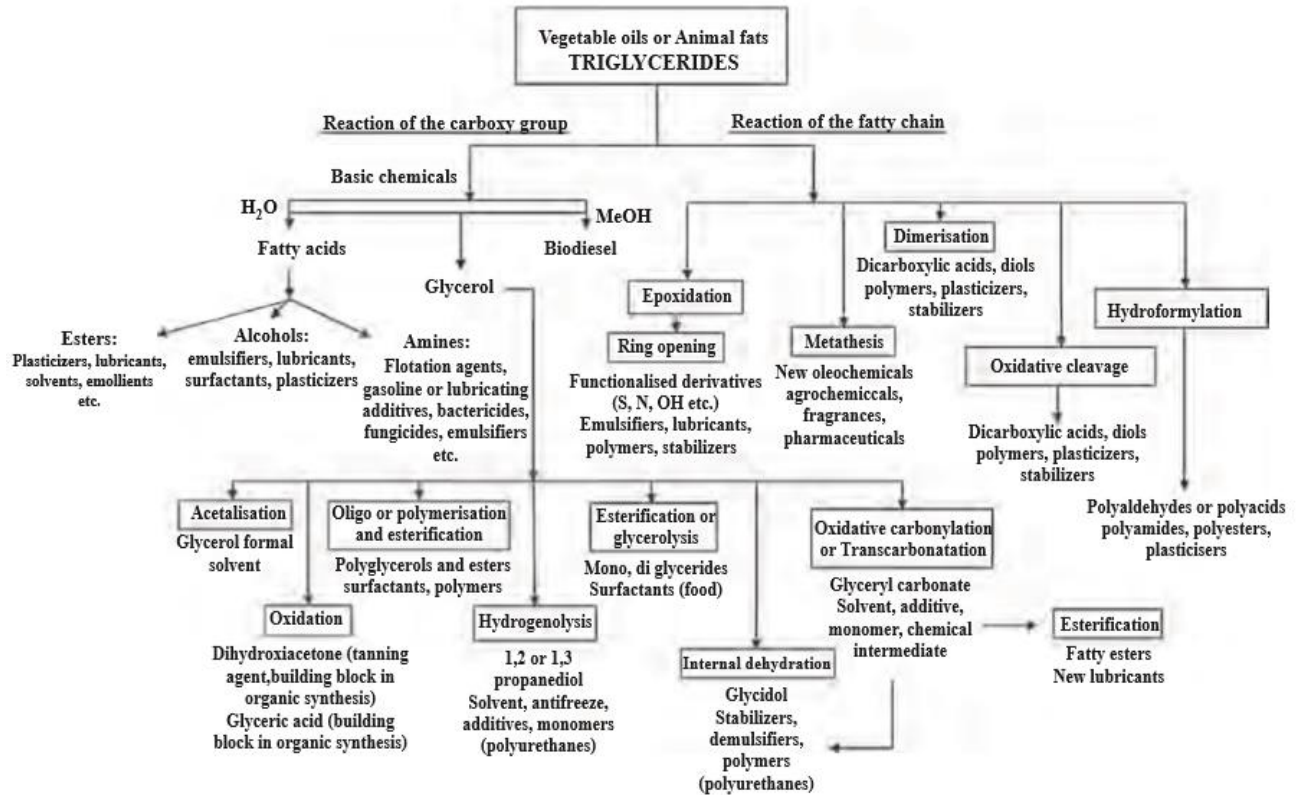
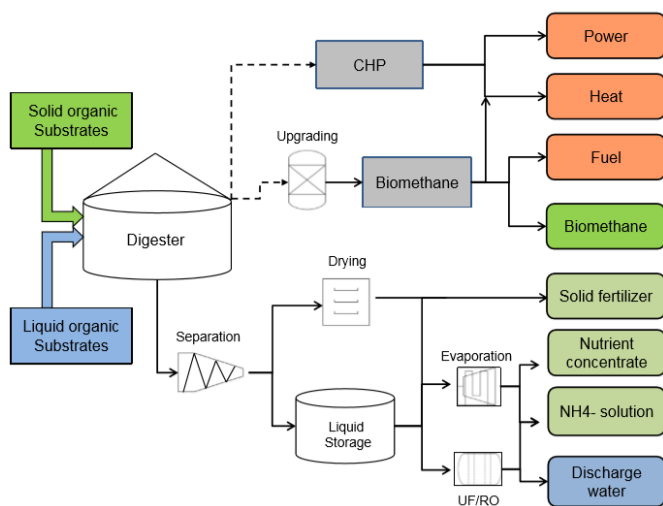


Figure 1.27: Oilseed biorefinery (Corma A, 2007)

It's important to highlights that, triglycerides can be converted to biodiesel (like in algae biorefinery), but also hydrolyzed in simple fatty acids and glycerol. Fatty acids can be transformed via thermochemical routes in esters and alcohols for the production of plasticizers, lubricants or solvents. Glycerol instead can be used as a building block in both biochemical process both in thermochemical way. Biotechnological routes (in yeast for example) can provide a green pathway for the production of citric acid (Priscilla F. Fonseca Amaral, 2009), instead thermochemical-catalyzed reaction can produce alcohol or other building blocks like 1,2 or 1,3 propanediol (Zhenle Yuana, 2010). Moreover, the lignocellulosic parts of oilseed crops can be integrated in the lignocellulosic – sugar/starch biorefinery.

## BIOGAS BIOREFINERY

Anaerobic digestion is a process where different types of substrate are subsequently converted in biogas, in different reaction steps catalyzed by different types of microorganism. Biogas is defined as a mixture of CH<sub>4</sub> (50%-75%) and CO<sub>2</sub> (50% - 25%) plus trace compounds as nitrogen, ammonia and hydrogen sulphite (Ashok Pandey, 2015). Because also anaerobic digestion for biomethane production will be a masterpiece of this dissertation, here are proposed only the principal biorefinery approaches excluding methanogenic process. In figure 1.28 is represented a simple biogas biorefinery.



**Figure 1.28:** Simple biogas biorefinery concept (Ashok Pandey, 2015)

After the conversion of different types of waste, like agro-food wastes or Organic Fraction of Municipal Solid Waste (OFMSW), the biogas predicted can be upgraded to biomethane for fuel or grid applications, or sent with a pipeline to a CHP process (Co-generation heat and power). This approach is extensively followed in Germany and Sweden where are present 208 of the 282 plants presents in Europe in 2013 (European Biogas Association, 2013). Methane is also considered an important platform in chemical industries. In table 1.4, are reported the compounds derived from the chemical treatment of methane.

Carbon disulfide:	$\text{CH}_4 + 4\text{S} \rightarrow \text{CS}_2 + 2\text{H}_2\text{S}$	(AlO <sub>2</sub> catalyst 700 °C)
Hydrocyanic acid:	$2\text{CH}_4 + 2\text{NH}_3 + 3\text{O}_2 \rightarrow 2\text{HCN} + 6\text{H}_2\text{O}$	(Platinum catalyst)
Dichloromethane:	$\text{CH}_4 + 2\text{Cl}_2 \rightarrow \text{CH}_2\text{Cl}_2 + 2\text{HCl}$	(Ultraviolet)
Ethyne:	$2\text{CH}_4 \rightarrow \text{C}_2\text{H}_2 + 3\text{H}_2$	(Vapor, 1400 °C)
Synthesis gas:	$\text{CH}_4 + \text{H}_2\text{O} \rightarrow \text{CO} + 3\text{H}_2$	(Steam reforming)

**Table 1.4:** Methane as a chemical building block (Ashok Pandey, 2015)

Most of these applications are still at laboratory scale, but a lot of peer reviewed papers are present in literature (Guo, 2014), (Dufour, 2015), (Conrado, 2014).

After the biomethane production, the main by-product is formed by a solid digestate. Due to its richness in P-N-K-S-Mg-Ca based micro and macronutrients, is commonly used as fertilizer. Sometimes it is necessary an upgrade of the digestate for fertilizing purpose, depending on specific national law. Moreover, the liquid fraction from the digestate can be separated, obtaining a concentrate liquid solution.

#### *1.4.3 Funding opportunity*

Synergy between academic research, big industrial company, broad communication and education programs is an essential parameter to build up an efficient green-oriented society. Thus, several projects have been funded by the European Commission under the last two framework programs and, in the near future, continuous support (€ 80 billion between 2014 and 2020) is foreseen in the frame of Horizon 2020 calls. In particular, the bio-based industries consortium received €975 million from Horizon 2020 funds, and €2.7 billion of private investments (Ana R.C. Morais, 2013). Ten biorefinery-based projects (“Biomass Energy Europe”, “Sustoil”, “Star-COLIBRI”, “Biocore”, “EuroBioRef”, and so on) are already ongoing with a total of €50 million from Horizon 2020, and a further € 28 million from the industry corporations (European Commission report, 2015).

## 1.5 LIGNOCELLULOSIC BIOMASS: FROM WASTE TO BIOCHEMICAL CONVERSION

Utilization of lignocellulosic biomass for the production of biofuel and bio-based chemicals has many advantage in terms of social and environmental concerns. Using a waste, there is no competition with food-related crops, and moreover, lignocellulosic ethanol generates 91% less GHG than fossil based petrol or diesel in transport applications (Vishnu Menon, 2012). A deep inside into lignocellulosic composition, and utilization in lignocellulosic - sugar/starch biorefinery are considered in this section.

### *1.5.1 Composition*

It was estimated that  $3.7 \times 10^9$  of agricultural residues is produced annually as by-products by agricultural industries worldwide (N.S. Bentsen, 2014). Those residues are composed by cellulose, (35%-45%), hemicellulose (25%-35%), lignin (20%-30%), mineral and various proteins (10%) (D. Pleissner, 2014). Based on raw estimation, it was calculated that  $1376 \times 10^6$  tons of cellulose,  $848 \times 10^6$  tons of hemicellulose and  $688 \times 10^6$  tons of lignin are produced worldwide (Daniel Pleissner, 2015). In table 1.5 is reported the composition of the principal lignocellulosic feedstocks, and in figure 1.29, are shows the principal components of lignocellulose.

Feedstocks	Carbohydrate composition (% dry wt)		
	Cellulose	Hemicellulose	Lignin
Barley hull	34	36	19
Barley straw	36–43	24–33	6.3–9.8
Bamboo	49–50	18–20	23
Banana waste	13	15	14
Corn cob	32.3–45.6	39.8	6.7–13.9
Corn stover	35.1–39.5	20.7–24.6	11.0–19.1
Cotton	85–95	5–15	0
Cotton stalk	31	11	30
Coffee pulp	33.7–36.9	44.2–47.5	15.6–19.1
Douglas fir	35–48	20–22	15–21
Eucalyptus	45–51	11–18	29
Hardwood stems	40–55	24–40	18–25
Rice straw	29.2–34.7	23–25.9	17–19
Rice husk	28.7–35.6	11.96–29.3	15.4–20
Wheat straw	35–39	22–30	12–16
Wheat bran	10.5–14.8	35.5–39.2	8.3–12.5
Grasses	25–40	25–50	10–30
Newspaper	40–55	24–39	18–30
Sugarcane bagasse	25–45	28–32	15–25
Sugarcane tops	35	32	14
Pine	42–49	13–25	23–29
Poplar wood	45–51	25–28	10–21
Olive tree biomass	25.2	15.8	19.1
Jute fibres	45–53	18–21	21–26
Switchgrass	35–40	25–30	15–20
Grasses	25–40	25–50	10–30
Winter rye	29–30	22–26	16.1
Oilseed rape	27.3	20.5	14.2
Softwood stem	45–50	24–40	18–25
Oat straw	31–35	20–26	10–15
Nut shells	25–30	22–28	30–40
Sorghum straw	32–35	24–27	15–21
Tamarind kernel powder	10–15	55–65	—
Water hyacinth	18.2–22.1	48.7–50.1	3.5–5.4

**Table 1.5:** Composition of the major representative lignocellulosic feedstocks (Vishnu Menon, 2012)

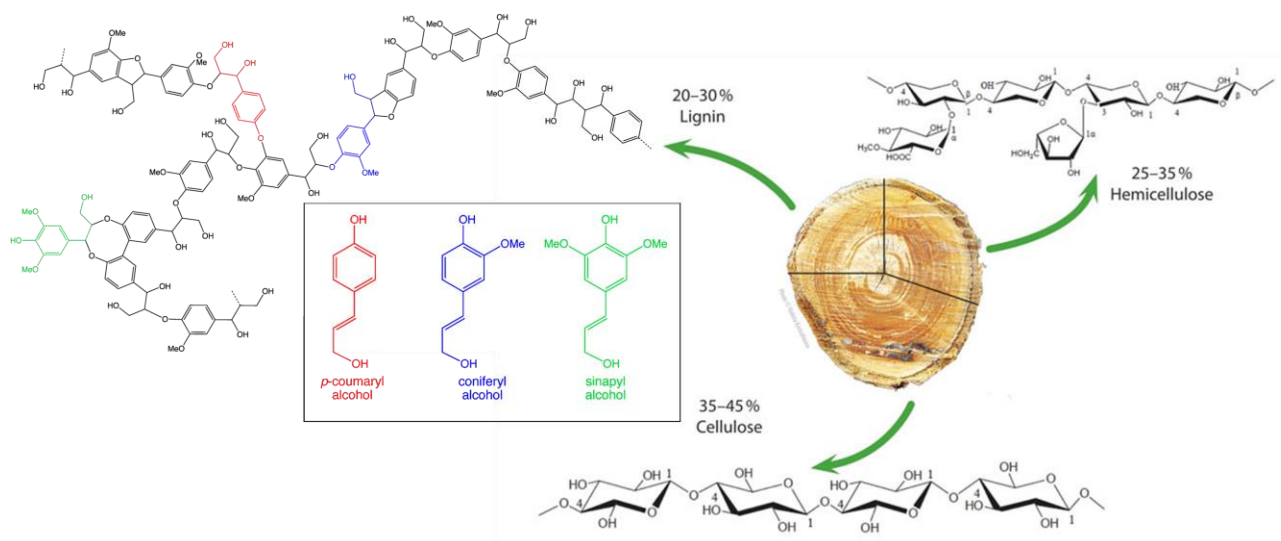


**Figure 1.29:** Structure of lignocellulose

Cellulose ( $C_6H_{10}O_5$ )<sub>n</sub> is a linear syndiotactic (alternating spatial arrangement of the side chains) polymer of glucose linked together by  $\beta$ -(1 / 4)-glycosidic bonds whereas hemicellulose ( $C_5H_8O_5$ )<sub>m</sub> is a branched heteropolymer of D-xylose, L-arabinose, D-mannose, D-glucose, D-galactose and D-glucuronic acid. Lignin is composed of three major phenolic components, namely p-coumaryl alcohol, coniferyl alcohol and sinapyl alcohol. The polymerization of these components and their ratio varies between different plants, wood tissues and cell wall layers (Vishnu Menon, 2012). The result is a strongly compacted network of long chain aromatic compounds.

These three components are interconnected by each other. Cellulose monomers are packed into a crystalline microfibrils, stabilized by hydrogen bonds. These microfibrils are further attached to each other by hemicelluloses and amorphous polymers of different sugars as well as other polymers such as pectin. All of this 3D structure is surrounded, protected and covered by lignin.

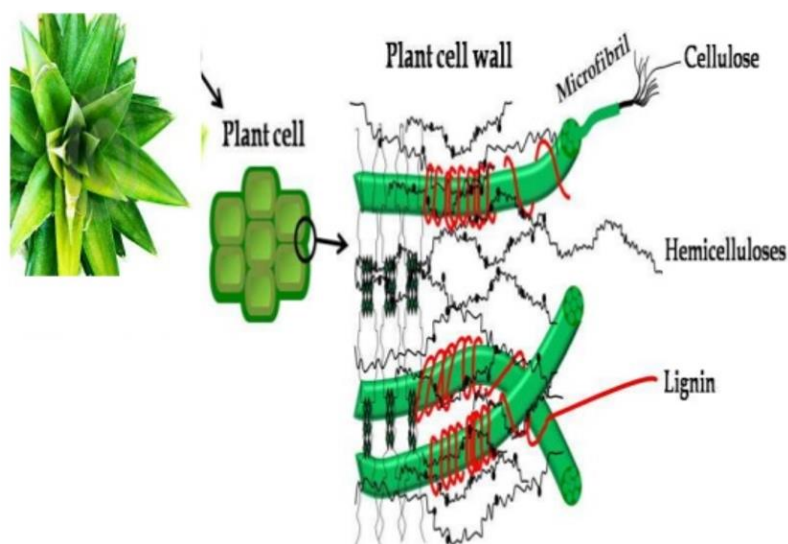


**Figure 10:** 3D structure of lignocellulosic biomass

This macrostructure is highly tightened, and the results is that not only big molecules (like enzymes), but also small components like single water molecules cannot enter in the network, making lignocellulose highly insoluble. Anyway, not all the parts of the microfibrils are compacted in the same way. Depending on the plant structure, some parts are less ordered, and the package of cellulose is not completely crystalline. This lead to an amorphous region in the plant cell wall (Arantes V, 2010). From this point of view is possible to estimate the crystallization index and the degree of

polymerization (DP). Biomasses with low DP and low crystallinity are more susceptible to cellulolytic enzymes, for the release of sugar monomers (Hallac BB, 2011). Is evident than a crucial step for the production of biofuel and bio-based chemicals using lignocellulosic and sugar/starch biorefinery, is the pretreatment of lignocellulose structure.

### 1.5.2 Pretreatments

Choosing the best pretreatment for lignocellulosic biomass in order to release the simple sugars, and enhance biodigestibility, is fundamental. It's important to say that doesn't exist a unique pretreatment for all lignocellulosic biomass. The choice of the right one must consider a lot of aspects, including compatibility with feedstocks, enzymes, and microorganism. Moreover, needs to be evaluated the cost impact itself, and in relationship to the other biorefinery stages. For example, the possibility and the price of eventually steam generation, the handling of liquid chemical residues and solid wastes, or the production and the possible re-utilization of by-products. Table 1.6 illustrates some of the most promising and used pre-treatment categories prevalently used for biofuel and bio-based products.

Method of pre-treatment	Sugar yield	Inhibitor formation	Byproduct generation	Reuse of chemicals	Applicability to different feedstock's	Equipment cost	Success at pilot scale	Advantages	Limitations & disadvantages
Mechanical	L	Nil	No	No	Yes	H	Yes	Reduce cellulose crystallinity	High Power consumption than inherent biomass energy
Mineral acids	H	H	H	Yes	Yes	H	Yes	Hydrolysis of cellulose and hemicellulose, alters lignin structure	Hazardous, toxic and corrosive
Alkali	H	L	H	Yes	Yes	Nil	Yes	Removal of lignin and hemicellulose, increases accessible surface area	Long residence time, irrecoverable salts formed
Liquid hot water	H	H	L	No	—	—	Yes	Removal of hemicellulose making enzymes accessible to cellulose	Long residence time, less lignin removal
Organosolv	H	H	H	Yes	Yes	H	Yes	Hydrolyze lignin and hemicellulose	Solvents needs to drained, evaporated, condensed and reused
Wet oxidation	H or L	Nil	L	No	—	H	—	Removal of lignin, dissolves hemicellulose and causes cellulose decrystallization	—
Ozonolysis	H	L	H	No	—	H	No	Reduces lignin content, no toxic residues	Large amount of ozone required
CO <sub>2</sub> explosion	H	L	L	No	—	H	—	Hemicellulose removal, cellulose decrystallization, cost-effective	Does not modify lignin
Steam explosion	H	H	L	—	Yes	H	Yes	Hemicellulose removal and alteration in lignin structure	Incomplete destruction of lignin—carbohydrate matrix
AFXE	H	L	—	Yes	—	H	—	Removal of lignin and hemicellulose	Not efficient for biomass with high lignin content
Ionic liquids	H/L	L	—	Yes	Yes	—	—	Dissolution of cellulose, increased amenability to cellulase	Still in initial stages

H:- High and L:- Low.

**Table 1.6:** Characteristic of the most common pre-treatments used for biofuel and bio-based production (Vishnu Menon, 2012)



Theoretically speaking, an effective pretreatment must have several features: avoiding size reduction, preserving hemicellulose fractions, limiting formation of inhibitors due to degradation products, minimizing energy input, and being cost-effective. Except for these criteria, several other factors are also needed to be considered, including recovery of high value added co-products (e.g., lignin and proteins), pretreatment catalyst, catalyst recycling, and waste treatment (Banerjee S, 2010).

Pretreatments can be divided into 4 big categories: physical, physico-chemical, chemical and biological pretreatments.

- Physical pretreatments:

Milling, irradiation with different types of rays (like gamma ray, electron beam or microwave radiations) or extrusion, requires higher energy consumption, and are not used in fully industrial scale. Anyway, when are the only applicable methods, they improve hydrolysis and biodegradability of lignocellulosic biomasses reducing particle size and crystallinity of cellulose (Vishnu Menon, 2012).

- Physico-chemical pretreatments:

They combine both physical and chemical techniques. The most used are steam explosion, AFEX (ammonia fiber explosion), liquid hot water (LHW) and microwave-chemical pretreatment. In *steam explosion* process, the raw biomass is treated at 160 – 260 °C with high pressure (until 4.83 MPa), for several seconds or minutes before reducing the pressure to atmospheric value. This lead to an explosive decompression with hemicellulose breakdown and lignin chemical transformation due to high temperature (Varga E, 2004). This is a consolidated industrial pre-treatment and is commonly used to improve biogas production from different type of biomass, like activated sludge (Ward A, 1998), cattle manure (Bougrier C D. J., 2007) or MSW (Mladenovska Z, 2006).

*AFEX – Ammonia Fiber Explosion*, is a pre-treatment where biomass is exposed to an ammonia solution (1 – 2 Kg/Kg dry biomass) at high temperature (90 °C) for several minutes. Temperature can be increased until 150 °C – 170 °C, with lower residence time, depending from biomass types. This process is commonly used with herbaceous crops and grasses, and leads to a decrystallization of cellulose, partial depolymerisation of hemicellulose, removal of acetyl groups predominantly on hemicellulose, cleavage of lignin carbohydrate complex linkages, lignin C-O-C bond cleavage,

increase in accessible surface area due to structural disruption, and increased wettability of the treated biomass (Gollapalli LE, 2002). Moreover, the ammonia solution can be isolated and recycled.

In *LHW – liquid hot water pretreatment*, high pressure is used to maintain water at liquid state at high temperature. Pressure and temperature values can be highly different depending on the percentage of lignin in the raw biomass. The main advantage of this process is the complete compatibility with the subsequent stages, because no toxic or inhibiting by-products are formed (Yu G, 2010), (Kobayashi N, 2009), (Ingram T, 2009).

Microwave – chemical treatment involves the utilization of different chemical compounds like acids, alkali,  $H_2O_2$  in combination with microwave to depolymerize the lignocellulosic biomass. Is an inexpensive pretreatment but usually are necessary more cycle with different chemical combination to obtain a good result (Zhu S, 2006).

- Chemical pretreatments:

*Acid pretreatments* are commonly used in the depolymerisation of hemicellulose. Usually  $H_2SO_4$  (0.2% – 2.5% w/w) is used in combination of continuous stirring and high temperature (130 °C – 210 °C) for a wide variety of biomass, e.g. switchgrass (Digman MF, 2010) and corn stover (Xu J, 2009). Sometimes, also other acids like HCl,  $HNO_3$ , or  $H_3PO_4$  can be used in alternative of sulphuric acid (Vishnu Menon, 2012).

*Alkaline pretreatments* are usually based on  $NH_4OH$  solution for the decomposition of high-lignin content biomasses. This leads to the degradation of ester and glycosidic side chain of lignin polymer together with cellulose swelling and decrystallization (Cheng YS, 2010). This is the most effective pretreatment for lignin depolymerisation, but a neutralizing step is necessary before further biomass conversion. Inhibitory compounds like furfural, aldehydes or phenolic salts are produced during the soaking of biomass (Vishnu Menon, 2012).

*Ionic liquids* are a new class of solvent entirely constituted by ionic species. They are salt characterized by low degree of symmetry, and for this reason are liquid at atmosphere conditions (Earle MJ, 2000). They are often used as a greener solvent in pharmaceutical and chemical industries but very recently they have been confirmed to be efficient for dissolution of lignocellulosic materials. Despite the large

number of peer-reviewed articles present in literature regarding this aspect (Liu LY, 2006), (Diego AF, 2007), (Zhao H, 2009), (Li Q, 2009), a lot of key points needs to be evaluated. For example, is necessary to verify the biocompatibility with the further biochemical transformation, all the toxicological aspects and a detailed knowledge regarding physico-chemical action mode on cellulose, hemicellulose and lignin (Vishnu Menon, 2012).

- Biological pretreatments:

They are based on the biologically modification of lignocellulosic biomasses made by the action of microorganism. In particularly, fungi are commonly used due to their deep degrading activity. Brown and soft rots mainly attack cellulose while imparting minor modifications to lignin, but white-rot fungi are more actively in degrading the lignin component (Sun Ye, 2002). They have main advantages like mild conditions, low energy input and no chemical requirements. Anyway their action is very slow, and a careful growth control is needed. Moreover, they can consume also hemicellulose and cellulose for growth, inhibiting the entire conversion process.

### *1.5.3 Biocatalytic valorization*

The treated biomass needs to be further valorized releasing the sugar monomers. In this paragraph will be considered only enzymatical process for the hydrolysis of hemicellulose and cellulose. As reported before (chapter 1.4.2) lignin continues along lignocellulose biorefinery and can be combusted for energy purpose or, more recently, converted to some building blocks both in thermochemical way (i.e. syngas production for further refinement as synthetic biofuels) both using biochemical routes (i.e. biological treatment for ferulic acid release used in vanillin bioproduction). As reported before, cellulose and hemicellulose needs to be enzymatically hydrolyzed to release fermentable sugars.

#### Cellulase enzymes

Three major type of enzymes are required for cellulose hydrolysis: endoglucanases (EG), exoglucanases (EXG), and  $\beta$  glucosidases (BGL) (Hasunuma T, 2013).

- ✓ Endoglucanase (EC 3.2.1.4) randomly hydrolyze the b-glycoside linkages of internal amorphous regions in cellulose to produce oligosaccharides of various degrees of polymerization and generate new chain ends.
- ✓ Exoglucanase hydrolyze cellulose in a processive manner from the reducing (EC 3.2.1.74 or cellodextrinase) or non-reducing ends (EC 3.2.1.91 or 1,4  $\beta$ - D glucan cellobiohydrolase) of cellulose chains to generate either glucose or cellobiose as major products.
- ✓  $\beta$  glucosidases (EC 3.2.1.21) cleaves soluble cellodextrins and cellobiose into glucose.

The most frequently reported source of cellulase is the fungus *Trichoderma reesei* (Jana SK, 1994), but nowadays a lot of microorganism are used for the production of these enzymes (table 1.7)

Microorganism	Method	Enzyme activities		
		FPase	CMCase	$\beta$ -glucosidase
<i>Acinetobacter anitratus</i>	SmF	ND	0.48 U/ml	ND
<i>Bacillus subtilis</i>	SSF	2.8 IU/gds	9.6 IU/gds	ND
<i>Bacillus pumilus</i>	SmF	ND	1.9 U/ml	ND
<i>Cellulomonas biazotea</i>	SmF	7450 nkat/g	13,933 nkat/g	2850 nkat/g
<i>Clostridium papyrosolvens</i>	SmF	35 IU/ml	45 IU/ml	ND
<i>Chaetomium globosum</i>	SmF	1.4 U/ml	30.4 U/ml	9.8 U/ml
<i>Streptomyces drowdowicz</i>	SmF	4.4 U/gds	595 U/L	ND
<i>Thermomonospora sp</i>	SmF	0.11 IU/ml	23 IU/ml	0.02 IU/ml
<i>Thermoascus auranticus</i>	SSF	4.4 U/gds	987 U/gds	48.8 U/gds
<i>Neurospora crassa</i>	SmF	1.33 U/ml	19.7 U/ml	0.58 U/ml
<i>Thermotoga maritima</i>	SmF	ND	ND	30 mU/ml
<i>Trichoderma reesei</i>	SmF	2.49 IU/ml	7.15 IU/ml	2.17 IU/ml
<i>T. reesei RUT C 30</i>	SmF	6.2 U/ml	54.2 U/ml	0.39 U/ml
<i>T. species A-001</i>	SmF	18 U/ml	167 U/ml	49 U/ml
<i>T. reesei ZU 02</i>	SmF	0.25 IU/ml	5.48 IU/ml	ND
<i>T. viridae</i>	SmF	0.88 U/ml	33.8 U/ml	0.33 U/ml
<i>Penicillium funiculosum</i>	SmF	1.4 IU/ml	4.55 IU/ml	9.29 IU/ml
<i>Penicillium pinnophilum</i>	SmF	2 U/ml	65 U/ml	10 U/ml
<i>P. janthinellum</i>	SmF	0.55 U/ml	21.5 U/ml	2.31 U/ml
<i>P. decumbans</i>	SSF	20.4 IU/g	ND	ND
<i>P. occitanis</i>	SmF-Fed	23 IU/ml	21 IU/ml	ND
<i>A. fumigatus IMI 246651</i>	SmF	40 EU/ml	0.5 EU/ml	1.73 EU/ml
<i>A. terreus</i>	SSF	243 U/g	581 U/g	128 U/g
<i>Fusarium oxysporum</i>	SSF	304 U/g	ND	0.140 U/g

**Table 1.7:** Production of cellulase using microorganism (Vishnu Menon, 2012).

### Hemicellulase enzymes

In the same manner of cellulose, also hemicellulose needs to be hydrolyzed. Based on the amino acid or nucleic acid sequence of their catalytic modules hemicellulases are grossly divided in glycoside hydrolases (GHs), and carbohydrate esterases (CEs) (Vishnu Menon, 2012).

- ✓ Glycoside hydrolases cleaves the glycosidic bonds in the xylan backbone, bringing about a reduction in the degree of polymerization of the substrate. Xylan is not attacked randomly, but

the bonds selected for hydrolysis depend on the nature of the substrate molecule, i.e., on the chain length, the degree of branching, and the presence of substituents (Li KC, 2000).

- ✓ Carbohydrate esterases, instead, are less characterized, and is known that the target of their action is the hydrolysis of the ester linkages of acetate or ferulic acid side groups (Biely P, 2012)

In table 1.8 are reported the most common used producing hemicellulases microorganism.

Enzyme	Organism	Substrate	Specific activity ( $\mu\text{mol min}^{-1} \text{mg}^{-1}$ )
Feruloyl esterase	<i>Clostridium stercoararium</i>	Ethyl ferulate	88
$\beta$ -1,4-xylosidase	<i>Thermoanaerobacter ethanolicus</i>	o-nitrophenyl- $\beta$ -D-xylopyranoside	1073
Exo- $\beta$ -1,4-mannosidase	<i>Pyrococcus furiosus</i>	p-nitrophenyl- $\beta$ -D-galactoside	31.1
Endo- $\beta$ -1,4-mannanase	<i>Bacillus subtilis</i>	Galactoglucomannan/glucomannans/mannan	514
$\alpha$ -L-arabinofuranosidase	<i>Clostridium stercoarium</i>	alkyl- $\alpha$ -arabinofuranoside/aryl- $\alpha$ -arabinofuranoside/ Larabinogalactan/L-arabinoxylan/ methylumbelliferyl- $\alpha$ -L-arabinofuranoside	883
$\alpha$ -Glucuronidase	<i>Thermoanaerobacterium saccharolyticum</i>	4-O-methyl-glucuronosyl-xylotriase	9.6
$\alpha$ -Galactosidase	<i>Escherichia coli</i>	raffinose	27,350
Endo-galactanase	<i>Bacillus subtilis</i>	arabinogalactan	1790
$\beta$ -Glucosidase	<i>Bacillus polymyxa</i>	4-nitrophenyl- $\beta$ -D-glucopyranoside	2417
Acetyl xylan esterase	<i>Fibrobacter succinogenes</i>	Acetylxylan/ $\alpha$ -naphthyl acetate	2933
Feruloyl esterase	<i>Aspergillus niger</i>	Methyl sinapinate	156
Endo-1,4- $\beta$ -xylanase	<i>Trichoderma longibrachiatum</i>	1,4- $\beta$ -D-xylan	6630
$\beta$ -1,4-xylosidase	<i>Aspergillus nidulans</i>	p-nitrophenyl- $\beta$ -D-xylopyranoside	107.1
Exo- $\beta$ -1,4-mannosidase	<i>A. niger</i>	$\beta$ -D-Man-(1-4)- $\beta$ -D-GlcNAc-(1-4)- $\beta$ -DGlcNAc-Asn-Lys	188
Endo- $\beta$ -1,4-mannanase	<i>Sclerotium rolfsii</i>	Galactoglucomannan/mannans galactomannans/ glucomannans/	380
Endo- $\alpha$ -1,5-arabinanase	<i>A. niger</i>	1,5- $\alpha$ -L-arabinan	90.2
$\alpha$ -L-arabinofuranosidase	<i>A. niger</i>	1,5- $\alpha$ -L-arabinofuranohexaose/1,5- $\alpha$ -L-arabinotriose/ 1,5-L-arabinan/ $\alpha$ -L-arabinofuranotriose	396.6
$\alpha$ -Glucuronidase	<i>Phanerochaete chrysosporium</i>	4-O-methyl-glucuronosyl-xylobiose	4.5
$\alpha$ -Galactosidase	<i>Mortierella vinacea</i>	melibiose	2000
Endo-galactanase	<i>A. niger</i>		6593
$\beta$ -glucosidase	<i>Humicola insolvens</i>	(2-hydroxy methylphenyl)- $\beta$ -Dglucopyranoside	266.9
Acetyl xylan esterase	<i>Schizophyllum commune</i>	4-methylumbelliferyl acetate/4-nitro phenyl acetate	227

**Table 1.8:**Principal characteristic of hemicellulose enzymes and principal producing microorganisms (Vishnu Menon, 2012)

Usually those enzymes (mainly cellulase) are produced in a bigger multi-enzymatic complex, called cellulosome. In this complex, different types of cellulose-degrading enzymes are assembled on the structural scaffold subunits through strong non-covalent protein–protein interactions between the docking modules (dockerin) and complementary modules (cohesins). In addition, scaffold contains a carbohydrate-binding module, which binds the entire enzymatic complex to the cellulose surface (Francisco, 1993). Due to the multiple necessity of different enzyme for a complete saccharification, a lot of protein engineering approaches are applied to obtain high specific enzyme complex with high rate of turnover and thermostability, and low products inhibition, using in particularly *E. coli* strain but also yeast as *Saccharomyces cerevisiae* or different types of *Bacillus* (Maki M, 2009).

## 1.6 BIOCONVERSION INTO BIOFUELS AND BIO-BASED CHEMICALS

After the release of the single sugar molecules, a further step of conversion is needed to obtain marketable products from lignocellulosic biomass. Focusing only on biochemical processing, the single sugar monomers are fermented to a large variety of compounds (see figure 1.26). Those can be divided in biofuel and bio-based chemicals.

### Biofuels

Biofuels are defined by Ludwig Gredmaier in his plenary lecture on “Bioenergy, Biofuels and Energy-from-waste” (Gredmaier, 2013) as a renewable, liquid, but also solid (e.g. wood) or gaseous fuels (e.g. biogas) made from recent, non-fossil biological plant matter (e.g. crops), that can be used in the transport sector but also for domestic and industrial heating. They can be divided into primary and secondary biofuels. Primary biofuels are wood chips or pellets, used in an unprocessed form mainly for heating and cooking. Secondary biofuels are those fuels that are produced by processing of biomass, that can be used in vehicles and various industrial processes. The principal secondary biofuels are bioalcohols (e.g. ethanol primarily derived both from sugar and syngas fermentation), biogas and biodiesel. In Appendix section, (table 7.1) are reported some literature examples with the principal consolidated bioprocess for large-scale ethanol production, whereas table 7.2 reports the most relevant bioconversion of synthesis gases in biomethane, biohydrogen and bioalcohols (including ethanol and butanol). Moreover, these secondary biofuels are categorized in first, second and third generation biofuels depending from the starting biomasses (Sudip Chakraborty, 2012).

- ✓ 1<sup>st</sup> generation biofuels are produced from sugar derived from edible crops. This category includes bioethanol produced from different types of plants (sugarcane in Brazil, corn in U.S.A. oilseed rape in Germany or palm oil in Malaysia), biodiesel from raw vegetable oils or biogas produced from anaerobic digestion of a plethora of green crops.

Those are well established technologies, but provides social concerns like competition with food, land and also water.

- ✓ 2<sup>nd</sup> generation biofuels are produced usually from non-edible crops (e.g. lignocellulosic feedstocks, or MSW).
- ✓ 3<sup>rd</sup> generation biofuels are, at this point, related to the utilization of CO<sub>2</sub> as a feedstock, in particularly as a carbon source.

In table 1.9 are summarized the principal differences in terms of biomass origin between 1<sup>st</sup> and 2<sup>nd</sup> biofuel generation. Note that, until now, 3<sup>rd</sup> generation biofuels are not technically and economically feasible for a large-scale industrial application.

Type of biofuel	1st generation	2nd generation
<b>biodiesel</b>	edible crops, e.g.	nonedible biomass
	soybean, sunflower, palm oil	waste cooking oil
<b>bioethanol</b>	edible crops, e.g.	nonedible biomass (cellulosic ethanol)
	sugar cane, maize, wheat	wood, straw, wastes
<b>biobutanol</b>	edible crops, e.g.	nonedible crops
	sugar cane, maize, wheat	
<b>biogas</b>	edible crops, e.g.	nonedible biomass
	maize, grass, sugar beet	manure, slurry, food waste, sewage
<b>biosyngas</b>	(coal)	municipal waste, waste wood,

**Table 1.9:** (Gredmaier, 2013).

### Bio-Based Chemicals

Bio-based products represent one of the most difficult challenges that our society needs to face. Due to the scientific progress in fermentation technologies and protein engineering, a large number of compounds can be produced (see the network in the Appendix section, figure 7.1). In 2014, the U.S.A. Department of energy (DOE) updates an already but incomplete list where are reported the most 12 representative and interested bio-based products, produced from biomass transformation (U.S. Department of Energy, 2014).

This list is redacted following 9 criteria used for evaluating the bio-based products status and future opportunity (table 1.10).

1. **The compound or technology has received significant attention in the literature.** A high level of reported research identifies both broad technology areas and structures of importance to the biorefinery.
2. **The compound illustrates a broad technology applicable to multiple products.** As in the petrochemical industry, the most valuable technologies are those that can be adapted to the production of several different structures.
3. **The technology provides direct substitutes for existing petrochemicals.** Products recognized by the chemical industry provide a valuable interface with existing infrastructure and utility.
4. **The technology is applicable to high volume products.** Conversion processes leading to high volume functional equivalents or utility within key industrial segments will have particular impact.
5. **A compound exhibits strong potential as a platform.** Compounds that serve as starting materials for the production of derivatives offer important flexibility and breadth to the biorefinery.
6. **Scaleup of the product or a technology to pilot, demo, or full scale is underway.** The impact of a biobased product and the technology for its production is greatly enhanced upon scaleup.
7. **The biobased compound is an existing commercial product, prepared at intermediate or commodity levels.** Research leading to production improvements or new uses for existing biobased chemicals improves their utility.
8. **The compound may serve as a primary building block of the biorefinery.** The petrochemical refinery is built on a small number of initial building blocks: olefins, BTX, methane, CO. Those compounds that are able to serve an analogous role in the biorefinery will be of high importance.
9. **Commercial production of the compound from renewable carbon is well established.** The potential utility of a given compound is improved if its manufacturing process is already recognized within the industry.



Succinic, fumaric and malic acids  
 2,5-Furan dicarboxylic acid  
 3-Hydroxypropionic acid  
 Aspartic acid  
 Glucaric acid  
 Glutamic acid  
 Itaconic acid  
 Levulinic acid  
 3-Hydroxybutyrolactone  
 Glycerol  
 Sorbitol  
 Xylitol/arabinitol

**Table 1.10:** Top 12 bio-based and the criteria used in the evaluation (Joseph J. Bozell, 2010)

This list is not exhaustive (i.e. lactic acid and ethanol are missing due to their well-established technologies), but is comprehensive of the most promising building blocks and bio-based products derived from biomass treatment. It will be impossible and pointless reviewing the principal biochemical pathway for the production of these molecules. For this reason, in Appendix section are reported some tables where are exemplified some industrial-scale processes for building block production, especially from lignocellulosic raw materials (figure 7.2).

There are a lot of industrial consolidated industrial strategies for the production of biofuel and bio-based chemicals (figure 1.31).

- ✓ SHF (separate hydrolysis and fermentation), is a conventional multistage process, where all the phases (pre-treatments, saccharification, C5 – C6 fermentation and recovery) are conducted in different vessels.
- ✓ SSF (simultaneous saccharification and fermentation) process combines hydrolysis and C6 fermentation. The compatibility of these processes in terms of pH, T° and substrate concentration, is the key factors for the success.



- ✓ SSCF (simultaneous saccharification and co-fermentation) process apply the same characteristic of the SSF process, but permits the contemporary C5 and C6 fermentation. This process has been recognized a feasible option in xylose rich material. A lot of engineered – based processes applies this technique.
- ✓ CPB (consolidated bioprocess) is the ultimate objective for an industrial bioprocess. All of the stage are condensed in one single operation, offering lower costs, and higher economically advantages. The key is the developing of the best microorganism. Up to date, only for 1<sup>st</sup> generation ethanol using particularly bacteria belonging to the *Clostridium* genus are reported some industrial examples (see Appendix section, table 7.3) (Vishnu Menon, 2012).

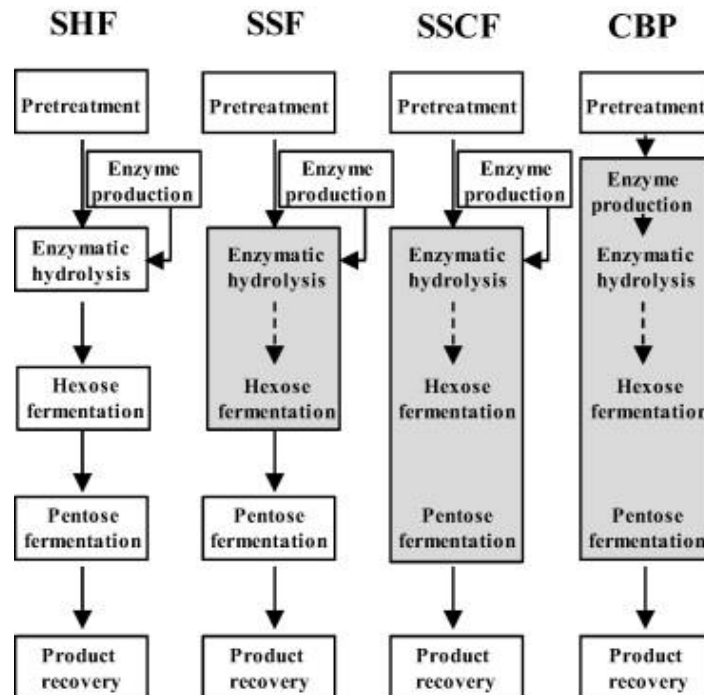


**Figure 11:** Various bioprocessing options available for the conversion of lignocellulosic biomass to useful products. SHF, separate hydrolysis and fermentation; SSF, simultaneous saccharification and fermentation; SSCF, simultaneous saccharification and co-fermentation; CBP, consolidated bioprocessing (Vinusevi Parisuthama, 2014).

## 2 AIM OF THIS WORK

---

The biorefinery concept is based on the valorization of organic carbon molecules from different types of waste, to replace the carbon obtained from fossil fuel. As extensively reported in the introduction section, this process can be the focus point for the instauration of a circular economy model with a deep shift vision toward a recycling-based society.

The final objective is to create a completely sustainable economy fully based on renewable products. The versatility of the biorefinery processes can provide different types of compounds. In particular energy (heat and biofuel), molecules (from building block to fine chemistry), materials (like plastics, solvent and composites), but also food ingredients.

The basic idea of this work was the valorization of different agro-industrial wastes and by-products exploiting different biorefineries approaches and integrate them, where was possible, for the biochemical production of different biofuel and bio-based chemicals. The main focus was, in particular, the development of different fermentation strategies, (i.e. pure culture/mixed consortia, batch/fed-batch/continuous approaches, suspended/biofilm process, single digestion or co-feeding), and the optimization of the most important fermentation parameters. The rationale of the project was the development of a plethora of small-scale tests, where the principal parameters are determined (e.g. production velocity, productivity, yield, kinetic parameters where possible), and the subsequent scale-up in pre-pilot scale, to improve the performances of the process. In addition to this, where was possible, an additional attention to the downstream phase was put. It is affirmed that downstream processes are one of the main bottleneck of biochemical conversion processes (CC Pegels, 2005), (Wingren, 2003). It is also evident that membrane-based systems coupled to emerging technologies for the integration in fermentation plant can provide further solutions to address the problem of the recovery of the interested molecule (Strathmann, 2001). Moreover, where mixed consortia were developed and acclimatized, molecular biology techniques were used for the phylogenetic determination of the microbial population.

Looking into the detail of the different projects, milk whey was used to test bio-hydrogen production using a pure culture of hyperthermophilic pure strain of *Thermotoga neapolitana*. This work was developed in the framework of “Bio-Hydro” project (Biological treatment for hydrogen production using agricultural waste), funded by MiPAAF (Ministry of Agricultural, Food and Forestry Policies). Dark fermentation experiments were developed both in small scale, both in a 19-L SPCSTR (Structured Packing Continuous Stirred Tank Reactor) adapted for suspended and biofilm fermentation. Additional studies for membrane – based gas separation directly coupled to the reactor are conducted, with the objective to increase biohydrogen purity.

Lactose, but also milk whey, was used for the production of succinic acid, one of the Top 12 building block according to the U.S.A. Department Of Energy (DOE). This project was the result of a deep collaboration between my department and the Flemish Instituted For Technological Research (VITO) where I spent 6 months during my PhD, in the framework of the “ReNew” project “Resource Innovation Network for European Waste” supported by Interreg. North West Europe IVB. In this work, both batch, both continuous fermentations were developed in 5-L bioreactor, and a deep focusing on electrodialysis (ED) separation system was posed. The main idea was the developing of an ISPR (In Situ Product Recovery) approach, where the fermenter was directly couple to the ED for succinic acid recovery, without cell retention steps. Moreover, small scale biofilm fermentation tests were performed in order to obtain a deep kinetic characterization of the immobilized process, and a further scale-up in 1-L Plug Flow Reactor was developed.

Biogas biorefinery versatility was also investigated, developing a lot of bio-CH<sub>4</sub> production tests, both in small scale, both in pre-pilot 30-L bioreactor using acclimatized mixed consortia. This work was, instead, developed in collaboration with different private companies. The rationale of this project considers a plethora of different type of raw (mainly lignocellulosic) biomasses (grape pomaces, tomato peels and maize silage), assessing their BMP (Bio-Methane-Potential) in different condition, and conduct long-term anaerobic digestion (AD) experiments, in order to evaluate the yield and the industrial feasibility of the process, combining low-cost pretreatments.

Then, from the main “methane biorefinery”, the main idea was to increase the potential of this biorefinery, using the same consortia for bioalcohol production, n-propanol in particular. In fact, during the acidogenic stage of anaerobic digestion process, a broad spectrum of short chain VFAs (Volatile Fatty Acids) are produced. They can be converted in acetic acid,  $H_2$  and  $CO_2$  and furthermore in biogas, following the “methane” biorefinery in the AD process, but also exploited as a chemical building blocks. Our idea, was to reduce propionic acid (one of the principal VFA together with acetic and butyric acid), in the respective alcohol (n-propanol), using the same consortia, changing only the experimental conditions. As all knows, propanol is one of the best candidate (with butanol) to replace not only fossil fuel for transport utilization, but also bioethanol, due to their higher energy density (Rakopoulos, 2011).

The knowledges gained in this work, could then be used to further implement future research for designing different biorefinery processes, and develop different strategies for the production of biofuels and chemical, using agro-industrial wastes.

In the next section, a brief state-of-the-art of every bioprocess considered in this dissertation, are reported, in order to better understand the results of the described experiment in chapter 4 and 5.

### 3 STATE OF THE ART

---

In this dissertation, biogas (e.g. biohydrogen and biomethane), alcohol fuels (e.g. n – propanol), and building blocks (e.g. succinic acid) are produced following specific fermentation biorefinery strategies, from different agro – industrial raw materials.

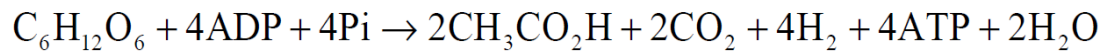
#### 3.1 BIO – HYDROGEN

Hydrogen is the simplest and most abundant element in the universe. Is usually present as biatomic gas ( $H_2$ ) at standard conditions, and due to its stability is poorly reactive in this form. On the earth surfaces, anyway, hydrogen is always present combined to other elements (e.g.  $H_2O$ ), because its biatomic form is 14,4 times higher than air (density  $0.0899\text{ Kg/m}_3$ ), and industrial processes are necessary for its production (Rigden, 2003). Hydrogen is a worldwide-accepted clean energy carrier for its fossil fuel-independent relationship and the high energy content per mass ( $120 - 142\text{ MJ/Kg}$ ) compared to petroleum ( $42,4\text{ MJ/Kg}$ ). Due to these advantages,  $H_2$  can be used as energy sources for different appliances, such for example, as hydrogen fuel cell vehicles (Dutta, 2014).

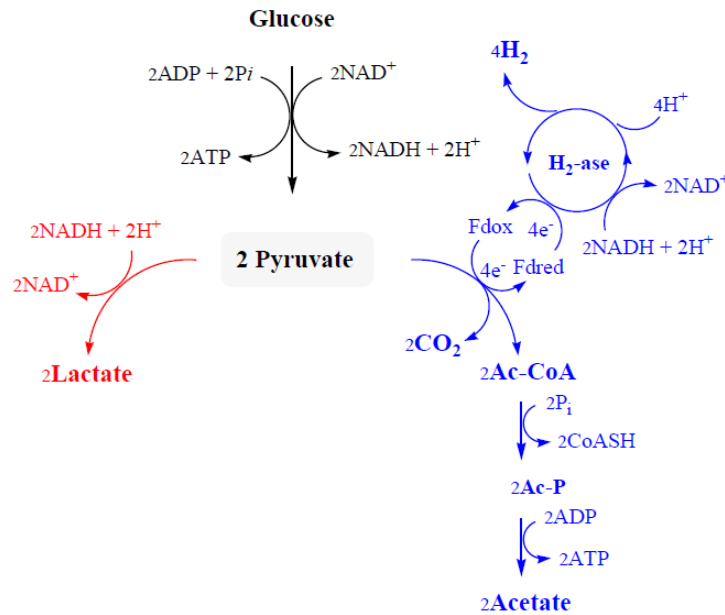
Hydrogen can be produced from a plethora of different technologies (renewables or not), like water electrolysis (Carmo, 2013), photosynthetic green algae production through direct photolysis (Ghirardi ML, 2006), coal gasification or lignocellulosic biomass pyrolysis (Akshat Tanksale, 2010) and high temperature steam reforming of biogas or biofuel, mostly ethanol or methanol (Haryanto, 2005). Recently, numerous biological – based techniques are reviewed in literature, for the production of hydrogen from agro industrial waste or by – products, exploiting two different fermentation processes: Photo – Fermentation and Dark – Fermentation.

Photo – Fermentation process is a biochemical pathway made by purple non-sulfur photosynthetic bacteria as *Rhodopseudomonas palustris*, *Rhodospirillum rubrum*, and *Rhodobacter spheroids*, and involves organic matter and solar light as carbon and electron donor. In this process, captured solar energy is used to produce ATP and high energy electrons (through reverse electron flow) with a reduction of a ferredoxin molecule. ATP and reduced ferredoxin drive proton reduction to hydrogen by an enzymatic complex, called nitrogenase. These organisms cannot derive electrons from water

and therefore use organic compounds, usually small VFAs (derived from sugar or other complex organic matter), as substrates. This process has a huge potential for water treatments for the complete conversion of acid wastes, but has low hydrogen yield and low light conversion efficiency. Moreover, photobioreactor plants have high initial and fixed costs (Hallenbeck, 2009). For this reason, the most used process for  $H_2$  is the dark fermentation process. In this process, a variety of different microbes can be used anaerobically to breakdown carbohydrate-rich substrates with Embden-Meyerhof pathway, to produce 2 pyruvic acids and 2 NADH, 2 ATP and  $2 H^+$  (water is omitted for simplicity) oxidizing 1  $C_6 H_{12} O_6$ . Then, the pyruvate is further converted to Ac-CoA and acetate with the production of 2 additional ATP. In this conversion,  $4 e^-$  are used to reduce ferredoxin molecule driving (together with two NADH molecules) proton reduction to  $H_2$  production, through an enzymatic complex called hydrogenase. The overall reaction is highlighted in figure 3.1 and graphically reproduced in figure 3.2



**Figure 3.1:** Overall reaction of hydrogen formation by *Thermotoga neapolitana* (Nirakar Pradhan, 2015)



**Figure 3.2:**  $H_2$  formation metabolic pathway in *T. neapolitana* (Nirakar Pradhan, 2015)

4 mol of H<sub>2</sub> can be theoretically produced per mole of consumed glucose. This limit represents the maximum theoretical yield of the process, but is evident that anabolic processes and growth necessity of the bacteria strain, limits the yield in a practical process.

The most used and well - characterized bacteria for hydrogen production with dark fermentation, is *Thermotoga neapolitana*, a Gram negative, hyperthermophilic bacteria was originally isolated from shallow submarine hot spring nears Lucrino in the Bay of Naples in 1986, with an optimal growth temperature of 77 °C (Belkin, Wirsén, & Jannasch, 1986), (Jannasch, Huber, Belkin, & Stetter, 1988). The *Thermotogales* order includes an assembly of rod-shaped, non-sporulating bacteria that are characterized by an unconventional outer envelope called the “toga”, which forms a large periplasmic space at the poles of each rod (figure 3.3) (Nirakar Pradhan, 2015).

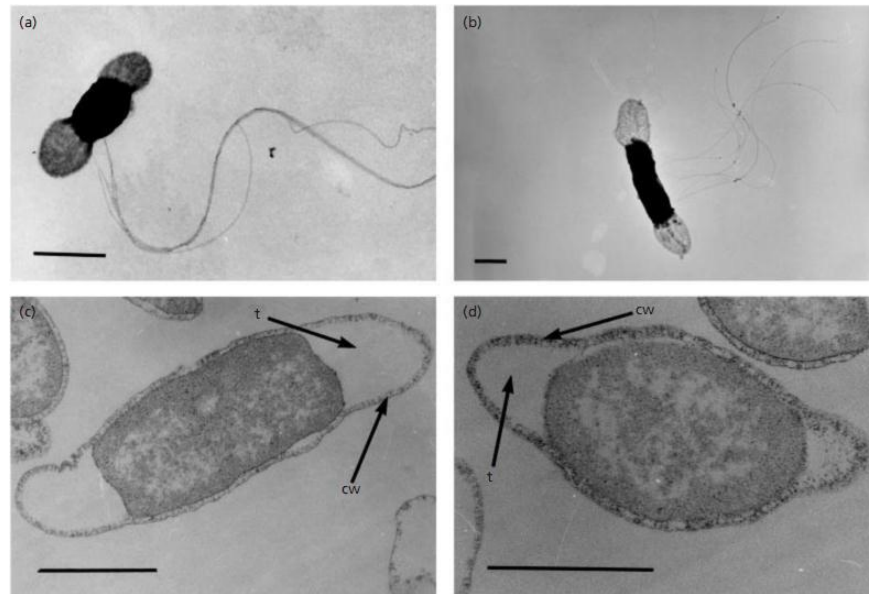


**Figure 3.3:** SEM images of *Thermotoga petrophila* (a), *Thermotoga naphthophila* (b). Electron micrographs of doubly stained ultrathin sections of cells of *T. petrophila* (c) and *T. naphthophila* (d). Black arrows indicate the “toga” and the cell wall. One bar is 1 μm (Takahata, 2001)

In table 3.1, is reported a summary of hydrogen production yield reported in the principal literature studies until now, associated with the fermentation type and the volume of the reactor.

Carbon Source	Substrate Load (g/L)	Culture Type	T(°C)/Start pH	Mixing Speed (rpm)	Reactor Volume (mL)	Working Volume (mL)	H <sub>2</sub> Yield	Byproducts
Glucose	5	B	80/7.5	250	3800	1000	2.8 mol H <sub>2</sub> /mol glucose	AA, LA, CO <sub>2</sub>
Glucose	5	B	80/7.1	250	2400	600	3.5 ± 0.1 mol H <sub>2</sub> /mol glucose <sup>a</sup>	AA, LA, CO <sub>2</sub>
Glucose	10	B	72/7.0	350	2000	1000	3.5 mol H <sub>2</sub> /mol glucose	AA, LA, CO <sub>2</sub>
Glucose	20	B	72/7.0	350	2000	1000	3.4 mol H <sub>2</sub> /mol glucose	AA, LA, CO <sub>2</sub>
Glucose/Fructose 7:3	10	B	72/7.0	350	2000	1000	3.3 mol H <sub>2</sub> /mol glucose	AA, LA, CO <sub>2</sub>
Glucose/Fructose 7:3	20	B	72/7.0	350	2000	1000	3.0 mol H <sub>2</sub> /mol glucose	AA, LA, CO <sub>2</sub>
Fructose	10	B	72/7.0	350	2000	1000	3.4 mol H <sub>2</sub> /mol fructose	AA, LA, CO <sub>2</sub>
Fructose	20	B	72/7.0	350	2000	1000	3.2 mol H <sub>2</sub> /mol fructose	AA, LA, CO <sub>2</sub>
Carrot pulp hydrolysate	10	B	72/7	350	2000	1000	2.7 mol H <sub>2</sub> /mol glucose	AA, LA, CO <sub>2</sub> , EtOH
Carrot pulp hydrolysate	20	B	72/7	350	2000	1000	2.4 mol H <sub>2</sub> /mol glucose	AA, LA, CO <sub>2</sub> , EtOH
Glycerol	5	B	75/7.5	-	120	40	2.7 ± 0.1 mol H <sub>2</sub> /mol glycerol	AA, LA, CO <sub>2</sub>
Molasses	20	B	77/8.5	100	116	40	2.6 ± 0.1 mol H <sub>2</sub> /mol glucose	AA, LA, CO <sub>2</sub>
Cheese whey	12.5	B	77/8.5	100	116	40	2.4 ± 0.1 mol H <sub>2</sub> /mol glucose	AA, LA, CO <sub>2</sub>
Diatom <sup>b</sup> water soluble sugars	2	B	80/7.5-8	250	3800	500	1.9 ± 0.1 mol H <sub>2</sub> /mol glucose	AA, LA, CO <sub>2</sub>
Glucose	5	B	80/8.0	200	120	60	3.8 ± 0.4 mol H <sub>2</sub> /mol glucose	AA, LA, CO <sub>2</sub>
Arabinose	5	B	80/8.0	200	120	60	3.8 ± 0.5 mol H <sub>2</sub> /mol arabinose	AA, LA, CO <sub>2</sub>
Xylose	5	B	80/8.0	200	120	60	3.4 ± 0.3 mol H <sub>2</sub> /mol xylose	AA, LA, CO <sub>2</sub>
Potato steam peels	10	B	75/6.9	350	2000	1000	3.8 mol H <sub>2</sub> /mol glucose	AA, LA, CO <sub>2</sub>
Glycerol	2.5	B	80/7.3	200	120/240	25/50	2.6 mol H <sub>2</sub> /mol glycerol	AA, LA, CO <sub>2</sub>

**Table 3.1:** H<sub>2</sub> yields from various substrates by hyperthermophilic eubacterium *T. neapolitana*. B = batch; FB = fed-batch; AA = Acetic acid; LA = Lactic acid; EtOH = Ethanol. In the black rectangle are underlined the study conducted in our department (Cappelletti et.al., 2012), (Dario Frascari, 2013).

In the framework of Bio-Hydro project, two study are published in peer reviewed journals (black rectangle in the table 3.1, references in the caption), and my contribution was to perform an integrated test bioreactor – membrane (see description in paragraph 4.3.2, unpublished result) and co-feeding experiments with molasses and milk whey (see description in paragraph 4.3.3 and 4.3.4, (Dario Frascari, 2013)).

### 3.2 ANAEROBIC DIGESTION AND BIO - METHANE

Anaerobic digestion is one of the best well – known multistep process for the production of alternative energy, especially biogas. Since 50 years ago, this process was studied and characterized, initially for the stabilization of sewage sludge derived from wastewater treatment (Tilche A., 1998), but then becomes one of the best technology for the production of renewable energy. In fact, more and more different types of substrates were used (alone or in co-digestion), for the production of biogas (and subsequent refined biomethane), used as a fuel or for domestic application. An incredible number of literature studies was performed to assess and define all the aspect of the process, kinetic, used wastes, inhibition, biochemical characterization, molecular identification of the involved bacteria, and so on. Generally speaking, anaerobic digestion is a multi – step biochemical process



performed by different types of bacteria and archaea that leads to a complete conversion of complex organic matter to CH<sub>4</sub>, and CO<sub>2</sub> (Centre, 2011). The typical composition of produced biogas is reported in table 3.2

Component	Formula	Concentration
Methane	CH <sub>4</sub>	50-75 Vol.-%
Carbon dioxide	CO <sub>2</sub>	25-45 Vol.-%
Water vapour	H <sub>2</sub> O	2-7 Vol.-%
Sulphide	H <sub>2</sub> S	0,002-2 Vol.-%
Nitrogen	N <sub>2</sub>	< 2 Vol.-%
Ammoniac	NH <sub>3</sub>	< 1 Vol.-%
Hydrogen	H <sub>2</sub>	< 1 Vol.-%
Trace gases		< 2 Vol.-%

*Table 3.2: Typical biogas composition*

Different type of wastes is used for bioCH<sub>4</sub> production, due to the extreme versatility and adaptability of the process. Lignocellulosic crops as rice (Gu Y, 2014), (Lei Z, 2010) corn (Song Z, 2014), (Zhu J, 2010), (Li Y, 2014) and wheat straw (Sambusiti C, 2013), (Lin Y, 2014), municipal waste as OFMSW (Fernández-Rodríguez J, 2014), (Hartmann H, 2005), (Forster-Carneiro T, 2008), different types of fruit and vegetables residues (Scano EA, 2014), (Liu G, 2009), dairy and cattle manure (Zhang C, 2013), (El-Mashad HM, 2010), and residues from waste activated sludge (Hasegawa S, 2000), (Feng Y, 2014), (Bougrier C B. A.-P., 2007) are only small examples of wastes utilization (alone or in co-digestion), in this process. Moreover, the residual of the process (commonly called “digestate”), is often used as a fertilizer in open field, obtaining a double advantage: energy production and valuable process waste. Due to the vastness of the topic, is evident that those literature examples represents only a minimum part of the global articles published. In fact, a lot of parameters needs to be optimized (e.g. reactor set-up, pretreatment of the waste, inoculum acclimatization...), and for this reason is impossible to make a unique classification. Every process is different and strictly depending on the experimental condition.

Besides that, the biochemical characteristics of the process are common to all the considered examples (figure 3.4)

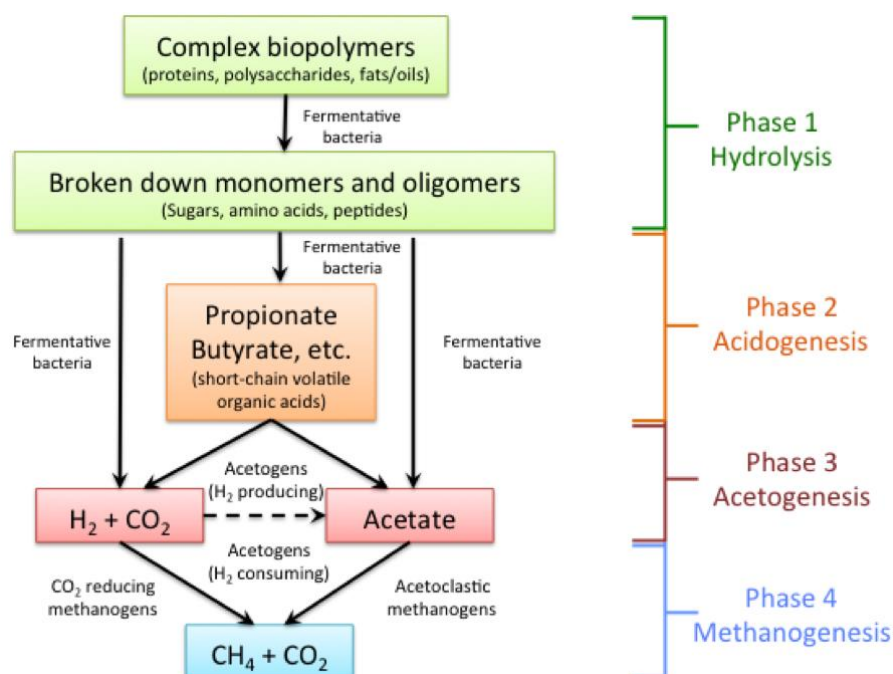
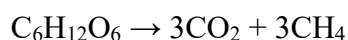


Figure 3.4: Biochemistry of anaerobic digestion process

From 1 mol of glucose, the overall process can be schematized as follow.



In the first hydrolytic step, the complex organic matter formed by polysaccharides, proteins and fats is hydrolyzed to the simple monomeric units (monosaccharides, amino acids, and fatty acids respectively). This process is mediated by a plethora of extracellular enzymes like lipases, proteases, cellulases, amylases, produced by different types of microorganism as *Clostridium*, *Bacteroides*, *Butyrivibrio*, *Clostridium*, *Fusobacterium*, *Selenomonas*, and *Streptococcus* genera (Heike Sträuber, 2012). This is the most variable stage of the process, due to the diversity of substrate and enzyme involved. Moreover, different variables can affect the velocity of this stage, like the dimension, shape and surface conformation of the raw materials and the biomass density. Generally, it is described as 1<sup>st</sup> order kinetic dependent only from substrate concentration (Pavlostathis, 1991).

In the second phase, acidogenic bacteria belonging to the genera *Pseudomonas*, *Bacillus*, *Clostridium*, *Micrococcus*, or *Flavobacterium*, transform water-soluble chemical substances into short-chain organic acids (formic, acetic, propionic and butyric, mainly), alcohols (methanol, ethanol), carbon dioxide, and hydrogen (Fayyaz Ali Shah, 2014). This is the only facultative anaerobic phase, and

sometimes also ammonia and hydrogen sulfide are produced giving an unpleasant smell (Claassen PAM, 1999).

In the next stage, acetogenic bacteria converts the broad spectrum of compounds produced in the acidogenic phase in acetate, carbon dioxide and hydrogen. In this acetogenic phase, bacteria including those of the genera of *Syntrophomonas* and *Syntrophobacter* convert the acid phase products into acetates and hydrogen which are used by methanogenic bacteria. For example, bacteria like *Methanobacterium suboxydans* transforms butyric acid to propionic acid, whereas *Methanobacterium propionicum* accounts for decomposition of propionic acid to acetic acid (Fayyaz Ali Shah, 2014). This is the key stage of the whole process, because approximately 70% of CH<sub>4</sub> arises in the process of acetates reduction.

All the bacteria involved in the first three phases have high duplication velocity (1 – 2 days), and huge adaptability to a lot of different environmental changes.

The last methanogenic phase, instead, is carried only by two types of archaea (mainly thermophilic and belonging to the *Euryarchaeota* phylum): the acetoclastic and hydrogenotrophic methanogens. This is the limiting step, due to the low duplication rate (5 – 6 days), and their sensitivity to changes in temperature and pH. Besides that, they are inhibited by a high level of volatile fatty acids and other compounds, e.g. hydrogen, ammonia, and sulphur hydrogen (Fayyaz Ali Shah, 2014). The acetoclastic methanogens produces more than 70% of the total methane in the process, with a disproportionation of acetic acid into CH<sub>4</sub> and CO<sub>2</sub>. The hydrogenotrophic pathways, instead, converts with low yields 4 mol of H<sub>2</sub> and 1 mol of CO<sub>2</sub> into 1 mol of methane and 2 mol of H<sub>2</sub>O. The total reactions are reported in table 3.3:

	<b>Reaction</b>	<b><math>\Delta G^\circ</math> (kJ/mol)</b>
Hydrogenotrophic methanogenesis	$4\text{H}_2 + \text{CO}_2 \rightarrow \text{CH}_4 + 2\text{H}_2\text{O}$	-135.0
Aceticlastic methanogenesis	$\text{CH}_3\text{COOH} \rightarrow \text{CH}_4 + \text{CO}_2$	-31.0

**Table 3.3:** Methanogenic reactions (Schink, 1997)

The main represented genera are *Methanobrevibacter*, *Methanogenium*, *Methanospirillum*, *Methanobacterium*, *Methanosarcina* e *Methanococcus*. In figure 3.5 are reported SEM images of the principal methanogenic archaea, whereas in tables 3.4 and 3.5, are represented some kinetic parameters estimated for two of the most famous methanogenic populations, and the principal methane – formation reactions.

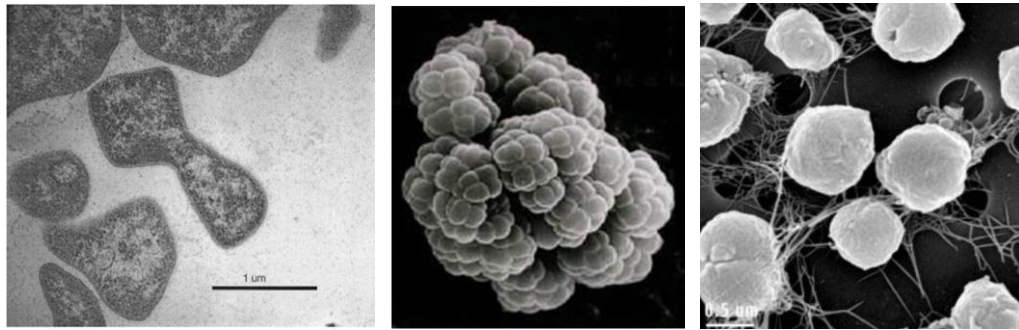


**Figure 3.5:** SEM images of the principal methanogenic genera. From left to right: *Methanosarcina*, *Methanobacterium*, *Methanococcus* (Corinna Bang, 2014)

Parameter	Methanosaeta	Methanosarcina
$U_{\max}$ (d <sup>-1</sup> )	0.20	0.60
$K_S$ (mg COD L <sup>-1</sup> )	10–50	200–280
NH <sub>4</sub> <sup>+</sup> (mg L <sup>-1</sup> )	<3000	<7000
Na <sup>+</sup> (mg L <sup>-1</sup> )	<10,000	<18,000
pH range	6.5–8.5	5–8
pH shock	<0.5	<0.8–1
Temperature range (°C)	7–6.5	1–70
Acetate concentration (mg L <sup>-1</sup> )	<3000	<15000

**Table 3.4:** Kinetics characteristics of methanogens (Fayyaz Ali Shah, 2014)

Hydrogen:	$4H_2 + CO_2 \rightarrow CH_4 + 2H_2O$
Acetate:	$CH_3COOH \rightarrow CH_4 + CO_2$
Formate:	$4HCOOH \rightarrow CH_4 + CO_2 + 2H_2O$
Methanol	$4CH_3OH \rightarrow 3CH_4 + CO_2 + 2H_2O$
Carbon monoxide:	$4CO + 2H_2O \rightarrow CH_4 + 3H_2CO_3$
Trimethylamine:	$4(CH_3)_3N + 6H_2O \rightarrow 9CH_4 + 3CO_2 + 4NH_3$
Dimethylamine:	$2(CH_3)_2NH + 2H_2O \rightarrow 3CH_4 + CO_2 + 2NH_3$
Methylamine:	$4(CH_3)NH_2 + 2H_2O \rightarrow 3CH_4 + CO_2 + 4NH_3$
Methyl mercaptans:	$2(CH_3)_2S + 3H_2O \rightarrow 3CH_4 + CO_2 + H_2S$
Metals:	$4Me^0 + 8H^+ + CO_2 \rightarrow 4Me^{++} + CH_4 + 2H_2O$

**Table 3.5:** Typical methanogenic reactions (Fayyaz Ali Shah, 2014)

After this overview of the anaerobic process, it's clear that every process is strictly dependent primarily from the inoculum and the waste used. For this reason, in paragraphs 4.1.2 and 4.4.2 both substrates and both inocula used in the experiments described in this dissertation, were deeply characterized in terms of physico – chemical characteristics (i.e. total and volatile solids, ashes...).

In the experiments described in this thesis, 2 inocula were used and four different types of wastes are used: grape pomaces, tomato peels, maize silage and olive mill wastewater. Except of olive mill

wastewater (that are dependent from the whole process of the plant), typical BMP values (Bio-Methane-Potential) of all of the other three wastes are described by E. Dinuccio, 2010. Those values (reported in table 3.6) are used as reference to determine the satisfactory of our biomethanization tests. Moreover, these values are only for single substrate; in this dissertation also co-feeding experiments were performed.

***Principal BMP Yields of grape pomace, tomato peels and maize silage reported in literature***

	NL <sub>CH4</sub> /Kg <sub>SV fed</sub>
<i>Grape pomace</i>	116
<i>Tomato peels</i>	218
<i>Maize silage</i>	317

**Table 3.6:** BMP Yields of the principal wastes used in this study reported by E. Dinuccio 2010

All the materials and methods necessary for these tests are reported in section 4.1 (for the waste characterization and inocula preparations), and in paragraph 4.4 (and subsequent sub-paragraph), for the tests detail.

### 3.3 ALCOHOL PRODUCTION: 1 - PROPANOL

Alcohols, in particularly the first four aliphatic alcohols (methanol, ethanol, n – propanol and n – butanol), are considered one of the best alternatives in replacing fossil fuels.

Table 3.7 reports the average octane number and the energy density of methanol, ethanol, n – propanol and n – butanol respect to gasoline.

Fuel	Energy Density(megajoules/liter)	Average Octane (AKI rating/RON)
Gasoline	~33	85-96/90-105
Methanol	~16	98.65/108.7
Ethanol	~20	99.5/108.6
Propanol	~24	108/118
Butanol	~30	97/103
AKI - Anti-Knock Index: This octane rating is used in countries like Canada and the United States.		
RON - Research Octane Number: This octane rating is used in Australia and most of Europe		

**Figure 3.7:** Principal characteristic of alcohol fuels respect to gasoline

Gasoline has a higher intrinsic energy density than alcohols, but the higher octane numbers of alcohols respect to petroleum – derived fuel, can compensate the lower density.

Ethanol is the most common biofuel produced worldwide. According to the last report of RFA (Renewable Fuel Association - 2015), more than 24.000 millions of gallons of bioethanol are produced in 2014 and 58% of the total amount is produced in U.S.A. and 25% in Brazil (Renewable Fuels Association, 2015). Ethanol is one of the best well – established industrial process, and a plethora of microorganism are used to ferment a large quantity of different raw materials with different examples of consolidated bioprocesses (Van Zyl WH, 2007), (Jin, 2011), (Yuan, 2012). It can be used directly in modified spark engines or can be blended with petrol. Moreover, it also improves fuel combustion in vehicles hence reduction emissions. In comparison with petrol, ethanol contains only a trace amount of sulfur, so mixing ethanol with petrol helps reduce the sulfur content of fuel, simultaneous lowering the emission of sulfur oxide that is the major component of acid rain (Sudip Chakraborty, 2012).

Besides ethanol, also methanol, n – propanol and n – butanol are recently considered other interesting alternative. Methanol is commonly produced by thermocatalytic conversion from syngas, but recently a particularly methane-oxidizing bacterium *Methylococcus capsulatus* was used to produce methanol from CH<sub>4</sub> as only carbon source (Steve S.F. Yu, 2003).

1 – propanol and 1 – butanol in particularly, represent the future of the bio – alcohols production, because combine ethanol advantages with higher octane number. As previously reported, biobutanol has a higher energy content than ethanol, almost 20% more by density. Due to its similarities to conventional gasoline, it is able to blend much better than ethanol with gasoline. Besides that, n –

butanol and n – propanol have a lot of applications as chemical intermediate and building blocks, not only as engines fuel. 1 – propanol is used as a solvent for waxes, vegetable oils, resins, cellulose esters, and ethers. It is found in inks, brake fluids and polishing compounds and has been used as a degreasing agent, an antiseptic, and a chemical intermediate. More recently, it is being used as a hand disinfectant by health care workers (James L. Unmack, 2011). The four butanol isomers, instead, represents a source of solvents for paints, resins, and dyes. Are also used in cosmetic industries, plasticizers, industrial cleaners, paint remover additives and a chemical intermediate for butyl esters or butyl ethers. Like ethanol, butanol is a biomass-based renewable fuel that can be easily produced by alcoholic fermentation of the biomass feedstocks, but with lower yields. Compared butanol yield by acetone butanol ethanol (ABE) fermentation to the classical yeast ethanol fermentation process, the yeast process has a 10–30 times higher yields (Chao Jin, 2011).

1 – propanol, instead is a most challenging process, because up to now, no natural high – yield biological process was reported in literature. For this reason, the main process for n – propanol production is still the chemical procedure: the catalytic hydrogenation of propionaldehyde derived from hydroformylation of ethylene using carbon monoxide and hydrogen in the presence of a catalyst such as cobalt octacarbonyl or a rhodium complex (Papa, 2011). In the last 20 years, anyway, several attempts to produce 1 – propanol are made, in particularly using metabolic engineering tools in GMO *E. coli* or syngas fermentation. Different literature works reports the manipulation of particularly biochemical pathway to produce 1 – propanol, for example the “sleeping beauty mutase operon” (Kajan Srirangan, 2013), the “1 – 2 propanediol way”, (R. Jain, 2011) or the “Citramalate pathway” (Shota Atsumi, 2008), reporting anyway small amount of propanol production, no more than few mg/L. Recently, also the keto – acid pathway involved in the aminoacids metabolism, was considered for alcohol production. The key intermediates of this aminoacids biosynthetic pathways are 2-ketoacids that can be converted to a wide range of chemically diverse compounds, including alcohols. (Pooja Jambunathan, 2014). As previously reported, no natural hosts can produce alcohols in significant quantities. A synthetic approach was developed to produce these alcohols using the 2-ketoacid intermediates of branched-chain amino acid biosynthetic pathways (see figure 3.8).

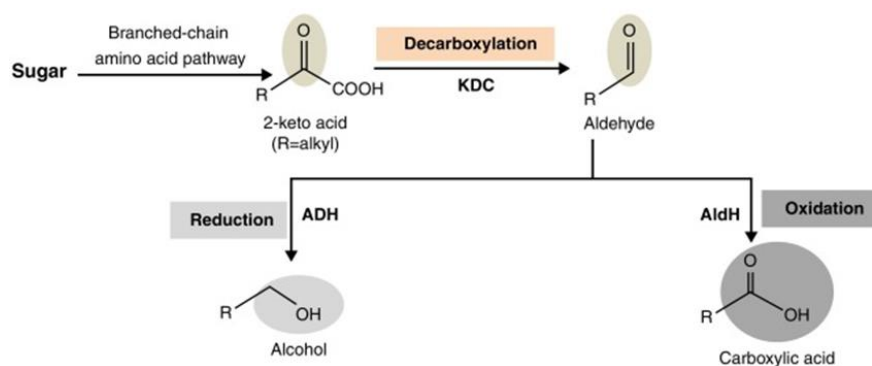


**Figure 3.8:** Keto – acids pathway for alcohol production (Pooja Jambunathan, 2014)

The limiting step is the reduction of the aldehyde derived by decarboxylation of the respective 2 – keto acid, to the respective alcohols. Thus, is necessary a synthetic approach to develop an efficient recombinant high – production. One of the best example reported in literature, is the metabolic engineering of *Escherichia coli* for the contemporary production of 1 – propanol and 1 – butanol production using threonine intermediate. Threonine is converted into 2 – ketobutyrate (the respective 2 – keto acid), and subsequent decarboxylated in propanal by KDC enzyme (2-keto acid decarboxylase) followed by reduction to n – propanol by ADH enzymes (alcohol dehydrogenase).

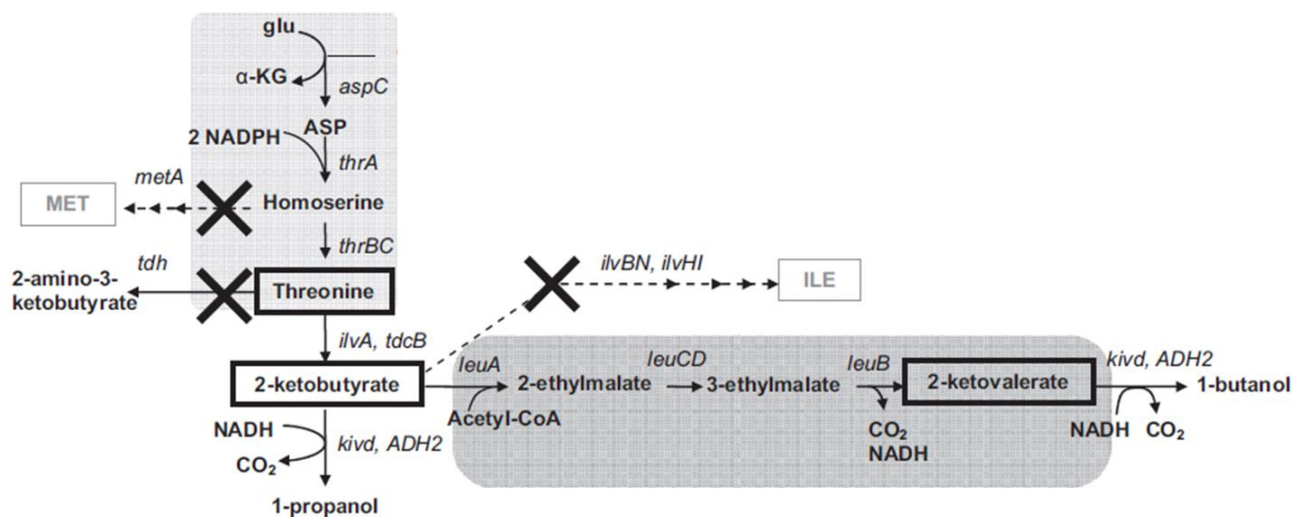


**Figure 3.9:** Metabolic engineering of *E. coli* for the production of 1 – propanol and 1 – butanol via keto acids pathway (C.R. Shen, 2008)

As previously reported, the yields are very low (less than 0,5 g/L of 1 – propanol).



Syngas fermentation, instead, is naturally carried out by different types of carboxydophilic bacteria belonging to *Clostridium* genus, e.g. *C. ljungdahlii*, *C. ragsdalei*, *C. coskatii*, *C. autoethanogenum* using Wood–Ljungdahl pathway. Ethanol, and acetic acid are usually the main products when only syngas is provided, but in presence of a small quantity of short chain carboxylic acid (from propionic to n – caproic acids), those acids were reduced using pressurized syngas as only electron donor (Perez et.al., 2012).

In table 3.7, are shown the principal results reported by Perez et.al., 2012 using two of the most promising carboxydophilic bacteria, and 15 mM of carboxylic acid in presence of 1,93 bar of syngas (60% v/v CO, 35% H<sub>2</sub>, 5% CO<sub>2</sub>) at pH 5,5.

Condition	Consumed carboxylic acid (mM)	Produced at end of experiment (mM)		
		Alcohol from carboxylic acid	Final acetic acid	Final ethanol
<i>C. ljungdahlii</i> ERI-2				
No carboxylic acid	NA	NA	123.27 ± 10.52	135.53 ± 20.10
Propionic acid	11.26 ± 1.03	10.44 ± 1.69 <i>n</i> -propanol	138.02 ± 22.99	169.05 ± 61.65
<i>n</i> -butyric acid	12.13 ± 1.79	8.27 ± 1.75 <i>n</i> -butanol	126.36 ± 20.85	129.87 ± 43.23
<i>n</i> -valeric acid	10.88 ± 1.07	5.63 ± 0.92 <i>n</i> -pentanol	100.48 ± 5.61	109.58 ± 25.88
<i>n</i> -caproic acid	11.11 ± 1.18	5.11 ± 0.68 <i>n</i> -hexanol	101.10 ± 14.31	102.58 ± 39.98
Isobutyric acid	7.47 ± 4.03	3.14 ± 1.89 isobutanol	112.90 ± 12.99	137.76 ± 46.10
<i>C. ragsdalei</i> P11				
No carboxylic acid	NA	NA	31.30 ± 3.15	59.65 ± 0.66
Propionic acid	10.39 ± 2.05	7.51 ± 2.01 <i>n</i> -propanol	39.43 ± 8.39	48.08 ± 24.17
<i>n</i> -butyric acid	6.85 ± 1.23	4.81 ± 1.55 <i>n</i> -butanol	64.13 ± 11.64	24.87 ± 9.75

**Table 3.7:** Alcohol production using *C. ljungdahlii* and *C. ragsdalei*, in presence of syngas and 15 mM of carboxylic acids

Also in this case, the yields are not comparable with industrial applications. Numerous literature works are published on this topic, in order to analyze the principal parameters of the process and increase the final yield (Kan Liu, 2014), (Kan Liu, 2014 a). One of these studies consider the possibility to use mixed consortia to reduce short volatile fatty acids to the respective alcohols, using hydrogen as electron donor (Kirsten J.J. Steinbusch, 2008). In particularly a mixed consortium was used to reduce acetic, propionic, and butyric acid to their respective alcohols in presence of 0,5 bar of hydrogen overpressure. According to this paper, and considering the anaerobic digestion process described in paragraph 3.2, the main idea of this topic was to enrich the biogas biorefinery, investigating if the

VFA produced in the first steps of the anaerobic digestion, can be converted to the respective alcohols, using one of the consortia present in our laboratory, changing only the physical conditions. We focused on the propionic acid, that is (after acetate) the most abundant VFA present in the anaerobic digestion process, and the most challenging process as previously reported. Three different consortia (described in section 4.2) are considered for the propanol production, and the screening, acclimatization and production tests, are extensively explained in the paragraph 4.5.1 and 4.5.2.

### 3.4 SUCCINIC ACID PRODUCTION

Succinic acid (S.A.) is one of the top 12 building block reported by the U.S.A. Department of energy (DOE) in 2014, produced from biomass transformation (U.S. Department of Energy, 2014). Due to its saturated structure, this dicarboxylic acid is one of the most promising building blocks for the production of a plethora of different types of molecules like 1-4 butanediol, gamma-butyrolactone, tetrahydrofuran, adipic acid, and so on. It's also used in the food industry as acidity corrector and neutralizer agent (E363) or in the perfume and detergent sectors. Moreover, numerous bioplastics are derived from succinic acid, e.g. PBS, Poly – Butylene Succinate (see figure 3.10) (Zeikus JG, 1999).

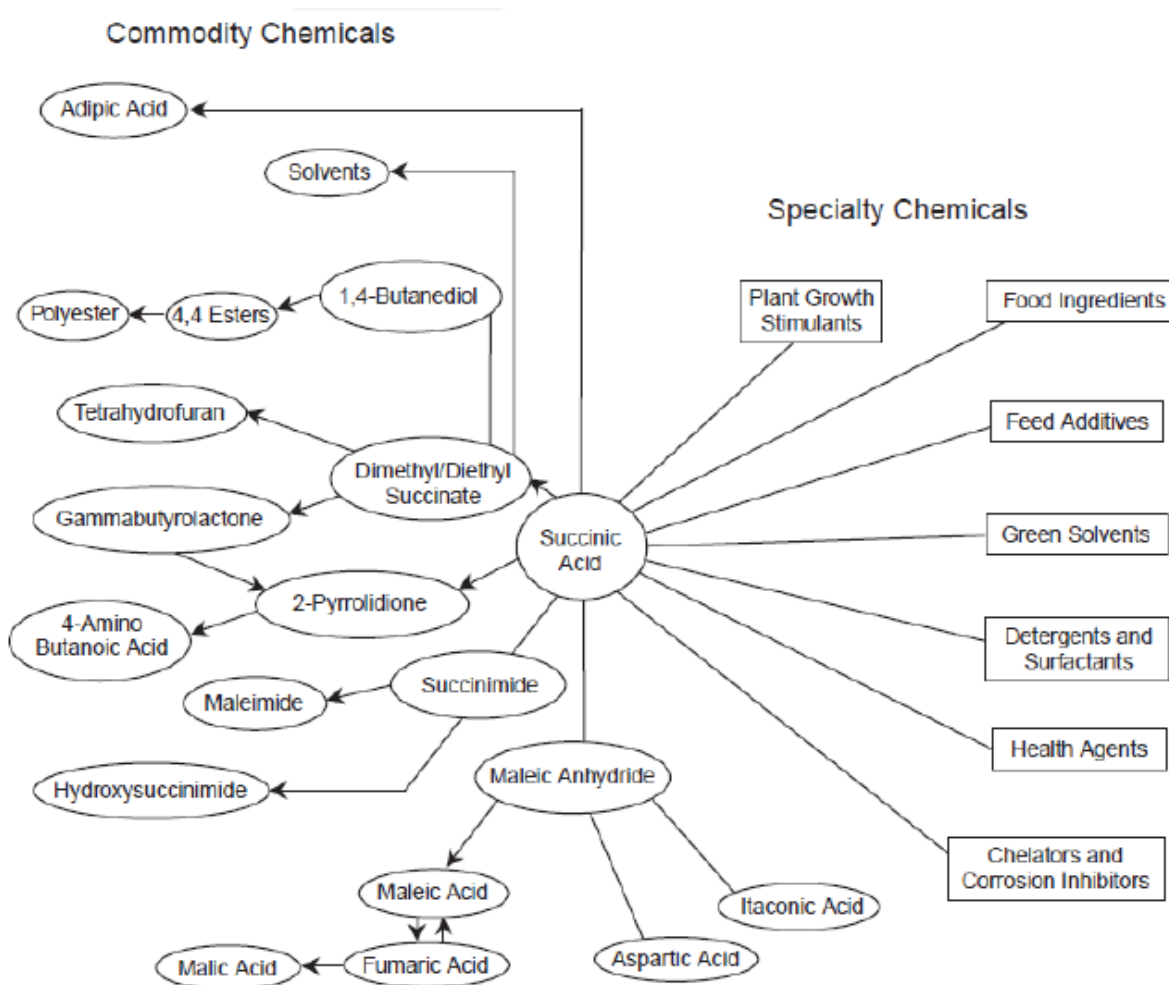


Figure 3.10: Succinic acid as intermediate molecules (Cheng K, 2012)

Besides the multiple uses of succinic acid, and the undoubted advantages derived from the renewable source, the fermentation process fix 1 mol of CO<sub>2</sub>, for every mol of succinic acid formed, with a maximum theoretical yield (in grams) of 1,31 g of succinic acid for 1 g of glucose consumed (Cheng K, 2012). For this reason, the establishment of high – yield succinic acid fermentation, represents one of the most promising bioengineering challenges for our society.

Up to now, only 0,2% of the global succinic acid market is covered by renewable processes (M.M. Bomgardner, 2011), and the petrochemical – based synthesis is still preferred due to the lower costs. Succinic acid is chemically derived from the hydrogenation of maleic anhydride formed from the oxidation of n – butane or from the carbonization reaction of acetylene (D. Vasudevan, 1995), but numerous studies in literature presents efficient alternatives to promote S.A. production from

biochemical process using different types of process and different types of waste as carbon source (Leung, 2012), (Li Q. e., 2010), (Dorado, 2009).

Different types of bacteria are able to produce succinic acid, because this molecule is an intermediate of Krebs cycle, one of the most common biochemical pathway in a large number of different microorganism species. Up to now, different types of bacteria and fungi are identified as natural succinic acid producer; besides that, also *E. coli*, and *C. glutamicum* and yeast like *S. cerevisiae* are used as engineered producing microorganism in recent literature works (table 3.8):

	Type	Species	Oxygen requirement
Natural producers	Bacteria	<i>Actinobacillus succinogenes</i>	Facultative anaerobe
	Bacteria	<i>Anaerobiospirillum succiniciproducens</i>	Strict anaerobe
	Bacteria	<i>Mannheimia succiniciproducens</i>	Facultative anaerobe
	Bacteria	<i>Bacteroides fragilis</i>	Strict anaerobe
	Bacteria	<i>Enterococcus faecalis</i>	Facultative anaerobe
	Bacteria	<i>Klebsiella pneumoniae</i>	Facultative anaerobe
	Bacteria	<i>Succinivibrio dextrinosolvens</i>	Strict anaerobe
	Fungi	<i>Aspergillus niger</i>	Facultative anaerobe
	Fungi	<i>Paecilomyces variotti</i>	Facultative anaerobe
	Fungi	<i>Penicillium simplicissimum</i>	Facultative anaerobe
Engineered producers	Bacteria	<i>Escherichia coli</i>	Facultative anaerobe
	Bacteria	<i>Corynebacterium glutamicum</i>	Aerobe
	Yeast	<i>Saccharomyces cerevisiae</i>	Facultative anaerobe

**Table 3.8:** List of the principal succinic acid producer microorganism (Cao Y, 2013)

The best and more exploited natural microorganism producers are *A. succinogenes*, *A. succinoproducens* e *M. succinoproducens*, but all the experiments reported in this dissertation are conducted with the Gram -, capnophylic, non-pathogenic and facultative anaerobic *Actinobacillus succinogenes* bacterium.

This strain was originally isolated from bovine rumen (Guettler MV R. D., 1999), and the genome was fully sequenced in 2003 (Hong SH, 2004). The obtained data confirmed shows that this microorganism doesn't have a complete Krebs cycle, and the genome includes different genes codifying for protein complexes involved in carbohydrates uptake, suggesting that this microorganism can ferment a plethora of different carbon sources (McKinlay J B, 2010).

The biochemical pathway for the S.A. production by *A. succinogenes*, is characterized by strict anaerobic conditions, and involves the fixation of inorganic carbon (figure 3.11):

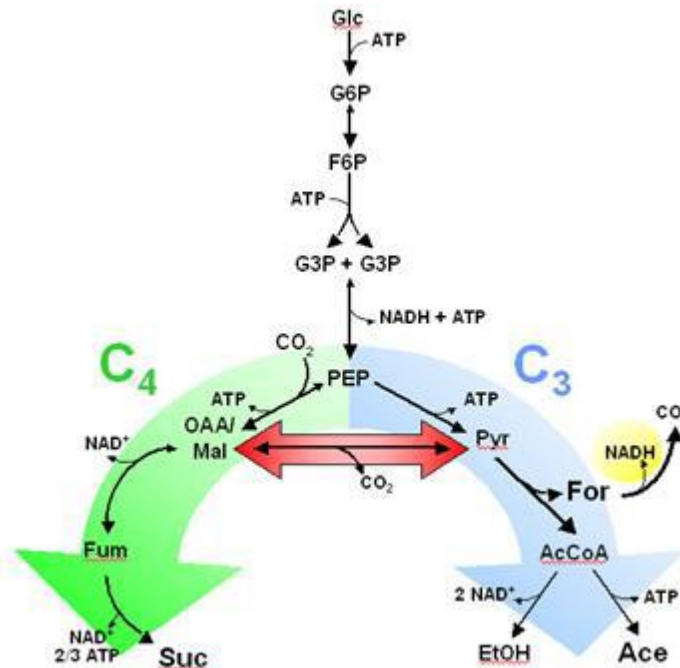


**Figure 3.11:** Biochemical pathway for succinic acid production by *A. succinogenes* (McKinlay JB, 2007)

From the glycolytic and pentose – phosphate pathways, the carbon source is converted to pyruvate and then to phosphoenolpyruvate (PEP). At this point the metabolic pathway is divided in two separate branches: the “C3 pathway”, and the “C4 pathway”. The “C4 pathway” leads to the succinate production and involves as a first step the transformation of PEP into oxalacetate through the action of phosphoenolpyruvate carboxykinase (PEP – K). Then, the oxalacetate is further converted into malate, fumarate and finally to succinate from malate dehydrogenase, fumarate reductase and succinate dehydrogenase. It’s evident that the PEP – K enzyme is the key for achieve and high yield of succinate. In fact, the oxidation of pyruvate that leads to acetate, formate and ethanol (C3 pathway), provides NADH and ATP, for the reductive C4 pathway, thus a delicate equilibrium is necessary to obtain high succinate titer. Moreover, high level of inorganic carbon (as CO<sub>2</sub>) promotes the succinate formation, because PEP – K fix the inorganic carbon molecule in presence of high level of inorganic carbon source. Is demonstrated

that the S.A. titer is 4 times higher when inorganic carbon is more than 1 mol C/mol glucose, respect to the experiments with low levels of CO<sub>2</sub> (< 0,1 mol C/mol glucose).

The overall reaction is stoichiometric: 1 mol of glucose and 1 mol of carbon dioxide leads to 1 mol of succinate, 1 mol of acetic acid and 1 mol of formate (Van der Werf MJ, 1997):



In table 3.9 is reported a summary of bio – succinic acid production yield, titer and productivity in the principal literature studies published until now, associated with the pretreatment process, microorganism used, and reactor configuration:

Feedstock	Pretreatment	Microorganisms	Configuration	Final conc. [g L <sup>-1</sup> ]	Productivity [g L <sup>-1</sup> h <sup>-1</sup> ]	Yield[g g <sup>-1</sup> sugar]
Glucose	NA	Rec. E. coli	Batch/bench top bioreactor	–	1.27	0.83
Fructose	NA	Rec. E. coli	Batch/bench top bioreactor	–	1.01	0.66
Xylose	NA	Rec. E. coli	Batch/bench top bioreactor	–	0.78	0.50
Glucose, Fructose	NA	Rec. E. coli	Batch/bench top bioreactor	–	0.79	0.58
Glucose, Xylose	NA	Rec. E. coli	Batch/bench top bioreactor	–	0.86	0.60
Raw whey (lactose)	NA	A. succinicproduces	Fed-batch	34.7	1.02	–
Food waste	A. awamori and A. oryzae	Rec. E. coli	Batch/bench top bioreactor	29.9	0.48	0.56
Wheat-based feedstock	A. awamori and A. oryzae	A. succinogenes	Batch/bench top bioreactor	64.2	1.19	0.81
Waste bread	A. awamori and A. oryzae	A. succinogenes	Batch/bench top bioreactor	47.3	1.12	1.16
Cakes	A. awamori and A. oryzae	A. succinogenes	Batch/bench top bioreactor	24.8	0.79	0.80
Pastries	A. awamori and A. oryzae	A. succinogenes	Batch/Bench top bioreactor	31.7	0.87	0.67
Cheese whey	NA	A. succinicproduces	Batch/bench top bioreactor	34.3	–	0.80
Cheese whey	NA	A. succinicproduces	Fed-batch/bench top bioreactor	34.7	–	0.91
Cheese whey	NA	A. succinicproduces	Continuous, bench top bioreactor	19.8	–	0.60
Cheese whey	NA	A. succinogenes	Batch/bench top bioreactor	27.9	0.44	0.57
Corn stover	Alkaline + enzymatic hydrolysis	A. succinogenes	Batch/bench top bioreactor	56.4	–	0.73
Corn stover	Alkaline, Acid, Alkaline peroxide, Aqueous ammonia soaking	A. succinogenes	SSF	47.4	–	0.72
Corn straw	Alkaline + enzymatic hydrolysis	A. succinogenes	Batch/bench top bioreactor	45.5	0.95	0.81
Corn straw	Alkaline + enzymatic hydrolysis	A. succinogenes	Fed-batch/bench top bioreactor	53.2	0.83	1.21
Corn core hydrolysate		A. succinogenes	Anaerobic bottle	32.1	–	0.89
Rice straw hydrolysate		A. succinogenes	Anaerobic bottle	17.6	–	0.63
Wheat straw hydrolysate		A. succinogenes	Anaerobic bottle	19.0	–	0.74
Rapeseed meal	Acid + enzymatic hydrolysis	A. succinogenes	SSF	15.5	–	0.12
Sake lees	Acid + enzymatic hydrolysis	A. succinogenes	Batch/bench top bioreactor	61.6	1.21	0.59
Sugar cane bagasse hydrolysates		Rec. E. coli	Fed-batch/bench top bioreactor	39.3	0.33	0.97
Cellobiose & sugars from sugarcane bagasse cellulose	Acid + enzymatic hydrolysis	A. succinogenes	Batch/bench top bioreactor	20	0.61	0.65

*Table 3.9: Principal fermentation processes reported in literature for the production of succinic acid (Daniel Pleissner, 2015 in press)*

This project was conducted in collaboration with the Flemish Institute For Technological Research (VITO), located in Mol, Belgium, and different aspects of the entire bioprocess was examined. In Belgium, after a preliminary experiment using both lactose and milk whey as a carbon source, the main project was focused to develop an integrated ISPR (“In Situ Product Recovery) pre – pilot plant with the fermenter directly couple to a electrodialysis system for the succinic acid recovery. In this configuration, no cell retention steps, e.g. micro or ultrafiltration were used. In paragraph 4.6.1 – 4.6.5 are extensively described the experiments and the configuration of the integrated plant.

In Bologna, instead, was developed a deep screening of different commercial support for biofilm growth, and the principal kinetic parameters were estimated (like  $\mu_{max}$  and  $K_s$ ), both with lactose and both with milk whey as carbon source. Moreover, a 1 L PFR type reactor was built, and preliminary biofilm fermentation test were performed, using the best carrier chosen in the previous screening. In paragraphs 4.7.1 – 4.7.4, are described the experiments for screening phase, for the kinetic model estimation, and also the 1 L plant.

## 4 MATERIALS AND METHODS

---

### 4.1 WASTES SUPPLYING

#### 4.1.1 Wastes collection

Grape pomaces (GPs), tomato peels (TPs), maize silage (MS) and olive mill wastewater (OMWs) were used for anaerobic digestion experiments. Red and white grape pomaces were collected from “*La Glicine*” winery, (Cesena – Italy), for white grape pomace (derived from “Verdicchio” grapes), and from “*Eridania – SADAM*”, a sub-holding of the agro-industrial compart of “Maccaferri Group” (Bologna – Italy), for red grape pomace (derived from “Sangiovese” and “Montepulciano” grapes). Tomato peels are obtained from “*CO.PAD.OR.*”, (Parma – Italy), and maize silage, instead, from “*Sebigas*”, a company controlled by Maccaferri Group, (Olgiate Olona - Italy). Olive mill wastewater, moreover, are collected from “*Olio Terra Nostra*” oil mill (Ugento – Italy). Before performing anaerobic digestion tests for biogas production, different physico – chemical analysis was performed on all these substrates in order to determine pH, density, total solids, volatile solids and ashes, following the protocols described below. All of this compounds were stored at – 20 °C until use (except for OMWs, that was kept at + 4 °C). Moreover, only grape pomaces were dried for 48 hours at 55 °C to eliminate water particles and grinded before use, due to the large dimension. For this reason, a sample of grinded red pomaces was sent to “*Bilfinger Sielv*” (Fossò – Italy) company for a granulometric distribution analysis, reported again in next chapter. No sterilization or filtration procedures was used before bioCH<sub>4</sub> production experiment, because a mixed acclimatized consortia was chosen as inoculum.

Milk whey and molasses were used as raw materials for biohydrogen project. Cheese whey powder was provided by “*Tosi & G*” (Vimercate - Italy), where molasses was produced and collected by the Trecasali sugar production plant of “*Eridania – SADAM*” (Parma – Italy). Both of the substrates were characterized in terms of composition (see next chapter). Also in this case, no sterilization or filtration procedures were necessary, due to the hyperthermophilic nature of the chosen microorganism.



Succinic acid production was evaluated using both lactose and both milk whey, performing experiment in Bologna and at VITO (Flemish Institute For Technological Research) – Mol, Belgium. Cheese whey used in Bologna was again a powder purchased from “*MILEI GmbH*” company (Hamburg – Germany), and cheese whey for the experiments conducted in Belgium was collected from a local industry. Also for these by-product, detailed data regarding the physico – chemical characterization are provided in the next chapter. In this project, milk whey was autoclaved at 121 °C for 20’ in the experiments performed at VITO, and filtered with sterile 0,22 µm VacuCap ® filter (Pall Corporation – USA), for the tests in Bologna.

#### 4.1.2 Physico – chemical characterization of the collected wastes

In table 4.1 are reported the characterization of grape pomaces (GPs), tomato peels (TPs), maize silage (MS) and olive mill wastewater (OMWs), used for biomethane production experiments, in terms of percentage of total solids (%TS), percentage of volatile solids (%VS), percentage of ashes (%AS), ratio between %VS / %TS, pH and density.

##### *Anaerobic digestion substrate characterization*

	% TS	% VS	% AS	% VS / % TS	pH	Density (g/ml)
<i>Grinded red GPs</i>	(88,5 ± 2,5)	(83,45 ± 2,72)	(5,04 ± 2,39)	(94,08 ± 6,14)	c.ca 4	c.ca 1,2
<i>Grinded white GPs</i>	(90,67 ± 3,54)	(86,84 ± 2,85)	(3,83 ± 0,68)	(95,78 ± 7,18)	c.ca 5	c.ca 1,2
<i>TPs</i>	(95,0 ± 0,52)	(92,67 ± 0,11)	(2,58 ± 0,02)	(97,54 ± 0,55)	c.ca 4	c.ca 1,2
<i>MS</i>	(55,56 ± 0,53)	(53,56 ± 0,51)	(2,00 ± 0,08)	(96,41 ± 0,04)	c.ca 5	c.ca 1,2
<i>OMWs</i>	(2,43 ± 0,11)	(2,06 ± 0,08)	(0,36 ± 0,09)	(85,03 ± 0,80)	c.ca 4	c.ca 1,2

**Table 4.1:** Physico – chemical properties of different types of substrate for anaerobic digestion experiments.

Figure 4.1, reports the granulometric distribution of red grape pomaces. 90% of grinded grape pomaces (red line) have an average diameter around 1 µm, instead most of the non-grinded grape pomaces have a diameter around 3.5 µm. Particle dimension has a big influence of biomethanization

experiments (Kouichi Izumi, 2010), for this reason a deep knowledge of grain size distribution is an important parameter to consider.

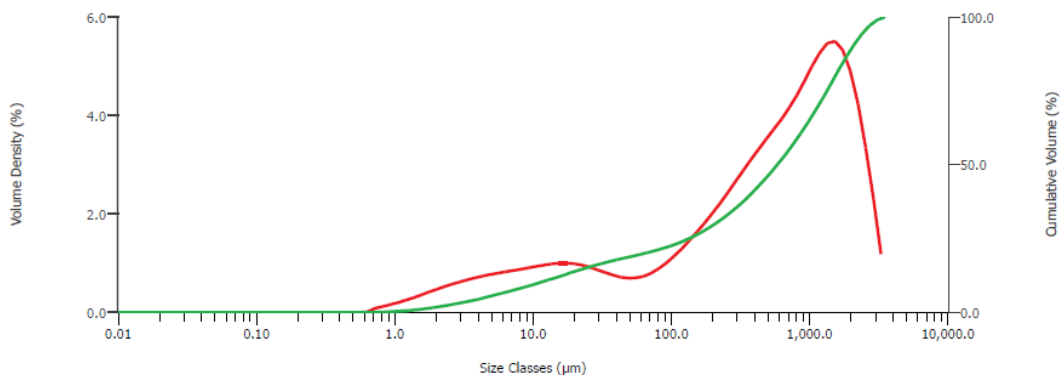


**Figure 4.1:** Grain size distribution of grinded and non-grinded red grape pomaces. Thanks to Bilfinger Sielv FM - IFMA

Composition of milk whey and molasses used for bio- $H_2$  tests is reported in table 4.2 and 4.3 (Values reported from the company data-sheet).

#### ***Milk whey for bio- $H_2$ tests***

	Lactose (%)	Proteins (%)	Fat (%)	Moisture (%)	Ash (%)	COD (g g <sup>-1</sup> cheese whey)	Microbial content mg <sub>dw</sub> g <sup>-1</sup> cheese whey
<i>Milk whey from “Tosi &amp; G”</i>	83	4	1	4	6	1,11	1,0 x 10 <sup>-6</sup>

**Table 4.2:** Composition of milk whey from “Tosi & G” according to product data sheet.

#### ***Molasses for bio- $H_2$ tests***

	Sucrose (%)	Fructose (%)	Glucose (%)	Proteins (%)	COD (g g <sup>-1</sup> molasses)	Microbial content mg <sub>dw</sub> g <sup>-1</sup> molasses
<i>Molasses from “Eridania - SADAM”</i>	24,5	14	9,5	6,1	0,85	1,2 x 10 <sup>-5</sup>

**Table 4.3:** Composition of molasses from “Eridania - SADAM” according to product data sheet

Milk whey for succinic acid production was also characterized in detail prior use, both in Bologna, both at VITO. Milk whey from “*MILEI GmbH*” was highly soluble whey derivate, manufactured by ultrafiltration, with principal properties expressed in the following data sheet.

#### Product properties

Characteristics	Specification	Test method
Bulk density	700 ± 50 g/l	ISO 8967
pH-value (10 %)	6.4 ± 0.3	IDF 104:2004
Scorched particles	Disc A/B	ADPI-Methode 916:2002

#### Typical composition

Protein	max. 4.0 %	ISO 8968-1
Fat	max. 1.0 %	ISO 1736
Ash	5.0 - 7.0 %	AOAC 930.30
Water	max. 3.0 %	ISO 5537
Lactose	77.0 - 87.0 %	ISO 5765
Nitrite	max. 1 ppm	Merckoquant

**Table 4.4:**

*Principal properties of Molkolac Instant milk whey used in Bologna.*

*Thanks to “MILEI GmbH”*

In addition to this, a detailed quantification of lactose in HPLC was performed. A value of 85,35% of equivalent lactose was founded in this milk whey, with a negligible amount of lactic acid.

Internal characterization was performed at Flemish Institute For Technological Research (VITO), of the used milk whey, in order to determine lactose composition and other technical characteristic.

Parameter	
Lactose (g/L)	49
Proteins (g/L)	2.2
Total N (g/L)	0.4
Total P (g/L)	0.4
pH	5.3
Conductivity (mS/cm)	6.2
Dry weight (%)	6
Ash content (%)	9

**Table 4.5:**

*Internal characterization of the milk whey used at VITO. Thanks to Garcia-Gonzales Linsey.*

It's evident that “Molkolac Instant” milk whey used in Bologna for succinic acid production was more concentrated (18 times higher), respect to VITO milk whey used for the same project.

## 4.2 STRAIN/CONSORTIA ACQUISITION AND STOCK PREPARATION

*Thermotoga neapolitana* DSMZ 4359<sup>T</sup> (Shimshon Belkin, 1986) was chosen after a long screening work reported in Cappelletti et. al, 2012 as the microorganism for all the bioH<sub>2</sub> tests. In the same article is reported that the strain was purchased from DSMZ (Braunschweig, Germany), and

initially growth on glucose (7.5 g L<sup>-1</sup>) at 77 °C, utilizing the complete culture medium reported in table 4.6

Component	
NaCl (g L <sup>-1</sup> )	10
NH <sub>4</sub> Cl (g L <sup>-1</sup> )	1
K <sub>2</sub> HPO <sub>4</sub> (g L <sup>-1</sup> )	0.7
MgCl <sub>2</sub> ·6H <sub>2</sub> O (g L <sup>-1</sup> )	0.2
CaCl <sub>2</sub> ·2H <sub>2</sub> O (g L <sup>-1</sup> )	0.1
KCl (g L <sup>-1</sup> )	0.10
Microelements (mg L <sup>-1</sup> )	<sup>a</sup>
Vitamins (μg L <sup>-1</sup> )	<sup>b</sup>
Yeast extract <sup>c</sup> (YE) (g L <sup>-1</sup> )	2
Tryptic soy broth <sup>d</sup> (TSB) (g L <sup>-1</sup> )	2
Cysteine (g L <sup>-1</sup> )	1
Hepes (g L <sup>-1</sup> )	23.8
Resazurin (g L <sup>-1</sup> )	0.02
pH	8.5

<sup>a</sup> Concentrations in mg L<sup>-1</sup>: nitrilotriacetic acid 15, MgSO<sub>4</sub>·7H<sub>2</sub>O 30, MnSO<sub>4</sub>·H<sub>2</sub>O 5, NaCl 10, FeSO<sub>4</sub>·7H<sub>2</sub>O 1, CoSO<sub>4</sub>·7H<sub>2</sub>O 1.8, CaCl<sub>2</sub>·2H<sub>2</sub>O 1, ZnSO<sub>4</sub>·7H<sub>2</sub>O 1.8, CuSO<sub>4</sub>·5H<sub>2</sub>O 0.1, KAl(SO<sub>4</sub>)<sub>2</sub>·12H<sub>2</sub>O 0.2, H<sub>3</sub>BO<sub>3</sub> 0.1, Na<sub>2</sub>MoO<sub>4</sub>·2H<sub>2</sub>O 0.1, NiCl<sub>2</sub>·6H<sub>2</sub>O 0.25, Na<sub>2</sub>SeO<sub>3</sub>·5H<sub>2</sub>O 0.003.

<sup>b</sup> Concentrations in μg L<sup>-1</sup>: biotine 20, folic acid 20, pyridoxine HCl 100, tiamine HCl 50, riboflavin 50, nicotinic acid 50, pantothenic acid 50, vitamine B12 1, *p*-aminobenzoic acid 50, lipoic acid 50.

**Table 4.6:** Medium for *T. neapolitana* stock. Source Cappelletti et. al. 2012.

The strain was then stocked at -80 °C in criovials containing 1 mL of cell suspension and 1 mL of fresh sterilized complete medium (table 4.6) supplemented with 40% glycerol and 5% DMSO, for further experiments (Cappelletti et.al., 2012).

Three different microbial consortia were tested for bioCH<sub>4</sub> production experiments. In the first part of the project, two inocula were collected for anaerobic digestion processes of red and white grape pomaces. The first one (called “SADAM” inoculum) was directly provided by “*Eridania – SADAM*” company, the second (called “DICAM” inoculum) was gently provided by Lorenzo Bertin research group, and was isolated from OFMSW (Organic Fraction Of Municipal Solid Waste) (Bertin, et al., 2012). Both of them were re-activated in a series of primary 116 ml small scale batch reactor (called “microcosm”) prepared under laminar flow hood and 100% nitrogen flow before being sealed with teflon-coated butyl stoppers and aluminum crimp sealers, as follow: 55 ml of total liquid volume divided in 20% (w/w) red grape pomaces, 10% (w/w) of inoculum and demi H<sub>2</sub>O, and incubated at 55°C, pH 7.5 – 8, and 100 rpm stirring. Subsequently, the consortia were propagated again as reported before, and half of that were supplemented with 20% of glycerol and kept at -20° C to

maintain a stock, and the other half were conserved at + 4 °C for the immediate use. Another already – enriched methanogenic consortium (called “SEBIGAS” consortium) was provided by “*Sebigas*” company when different types of agro-industrial waste were tested in addition to grape pomaces (i.e. tomato peels, maize silage and olive mill wastewater). This consortium was collected from a primary tomato peels digester, and immediately frozen at – 20 °C under 100% nitrogen condition and supplemented with 20% of glycerol, in a series of microcosm prepared as described before. Another part of the series (without glycerol) was kept at 4 °C for immediate experiments.

1 - Propanol production experiments were performed testing three different consortia. One of them was the DICAM consortium already used for the anaerobic digestion project. The second (OMW inoculum) one was again gently provided by Lorenzo Bertin research group (Bertin, et al., 2010) and was isolated from an oil mill wastewater, and subsequently acclimatized for volatile fatty acid production. The “*Sebigas*” company collected and provide the third inoculum (called “MAIS” inoculum), from a CSTR anaerobic reactor fed with maize silage. Both “OMW”, both “MAIS” consortia were resuspended in ATCC medium 1754 (PETC Medium) adapted by Perez et.al., 2012 for consortia (table 4.7) for the preparation of a series of 116 ml microcosms, as follow: 40 ml of total liquid volume with 20% of proper inoculum under laminar flow hood and 100% nitrogen flow before being sealed with teflon-coated butyl stoppers and aluminum crimp sealers. Incubation was performed at 30 °C, pH 6 and 100 rpm. The consortia were then stocked at –20 °C in microcosms under 100% N<sub>2</sub> atmosphere, containing 8 mL of cell suspension and 32 mL of fresh complete medium (table 4.7) supplemented with 20% glycerol. Another series was prepared in the same manner, and kept at + 4 °C without glycerol, for immediate use.

Component	Quantity
Glucose	10 g/L
NH <sub>4</sub> Cl	1.0 g/L
NaHCO <sub>3</sub>	2 g/L
KCl	0.1 g/L
MgSO <sub>4</sub> * 7 H <sub>2</sub> O	0.2 g/L
NaCl	0.8 g/L
KH <sub>2</sub> PO <sub>4</sub>	0.1 g/L
CaCl <sub>2</sub> * 2H <sub>2</sub> O	0.02 g/L
HEPES	1 g/L
Yeast Extract (YE)	1 g/L
Microelements (*)	10 ml
Vitamin (*)	10 ml
Cysteine	40 g/L

\* Microelements (g/L): Nitriloacetic acid 2; MnSO<sub>4</sub> \* H<sub>2</sub>O 1; Fe(SO<sub>4</sub>)<sub>2</sub>(NH<sub>4</sub>)<sub>2</sub> \* 6H<sub>2</sub>O: 0,8; CoCl<sub>2</sub> \* 6H<sub>2</sub>O g/L; ZnSO<sub>4</sub> \* 7H<sub>2</sub>O; 0,0002; CuCl<sub>2</sub> \* 2H<sub>2</sub>O: 0,02; NiCl<sub>2</sub> \* 6H<sub>2</sub>O: 0,02; Na<sub>2</sub>MoO<sub>4</sub> \* 2H<sub>2</sub>O 0,02; Na<sub>2</sub>SeO<sub>4</sub>: 0,02; Na<sub>2</sub>WO<sub>4</sub>: 0,02

\* Vitamin (mg/L): Biotin: 2; Folic acid: 2; Pyridoxine hydrochloride: 10; Thiamine HCl: 5; Riboflavin 5; Nicotinic acid: 5; Calcium D-(+)-pantothenate: 5; B12: 0,1; p-Aminobenzoic acid: 5; Lipoic acid: 5

**Table 4.7:** ATCC medium 1754 (PETC Medium) adapted by Perez et.al., 2012

*Actinobacillus succinogenes* ATCC55618 (Guettler MV R. D., 1999), was used as a pure culture both at VITO both at Bologna university for the bioproduction of succinic acid. At VITO, already pre-existing 1 ml frozen stock supplemented with 20% sterile glycerol, were re-activated in two subsequent steps (as described later), for fermentation experiments. In Bologna, the strain was purchased from DSMZ (Braunschweig, Germany), and cultivated using Hungate technique (Hungate RE, 1969). The freeze – dried *A. succinogenes* powder was re-activated anaerobically (under 100% of sterile – filtered N<sub>2</sub>) in sterile anaerobic tube sealed with autoclaved teflon-coated butyl stoppers and autoclaved aluminum crimp sealers, with 20 ml of sterile 545 DSMZ medium (as reported in DSMZ instructions) for 24 hours at 37 °C and 100 rpm. The strain was then stocked at –80 °C in autoclaved criovials containing 0,5 mL of cell suspension and 0,5 mL of fresh sterile 545 DSMZ medium, supplemented with 20% of sterile glycerol.

## 4.3 H<sub>2</sub> PROJECT

### 4.3.1 Bioreactor set - up

The configuration of the reactor used for dark fermentation tests is reported in the process and instrumentations diagram (P&ID) in figure 4.2

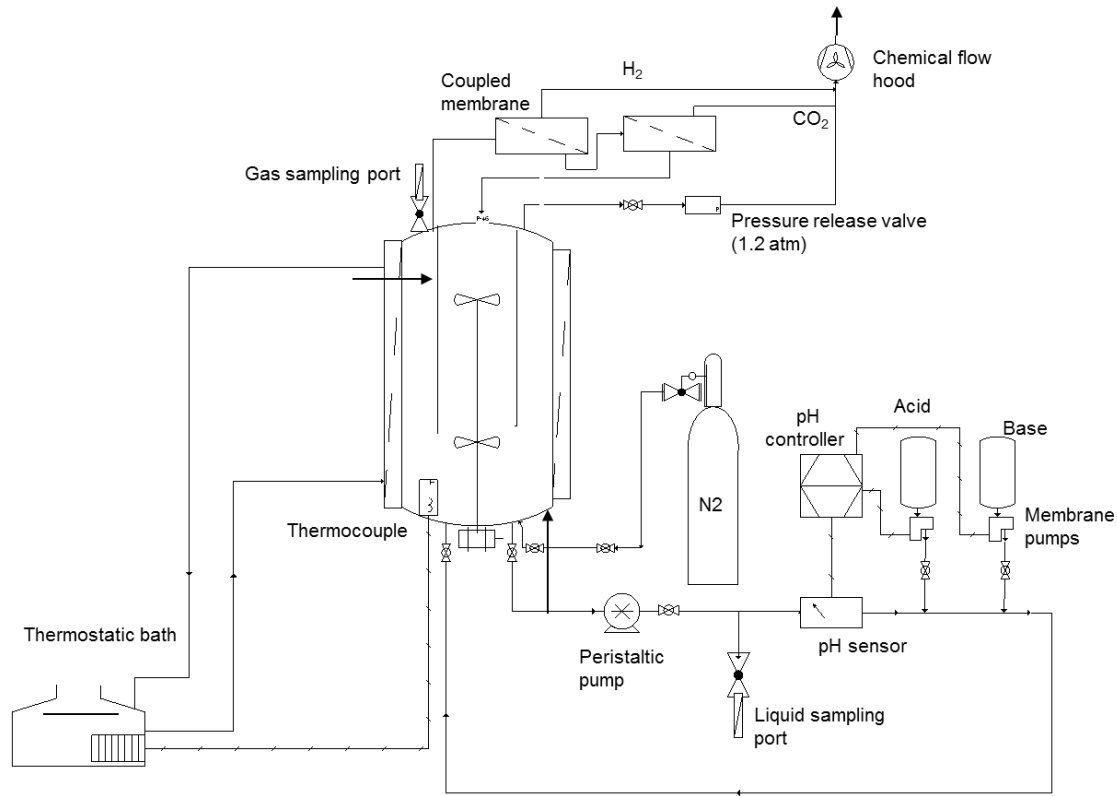


**Figure 4.2:** P&ID scheme of the SPCSTR used for biohydrogen tests

The reactor can be classified as a *structured packing continuous stirred tank reactor* (SPCSTR), and was entirely projected in our department, in particularly in collaboration with the Applied Fluid Dynamics and Mixing Group of Prof. A. Paglianti and Prof.ssa G. Montante, and the Diffusion in Polymers and Membrane Separation Group of Prof. M. G. Baschetti and G. C. Sarti. A lot of preliminary studies were performed in order to determine the mixing and the fluidodynamic behavior of the reactor, and the best membrane configuration (G. Montante F. L., 2010), (G. Montante A. P., 2012), (G. Montante M. C., 2013), (J. Catalano, 2012), (M. Giacinti Baschetti, 2013).

The reactor is a thermally - insulated 19 L cylinder stained steel vessel of 23,2 cm diameter ( $\varnothing$ ) and 46,4 cm highness (h) and equipped with an automatic pH correction system and a thermostatic bath

(MPM mod. M428 – MPM Instrument. Bernareggio, Milano) with a thermocouple for temperature control. The pH control system is a PID type formed by a temperature – resistant pH probe (Crison – pH 5330 – Crison Instrument. Barcelona, Spain), connected to a membrane pump (ITACA mod. PUMP KMF 1802 EP), controlled by an automatic control unit (CRISON pH29 – Crison Instrument. Barcelona, Spain). This pump was also connected to a two separate 2 L bottles of 2M phosphoric acid and 2M NaOH, for the pH adjustment. The pH was strictly controlled in the range between 7,4 and 7,6 (77 °C value). Mechanical stirring (150 rpm), pumps the liquid – gas phase into an internal “draft tube” of 9,6 cm diameter ( $\varnothing$ ) and 31,6 cm highness, towards the bottom of the reactor. Two PBT impellers (Pitch Blade Turbine) with different diameters (1,8 cm and 7,5 cm) were respectively positioned at 30,9 cm from the bottom (the smaller one) and 15,5 cm from the bottom (the bigger one). This innovative configuration allows the biphasic mixture ( $H_2$  – liquid medium) to continuously flowing from the upper impeller through the draft tube, toward the second impeller. Then, the second impeller pushes the gas – liquid mixture out from the bottom side of the draft tube (through small holes), distributing the gaseous phase to the whole surface of the reactor, outside the draft tube. In this configuration, the mixture is continuously pushed outside from the internal bottom part of the draft tube to the upper side of the vessel until the free surface. At this point, the biphasic mixture is separated, most of the  $H_2$  – rich gaseous phase flows externally to the reactor to a condenser and then to the separation module, the liquid medium re-enter in the draft tube through tailor – made big holes. In this configuration, no external pump or recirculating systems is needed to push the hydrogen towards the membrane, reducing fixed costs, and increasing the security of the entire plant. Moreover, a pressure difference from the two side of the membrane is created, allowing a better performance of the separation module. Internally to the draft tube, the carriers for the biofilm growth were enclosed in multiple tailor – made stained steel bags. To increase the security of the plant, an hydraulic guard at the end of the methane pipeline to avoid overpressure, together with a  $N_2$  bag (connected to the headspace of the reactor) to avoid depression, were added. In addition to this, a pressure relief valve is present to ensure a major control of the plant, and a connection with a 100% nitrogen line allows to create anaerobic condition for microbial growth. The  $H_2$  – rich biogas was sent through tap-water



condenser to a non-return valve towards a volumetric counter (*MilliGascounter Type MGC – 1*. Ritter Company – Bochum Germany) with a sensibility of  $\pm 3$  ml, and then aspirated by a chemical flow hood. A connection between the reactor and a 100% N<sub>2</sub> line was added, in order to permit the continuously flushing of the reactor for the removal of the oxygen.

In figure 4.3 and 4.4 are reported the “draft tube” configuration with a schematically direction of the gas – liquid mixture in the vessel, and a detail of the stained steel bags for the carrier. Figure 4.5, instead, shows a real picture of the plant.

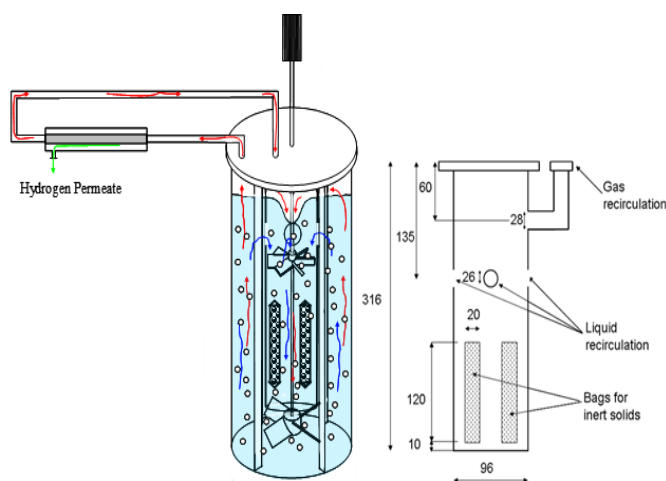


**Figure 4.3**

**Figure 4.3:** P&ID of the draft tube, and schematic recirculation flow



**Figure 4.4**

**Figure 4.4:** Detail of the stained steel bags for the carrier, and their disposition inside the draft tube



**Figure 4.5:** Real bio – H<sub>2</sub> plant

In all the experiments, the reactor was filled with 15 L of appropriate culture medium, and 4 L of headspace was kept.

#### 4.3.2 Bioreactor membrane coupled test

In addition to the described bioreactor set-up, during the coupling of the module for membrane – based bio – H<sub>2</sub> separation, the batch system was modified as follow.

The Diffusion in Polymers and Membrane Separation Group, after a deep screening, developed an innovative membrane based on Matrimid® 5218 polymer, (poly (3,3',4,4'-benzophenone tetracarboxylic dianhydride and diaminophenylindane)) a polyamide often used in membrane – based downstream processes (M. Giacinti Baschetti, 2013). The thickness and the area of the membrane were respectively 37 µm and 0.01 m<sup>2</sup> with an optimal work temperature of 65 °C. To avoid membrane disruption, in the permeate side, a 100 % nitrogen flux was continuously provided at 0,5 NL/min, together with an ejector system that ensure a depression of ~ 0,6 atm to force the biogas through the membrane module.

The membrane was prepared from a 5% Matrimid ® solution in dichloromethane left for 24 h under chemical flow hood for a slow evaporation of the solvent. Then, other 24 h at 200 °C was necessary to ensure the complete evaporation of the dichloromethane. Then, the membrane was inserted in the tailor – made stained steel support reported in figure 4.6.

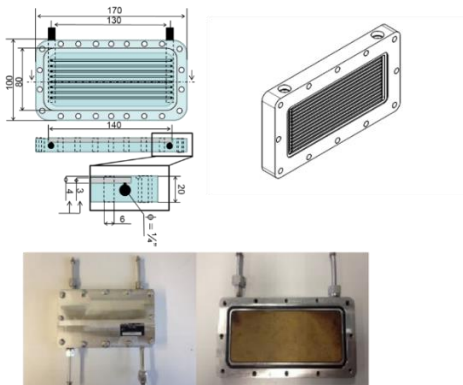


**Figure 4.6:**

*P&ID and real photos of membrane support. The reported values are in mm.*

The module with the membrane was coupled to the reactor after the condenser, in order to remove the major quantity of aqueous vapor, as depicted in the following P&ID (figure 4.7).

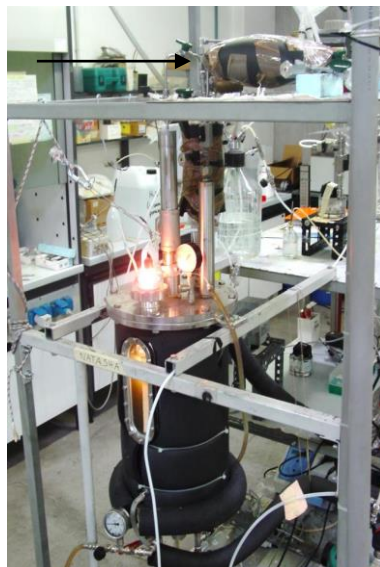
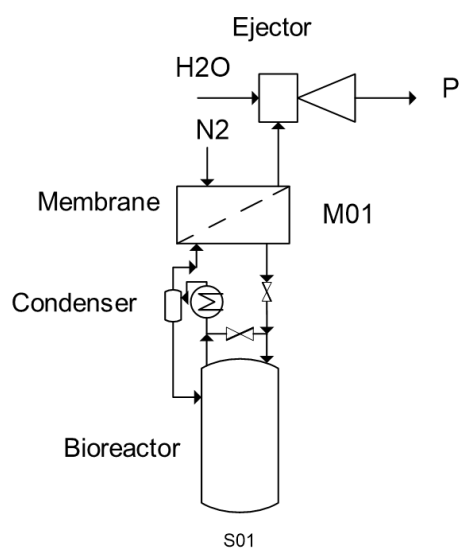


**Figure 4.7:**

On the left, a P&ID of the connection between reactor and membrane module. An overview of the entire plant is reported in figure 3.2

On the right, a real photo taken during the experiment. A black arrows indicates the membrane separation system

Due to the innovative nature of the experiment, in order to assess the feasibility of the integrated plant, a rich medium was used with glucose as a primary carbon source, and the reactor was inoculated with a 2% (v/v) pre-culture of *Thermotoga neapolitana*.

The pre-cultures were prepared in a series of 116 ml microcosm as follow: one criovial (2 ml) was added to 38 mL of 100% N<sub>2</sub>-stripped complete growth medium (table 4.6), closed with teflon-coated butyl stoppers and aluminum crimp sealers, and incubated at 77 °C for 24h at 100 rpm stirring in a Dubnoff orbital shaker (General Laboratory Supply, Pasadena, USA). The day after, 2% v/v (300 ml) of pre-cultures was used as inoculum for the reactor, filled with 14,7 L of the medium reported in table 4.6 without HEPES and resazurin. Prior to inoculum, the reactor was sparged with 100% N<sub>2</sub> flux for ~ 30', to ensure anaerobic condition. The experiment was performed for 260 hours at 77 °C and 250 rpm/min stirring (tip speed 0,61 m s<sup>-1</sup>), with a subsequent double feed of 2 g/L and 1,5 g/L of 100% N<sub>2</sub>-stripped glucose solution prepared in 120 ml bottle closed with teflon-coated butyl stoppers and aluminum crimp sealers, after 21 hours and 26 hours respectively, to ensure a high biomass concentration. The reactor was monitored (amount of biogas produced) and sampled 3 times/day, for

HPLC, GC and biomass analysis. The biogas was forced through the membrane after 48,5 hours (corresponding to the exponential phase of the microbial growth), and the integrated experiment continued for other 48,5 hours with a constant depression in the permeate side of the membrane between 0,5 and 0,6 bar. The biogas composition was determined both at the entry side of the module, and both at the permeate side 3 times/day. Also the retentate fluxed back to the reactor was monitored with the same frequency.

### *4.3.3 Microcosm Co-Feeding experiments*

In Cappelletti et.al., 2012, 116 ml microcosms - biohydrogen production tests using molasses and cheese whey were performed, in order to determine the  $H_2$  productivity (expressed in  $mmol\ H_2\ L^{-1}\ h^{-1}$ ), and  $H_2$  yield (expressed in  $mmol\ H_2\ g^{-1}\ SUGAR$ ). The tests were performed in triplicate, preparing the pre-inocula using the same procedure described above. The complete medium listed in table 4.6 was used for bioproduction tests, using molasses (20 g/L) or milk (12,5 g/L) whey in substitution of glucose, using 5% v/v of pre-culture as inoculum. All the molasses and milk whey concentration were chosen to start with the same total sugar concentration (10 g/L). The microcosms were prepared with 38 ml of medium, flushed with 100%  $N_2$  to ensure anaerobic condition, closed with teflon-coated butyl stoppers and aluminum crimp sealers, and inoculated for the fermentation at 77 °C and 100 rpm stirring in a Dubnoff orbital shaker (General Laboratory Supply, Pasadena, USA).

The same principles were used during the co-feeding experiments. Pre-inocula were prepared as described before, and 5% v/v was used to inoculate the 116 ml microcosms series, prepared in triplicate with media reported in table 4.6 without glucose, as follow. 12 microcosms (4 conditions in triplicate) with 38 ml of medium and 2 ml of inoculum, following this substrate scheme:

- ✓ 75% - 25% of molasses (20 g/L) and milk whey (12,5 g/L)
- ✓ 50% - 50% of molasses (20 g/L) and milk whey (12,5 g/L)
- ✓ 25% - 75% of molasses (20 g/L) and milk whey (12,5 g/L)
- ✓ Abiotic controls with no substrate and sterilized with 3 g/L of  $NaN_3$

Before inoculation, microcosms were prepared under laminar flow hood, flushed with 100% N<sub>2</sub> to ensure anaerobic condition, and closed with teflon-coated butyl stoppers and aluminum crimp sealers. The incubation conditions were the same as previously described (77 °C in a Dubnoff orbital shaker (General Laboratory Supply, Pasadena, USA), with 100 rpm stirring). The microcosms were monitored 2 times/day for 184,5 hours, analyzing quantity and composition of the biogas produced, and sampled for GC, HPLC and biomass analysis.

## 4.4 CH<sub>4</sub> PROJECT

### 4.4.1 Bioreactor set-up

The configuration of the reactor used for anaerobic digestion tests is reported in the process and instrumentations diagram (P&ID) in figure 4.7:

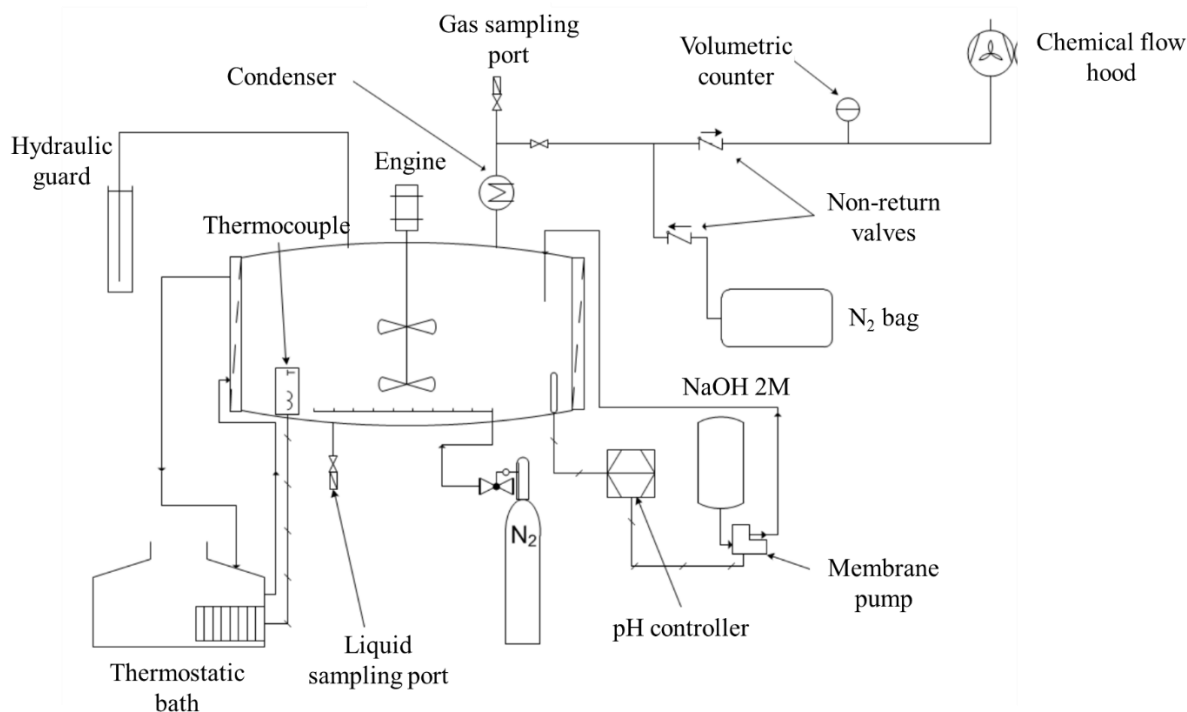


**Figure 4.7:** P&ID scheme of the CSTR used for anaerobic digestion tests

The reactor is a 29,7 L CSTR (*continuous stirred tank reactor*) stainless steel scale down (1:55 scale factor) of a “Sebigas” property industrial digester of 43,5 cm internal diameter ( $\varnothing$ ) and 20,0 cm highness (h) and equipped with an automatic pH correction system and a thermostatic bath (MPM mod. M428 – MPM Instrument. Bernareggio, Milano), with a thermocouple for temperature control. The pH control system is a PID type formed by a temperature – resistant pH probe (Crison – pH 5330 – Crison Instrument. Barcelona, Spain), connected to a membrane pump (ITACA mod. PUMP KMF 1802 EP), controlled by an automatic control unit (CRISON pH29 – Crison Instrument. Barcelona, Spain). The pump was also connected to a 2 L bottle of 2M NaOH, for the pH adjustment. The pH was strictly controlled in the range between 7,6 and 7,8 (55 °C value), optimum for the methanogenic activity (Jin-Young Jung, 2000). The mechanical stirring was performed with two impellers and principal turbine located eccentrically at  $\varnothing/3$  from the right side of the reactor. The mixing velocity was scaled down from the industrial value, keeping constant the tip speed of the impellers (2,85 m/s), and resulted in 679 rpm/min. Numerous fluidodynamic PIV studies were performed by our department in collaboration with the company and the Applied Fluid Dynamics and Mixing Group of Prof. A. Paglianti and Prof.ssa G. Montante, to determine the best impellers configuration for this eccentric mixing. A tailor made three – phase impeller was chosen to ensure an optimal miscelation (figure 4.8).

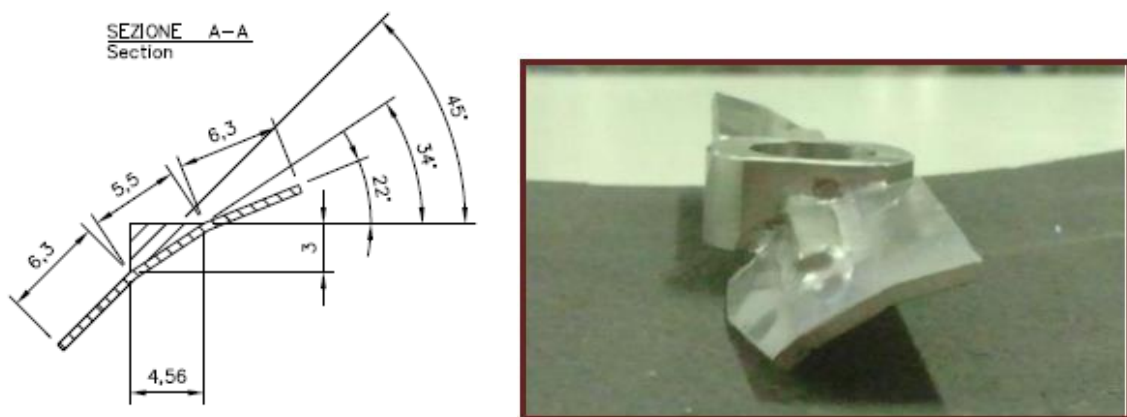


**Figure 4.8:** Detail of the two impellers used in the reactor. The expressed values are in mm

To increase the security of the plant, an hydraulic guard at the end of the methane pipeline to avoid overpressure, together with a N<sub>2</sub> bag (connected to the headspace of the reactor) to avoid depression,

were added. In addition to this, a pressure relief valve is present to ensure a major control of the plant, and a connection with a 100% nitrogen line allows to create anaerobic condition for microbial growth. Moreover, the  $\text{CH}_4$  – rich biogas was sent through a tap water condenser to non-return valve towards a volumetric counter (*MilliGascounter Type MGC – 1*. Ritter Company – Bochum Germany) with a sensibility of  $\pm 3$  ml, and then aspirated by a chemical flow hood.

In all the performed tests, the reactor was filled with 19,4 L of medium and 10 L of headspace was kept. The optimal temperature was set at 55 °C.

In the figure 4.9 is reported a vertical section and a real photo of the plant:

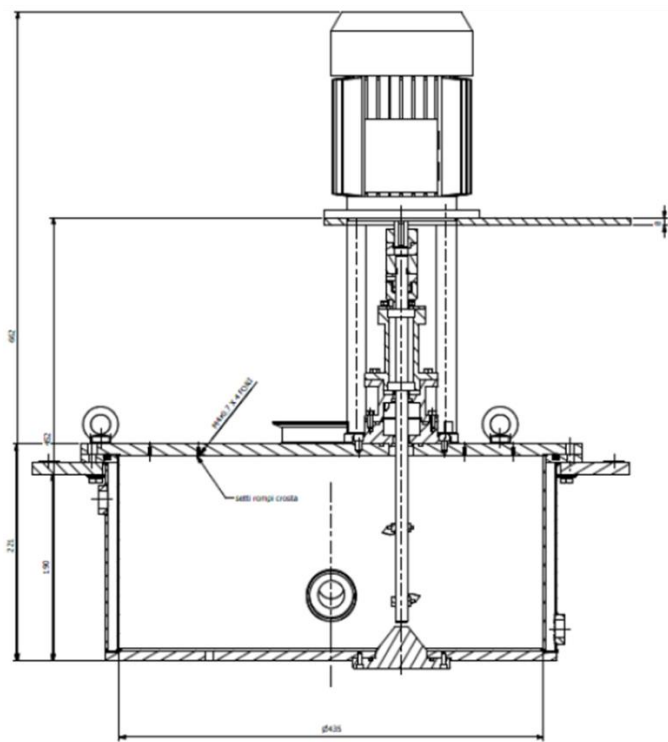


**Figure 4.9:** Vertical section and real photo of the bio-CH<sub>4</sub> plant

#### 4.4.2 Red grape pomace digestion with “DICAM” inoculum. Batch, - fed batch and continuous bioreactor tests

In these tests only grinded red grape pomaces as substrate and “SADAM” / “DICAM” inocula were used. Grape pomaces were analyzed in terms of % TS, % VS, % AS, % VS / % TS, pH and density (g/ml) as reported in table 4.1. Also the two inocula were characterized in terms of % TS, % VS and % VS / % TS (see table 4.8).

**“DICAM” & “SADAM” preliminary inocula characterization**

	% TS	% VS	% VS / % TS
“DICAM”	3,15	1,34	42,65
“SADAM”	4,00	3,07	76,71

**Table 4.8:** Physical characterization of the two methanogenic inocula.

With preliminary tests made by L. Bertin research group and published in peer – reviewed journal (Bertin, et al., 2012) and (L. Bertin et.al., 2012 (a)), the DICAM inoculum was chosen, due to the higher BMP (Bio-Methane Potential) and lower VFA (Volatile Fatty Acids) accumulation at 55 °C. From two of the pre-inocula kept at + 4 °C (see paragraph 4.2), two subsequentially propagation were made, in one bottle of 2 L and two bottles of 5 L respectively, prior reactor inoculation. No specific medium was used, only demi H<sub>2</sub>O and red grape pomaces as carbon and energy sources were used, in order to continue the acclimatization process of the chosen inocula. For every step the fermentation 2/3 of the total bottle volume was kept as headspace, and only 1/3 was filled with liquid, to ensure enough space for biomethane production, avoiding overpressure. Every propagation step was prepared as follow: 20% (w/w) of dried and grinded red grape pomaces and 10% (w/w) of the initial culture. Demi H<sub>2</sub>O was used to reach the right volume. This procedure was made under laminar flow hood and continuous 100% N<sub>2</sub> flux to limit oxygen contact. The pH was adjusted with NaOH 2M in the range between 7 - 8 and the bottle was closed with a tailor-made screw cap equipped with a manometer and two sampling port for liquid and gas (figure 4.10). Prior incubation in static condition at 55 °C, a continuous flux for ~ 30’ with 100% N<sub>2</sub> was necessary to obtain anaerobic conditions. The 2 L bottle



was monitored systematically every 2 – 3 days for biogas production and composition, pH and amount of VFA, until the acetic acid trend was descending and concentration was nearby 1 g/L. Then, two 5 L bottles were inoculated with the same procedure and in the same condition as reported before and monitored in the same way.



**Figure 4.10:** Real photo of the used 2 L bottle and detail of the tailor – made screw cap

For the first BATCH TEST with dried and grinded red grape pomace, the reactor was prepared as in the following table:

***Anaerobic digestion BATCH experiment: experimental conditions***

<i>Total reactor volume (L)</i>	29,7
<i>Total liquid volume (L)</i>	19,4
<i>Total headspace volume (L)</i>	10,3
<i>Substrate concentration (% w/w)</i>	20
<i>Inoculum</i>	“DICAM”
<i>Inoculum concentration (% w/w)</i>	10
<i>Temperature (° C)</i>	55
<i>Initial pH</i>	7,86
<i>Stirring (rpm/min)</i>	679

**Table 4.9:** Experimental conditions of the first batch test

The reactor was sparged for ~ 30' with 100% N<sub>2</sub> gas, and then monitored once a day for 84,85 days, in terms of volume and biogas composition, and 2 times/week in terms of volatile fatty acids determination. Moreover, two sample for total and volatile solids determination were taken at the beginning and at the end of the experiments, in order to determine the volatile solid conversion during the overall test.

For the second test performed in FED – BATCH condition, an integrated approach was necessary. Due to the necessity of a dilution of the digestate as soon as the acetic acid concentration was near 8 g/L, the experiment was performed in the initial stage in different bottle with increasing volume, and then in bioreactor, when the volume was enough to permit a good mixing. For every bottle – step, 2/3 of the total bottle volume was kept as headspace, and only 1/3 was filled with liquid, to ensure enough space for biomethane production, avoiding overpressure.

From the pre-inocula prepared as described in paragraph 4.2, a first scale – up was prepared in 1 L bottle equipped with a tailor-made screw cap equipped with a manometer and two sampling port for liquid and gas (figure 4.10). The bottle was composed by a 20% w/w of grinded red pomace as a substrate, and inoculated with 10% w/w of pre-inoculum. Demi H<sub>2</sub>O was used to reach the right volume, and pH was corrected in the range between 7 - 8. Prior incubation, a continuous flux for ~ 30' with 100% N<sub>2</sub> was necessary to obtain anaerobic conditions. For 19,5 days, the bottle was incubated without stirring at 55 °C and monitored one day for biogas production and composition, and twice a week for VFAs concentration. Moreover, two sample for total and volatile solids determination were taken at the beginning and at the end of this phase, in order to determine the volatile solid conversion. Then, a second dilution step was performed from 1 L bottle to a 6 L bottle, maintaining the same condition as described before, adding a solution of demi H<sub>2</sub>O and 20% w/w grinded red grape pomace. The 6 L bottle was prepared and incubated in the same condition, and monitored with the same frequency. After 41,6 days, another dilution was performed from 6 L bottle to 13 L in bioreactor, maintaining 16,7 L of headspace. In this phase, only demi water was used and no grape pomace were added. Moreover, no inoculation was performed. The temperature was set at 55 °C, and the pH was automatically maintained in the range between 7,6 and 7,8 with a constant

stirring (679 rpm/min). After a 30' flux of 100% N<sub>2</sub> to ensure anaerobic condition, the reactor was monitored until 87,9 days, one a day for biogas quantity and determination, and twice a week for HPLC analysis of VFAs. Again, a sample for total and volatile solids at the beginning and at the end of the fermentation was kept, to determine the total conversion.

The last biomethane experiment performed in this bioreactor, was a long CONTINUOUS test monitored for 246 days. Two main parameters ruled this long test, besides the VFAs concentration: the Hydraulic Retention Time (HRT) and the Organic Loading Rate (OLR)

$$HRT \text{ (day)} = \frac{V_L}{Q} \frac{\text{(liters)}}{\text{(liters/day)}}$$

$$OLR \text{ (grams * liter}^{-1} \text{ * day}^{-1}) = \frac{(g_{sub}/V_L)}{\Delta t} \frac{\text{grams}}{\text{liter day}}$$

Where V<sub>L</sub> is the liquid volume, Q is the volumetric flow rate in the reactor, g<sub>sub</sub> are referred to the grams of volatile solid fed every unit of time, and Δt is the time interval between two feeding of the reactor. The Hydraulic Retention Time represents the permanence time of a fluid elements in the reactor, and is a characteristic parameter of the chemostat – type reactors. The Organic Loading Rate instead, represents, the amount of substrate fed for every unit of reactor and every unit of time considered, and is a typical criterion for the continuous process. In this case, the amount of substrate was referred only to the volatile solid in the substrate, considering the percentage of volatile solids reported in table 4.1.

Is evident that the two parameters are strictly interconnected. In fact, the HRT depends from the volumetric flow rate, that depends from the substrate fed to the reactor. But the substrate fed is related to the OLR set. In this experiment, an initial volumetric flow rate (Q) of 0,22 L/day was set, that leads to a 68 days of HRT. According to the company partner of the project, the objective of the experiment was to increase systemically the OLR (keeping constant the HRT), from very low value (i.e. 0,4 g<sub>sv</sub>/L/day) to, at least, 1 g<sub>sv</sub>/L/day, and evaluate the performance of the plant.

In this assay, the digestate from the fed-batch experiment was used as inoculum, because the 87,4 days of continuous test increased the acclimatization of the consortium to a high value of VFAs. From the previous fed-batch experiment, the liquid volume was increased to 13,7 L, with a 16 L of headspace, and all the other conditions (pH, T °C, and stirring velocity) were the same. After a preliminary phase of discontinuous alimentation in the range of 0,1 – 0,3 g<sub>sv</sub>/L/day, to avoid higher amount of VFA in the reactor, the starting point was set with an OLR = 0,4 g<sub>sv</sub>/L/day. When the acetic acid detected was  $\approx$  to 1 g/L, an increasing of OLR from 0,4 g<sub>sv</sub>/L/day to 0,6 g<sub>sv</sub>/L/day was performed. Again, after a short period of stabilization, between 0,6 g<sub>sv</sub>/L/day and 0,9 g<sub>sv</sub>/L/day, the OLR was further increased from 0,9 g<sub>sv</sub>/L/day to 1,2 g<sub>sv</sub>/L/day. In the next table are reported the substrate solution fed (in terms of grams of grape pomace and VS of grape pomace, and water content), and the grams of the digestate discharged from the reactor.

***Anaerobic digestion CONTINUOUS experiment: OLR variation***

	Grape pomace fed (total g)	Grape pomace fed (total ml)	Grape pomace fed (total VS)	Demi H <sub>2</sub> O fed (total ml)	Digestate discharged (total ml)
0,4 g <sub>sv</sub> /L/day	7,2	5,99	6,00	214,01	220,00
0,6 g <sub>sv</sub> /L/day	10,80	8,99	9,00	211,01	220,00
0,9 g <sub>sv</sub> /L/day	16,2	13,48	13,50	206,52	220,00
1,2 g <sub>sv</sub> /L/day	21,69	17,97	18,00	202,03	220,00

**Table 4.10:** Grape pomace fed (in terms of total grams, total ml, and total VS) and amount of discharged digestate for every OLR. The value of grape pomace density and VS percentage reported in table 3.1 was used for the calculation of the ml of grape pomace and the grams of VS fed.

To ensure continuous conditions, every day the reactor was fed with the right amount of substrates. The used procedure is described as follow. Primarily, the right amount of the digestate was discharged

from the reactor, then in a 100% N<sub>2</sub> controlled atmosphere, grape pomaces and water separately (to avoid clogging of the valve), were added. On Friday, a cumulative fed until next Monday was performed, to ensure the fed of right amount of substrate/day. The reactor was monitored until the end of the experiment every 1 or 2 days for biogas quantity and determination, and twice a week for HPLC analysis of VFAs. Again, a sample for total and volatile solids at the beginning and at the end of the fermentation was kept, to determine the total conversion. Periodically, TS and VS analysis of the digestate were also performed.

#### *4.4.3 White pomace digestion with “DICAM” inoculum. BioMethane Potential (BMP) microcosms test*

In the meanwhile of the continuous bioreactor test with red grape pomace, a BMP (Bio Methane Potential) test was performed, in order to evaluate the yield and the production rate, using white grape pomace. A lot of literature studies (Kammerer, 2004), (Guerrero, 2008), reports the present of high content of polyphenols in white pomace, and their extraction. Moreover, polyphenols have a well – established toxic activity towards microbial growth (tannins, in particular) (Field J. A., 1987), (Field J. A., 1989), and for this reason, white pomace are less used in the anaerobic digestion process. A series of 8 microcosms, with two negative controls (digestate discharged from the reactor at 43,94 days at 0,4 g<sub>sv</sub>/L/day), three positive control (same digestate discharged from the reactor at 43,94 days at OLR = 0,4 g<sub>sv</sub>/L/day and fed with red grape pomace representative of the same OLR), and other three microcosms with the same digestate and fed with the same OLR with white pomace. Two of them were duplicate, and in the third one was added a microelement & vitamin solution, composed as follow.

- Microelements (g/L): Nitriloacetic acid: 2; MsSO<sub>4</sub> \* H<sub>2</sub>O: 1; Fe(SO<sub>4</sub>)<sub>2</sub>(NH<sub>4</sub>)<sub>2</sub> \* 6H<sub>2</sub>O: 0,8; CoCl<sub>2</sub> \* 6H<sub>2</sub>O: 0,2; ZnSO<sub>4</sub> \* 7H<sub>2</sub>O: 0,0002; CuCl<sub>2</sub> \* 2H<sub>2</sub>O: 0,02; NiCl<sub>2</sub> \* 6H<sub>2</sub>O: 0,02; Na<sub>2</sub>MoO<sub>4</sub> \* 2H<sub>2</sub>O: 0,02; Na<sub>2</sub>SeO<sub>4</sub>: 0,02; Na<sub>2</sub>WO<sub>4</sub>: 0,02.

- Vitamins (g/L): Biotin: 0,002; Folic acid: 0,002; Pyridoxine hydrochloride: 0,01; Thiamine HCl: 0,005; Riboflavin 0,005; Nicotinic acid: 0,005; Calcium D-(+)-pantothenate: 0,005; B12: 0,0001; p-Aminobenzoic acid: 0,005; Lipoic acid: 0,005.

As usual, to determine the initial conditions of the consortium in the digestate used as inoculum, %TS, %VS, ratio between %VS / % TS, and VFAs concentration, were determined prior inoculation.

The microcosm were prepared with 40 ml of digestate in 116 ml microcosms under laminar flow hood in presence of 100% N<sub>2</sub> flux to limit the oxygen contact. To maintain the same daily OLR, 1,346 g of red / white grape pomace were added to each microcosm, (except negative controls) calculated as the follow.

Daily grape pomace added to the reactor (g)	7,2
Daily demi H <sub>2</sub> O added to the reactor (g)	214,01
Corresponding g/L	$\frac{7,2}{\frac{214,01}{1000}} = 33,643$
Liquid volume in each microcosm	40
OLR <sub>REACTOR</sub> at 43,94 days (g <sub>SV</sub> * L <sup>-1</sup> * d <sup>-1</sup> )	0,4
Grape pomace/microcosm (g)	$\frac{33,643 * 40}{1000} = 1,346$

**Table 4.11:** Calculation for the feed of red/white grape pomace for every microcosm (except negative controls). Values of daily grape pomaces, and demi H<sub>2</sub>O added to the reactor was taken from table 3.10

Then, the microcosms were closed with teflon-coated butyl stoppers and aluminum crimp sealers and fluxed with 100% N<sub>2</sub> to ensure anaerobic condition for ~ 30'. Subsequently, they were incubated at 55 °C, for 44,05 days, at pH in the range between 7 – 8, and 100 rpm/minute stirring. Every 2 – 3 days, the biogas production and composition was monitored, and the concentration of VFAs was determined by HPLC.

#### 4.4.4 *Microcosms inhibition tests with “DICAM” inoculum*

Oxygen, acetic acid, and lignocellulosic – derived compounds, (HMF, syringaldehyde and ferulic acid), are three of the main inhibitory compounds of the anaerobic digestion process (Ye Chen, 2008), (Barakat et.al., 2012). With the “DICAM” consortium used for the bioreactor tests, two different experiments were made to determine quantitatively the amount of these inhibition.

##### ✓ O<sub>2</sub> INHIBITION

Starting from the digestate taken from the bioreactor at the end of the batch experiment (it means a consortium in an active methanogenic phase), a series of 15 microcosms were prepared (five different percentage of oxygen, from 1% to 4%, and a negative control with 0%, all the conditions tested in triplicate), as follow. 40 ml of methanogenic digestate in a 116 ml microcosm under laminar flow hood in presence of 100% N<sub>2</sub> flux to limit the oxygen contact. Then, the microcosms were closed with teflon-coated butyl stoppers and aluminum crimp sealers, and fluxed with 100% N<sub>2</sub> to ensure anaerobic condition for ~ 30'. No substrate was necessary, because the residual concentration of acetic acid from the previous batch test was 2,64 g/l, more than enough to observe and determine the initial velocity of the process. Anyway, to check the principal parameters of the consortia, the %TS, VS and the ratio %VS / %TS of the digestate – inocula were determined, prior inoculation. The microcosms, then, were spiked with the right amount of pure oxygen, as reported in the followed table 4.12, and subsequently incubated at 55 °C, for 51,29 days, at pH in the range between 7 – 8, and 100 rpm/minute stirring. Every day the headspace composition and the produced biogas were monitored. After 9,42 and 28,13 days, the microcosms were opened under 100% N<sub>2</sub>, a sample for VFAs analysis was taken, re-closed again with teflon-coated butyl stoppers and aluminum crimp sealers, fluxed for ~ 30' with pure N<sub>2</sub>, and spiked again with the same amount of oxygen, prior incubation in the same conditions as before.

***O<sub>2</sub> inhibition experiments: oxygen amount in the microcosms headspace***

	Negative control	1%	2%	3%	4%
<i>Oxygen amount (ml)</i>	0,00	0,76	1,52	2,28	3,04

**Table 4.12:** *Oxygen amount (in ml) spiked in every microcosm*

✓ **ACETIC ACID INHIBITION**

Starting from the digestate taken from the bioreactor at the interface between 0,4 g<sub>sv</sub>/L/day and 0,6 g<sub>sv</sub>/L/day (55 days of continuous experiment) a set of 21 microcosms were prepared in order to screen six acetic acid concentrations plus negative control (all the tests were performed in triplicate, and listed in table 4.13). To determine the initial acetic acid concentration of the negative control, a VFAs analysis was performed together with the determination of %VS, %TS and ratio %VS / %TS to ensure the best inoculum performance. In table 4.13 are listed the acetic acid screened concentration.

***Acetic acid inhibition experiments: CH<sub>3</sub>COOH amount in the microcosms liquid phase***

	Negative control						
<i>CH<sub>3</sub>COOH (g/L) final concentration</i>	0,79	1,95	4,81	5,98	7,85	10,63	12,51
<i>Pure CH<sub>3</sub>COOH (μl) added to the microcosm</i>	0,00	46,14	120,88	197,14	273,40	387,80	502,19

**Table 4.13:** *CH<sub>3</sub>COOH amount (in g/L) spiked in every microcosm*

The microcosms were prepared as follow. 40 ml of methanogenic digestate in a 116 ml microcosm under laminar flow hood in presence of 100% N<sub>2</sub> flux to limit the oxygen contact. Then, pure acetic acid was added to the microcosm with two 50 μl / 500 μl Hamilton ® liquid syringe (Hamilton company. Bonaduz – CH), and the pH was corrected in the range between 7 – 8. The microcosms were closed with teflon-coated butyl stoppers and aluminum crimp sealers and fluxed with 100% N<sub>2</sub>



to ensure anaerobic condition for ~ 30'. The spiked microcosms were incubated at 55 °C for 20,63 days with 100 rpm/minute stirring velocity, and monitored once every 1 – 2 days for biogas production, composition, and VFAs production.

✓ LIGNOCELLULOSIC DERIVED COMPOUNDS INHIBITION

At the end of the continuous test, to verify the status of the consortium and the possible inhibition from lignocellulosic derived compounds, BMP – Bio Methane Potential Test was performed according to the procedure reported in Angelidaki, M. et.al., 2009. From the exasusthed digestate of the reactor, a series of 6 micocosms, (one conditions plus negative control in triplicate), were prepared as follow. For the negative control, after an accurate determination of % TS, %VS, ratio between %VS / % TS, and VFAs concentration, to check the presence of enough substrate to continue the anaerobic digestion process, 40 ml of the digestate was used as negative control in 116 ml microcosms prepared under laminar flow hood, in presence of 100% N<sub>2</sub> flux to limit oxygen contact. After pH correction in the range between 7 – 8, the bottles were closed with teflon-coated butyl stoppers and aluminum crimp sealers, and fluxed for ~ 30' with 100% N<sub>2</sub> to ensure anaerobic conditions. Then, a 12,85 days of incubation were performed at 55 °C, and 100 rpm stirring velocity, sampling every 2 – 3 days for biogas volume and composition, and VFAs concentration. On the other hand, the principal test was prepared as follow. 120 ml of the same digestate of the reactor, was centrifuged at 1000 rpm for 10', 25 °C to precipitate only the particulate matter. Again, another centrifuge cycle was performed, at 8000 rpm for 10' at 4 °C, to precipitate the cells. Both particulate matter from the first centrifuge, both supernatant from the second one, was kept for a future chemical analysis, in order to individuate lignocellulosic – derivates compounds. The precipitate cells were, then, resuspendend (40ml/for every 116 ml bottle) in a sysntethic medium at pH 7,5 from Angelidaki, M. et.al. 2009, reported in table 4.14, with 2 g/L of glucose as only carbon source. It's evident that also the negative control was supplemented with the same amount of glucose.

Component	Quantity
NH <sub>4</sub> Cl	1.0 g/L
NaCl	0.1 g/L
MgCl <sub>2</sub> * 6 H <sub>2</sub> O	0.1 g/L
CaCl <sub>2</sub> * 2H <sub>2</sub> O	0.005 g/L
K <sub>2</sub> HPO <sub>4</sub>	1 g/L
Cysteine	0,5 g/L
NaHCO <sub>3</sub>	2,6 g/L
Microelements (*)	540 µl
Vitamins (*)	5,4 µl

\* Microelements 1X (g/L) FeCl<sub>2</sub> \* 4H<sub>2</sub>O 2; H<sub>3</sub>BO<sub>3</sub> 0,05; ZnCl<sub>2</sub>: 0,05; CuCl<sub>2</sub> \* 2H<sub>2</sub>O 0,038; MnCl<sub>2</sub> \* 4H<sub>2</sub>O: 0,05; (NH<sub>4</sub>)<sub>6</sub>Mo<sub>7</sub>O<sub>24</sub> \* 4H<sub>2</sub>O: 0,05; AlCl<sub>3</sub>: 0,05; CoCl<sub>2</sub> \* 6H<sub>2</sub>O 0,05; NiCl<sub>2</sub> \* 6H<sub>2</sub>O: 0,092; Na<sub>2</sub>SO<sub>3</sub> \* 5H<sub>2</sub>O: 0,1

\* Vitamins 100X (g/L): Biotin: 0,02; Folic acid: 0,02; Pyridoxine hydrochloride: 0,1; Thiamine HCl: 0,05; Riboflavin 0,05; Nicotinic acid: 0,05; Calcium D-(+)-pantothenate: 0,05; B12: 0,001; p-Aminobenzoic acid: 0,05; Lipoic acid: 0,05

Table 4.14: Synthetic medium for BMP assay, from Angelidaki, M. et.al. 2009

The microcosms were prepared under laminar flow hood, in presence of 100% N<sub>2</sub> flux to limit oxygen contact. The bottles were, then, closed with teflon-coated butyl stoppers and aluminum crimp sealers, and fluxed for ~ 30' with 100% N<sub>2</sub> to ensure anaerobic conditions. Then, a 12,85 days of incubation were performed at 55 °C, and 100 rpm stirring velocity, sampling every 2 – 3 days for biogas volume and composition, and VFAs concentration.

#### 4.4.5 Microcosms co-digestion of grape pomace with other by-products with “SEBIGAS” inoculum

The “SEBIGAS” consortium, a property of the company partner of the project, was used to screen different types of by-products for biomethane production, both alone, both in co-digestion with red grape pomace. In tables 4.1 are reported the physical characterization of the agro – industrial wastes used, in this experiment, instead, in table 4.15 are reported the same characteristics identified for the “SEBIGAS” inoculum:

##### “SEBIGAS” preliminary inoculum characterization

	% TS	% VS	% VS / % TS
“SEBIGAS”	7,63	5,93	77,80

Table 4.15: Physical characterization of the “SADAM” methanogenic inoculum.

Due to the high content of volatile solids ( $59,01 \pm 1,5$ ) g/L of the analyzed inoculum (the inoculum was isolated from an active digester fed with tomato peels), 1 liter of inoculum kept at  $+ 4\text{ }^{\circ}\text{C}$  was corrected with NaOH 2M to correct the pH in the range between 7 – 8, and closed with a tailor-made screw cap equipped with a manometer and two sampling port for liquid and gas (figure 4.10), and fluxed for  $\sim 30'$  with 100%  $\text{N}_2$  to ensure anaerobic conditions under laminar flow hood. Then, the bottle was incubated at  $40\text{ }^{\circ}\text{C}$  for 10,85 days in static condition and periodically monitored, in terms of volume and composition of biogas, and volatile solids. No substrate was added in order to reduce the amount of volatile solids below 10 g/L (comparable to the value of “DICAM” inoculum used for the previous test), and limit the contribution of the volatile solids of the inoculum, to the entire process. After this step, the inoculum was split in 24 microcosms to analyze 8 conditions, each one in triplicate: negative control with no substrate, four single by-products (red grape pomace, tomato peels, maize silage and olive mill waste), and three co-digestion indicated by the company (maize silage – tomato peels, maize silage – red grape pomace, and tomato peels – red grape pomace).

There were two principal conditions in this test:

- ✓ The ratio between the grams of volatile solids of the inoculum and the total grams of volatile solids of the substrates must be: 4:1

Equation 1:

$$\frac{g\text{ }VS_{inoculum}}{g\text{ }VS_{substrate\ 1} + g\text{ }VS_{substrate\ 2}} = 4$$

- ✓ The co-digestion ratio between the two substrates in terms of volatile solids must be 1:1, so:

Equation 2:

$$g\text{ }VS_{substrate\ 1} = g\text{ }VS_{substrate\ 2}$$

Considering the Equation 3 where:

$$g_{VS} = total\ mass * \% VS$$

And setting the total inoculum mass at 40,00 g for each microcosm, it's possible to calculate the mass (g) of every substrate to add in each microcosm. Substituting the Equation 3, in Equation 1, and considering (from Equation 2) equivalent the contribution of the volatile solids of the two substrates, the Equation 4 is derived:

Equation 4: 
$$\frac{\text{total mass}_{\text{inoculum}} * \% \text{VS}_{\text{inoculum}}}{2 * (\text{total mass}_{\text{substrate 1}} * \% \text{VS}_{\text{substrate 1}})} = 4$$

(substrate 1 was used as reference in the denominator, from Equation 2)

Solving this Equation 4, it's possible to obtain the mass (g) of every substrate to add in each microcosm, to respect the conditions imposed in Equation 1 and 2.

The microcosms were prepared as follow. Under laminar flow hood and a constant 100% N<sub>2</sub> flow to avoid oxygen contact, 116 ml bottles with 40 grams of liquid inoculum was prepared, and substrates were added as reported in table 4.16 (total mass columns):

Test	Inoculum		Substrate 1		Substrate 2		Total VS substrates	VS inoculum / VS substrates
	total mass (g)	VS (g)	total mass (g)	VS (g)	total mass (g)	VS (g)	g	
Negative control	40,000							
Grape Pomace	40,000	2,374	0,674	0,594			0,594	4,00
Maize Silage	40,000	2,374	1,108	0,594			0,594	4,00
Tomato Peels	40,000	2,374	1,054	0,594			0,594	4,00
Maize Silage - Tomato Peels	40,000	2,374	0,554	0,297	0,527	0,297	0,594	4,00
Maize Silage - Grape Pomace	40,000	2,374	0,554	0,297	0,337	0,297	0,594	4,00
Tomato Peels - Grape Pomace	40,000	2,374	0,527	0,297	0,337	0,297	0,594	4,00
Olive Mill Wastewater	40,000	2,374	28,811	0,594			0,594	4,00

**Table 4.16:** Microcosm co-feeding scheme

The bottles were, then, supplemented with 0,4 ml of a trace elements and vitamins solution 1:100 provided by the company, closed with teflon-coated butyl stoppers and aluminum crimp sealers, and fluxed for ~ 30' with 100% N<sub>2</sub> to ensure anaerobic conditions. Then, a 32,04 days of incubation were performed for grape pomace microcosms, 33,75 for maize silage and negative control, and 54,79 days for all the other microcosms, at 55 °C, and 100 rpm stirring velocity, sampling every day for biogas volume and composition, and every 3 – 4 days for VFAs concentration.

## 4.5 PROPANOL PROJECT

### 4.5.1 Screening and acclimatization of the consortia

Starting from the three initial consortia (“DICAM”, “OMW” and “MAIS”), kept at 4 °C, the main idea was to perform subsequent steps of growth, selection and acclimatization, in order to obtain an enriched consortium to tests for n-propanol production. In this tests, the main substrate will be the propionic acid, and an electron donor (pure H<sub>2</sub>) is necessary to perform the reduction reaction. Then, a DGGE analysis followed by sequencing process (described later), was performed to identify the main bacteria involved in the reaction.

For the GROWTH PHASE, 9 microcosms (a triplicate for each consortium) were set-up, as follow. Under laminar flow hood and a constant 100% N<sub>2</sub> flow to avoid oxygen contact, 116 ml bottles containing 32 ml of the following media (with 10 g/L of glucose as a carbon source), were prepared:

Component	Quantity
NH <sub>4</sub> Cl	1.0 g/L
NaHCO <sub>3</sub>	2,0 g/L
KCl	0,1 g/L
MgSO <sub>4</sub> * 7 H <sub>2</sub> O	0.2 g/L
NaCl	0,8 g/L
KH <sub>2</sub> PO <sub>4</sub>	0,1 g/L
CaCl <sub>2</sub> * 2H <sub>2</sub> O	0.02 g/L
HEPES	23,8 g/L
Yeast Extract	1 g/L
Cysteine	40 g/L
Microelements (*)	10 ml
Vitamins (*)	10 ml

\* Microelements 1X (g/L): Nitriloacetic acid: 2; MnSO<sub>4</sub> \* H<sub>2</sub>O 1; Fe(SO<sub>4</sub>)<sub>2</sub>(NH<sub>4</sub>)<sub>2</sub> :0,8; CoCl<sub>2</sub> \* 6 H<sub>2</sub>O: 0,2; ZnSO<sub>4</sub> \* 7H<sub>2</sub>O 0,0002; CuCl<sub>2</sub> \* 2H<sub>2</sub>O; 0,02; NiCl<sub>2</sub> \* 6H<sub>2</sub>O: 0,02; Na<sub>2</sub>MoO<sub>4</sub> \* 2H<sub>2</sub>O: 0,02; Na<sub>2</sub>SeO<sub>4</sub> 0,02; Na<sub>2</sub>WO<sub>4</sub>: 0,02.

\* Vitamins 1X (g/L): Biotin: 0,002; Folic acid: 0,002; Pyridoxine hydrochloride: 0,01; Thiamine HCl: 0,005; Riboflavin 0,005; Nicotinic acid: 0,005; Calcium D-(+)-pantothenate: 0,005; B12: 0,0001; p-Aminobenzoic acid: 0,005; Lipoic acid: 0,005

**Table 4.17:** Synthetic medium for growth phase of all the three consortia, derived and modified from Perez et.al., 2014.

Then, 8 ml of each consortium (20% v/v), were inoculated for a total liquid volume of 40 ml, and 76 ml of headspace. The pH was set at 6 with NaOH 2M, and the bottles were, then, closed with teflon-coated butyl stoppers and aluminum crimp sealers, and fluxed for ~ 30’ with 100% N<sub>2</sub> to ensure

anaerobic conditions. Then, a 4,98 days of incubation were performed at 30 °C and 100 rpm/min stirring velocity, monitoring daily the biogas production and composition, acid, alcohol and sugar concentration. Biomass was also quantified with Lowry's method. Five ml of each culture was sampled, supplemented with 20% v/v of glycerol, and kept at – 20 °C for PCR – DGGE analysis.

The SELECTION PHASE was developed with three subsequent cycles of pasteurization. There are literature evidences that the *Clostridia* class can represent the major types of bacteria that can reduce the short volatile fatty acid in the respective alcohol (Day, 1970), (Peralta-Yahya, 2012), (Isom, 2015). Moreover, all the *Clostridia* species form spores in response to environmental stress (e.g. high temperature), and this spores are resistant to very high temperature, (> 100 °C) (W.-W. Yang, 2009). In addition to this, thermic treatment inhibits the methanogenic part of the consortia, very sensitive to the temperature variations. S. H. Zinder et.al., 1984 demonstrate that in a thermophilic methanogenic reactor, more than 95% of the methanogenic activity was completely inhibited at 65 °C. For this double reason, 3 cycle of pasteurization at 63 °C for 30' each, were developed. Between each cycle, an incubation step with the same – rich medium reported in table 4.17 with 1,5 g/L of glucose as only carbon source, was performed.

Each of the nine microcosms derived from the growth phase, was propagated in two different 116 ml bottles; a total of 18 microcosms were prepared as follow. Under laminar flow hood and a constant 100% N<sub>2</sub> flow, 18 bottles were prepared with 31 ml of the same medium reported in table 4.17 (with no carbon source), and from each microcosm of the previous phase, two bottles were inoculated with 8 ml (20% v/v) of consortium. Then , the pH was set at 6 with NaOH 2M, and the bottles were, then, closed with teflon-coated butyl stoppers and aluminum crimp sealers. Immediately, one bottle for each couple was pasteurized, and the other one was left at room temperature. In the meanwhile, eighteen 1 ml solution of glucose 60 g/L for each microcosm was prepared in a small vial and adjusted at pH 6. At the end of the pasteurization process, to both of the vial for each couple, was added the entire glucose solution with a Hamilton 1 ml – precision liquid syringe (Hamilton Company. Bonaduz – CH), to reach a final concentration of 1,5 g/L and a total liquid volume of 40 ml. All the 18 microcosm

were fluxed for ~ 30' with 100% N<sub>2</sub> to ensure anaerobic conditions, and incubated for 24 hours at 30 °C and 100 rpm/min stirring velocity. The same procedure for all the 18 microcosms was repeated twice (pasteurization and glucose incubation), with the 1 ml glucose stock solution adjusted to 61,5 g/L the second day, and 63 g/L the third day, due to the increase of the liquid volume from 40 ml to 42 ml. No samples were taken.

For the ACCLIMATIZATION PHASE only propionic acid was used as a carbon source. All the 18 microcosms from the selection phase (3 consortia, each one pasteurized or not → 6 total consortia, each one in triplicate), were propagated again in new 116 ml bottles, with 32 ml of the same medium reported in table 4.17, at pH 6 without yeast extract, and with 2 g/L of propionic acid as only carbon source. The 18 microcosms were prepared in 116 ml bottles under laminar flow hood and a constant 100% N<sub>2</sub> flow to avoid oxygen contact, with 32 ml of the medium listed in table 3.14, at pH 6 (adjusted with NaOH 2M), with 2 g/L of propionic acid as only carbon source in presence or absence of 15 mM of sodium molybdate. Totally, 36 microcosms were analyzed. As reported by D.R. Ranade, 1999, sodium molybdate (Na<sub>2</sub>MoO<sub>4</sub>) is often used to inhibit the activity of sulphate reducing bacteria (SRB), inhibiting the adenosine 5 phosphosulphate reductase enzyme. This enzyme catalyze the reductive cleavage of APS (adenosine-5'-phosphosulfate) to sulfite plus AMP, and is a key protein in the metabolism of SRB (Alexander Schiffer, 2010), (João C. Queiroz, 2010). SRB, in fact, are anaerobic microorganisms that are widespread in anoxic environment, where they use sulphate (SO<sub>4</sub><sup>2-</sup>) as a terminal electron acceptor, resulting in the production of sulphide (HS<sup>-</sup>). The ubiquity of this type of microorganism, is absolutely related to the high metabolic adaptability, in fact, the can growth in presence of sulphate, both on dissimilatory metabolism using hydrogen as electron donor, both using fermentative metabolism where volatile fatty acids are used an electrons donor, and further oxidized to acetate and sulphide (Gerard Muyzer, 2008).

Due to the presence of propionate and sulphate in the media, in this phase the fermentative metabolism of SRB can compete with the desired VFA reduction metabolism of clostridia. For this reason, the

effect of supplementation of 15 mM of sodium molybdate was evaluated, in order to avoid undesired metabolisms.

All the bottles were inoculated (20% v/v) with 8 ml of the previous microcosms, and closed with teflon-coated butyl stoppers and aluminum crimp sealers. After 30' of 100% N<sub>2</sub> to ensure anaerobic conditions, a 29,63 days of incubation were performed at pH 6, 30 °C and 100 rpm/min stirring velocity. No samples were taken.

#### *4.5.2 Production tests*

As reported in the acclimatization phase, only propionic acid was used as carbon source. Moreover, in the test phase, the microcosms headspace was firstly replaced with nitrogen to ensure oxygen absence, then replaced with pure hydrogen, and finally pressurized to 1.5 bar of pure hydrogen. Hydrogen was used as electron donor to reduce short chain fatty acid to the respective alcohol, and the overpressure was necessary, (according to Kirsten J.J. Steinbusch et.al., 2008) since thermodynamic calculations pointed out that high hydrogen pressure decreases the  $\Delta G$  of the reaction. All the 36 microcosms from the acclimatization phase were propagated again in new 116 ml bottles, with 32 ml of the same medium reported in table 4.17, at pH 6 without yeast extract, and with 2 g/L of propionic acid as only carbon source. To be more clear, in table 4.18, are listed all the condition obtained after the acclimatization phase:



***Start conditions after the acclimatization phase***

<i>“DICAM” consortium</i>	NP <sub>DICAM</sub> (I)	NP <sub>DICAM</sub> (II)	NP <sub>DICAM</sub> (III)	P <sub>DICAM</sub> (I)	P <sub>DICAM</sub> (II)	P <sub>DICAM</sub> (III)
<i>“DICAM” consortium + sodium molybdate</i>	NP <sub>DICAM</sub> (I)	NP <sub>DICAM</sub> (II)	NP <sub>DICAM</sub> (III)	P <sub>DICAM</sub> (I)	P <sub>DICAM</sub> (II)	P <sub>DICAM</sub> (III)
<i>“OMW” consortium</i>	NP <sub>OMW</sub> (I)	NP <sub>OMW</sub> (II)	NP <sub>OMW</sub> (III)	P <sub>OMW</sub> (I)	P <sub>OMW</sub> (II)	P <sub>OMW</sub> (III)
<i>“OMW” consortium + sodium molybdate</i>	NP <sub>OMW</sub> (I)	NP <sub>OMW</sub> (II)	NP <sub>OMW</sub> (III)	P <sub>OMW</sub> (I)	P <sub>OMW</sub> (II)	P <sub>OMW</sub> (III)
<i>“MAIS” consortium</i>	NP <sub>MAIS</sub> (I)	NP <sub>MAIS</sub> (II)	NP <sub>MAIS</sub> (III)	P <sub>MAIS</sub> (I)	P <sub>MAIS</sub> (II)	P <sub>MAIS</sub> (III)
<i>“MAIS” consortium + sodium molybdate</i>	NP <sub>MAIS</sub> (I)	NP <sub>MAIS</sub> (II)	NP <sub>MAIS</sub> (III)	P <sub>MAIS</sub> (I)	P <sub>MAIS</sub> (II)	P <sub>MAIS</sub> (III)

**Table 4.18:** For every consortium (listed at left), are reported all the screened conditions for propanol production. NP / P means “Not Pasteurized / Pasteurized”, and I / II / III means the number of the replicate

Every triplicate was propagated as described before (2 g/L of propionic acid, and H<sub>2</sub> as electron donor). Two bottles were immediately incubated, the third was supplemented with 20 mM of sodium molybdate (Na<sub>2</sub>MoO<sub>4</sub>) to inhibit sulphate – reducing bacteria, and incubated.

The 18 microcosms were prepared in 116 ml bottles under laminar flow hood and a constant 100% N<sub>2</sub> flow to avoid oxygen contact, with 32 ml of the medium listed in table 4.17, at pH 6 (adjusted with NaOH 2M), with 2 g/L of propionic acid as only carbon source (and sodium molybdate where necessary). Then, all the bottles were inoculated (20% v/v) with 8 ml of the previous microcosms, and closed with teflon-coated butyl stoppers and aluminum crimp sealers. After 30’ of 100% N<sub>2</sub> to ensure anaerobic conditions, other 30’ with 100% H<sub>2</sub> was necessary to replace all the nitrogen. Hydrogen was correctly disposed under chemical flow hood during the procedure. After that, 0,5 bar of pure hydrogen relative pressure was instaurated in the 76 ml – headspace. The microcosms were incubated for 24,92 days and monitored two – three times per week, in terms of produced biogas and relative composition, alcohol, acids and biomass concentrations respectively with HPLC and Lowry’s method. Pressure, was re-established when the relative value was lower than 0,25 bar.

At the end of the experiment, 5 ml of each culture was sampled, supplemented with 20 %v/v glycerol and kept at – 20 °C for PCR – DGGE analysis.

## 4.6 SUCCINIC ACID PROJECT (VITO)

### *4.6.1 Bioreactor & Electrodialysis plants set - up*

This project was born with a deep collaboration between DICAM department in Bologna and the Flemish Institute For Technological Research (VITO) located in Mol (Flanders Region – Belgium) where I spent six month during my PhD period. In this period, the main idea was to develop a couple of batch/continuous fermentation in a 5 L bioreactor, to produce succinic acid (S.A.) and, in the meanwhile, perform a series of offline downstream studies with an electrodialysis (ED) separation plant, in order to couple directly the reactor to the ED plant, without cell retention steps.

ED is one of the most common downstream processes for the recovery of charged molecules produced by fermentation (Kurzrock, 2010), (Xiu, 2008), (Boyaval, 1987). Moreover, is used as a standard technique used in the desalination of sea-water (Lee, 2002), (Banasiak, 2007). In the case of organic molecules recovery, this process is always used after a cell retention step (ultra or microfiltration, usually). The innovation of this approach, is to avoid cell retention step, decreasing the complexity and the cost of the plant. ED, basically, is formed by the alternating of cation and anion membranes, that allows the transportation of ions under the influence of an electric field. More details, and physical principles explanation are given in the appropriate results section.

These are the P&ID flow diagrams of the separate fermenter and ED plant (figures 4.11 and 4.12).

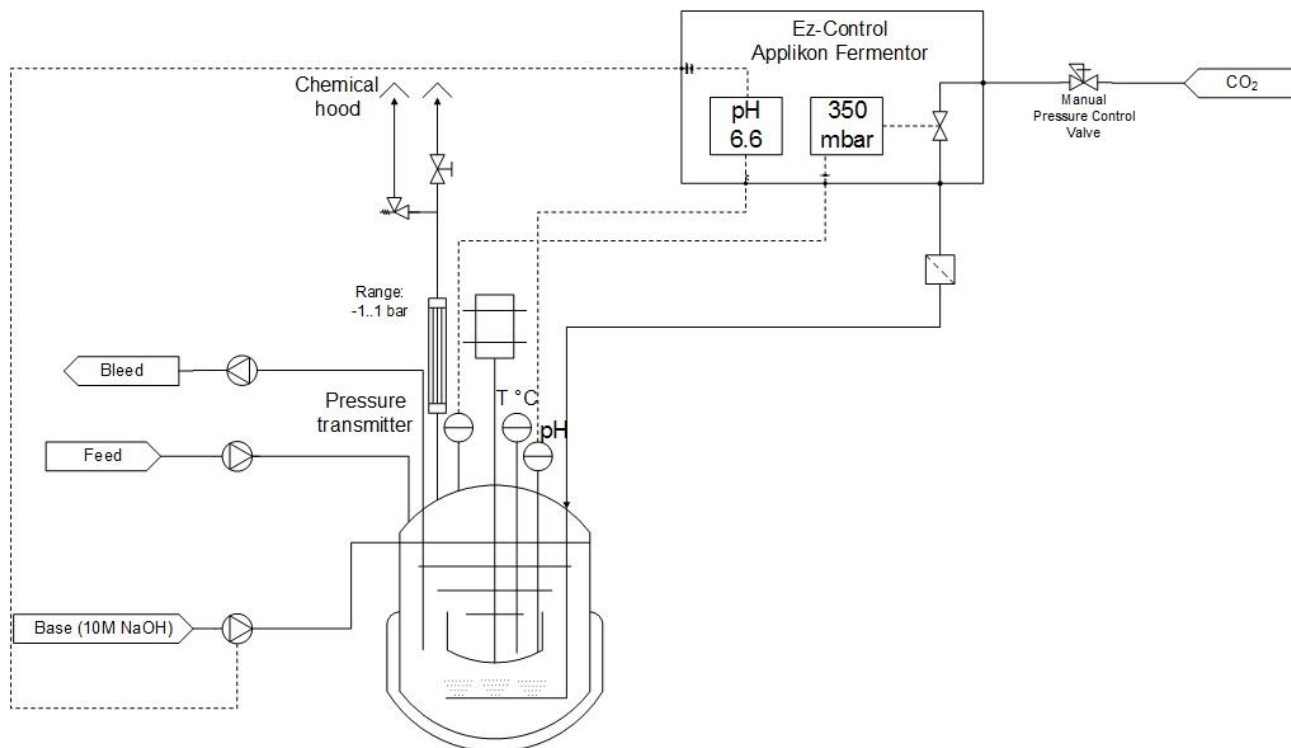


**Figure 4.11:** Scheme of the CSTR used for S.A production. “Bleed” and “Feed” units were only used in the continuous experiments

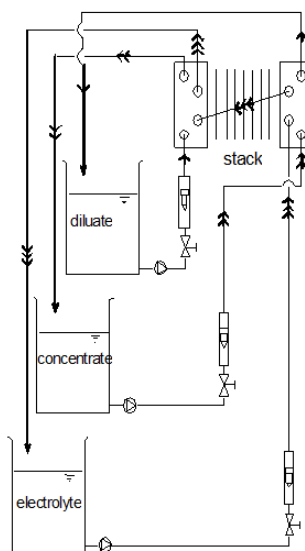


**Figure 4.12:** Scheme of the ED plant for offline tests

The reactor is a CSTR (*Continuous Stirred Tank Reactor*) 5 L jacketed and complete autoclavable glass vessel, with 3.4 L working volume, with a mechanical stirring system and two Rushton 45mm diameters impellers. 1,5 L was occupied by liquid medium and 1,9 L was headspace. A safety relief valve (+ 1 relative bar) and a sampling port pipe (4 mm diameters) with a threaded and interchangeable

20 ml glass bottle were present on the top side of the fermenter. 12 mm  $\text{dO}_2$ , pH and antifoam probes, interfaced with a E-Z automatic control, connected to a PC containing the supervisory control and data acquisition software BioXpert V2, were included in the system, with respective membrane – based pumps. Internal 12 mm L – type gas sparger, connected to a SUB 1000 pressure transmitter regulated by E-Z automatic control by PC software was present, in order to keep continuously the fermenter at 350 mbar relative pressure. The amount of gas inlet was regulated by an automatic rotameter. A PT 100 Temperature control present in the external jacket allows a precise temperature control ( $\pm 0,1$  °C). All the equipment was supplied by Applikon Biotechnology. Schiedam – The Nederland. Two additional peristaltic pumps (Watson-Marlow 520U. Cornwall UK) was used in the continuous experiments for the feed and the bleed sub-units, controlled by an automatic level sensor (Applikon Biotechnology. Schiedam – The Nederland).

The pre-pilot ED plant consists mainly of three independent storage tanks (concentrate, diluate, electrolyte solution) connected by separates loops to a multi – layer membrane stack, formed by alternate layer of anionic (PC-200D - Polymerchemie Altmeier GmbH – Germany) and cationic membranes (CMX - Neosepta, Tokuyama Soda, Japan). Three peristaltic pumps recirculate continuously the liquid between the compartments and the membrane stack. In this way, the ions present in the diluate compartment passes in the concentrate compartment, pushed by the electric field. The electrolyte solution (0,5M of  $\text{Na}_2\text{SO}_4$ ) re-equilibrates constantly the ion balance through anode and cathode compartments. Conductivity (an indirect measurement of ion migration) and pH are measured in the connection between the vessel and the stack for every loop. The voltage and the current across the stack are set by a direct current power supply. All these parameters are recorded and controlled by a computer, (including pumps flow rates and the relative pressure in the stack) equipped with “Labview” based software developed at VITO. Moreover, HPLC analysis of diluate and concentrate compartment were performed, in order to determine the succinic acid concentration in both diluate and concentrate compartment. In figures 4.13 is reported real photos of the fermenter:



**Figure 4.13:** Real photos of the CSTR fermenter.

The center of the separation process, is the membrane stack, formed by a variable number of layers of alternate cationic / anionic membranes (6 layers for the offline tests and 1 layer for the coupled experiment, see calculation later), separated by spacers and rubber gaskets.

In table 4.19 are reported the principal characteristics of the two membranes:

***Physico – mechanical characteristic of the ED membranes***

	Electric resistance ( $\Omega \cdot \text{cm}^2$ )	Burst strength (MPa)	Thickness (mm)	Temperature ( $^{\circ}\text{C}$ )	pH
<i>“CMX” cationic membrane</i>	3	c.ca 0,4	0,17	< 40	0 – 10
<i>PC-200D anionic membrane</i>	2	0,39 – 0,49	0,08 – 0,1	< 40	< 7

**Table 4.19:** Membrane characteristic. Sources: Neosepta Tokuyama Soda and GmbH – Germany.

In all the offline tests, the diluate solution was a 10 L synthetic fermentation media with succinic acid (S.A.) at different concentration (depending on the necessity), and acetic acid at 10 g/L. Moreover, pH was set at 6.6 and  $\text{NaHCO}_3$  10 g/L was added, to avoid pH troubles.

The concentrate solution was formed by S.A. 50, 60 or 70 g/L of S.A at pH 6,6. (depending on the necessity), and electrolyte was always 3 L of 0,5  $\text{Na}_2\text{SO}_4$ .

All the tests, both offline, both online, were performed at 180 L/h, 100 L/h and 150 L/h flow rate, respectively of diluate, concentrate and electrolyte compartment, to avoid difference in pressure through the membranes (that can increase the possibilities of leakages in the stack).

The coupled experiment was performed coupling the continuous – reactor experiment, to the concentrate compartment, and flowing directly the fermentation medium through the membranes, allowing the S.A. transfer to the concentrate solution. After that, a return – loop to the reactor was built, and the depleted media returned to the fermenter. The conditions of the experiment were the same as reported before, in terms of concentration of concentrate and diluate compartments, and flow rates.

#### 4.6.2 Reactor batch experiments

During preliminarily batch tests, both lactose, both milk whey, were used as substrates. For every experiments, two fixed pre-cultures step were performed, prior bioreactor inoculation.

##### ✓ Pre culture 1

The necessary medium is detailed in the following table.

Component	Quantity (g/L)
Glucose	20
Bacteriological peptone	10
Yeast extract	10
K <sub>2</sub> HPO <sub>4</sub>	3
NaCl	1
(NH <sub>4</sub> ) <sub>2</sub> SO <sub>4</sub>	3
MgCl <sub>2</sub> * 6H <sub>2</sub> O	0,3
CaCl <sub>2</sub> * 2H <sub>2</sub> O	0,3
Na <sub>2</sub> CO <sub>3</sub>	5
BIS-TRIS	20
FeSO <sub>4</sub> * 7H <sub>2</sub> O	0,005

*Table 4.20: S.A. production pre – culture 1 medium.*

Bacteriological peptone, yeast extract,  $K_2HPO_4$ , NaCl and  $(NH_4)_2SO_4$  were dissolved in 600 ml of demi  $H_2O$  (for 1 L preparation), adjusted at pH 6,6, and autoclaved. All the other components were dissolved in 400 ml of demi  $H_2O$  (for 1 L preparation), adjusted at pH 6,6 and sterile filtered in the autoclaved bottle with 0,22 VacuCap® sterile filter (Pall corporation U.S.A.), under laminar flow hood. Then, with this medium, three separate sterile 15 ml pre – culture tubes were prepared: two of them were inoculated under laminar flow hood with 1 ml of frozen culture (see paragraph 4.2), in 9 ml of medium (10 % v/v), the other was filled with 10 ml of medium, as negative control. All the tubes are closed in an anaerobic jar equipped with an AN0035 - AnaeroGen bag (Thermo Fisher Scientific U.S.A.) to create anaerobic conditions and a BR0055 – AnaeroIndicator (Thermo Fisher Scientific U.S.A.) to check the oxygen absence, and incubated for 24 hours at 37 °C and 150 rpm/min stirring velocity. No samples were taken; only at the end of the incubation period, OD was determined by a spectrophotometer (ASD19-N 10 mm single pathway. Optek-Danulet. Essen – Germany).

#### ✓ Pre culture 2

The necessary medium is equivalent to the previous one reported in table 4.20, except for the presence of lactose 20 g/L instead of glucose 20 g/L. The preparation procedure is the same. With this medium, three separate sterile 150 ml pre – culture flasks were prepared: two of them were inoculated in glove-box chamber (GP Campus series. Jacomex company Dagneux - France) with all the previous pre – culture 1, in 90 ml of medium with lactose (10 % v/v), the other was filled with 100 ml of medium, as negative control. All the flasks are closed in an anaerobic jar equipped with an AN0035 - AnaeroGen bag (Thermo Fisher Scientific U.S.A.) to create anaerobic conditions and a BR0055 – AnaeroIndicator (Thermo Fisher Scientific U.S.A.) to check the oxygen absence, and incubated for 24 hours at 37 °C and 150 rpm/min stirring velocity. No sample were taken; only at the end of the incubation period, OD was determined spectrophotometrically.

After the pre-culture steps, the fermenter medium was prepared as follow (final liquid volume 1,5 L).

Component	Quantity (g/L)
Lactose	40
Bacteriological peptone	10
Yeast extract	10
K <sub>2</sub> HPO <sub>4</sub>	3
NaCl	1
(NH <sub>4</sub> ) <sub>2</sub> SO <sub>4</sub>	3
MgCl <sub>2</sub> * 6H <sub>2</sub> O	0,3
CaCl <sub>2</sub> * 2H <sub>2</sub> O	0,3
Biotin	0,0002
FeSO <sub>4</sub> * 7H <sub>2</sub> O	0,005

*Table 4.21: Medium for the fermenter with lactose test*

Component	Quantity (g/L)
Milk whey (equivalent lactose)	40
Bacteriological peptone	10
K <sub>2</sub> HPO <sub>4</sub>	3
NaCl	1
(NH <sub>4</sub> ) <sub>2</sub> SO <sub>4</sub>	3
MgCl <sub>2</sub> * 6H <sub>2</sub> O	0,3
CaCl <sub>2</sub> * 2H <sub>2</sub> O	0,3
Biotin	0,0002
FeSO <sub>4</sub> * 7H <sub>2</sub> O	0,005

*Table 4.22: Medium for the fermenter with milk whey test*

For every test, the fermenter was prepared with bacteriological peptone, yeast extract (only for lactose test), K<sub>2</sub>HPO<sub>4</sub>, NaCl and (NH<sub>4</sub>)<sub>2</sub>SO<sub>4</sub> in 900 ml of demi H<sub>2</sub>O, adjusted at pH 6,6, and autoclaved with only the relief valve open, without pressure transmitter. All the other medium components were dissolved in 450 ml of demi H<sub>2</sub>O (for 1 L preparation), adjusted at pH 6,6 and sterile filtered in an autoclaved bottle with 0,22 VacuCap® sterile filter (Pall corporation U.S.A.), under laminar flow hood. With sterile tubes (Masterflex Norprene tubing A 60 G. Cole Parmer company Vernon Hills U.S.A.), and the equipped peristaltic pump, the second part of the media were mixed into the autoclaved fermenter (with closed relief valve), in a sterile environment. The pressure transmitter was, then, connected to the headspace fermenter (in sterile conditions), and all the probes (pH & dissolved O<sub>2</sub>), and pumps were properly calibrated. Prior inoculation, a 30' CO<sub>2</sub> sparging in the fermenter was necessary, to avoid oxygen presence, and to ensure enough carbon dioxide. CO<sub>2</sub>, in fact, is necessary for S.A. production because CO<sub>2</sub> is a carbon source, together with lactose (Ke-Ke Cheng, 2012). After 30' the dissolved O<sub>2</sub> was generally lower than 1%, and the fermenter was sterile inoculated with 150 ml of pre – culture 2 (10% v/v), with a peristaltic pump. The pH was set at 6,6 and a bottle of sterile 10M NaOH was connected to keep the right value during the fermentation. Lastly, the pressure was set at 350 relative mbar, the temperature at 37 °C, and the stirring value at 200 rpm/min. The fermenter was sampled 2 – 3 times day to check pH, OD, and medium composition.



#### 4.6.3 Electrodialysis optimization: LCD determination

LCD (Limiting Current Density), is defined as the current value applied to the membranes to ensure the maximum transportation efficiency. The maximum efficiency is reached when during the transport across the membranes, the ion concentration becomes zero on the surface of ion exchange membranes (more detail are provided in 5.4.2). Therefore, it is important to determine LCD for designing and operating with electrodialysis systems.

In this test, the ED plant was prepared as follow. Six membrane layers closed in a compact stack, connected to the three compartment (concentrate, diluate and electrolyte). The 2 L concentrate was prepared with 50 g/L of succinic acid at pH 6,6, and the 3 L concentrate with 0,5M of Na<sub>2</sub>SO<sub>4</sub>. Then, five different type of 10 L diluate solution (A – E) were prepared (pH 6,6).

***Diluate solution used in the ED determination test***

	Succinic acid (g/L)	Acetic acid (g/L)	NaHCO <sub>3</sub> (g/L)
<i>A</i>	30	10	10
<i>B</i>	20	6,67	6,67
<i>C</i>	10	3,33	3,33
<i>D</i>	5	1,67	1,67
<i>E</i>	2,5	0,83	0,83

***Table 4.23: LCD determination: Diluate solution composition***

The flow rates were the same as described previously. For every diluate solution tested, the system was refilled with new concentrate and electrolyte solutions.

After a few minutes of flow rates equilibration, an electric field was applied was applied to the system. The value was stepwisely increased slowly (60 mA/min), and every minute were monitored the applied current (A), voltage (V) and resistance ( $\Omega$ ) values in the system. Moreover, at the beginning and at the end of the experiments, pH and conductivity (mS/cm) were checked for all the three solution, and succinic acid titer in the concentrate and diluate compartments was analyzed by HPLC. The test with the solution A was monitored for 93', the tests with the solutions B, C, D, and E were

monitored respectively for 63', 34' 17' and 11'. For every test, the reciprocal of the current set value every minutes was plotted against the resistance registered from the system. The minimum of the resulting curve is the reciprocal of the desired LCD value. Reporting the conductivity (continuously monitored online in every test through the PC software) in function of the obtained LCD from the previous graphs, it's possible to obtain an experimental relationship that tell us which current is necessary to apply to the system, to ensure the best performance of the process for every conductivity value of the diluate solution.

The same LCD determination was performed with a real centrifuged fermentation broth (20' 4 °C, 8000 rpm/min), with a well – known succinate/acetate concentrations, as diluate compartment. All the other solutions, flow rates and operational procedures were the same. the experiment was performed for 50', sampling as reported previously every minutes.

#### *4.6.4 Electrodialysis tests with synthetic and real broth*

After the LCD determination, numerous separation tests were performed offline both with synthetic both with real broth, prior coupling to the fermenter.

Following the relationship established in the LCD experiment between LCD and conductivity, a separation test was performed using a synthetic solution in the diluate compartment. In this test, the concentrate and the electrolyte compartment was prepared as previously reported, and for the diluate synthetic medium was used the solution “A” of the LCD determination assay. The conductivity in both diluate and concentrate compartment was measured and registered online (every 15 seconds) and the applied current was manually set-up following the previous relationship. Moreover, the current and the resulting voltage are monitored continuously online, instead the pH, the volume changing in every compartments and the titer of acetate and succinate was measured offline, sampling 20 ml from all the compartments 3 – 4 times/day. The experiment was followed for 20,43 hours until the diluate conductivity was below 7 mS/cm. At this point, the diluate compartment was refilled with another solution “A” without change neither the concentrate, nor the electrolyte compartment. The applied

current was again set-up to the right value flowing the conductivity, and the second part of this experiment was prolonged for other 6,16 hours, monitoring the same parameters with the same frequency as described in the previous description.

Then, a real experiment, with both centrifuged and both non – centrifuged real culture broth with a well – known succinate/acetate concentrations, as diluate compartment was developed. A LCD determination for 50' was performed with centrifuged broth, and a real separation test with real non – centrifuged broth was performed and followed for 11,91 h sampling every hour. All the conditions (flow rates, concentrate and electrolyte volume and concentrations, relationship conductivity/LCD and sampling frequency), were initially the same as the previous test. Due to unexpected results (explained in the appropriate results section), after 6 hours, the energy supplying was switched to constant voltage value, fixed at 4,2 V, resulting in 0,8 Ampère, till the end of the experiment, without following anymore the conductivity/LCD relationship.

#### 4.6.5 *Fermenter – ED coupled test*

The integrated experiment was performed coupling the fermenter working in steady state condition, to the ED plant. The fermenter was prepared in a batch mode from the frozen inoculum as described in paragraph 4.6.2, using 50 g/L as lactose concentration, instead of 40 g/L. After 23,78 hours of batch phase (where the reactor was sampled 2 times/day), the continuous mode was set-up with 16,8 hours as  $\tau$  (residence time). So, the “feed” flow rate was calculated as follow:

$$Flow\ rate\ \left(\frac{L}{h}\right) = \frac{working\ volume\ (L)}{\tau\ (h)}$$

and results in 0,089 L/h (1,49 ml/min), with a corresponding dilution rate (“D”) of 0,059 h<sup>-1</sup>, calculated as follow.

$$D\ (h^{-1}) = \frac{1}{\tau\ (h)}$$

The fermenter was sampled 3 times/day. In the meanwhile, the ED plant (1 membrane layer was used instead of six. Explanation in the appropriate paragraph in the result section) was prepared as follow. Both membrane and the supporting part of the stack, were kept in ethanol 80% for 72 hours. Then, the stack was built under laminar flow hood and connected in sterile environment with concentrate and electrolyte compartment. The concentrate compartment was equipped with a UV lamp (Sadechaf company. Turnhout – BE), between the tank and the stack. This part of the plant was sterilized using a EPA registered antimicrobial agent: Oxonia ® solution 3% (v/v) (Ecolab Industries St.Paul – MN. U.S.A.). Concentrate and electrolyte compartment were filled with 5 L of Oxonia ® solution and flowed through the membrane stack for 2 hours (same flow rates as reported previously), and fluxed overnight with the same amount of sterile H<sub>2</sub>O, to eliminate all the traces of Oxonia ® detergent. Then, the concentrate compartment was filled with a 2 L sterile solution of 50 g/L of succinic acid, and the electrolyte with a 3 L sterile solution of Na<sub>2</sub>SO<sub>4</sub>, and fluxed for 1 hour to remove all the water from the pipeline. The entire plant was kept in this conditions (only the recirculation between stack and electrolyte/concentrate compartment was switched off), until the moment of the real coupling. After 150,73 hours of continuous fermentation, the diluate side of the ED plant was coupled to the fermenter with autoclaved tubes, and the pumps of all the three compartments were switched on. After 5 minutes of stabilization, 4,2 Volt was supplied through the platinum electrodes of the stack. The experiment was prolonged until 333,15 total hours, and sampled 3 times/day. 5 ml of liquid medium were taken from the fermenter, and analyzed in terms of pH, OD, conductivity and medium composition. Other 5 ml were taken from the concentrate tank and analyzed in terms of pH, conductivity and composition. Moreover, pressure and flow rate of each compartment, with voltage and current supplied were registered.

To have an idea of the fouling effect on the membranes performance, three LCD determination were performed during the experiment, at 167,21 hours – 215,07 hours and 311,23 hours. In those moments, the power was switched from constant voltage to constant current, and slowly incremented (60 mA/min). The resulting resistance was monitored every minutes and plotted in the same graph described in section 3.6.3 (1/current vs resistance). The minimum value was the LCD; no sample were

taken during LCD determination. The first experiment (167,21 h) was prolonged for 45', the second (215,07 h) and the third one (311,23 h) for 44'. At the end of every test, the power was switched again to constant voltage (4,2 V).

## 4.7 SUCCINIC ACID PROJECT (DICAM)

In Bologna, the main idea of the project, was to develop a suitable process for biofilm growth, choosing the best support for microbial growth, evaluate the principal kinetic parameters of the immobilized process ( $\mu_{\max}$ ,  $K_s$ ), both for lactose, both for milk whey in microcosms tests, and evaluate the performance on a 1 L scale plant formed by a column packed with the best identified support.

### 4.7.1 Bioreactor set - up

The configuration of the reactor used for S.A. production tests is reported in the process and instrumentations diagram (P&ID) in figure 4.14:

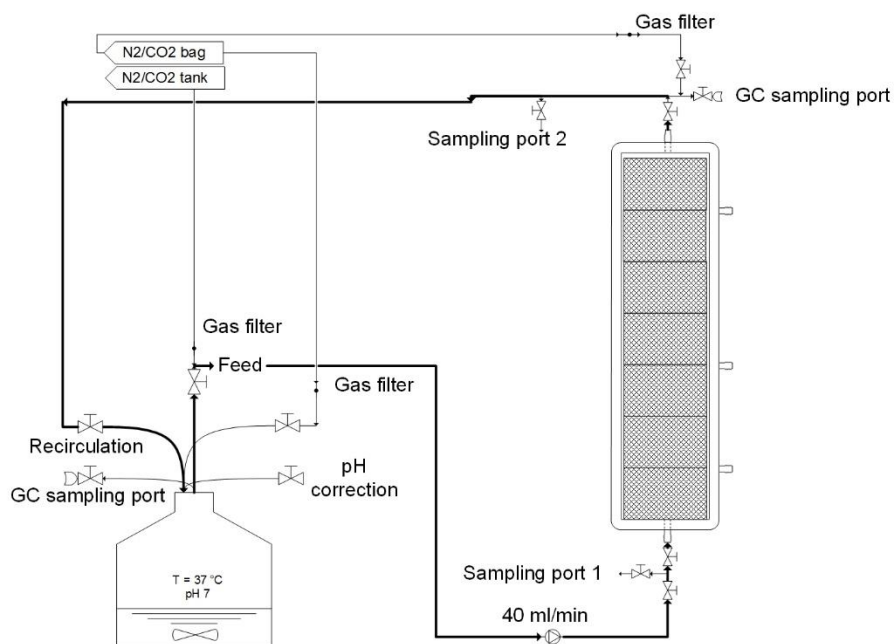


**Figure 4.14:** P&ID scheme of the PFR used for succinic acid production tests

The principal part of the plant is formed by a sterile vacuum-sealed 1,04 L glass column (4,9 cm internal diameter and 58,5 cm highness) packed with 840 grams of Glaxstone®, the chosen carrier (see next paragraph for the characteristic), with two sampling ports at the entrance (bottom side – sampling port 1) and at the exit of the column (upper side – sampling port 2), and other three additional sampling ports all along the length (FAVS Company. Bologna – Italy). The packed column has a bulk density of  $808 \text{ g}_{\text{solid carrier}} / \text{L}_{\text{reactor}}$  and a total liquid volume of 579 ml. The bottom side of the column was connected through a Masterflex L/S 0.1 HP 1-100 RPM peristaltic pump and an autoclaved Norprene® tube (A60 G) (Cole-Parmer. Vernon Hill – USA), with a sterile 2 L bottle closed with a tailor-made screw cap (figure 3.10) equipped with a gas sampling port, and a valve for manual pH adjustment. Both column headspace, both the upper side of the column were connected to a pure CO<sub>2</sub> bag, to maintain atmospheric pressure, anaerobic environment and ensure enough carbon dioxide for the production phase. The sterile condition was provided by GVS 0,22 µm cellulose acetate filter, (GVS Filter Technology. Stanford – ME – U.S.A.). The same connections were used to connect the reactor to another bag, filled with 13% of CO<sub>2</sub> and 87% of N<sub>2</sub>, during the biofilm growth phase. Moreover, a 100% N<sub>2</sub> supply line was used to flux the reactor and the bottle in the preparation phases, to strip all the oxygen. At the upper side of the column, a gas sampling port was added, to check the gas composition, during all the phases. The liquid from the bottle (stirred at 500 rpm/min, to increase gas – liquid mass exchange), flows through the column (and through the carrier) from the bottom side at 40 ml/min, and recirculated again into the bottle. All the plant was kept at constant 37 °C. In figure 4.15 there is a real photo of the plant:



*Figure 4.15: Real photo of the succinic acid bioproduction packed – column plant*

### 4.7.2 Carrier screening

In the first part of the project, 5 different commercial carriers were screened, in order to identify the best for the biofilm growth. The principal characteristics are reported in table 4.24:

**Carrier specifics for *A. succinogenes* immobilization**

	Material	Surface Area (m <sup>2</sup> /m <sup>3</sup> )	Bulk Density (g/L)	Porosity (%)	Ø (cm)	h (cm)	Company
<i>Biomax</i> ®	Ceramic	250	753,2	65,9	(0,91 ± 0,04)	(1,10 ± 0,04)	Askoll ®
<i>Kaldnes K1</i> ®	HDPE	950	165,5	/	(1,06 ± 0,05)	(0,75 ± 0,01)	EvolutionAcqua ®
<i>Bio-Flo 9 Sinker</i> ®	HDPE	800	190,9	/	(1,05 ± 0,10)	(0,80 ± 0,01)	SmokyMountain ®
<i>Poraver</i> ®	Expanded glass	/	205,5	38,1	(0,29 ± 0,05)	/	Poraver ®
<i>Glaxstone</i> ®	Syntherize d glass	270	717,9	76,4	(1,99 ± 0,28)	(1,00 ± 0,01)	WaveAcquaristic ®

**Table 4.24:** Principal characteristic of the tested carriers for *A. succinogenes* immobilization

Figure 4.16 reports real photos of every carrier. Every support was autoclaved prior utilization.



**Figure 4.16:** From left side: Poraver ®, Glaxstone ®, Bio-Flo 9 sinker ®, Kaldnes K1 ®, Biomax ®

The screening experiment was formed by three different steps. In the first one, a pre- culture 1 was performed from frozen culture. Then a second phase of biofilm immobilization, and the last step of bioproduction. Every carrier was screened in triplicate.



✓ Pre – culture 1

From 1 ml frozen inoculum of *A. succinogenes* (see paragraph 4.2 for stock preparation), a first pre-culture step was performed in the same manner as described in paragraph 4.6.2., Pre – culture 1. In this case, 15 tubes were necessary, and no samples were taken.

✓ Biofilm growth

This phase was entirely developed in our laboratory. From the previous phase, 15 microcosms (5 microcosms in triplicate) were prepared under laminar flow hood, as follow. 60 ml of every carrier were packed into the 116 ml bottles, and autoclaved. Then, enough medium listed in table 4.20 and prepared as in section 4.6.2 (pre – culture 2), with lactose 20 g/L instead of glucose 20 g/L, to cover all the carrier was added to the microcosms. In this case, 70 ml were necessary with Kaldnes K1 ®, and Bio-Flo 9 sinker ®, and only 50 ml with the other carriers. These microcosms were inoculated from the pre – culture 1 tubes (10% v/v), and 1 ml of liquid sample was taken to analyze initial biomass with Lowry's method and liquid medium by HPLC. All the bottles were closed in an anaerobic jar equipped with an AN0035 - AnaeroGen bag (Thermo Fisher Scientific U.S.A.) to create anaerobic conditions and a BR0055 – AnaeroIndicator (Thermo Fisher Scientific U.S.A.) to check the oxygen absence, and incubated for 24 hours at 37 °C and 150 rpm/min stirring velocity.

Also in this case, no samples were taken during the incubation.

✓ Bioproduction phase.

After the 24 hours of biofilm growth, the exhausted media was discharged and 1 ml of liquid sample was taken for HPLC analysis, and biomass quantification. Moreover, 5 carriers for each bottle were sampled and analyzed with modified Lowry's method (see analytical techniques), for the quantifications of the developed biofilm. Then, the microcosms were filled with the same amount of medium reported in table 4.25 (70 ml for Kaldnes K1 ®, and Bio-Flo 9 sinker ®, and 50 ml for all the other carriers):

Component	Quantity (g/L)
Lactose	7
Bacteriological peptone	10
Yeast extract	10
K <sub>2</sub> HPO <sub>4</sub>	3
NaCl	1
(NH <sub>4</sub> ) <sub>2</sub> SO <sub>4</sub>	3
MgCl <sub>2</sub> * 6H <sub>2</sub> O	0.3
CaCl <sub>2</sub> * 2H <sub>2</sub> O	0.3
Biotin	0,0002
FeSO <sub>4</sub> * 7H <sub>2</sub> O	0,005
BIS – TRIS	20

*Table 4.25: Medium composition for succinic acid production in the experiments for the identification of the best carrier for biofilm development*

The preparation of the medium was the same as described before. Bacteriological peptone, yeast extract, K<sub>2</sub>HPO<sub>4</sub>, NaCl and (NH<sub>4</sub>)<sub>2</sub>SO<sub>4</sub> were dissolved in 600 ml of demi H<sub>2</sub>O (for 1 L preparation), adjusted at pH 6,6, and autoclaved. All the other components were dissolved in 400 ml of demi H<sub>2</sub>O (for 1 L preparation), adjusted at pH 6,6 and sterile filtered in the autoclaved bottle with 0,22 VacuCap® sterile filter (Pall corporation U.S.A.), under laminar flow hood. The pH was set at 7 with autoclaved NaOH 2M, and a 1 ml of liquid sample was taken for HPLC and biomass analysis. The bottles were, then, closed with teflon-coated butyl stoppers and aluminum crimp sealers, and fluxed for ~ 30' with 100% sterile – filtered CO<sub>2</sub> to ensure anaerobic conditions (GVS 0,22 µm cellulose acetate filter - GVS Filter Technology. Stanford – ME – U.S.A.). No inoculation was performed. Finally, the microcosms were connected to a 100% CO<sub>2</sub> bag to provide the right amount of carbon dioxide for the reaction. The sterility was ensured by GVS 0,22 µm cellulose acetate filter. The incubation was performed for 29 hours, at 100 rpm/min at 37 °C, and the pH was controlled every 3 hours and corrected (if necessary) with sterile NaOH 2M. Every hour all the microcosms were sampled: 1 ml of liquid medium was taken for HPLC and biomass analysis. Moreover, at the end of the experiment, 5 carriers were sampled in order to analyze the biofilm concentration with the modified Lowry's method (see analytical techniques).

### 4.7.3 Kinetic parameters estimation: lactose and milk whey tests

In the previous tests, two of the most promising carriers was selected (Glaxstone ®, Poraver ®, see appropriate result section). For both of them, a series of microcosms experiments were performed (in triplicate) in order to determine the kinetic parameters  $\mu_{max}$  and  $K_s$  with lactose as only carbon source. With this quantitative results, the best carrier was chosen (Glaxstone ®, see appropriate result section), and another series of microcosms test was performed (in triplicate), to evaluate the same kinetic parameters with milk whey as substrate.

The procedure for this experiments was very similar to the procedure adopted for the screening of the carriers. In this case different substrate concentrations were tested in the bioproduction phase, in order to determine the initial absolute velocity of production of S.A. and consumption of substrate. From the absolute velocity, the relative velocity was calculated making the ratio between absolute velocity and biomass quantity. At this point, the tested concentrations (reported in table 4.26), are plotted in function of the initial specific velocity, and related with a Monod model, using a best-fit procedure minimizing the mean square deviation for every parameter. The lactose equivalent in the table are the concentration present in the milk whey.

***Substrate concentrations tested in kinetic parameters determination***

	g/L	g/L	g/L	g/L	g/L	g/L
<i>Lactose (Glaxstone ®)</i>	1,8	2,4	4,7	7,3	9,3	11,5
<i>Lactose (Poraver ®)</i>	/	2,2	4,6	7,4	9,4	11,7
<i>Lactose equivalent in milk whey (Glaxstone ®)</i>	1,8	5,5	8,6	11,8	14,72	/

**Table 4.26:** Different substrate concentration tested in the S.A. bioproduction phase with biofilm fermentation for the estimation of  $\mu_{max}$  and  $K_s$

The pre – culture 1 phase and the biofilm growth phase were developed (and sampled) as described before in the carrier screening section. For the lactose experiments, 33 tubes were inoculated (18 for lactose – Glaxstone ® experiments to test six concentrations in triplicate, and 15 for lactose – Poraver ® experiments to test five concentrations in triplicate) from 1 ml of frozen inoculum, as previously

reported. Again, the biofilm growth phase, was prepared in the same manner as depicted in section 3.7.2 for all the microcosms, using 60 ml of carriers and 50 ml of medium.

For the bioproduction phase, also in this case, the exhausted media was discharged and 1 ml of liquid sample was taken for HPLC analysis, and biomass quantification, together with 5 carriers for biofilm estimation with modified Lowry's method (see analytical techniques). The sterile microcosms were filled with 50 ml of medium reported in table 4.25, without inoculation, and 1 ml of liquid sample was taken for HPLC and biomass analysis. The bottles were, then, closed with teflon-coated butyl stoppers and aluminum crimp sealers, and fluxed for ~ 30' with 100% sterile – filtered CO<sub>2</sub> to ensure anaerobic conditions (GVS 0,22 µm cellulose acetate filter - GVS Filter Technology. Stanford – ME – U.S.A.). Finally, the microcosms were connected to a 100% CO<sub>2</sub> bag to provide the right amount of carbon dioxide for the reaction with GVS 0,22 µm cellulose acetate filter to assure the sterility of the gas inlet. The incubation was performed for 6 hours (except for the higher concentration of substrate, where 8 hours of incubation were necessary), at 100 rpm/min at 37 °C. The pH was controlled every 3 hours and corrected (if necessary) with sterile NaOH 2M. Every hour all the microcosms were sampled: 1 ml of liquid medium was taken for HPLC and suspended biomass analysis. Moreover, at the end of the experiment, 5 carriers were sampled in order to analyze the biofilm concentration with the modified Lowry's method (see analytical techniques).

The same concept was applied for the 5 concentrations (15 total microcosms) with milk whey. Only Glaxstone ® was used, because was identified as the best carrier for biosuccinic acid production (see results section). All the conditions for the three phase were exactly the same, only in the bioproduction phase, the microcosms were monitored every hour for 9 hours.

#### *4.7.4 Bioprocess scale – up in 1 L plant*

After the kinetic characterization of the process, the scale – up in 1 L plant (described in section 4.7.1) was performed, using lactose as carbon source. Five tests with increasing lactose concentrations were developed, in order to determine the sustainability of the process.

A preliminary fluidodynamic experiment was necessary to determine the principal parameter of the plant. The whole plant was filled with demi H<sub>2</sub>O, and recirculated for 30', in the operative conditions (40 ml/min flow rate, 37 °C, and 500 rpm/min stirring in the liquid bottle), and the conductivity was measured (μS/cm) from the sampling port 2 at the top of the column. Then, the feed bottle was changed with a 50 mM NaCl solution, and the conductivity was continuously measured (μS/cm) from the sampling port 2 at the top of the column every 30 seconds during the recirculation of the solution. Plotting the conductivity values in function of time, the resulting profile concentration is a sigmoid function, where the inflection point corresponds to the filling time of the column ( $\tau_{\text{column}}$ ). This value represents, the minimum amount of time necessary to change completely the medium inside the PFR. Moreover, it's possible to calculate the minimum flow rate necessary to maintain a perfectly mixed phase inside the whole system. A perfectly mixed phase is defined when the total residence time of the plant (HRT), is, at least, 1 order of magnitude less of the characteristic time of the reaction (Fogler, 2014). In this case, no significant variation of the parameters inside the column is observed, and all the process can be considered a perfectly mixed phase. In our experiment, the characteristic time of the reaction is considered when the 75% of lactose conversion to S.A. was reached in the microcosms tests with Glaxstone ® and lactose 7 g/L.

Assuming that the ratio between the liquid volume in the column and the liquid volume in the bottle (considering negligible the dead volume of the tubes) will be 1,5, it's possible to estimate the column residence time ( $\text{HRT}_{\text{column}}$ ) as the ratio between  $1/10_{\text{characteristic reaction time}} / 1,5$ .

Dividing the total liquid volume in the column and the estimated  $\text{HRT}_{\text{column}}$ , the desired minimum flow rate to obtain a perfected mixing phase in the glass column, was calculated.

After this characterization, five bioproduction tests are performed.

The principle of these tests was to limit the growth of the suspended biomass in the feed bottle during the recirculation. For this reason, the liquid volume in the feed bottle was kept lower as possible, only 50 ml to ensure the working of the peristaltic pump. The total liquid volume in the plant results in 629 ml (579 ml of useful volume in the column and 50 ml in the feed).

The three phases, pre – culture 1, biofilm growth and bioproduction, were modified as follow. The first pre – culture phase was developed in a sterile 250 ml bottle with 100 ml of total liquid volume, inoculated with 10% v/v of inoculum (90 ml of medium reported in table 4.20, and 10 ml from ten 1 ml frozen criovial stock). As reported in paragraph 4.6.2, this bottle was closed in an anaerobic jar equipped with an AN0035 - AnaeroGen bag (Thermo Fisher Scientific U.S.A.) to create anaerobic conditions and a BR0055 – AnaeroIndicator (Thermo Fisher Scientific U.S.A.) to check the oxygen absence, and incubated for 24 hours at 37 °C and 150 rpm/min stirring velocity. No samples were taken. After 24 hours the 2 L “feed” bottle was sterilized in autoclave and filled with 566,1 ml of medium reported in table 4.20, with 20 g/L of lactose ad carbon source instead of 20 g/L of glucose, and inoculated under laminar flow hood with 62,9 ml (10% v/v) of *A. succinogenes* from pre – culture 1. The bottle was closed with the tailor made screw cap described in section 4.7.1, and connected under sterile condition to the plant. All the system was fluxed for 30’ with sterile – filtered N<sub>2</sub> gas (GVS 0,22 µm cellulose acetate filter - GVS Filter Technology. Stanford – ME – U.S.A.) to eliminate air residues. The 13% CO<sub>2</sub> - 87% N<sub>2</sub> bag was connected, the peristaltic pump was turned on to ensure continuous recycle between column and bottle, and 5 ml of liquid was sampled from the column for HPLC and biomass analysis. No carriers were sampled to maintain the sterility. The plant was kept at 37 °C for 24 h, and monitored at the beginning and at the end of the growth phase. The pH was monitored, and adjusted at 6,6 manually every 3 hours.

In the bioproduction phase, another 2 L bottle with the same configuration of the previous one was autoclaved and filled with 629 ml of medium reported in table 4.25 changing only the lactose concentration: 8 g/L in the first experiment, 12 g/L in the second, and 16 g/L in the last three experiments. After 24 hours of biofilm growth, the pump flux was inverted, the last sample was taken and the column emptied. Then, the bottle with the new medium was connected in a sterile environment, replacing the previous with the exhausted culture medium. To remove nitrogen, the whole plant was fluxed for 30’ with sterile – filtered CO<sub>2</sub> gas (GVS 0,22 µm cellulose acetate filter - GVS Filter Technology. Stanford – ME – U.S.A.) to eliminate air residues. The 100% CO<sub>2</sub> bag was connected replacing the previous one, the peristaltic pump was turned on to ensure continuous recycle

between column and bottle, and 5 ml of liquid was sampled from the column for HPLC and biomass analysis. No carriers were sampled to maintain the sterility. The plant was kept at 37 °C for 9 h, and sampled every hour for medium composition. The pH was monitored, and adjusted at 6,6 manually every 3 hours. At the beginning and at the end of the bioproduction phase, a biomass analysis with Lowry's method was performed.

After the 8 g/L and 12 g/L experiment, a biofilm growth phase was performed (as described in this section) before the three experiments with 16 g/L of lactose. Only at the end of the last experiments, 5 carriers from the bottom, the middle and the top part of the column were sampled to perform biofilm quantification in triplicate.

## 4.8 PRINCIPAL ANALYTICAL TECHNIQUES

### 4.8.1 DNA extraction and PCR - DGGE

In the propanol project, a PCR – DGGE (*Polymerase Chain Reaction – Denaturing Gradient Gel Electrophoresis*) approach was used to identify the main bacteria present in the consortia, responsible for the conversion of propionic acid into propanol. All of the analysis were performed in duplicate.

Metagenomic DNA was extracted from 1,5 ml of samples conserved at – 20 °C and supplemented with 20% v/v of glycerol using Power Soil DNA Isolation Kit (MoBio ® Laboratories, Carlsbad, CA, USA) according to the protocol “for maximum yield”. All of the samples were previously gently vortexed and centrifuged at  $10.000 \times g$  for 2' at 4 °C (SL 16R series – Thermo Scientific ®). After the removal of the supernatant, the protocol was followed as provided by the manufacturer. The quality of the genomic extract was controlled through electrophoresis on 1% agarose gel dissolved in TAE buffer 1X, migrated at 120 Volt for 40' (Bio-Rad Laboratories ® S.r.l. Segrate (MI) - Italy). The staining was performed in 0.5 µg/ml ethidium bromide solution for 20' and the images was captured in UV transilluminator with a digital camera supported by a Gel Doc apparatus (Bio-Rad Laboratories

® S.r.l. Segrate (MI) - Italy). When necessary, DNA samples were quantified using nanophotometer P-330 model (Implen GmbH ®. München, Germany).

For the DGGE analysis, 16S rRNA gene of the metagenomic DNA previously extracted from the microbial community samples, was amplified in PCR reaction with the GC-clamped forward primer “GC-357F” (5’ –CGCCCCGCCGCGCCCCGCGCCCGGCCCGCCGCCCCCGCCCCCTACGGGAGGCAGCAG – 3’) and “907r” (5’-CCGTCAATTCCTTTGAGTTT-3’). (Sass AM, 2001). The 25 µl total reaction volume was formed by: 17,4 µl of sterile demi H<sub>2</sub>O, 2,5 µl of 1 x PCR buffer (Invitrogen. Paisley UK), 1,5 µl of 25 mM Mg<sup>++</sup>, 0,5 µl of 10 mM dNTPs solution, 0,5 µl of each 20 µM primer solution, 0,1 µl of Taq polymerase (5U/ µl), (Invitrogen, Paisley - UK), and 2 µl of total extracted DNA. The PCR conditions were the following: hot start at 60 °C, initial temperature 94 °C for 5’ and then 30 cycles of denaturation at 95 °C for 30”, annealing at 55 °C for 30”, extension at 72 °C for 1’, followed by a last extension step at 72 °C for 10’ (Zanaroli G., 2012).

The DGGE analysis, (with c.ca 400 ng DNA each lane), were performed in a D-Code system (Bio-Rad Laboratories S.r.l. Segrate (MI) - Italy) with 7% (w/v) polyacrylamide gel (acrylamide-N,N'-methylenebisacrylamide, 37:1) in 1x TAE buffer, with a denaturing gradient from 40% to 60% denaturant (100% denaturant was set at 7 M urea and 40% (v/v) formamide) (Zanaroli G., 2010).

The amplicons were resolved at 55 V for 16 h, 60 °C. The gel was stained in a solution of 1× SYBR-Green (Sigma–Aldrich, Milwaukee, WI) in 1× TAE for 30 min and the images were captured in UV transillumination with a digital camera supported by a Gel Doc apparatus (Bio-Rad Laboratories ® S.r.l. Segrate (MI) - Italy).

For the sequencing process, the most relevant bands were cut from the gel with a sterile scalpel and the DNA was eluted by incubating the gel fragments for 4 h in 50 µL of sterile deionized water at 30 °C and 150 rpm/min stirring. The eluted DNA was re-amplified in the same PCR condition as previously reported (adding 5% of sterile DMSO to the mix), and resolved in another DGGE, to confirm the purity of the DNA. After elution from the second polyacrylamide gel, another PCR was performed using the same primer (“357F” and “907r”) without GC clamp, and 5 µl of each amplicon was purified with 0,5 µl of 20 U/µl of Exonuclease I (ExoI) enzyme (Thermo Scientific – U.S.A.),



and 1 µl of 1 U/µl of Alkaline Phosphatase (FastAP), (Thermo Scientific ® – U.S.A.) at 37 °C for 30', with a subsequent enzyme inactivation step for 15' at 80 °C. In presence of the corresponding primer (5,2 µl of “357 F” 20 µM, in 50µl of sterile demi H<sub>2</sub>O), the products were dried at 60 °C for maximum 30', and sent to BMR Genomics (Padova, Italy), for the sequencing reaction.

Each 16S rRNA gene sequence obtained, was aligned to Ribosomal Database Project-II (RDP, release 11, <http://rdp.cme.msu.edu>) using “Seqmatch” tool. The phylogenetic affiliation of every sequence was obtained from the same website through the “Classifier” tool.

#### 4.8.2 HPLC & GC

HPLC (*High Performance Liquid Chromatography*) and GC (*Gas Chromatography*), are two techniques used to determine the composition of both liquid medium, and both headspace, in the performed experiments.

##### ✓ HPLC

In Bologna, (DICAM department), a “Prominence” series modular HPLC (Shimadzu Corporation ®. Kyoto – Japan), was used to determine sugars (glucose, lactose and galactose) VFAs, (acetic, propionic, butyric, isobutyric, valeric, isovaleric, caproic, isocaproic and eptanoic acid), alcohols (ethanol, n-propanol and n-butanol), succinic acid and other fermentation by-products, as formic, pyruvic and lactic acid. The HPLC is equipped with 5 different modules. A “CBM-20A/20Alite” system controller connected to a PC through “LC LabSolutions Series Workstation” software; a “LC-30AD” solvent delivery unit with a wide range of flow rates, from 0.0001 to 3.0000 mL/min; a “SIL-20A” series autosampler for maximum 105 - 1,5 ml vials, a “CTO-20A” column oven with a forced air-circulation-type, from 10 °C above room temperature to 85 °C, and a “RID-20A” refractive index detector with temperature control between 30 °C to 60 °C, operating in the range between 1 to 1.75 RIU. The column is a 7,8 x 300mm “IC – Sep ICE - Coregel 87H3” (Transgenomic ®. Manchester – UK), used at 40 °C with a H<sub>2</sub>SO<sub>4</sub> 0,12 M as mobile phase. All the analytes were detected using

appropriate methods based on standard linear calibrations in the range between 1 g/L and 50 g/L, with a coefficient of determination ( $R^2$ ) in the range between 0,96 and 1,00.

Prior injection, all the samples were centrifuged at 14.000 rpm/min at 8 °C for 10', and filtered in 1,5 ml vial (Agilent Technologies. Santa Clara – U.S.A.), using 0,22  $\mu$ m “Millex - 49 GV” PVDF filters (Millipore ®. Vimodrone (MI) – Italy).

At VITO, a “Agilent 1200 series” HPLC was used (Agilent Technologies ® Santa Clara – U.S.A.), equipped with equipped with 4 different modules. A “Agilent binary pump SL series” system controller connected to a PC through “Agilent ChemStation Series” software with a wide range of flow rates, from 0.0001 to 5.0000 mL/min; a “HiP-ALS-SL” autosampler for maximum 96 - 1,5 ml vials, a “TCC SL unit” column oven with a forced air-circulation-type, from 10 °C above room temperature to 85 °C, and a “Agilent 1260” refractive index detector, operating in the range between 1 to 1.75 RIU. The column is a 7,7 x 300mm “Agilent Hi-Plex - H” (Agilent Technologies ® Santa Clara – U.S.A.), used at 60 °C with a H<sub>2</sub>SO<sub>4</sub> 0,01 M as mobile phase. All the analytes were detected using appropriate methods based on standard linear calibrations in the range between 1 g/L and 50 g/L, with a coefficient of determination ( $R^2$ ) in the range between 0,95 and 0,99.

Prior injection, all the samples were centrifuged at 14.000 rpm/min at 8 °C for 10', dilute when necessary with demi – H<sub>2</sub>O and filtered in 1,5 ml vial (Agilent Technologies. Santa Clara – U.S.A.), using 0,22  $\mu$ m “Spartan - 13 GV” regenerate cellulose filters (GE Healthcare ®. Diegen – Belgium).

#### ✓ GC

The bioreactor headspace (in Bologna) was monitored by gas chromatography analysis using a “Agilent 5890 SERIES II Plus” chromatograph (Agilent Technologies ® Santa Clara – U.S.A) with a 7,06 ml/min nitrogen flow rate as a gas carrier. The column was a 30 meters Carboxen®-1010 PLOT with an average diameter of 5,3 mm and 30  $\mu$ m thickness (Supelco Analytical ®. Bellefonte (PE) – U.S.A.), and the gas flows through the column towards a TCD detector, using a constant temperature of 150 °C. The instrument was connected to a PC using as interface the “ChemStationRev.A.10.02” software. The monitored compounds, H<sub>2</sub>, O<sub>2</sub>, CH<sub>4</sub> and CO<sub>2</sub> were calibrated using appropriate methods

based on standard linear calibrations in the range between 0,5% and 100%, with a coefficient of determination ( $R^2$ ) in the range between 0,94 and 1,00. Only oxygen was monitored only in the range between 0,5% and 20%.

The biogas in the headspace was sampled using a 500  $\mu$ l “Hamilton Bonaduz Schweiz ® - GASTIGHT#1750” syringe (Hamilton Company ®. Bonaduz CH) with a “Side Port – Point#5 style” needle (Hamilton Company ®. Bonaduz CH), and 200  $\mu$ l were injected in the instrument.

For every compounds monitored by HPLC and GC, a proper control chart (known also as “Shewhart charts”) was created, in order to ensure the reliability of the measures. These charts were made associating to the real value, two different “warning” limits denominated “attention” and “control”. Those limits were calculated from the medium value of a preliminary measures data set of the compound analyzed at defined concentration, analyzing the standard deviation and the T Student coefficient (for  $\alpha = 0,05$  and  $\alpha = 0,01$  respectively). The experimental data must stay in this limits range, to ensure the reliability of the process.

#### *4.8.3 Total solids (TS) and volatile solids (VS) determination*

In the bio-CH<sub>4</sub> was necessary to characterize both inoculum, both substrates in terms of total and volatile solids, in order to set-up the experiments and express yields and production velocities. The total solids number (TS) represent the summary of the organic and the inert fraction (ashes) of the considered materials. The volatile solids number (VS), instead, represents only the organic part of the dry matter. A simple procedure was developed as reported by U.S.A Official Department Of Energy through NREL report (A. Sluiter, 2008).

On an analytical balance ME – T series (Mettler Toledo ® Novate Milanese – Italy), the tare weight of a ceramic crucible was determined. Then, a defined quantity of the substrate / inoculum was weighted (net value). After 24 hours at 105 °C to eliminate only the water from the sample, again the

crucible was weighted on the analytical balance. The difference between this value and the tare weight represents the grams of total solids (TS) of the sample.

After that, the crucible was incubated for 1 hour at 600 °C, and weighted again. The difference between this value (post 600 °C) and the tare weight represents the grams of inert part (ashes and mineral compounds mostly) of the sample. The grams of volatile solids are calculated from the difference between the TS previously determined and the inert part. The most important value for our experiment, is the % VS, calculated as the ratio between the grams of volatile solids and the defined quantity of the substrate analyzed.

$$VS (g) = TS (g) - Inert\ part (g)$$

$$\% VS \frac{VS (g)}{net\ quantity (g)}$$

#### 4.8.4 Biomass determination: Lowry's method

To determine the biomass concentration, Lowry's method was used (Lowry, 1951). This method was used as described in the article both for suspended and attached biomass determination, only the pretreatments of the samples were re-adapted, in order to estimate correctly the amount of biofilm growth. All the tests were performed in triplicate. For this assay, numerous solutions were necessary:

- Solution A: 2% di Na<sub>2</sub>CO<sub>3</sub> in NaOH 0.1 N
- Solution A2: 2% di Na<sub>2</sub>CO<sub>3</sub> in H<sub>2</sub>O
- Solution B1: 1% CuSO<sub>4</sub> · 5H<sub>2</sub>O in demi H<sub>2</sub>O (light sensible)
- Solution B2: 2% Na-tartrate (C<sub>4</sub>H<sub>4</sub>Na<sub>2</sub>O<sub>6</sub>) in demi H<sub>2</sub>O
- Solution C: mix of A, B1 e B2 (100:1:1) (light sensible)
- Solution D: mix of A2, B1 e B2 (100:1:1) (light sensible)

- Solution E: 1:1 dilution of Folin-Ciocalteu ® reagent 2N in demi H<sub>2</sub>O (light sensible)
- NaOH 0.5 N in demi H<sub>2</sub>O
- NaOH 1 N in demi H<sub>2</sub>O
- NaCl 0.9 % in demi H<sub>2</sub>O

#### ✓ Suspended biomass analysis

The liquid culture medium sample were centrifuged at 14000 rpm/min at 8 °C for 5', and washed with 1 ml of NaCl 0,9% solution, after supernatant removal. This procedure was performed twice, and at the end, the biomass pellet was resuspended in the same volume of demi H<sub>2</sub>O of the starting sample volume. In a new eppendorf, 200 µl of the resuspended sample was mixed with, 200 µl of demi H<sub>2</sub>O and 100 µl of NaOH 0,5 M.

After this pre-treatment, the real Lowry's test was performed. The prepared samples were boiled for 1' and immediately kept at – 20 °C for another minute. Then, they are transferred in a 15 ml clean glass tubes previously filled with 2,5 ml of solution C, and vortexed for a couple of seconds. After ten minutes, 250 µl of solution E were added to the tubes, and vortexed again. After 40 minutes at room temperature, the samples were read at 540 nm using demi H<sub>2</sub>O as blank.

#### ✓ Biofilm analysis

For the biofilm estimation, two different types of analysis were performed. The biomass can be classified as “strongly attached” and “weakly attached” on the surface. The “weakly attached” term is referred to the biofilm on the surface of the carrier, in equilibrium with the suspended part of the culture. The “strongly attached” term, is referred to the inner part of the biofilm. To determine both strongly, both weakly attached biomass, 5 carriers were sampled, transferred in a 15 ml falcon and washed with 7 ml of NaCl 0,9% solution for 1 hour at 90 rpm/min stirring at room temperature. Then, 2 ml of the supernatant were conserved and labeled as “weakly biomass”. This sample is treated as a suspended biomass, and analyzed as previously reported.

The other 5 ml of supernatant were centrifuged at 5000 rpm, 8 °C for 25' and subsequently discharged. Another washing procedure with 7 ml of NaOH 1 M for 1,5 hours at 30 °C and 90 rpm/min stirring was performed, in order to remove the “strongly attached” biomass from the carrier. 500 µl of the solution was, then, transferred to a new eppendorf, and analyzed with the Lowry's method. The prepared samples were boiled for 1' and immediately kept at – 20 °C for another minute. Then, they are transferred in a 15 ml clean glass tubes previously filled with 2,5 ml of solution C, and vortexed for a couple of seconds. After ten minutes, 250 µl of solution E were added to the tubes, and vortexed again. After 40 minutes at room temperature, the samples were read at 540 nm using a treated solution from a virgin carrier as blank, to avoid interferences from the carrier material. The obtained values were interpolated with a linear correlation resulted from BSA (Bovine Serum Albumin – Sigma Aldrich ®. U.S.A.) analysis in the range from 0 – 150 mg/L ( $R^2 = 0,9921$ ).

The suspended and “weakly attached” biomass were expressed in  $\text{mg}_{\text{proteins}}/\text{L}$ , simply obtained from the interpolation with BSA correlation. The “strongly attached” biomass, instead, was expressed in  $\text{mg}_{\text{proteins}}/\text{L}_{\text{reactor}}$ . For this reason, the obtained value needs to be normalized for the net quantity of analyzed support. Every carrier, then, is weighted and dried at 105 °C for one night. The same carrier was subsequently left 1 hour at 600 °C, and weighted again, to obtain the net amount of analyzed carrier (grams). Then, the interpolated values obtained from Lowry's method (in  $\text{mg}_{\text{proteins}}/\text{L}$ ) were multiplied for the volume of NaOH 1M present in the initial falcon (in liter), to obtain the  $\text{mg}_{\text{protein}}$ . These values are divided by the net grams of the carrier previously determined, to obtain  $\text{mg}_{\text{protein}}/\text{g}_{\text{carrier}}$ . Multiplying for the bulk density ( $\text{g}/\text{L}$ ) of each carrier, the desired values in  $\text{mg}_{\text{proteins}}/\text{L}_{\text{reactor}}$  are obtained.

Another biomass type that was only characterized in the succinic acid PFR plant, is the entrapped biomass, that represent the cells that remained entrapped between the dead space of the carrier during the experiment (and for this reason are not detected in the analysis of suspended sample), but is unable to form biofilm. This type of biomass was estimated in the same manner as made with suspended biomass, with only a small pretreatment to remove these cells from the column. After the bioproduction test, the column was emptied, and the carriers were gently and carefully removed with

a pair of tweezers. The column was then washed with 580 ml of demi water, and strongly agitated, in order to remove all the entrapped biomass. Then, the samples (in triplicate) were analyzed as a simple suspended biomass sample.

#### *4.8.5 Chemicals*

If not specified, all the chemical compounds were supplied by Sigma Aldrich S.r.l. (Milan, Italy).

## 5 RESULTS AND DISCUSSION

### 5.1 BIO – H<sub>2</sub> PROJECT

#### 5.1.1 Integrated bioreactor – membrane experiment

The innovative approach used in this experiment is described in section 4.3.2. Up to now, only few literature studies was published (Juan E. Ramírez-Morales, 2015), (Barelli, 2008), (Gallucci, 2013) regarding the integrated bioproduction of hydrogen from renewable sources, coupled to membrane separation. Anyway, these process was conducted with mixed consortia, or with different type of reactor configuration. Moreover, no study was reported for the commercial membrane used in this experiment. Thus, this study represents the first of its kind with this configuration. The overall results are reported in the graphs below.

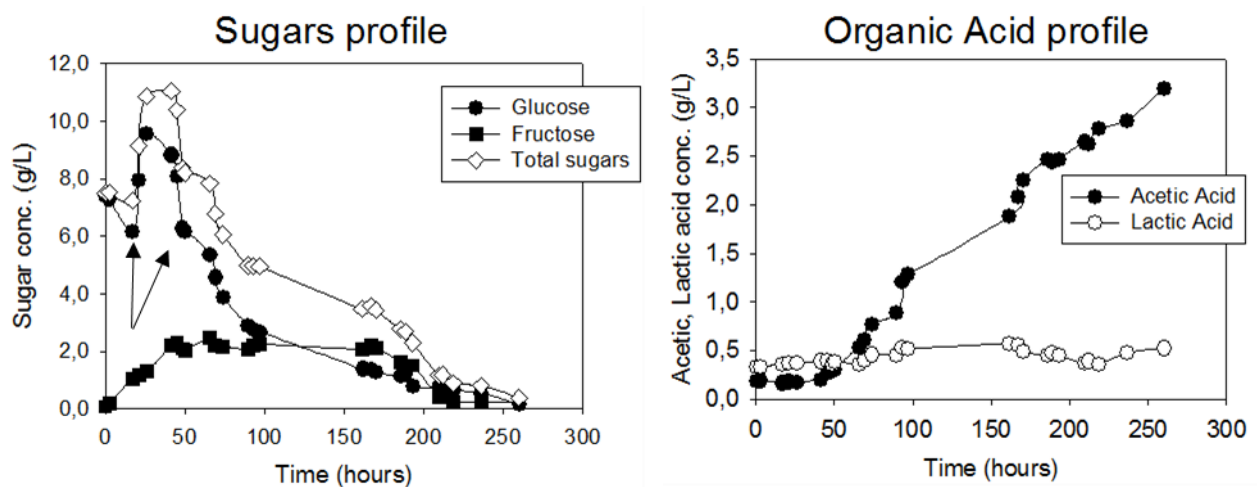


**Figure 5.1:** Sugars and acids concentration in the Bio – H<sub>2</sub> production experiments reactor coupled with membrane separation module

The starting glucose concentration was 7,51 g/L (0,58 mol), and after 260 hours of total experiment, the resulting concentration of total sugars was 0,39 g/L, with a total carbohydrates utilization as 94,7 % and 0,03 g/L/h as carbohydrates consumption rate. As it's reported in the description section, 2 subsequent addition of 2 g/L and 1,5 g/L glucose were performed (black arrows in the graph) after 21 hours and 26 hours of fermentation, in order to ensure high biomass concentration and elevated



hydrogen productivity for the membrane test. Fructose was produced during the initial 50 h of fermentation with a production rates between 0,08 and 0,05 g/L/h, and then slowly but completely consumed. To investigate the possible role of *T. neapolitana* in the reaction of glucose isomerization to fructose, three non-inoculated batch tests conducted with 9,5 g/L of glucose at 77 °C was sterilized by adding 3.5 g/L of NaN<sub>3</sub>. The abiotic test resulted in an initial rate of fructose production similar to this experiment ( $0,04 \pm 0,01$ ) g/L/h. This results suggests that the observed fructose production can be ascribed to abiotic phenomena, in agreement with numerous studies that document the chemical isomerization of glucose to fructose mediated by high temperature (Román-Leshkov, 2010). Moreover, other literature studies, reports biological fructose production by *T. neapolitana* (De Vrije, 2009), (D'Ippolito, 2010).

The acetate concentration followed a linear and constant increasing until a final concentration of 3,2 g/L (0,75 mol) whereas lactate concentration remained quite stable with an initial concentration of 0,34 g/L and a final concentration of 0,53 g/L. This organic acid profile is a strong indicator of hydrogenase activity (see metabolic pathway in figure 4.2). Theoretically, 2 mol of acetate are produced from the oxidation of 1 mol of glucose. In this experiment the ratio is 1,47 mol of acetate produced for every mol of glucose consumed.

In figure 5.2 are reported the main parameters of the fermentation: hydrogen productivity (in terms of mmol H<sub>2</sub> /L/h), biogas volumetric flow rate (L/d), and composition (%).

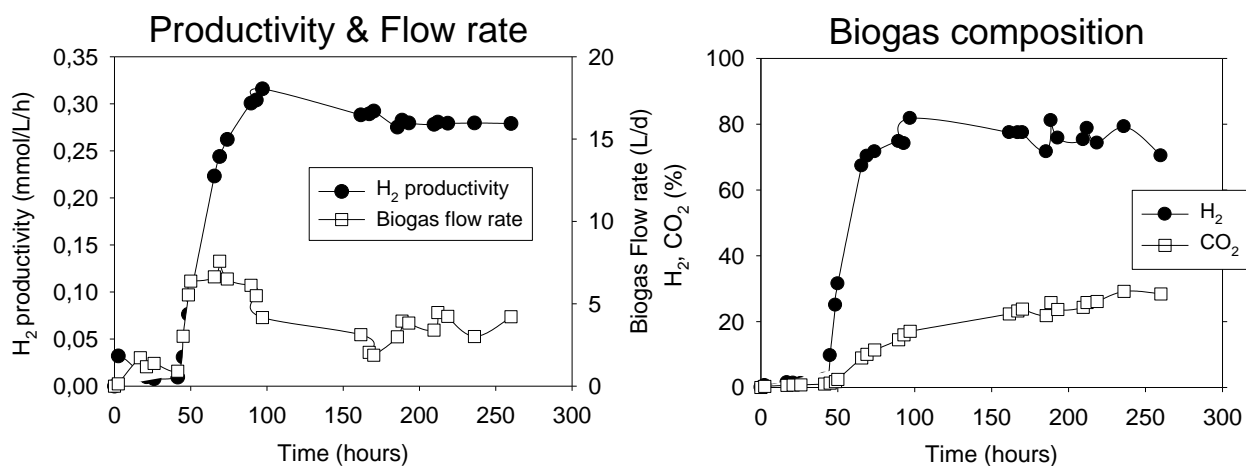


**Figure 5.2:** H<sub>2</sub> productivity, biogas flow rate and composition in the coupled bioreactor test for biohydrogen production

The exponential phase of the process starts after 41,5 hours of lag phase, and finished after 97 hours of fermentation. The hydrogen productivity reached a maximum value of 0,31 mmol  $H_2$  /L/h, corresponding to 8,4 mmol  $H_2$  /mol glucose consumed. The carbon dioxide productivity was very low, and stays between 0,01 and 0,05 mmol  $CO_2$  /L/h. At the end of the fermentation, 38,6 L of biogas were produced, with maximum volumetric flow rate of 7,5 L/d after 69 hours, in the middle of exponential phase. The biogas composition measured after the reactor condenser (without membrane module) reached the maximum hydrogen percentage (79,9 %) after 97 hours of fermentation, and stays constant until the end of the experiment. The figure 5.3 reports the suspended biomass estimated with Lowry's method:

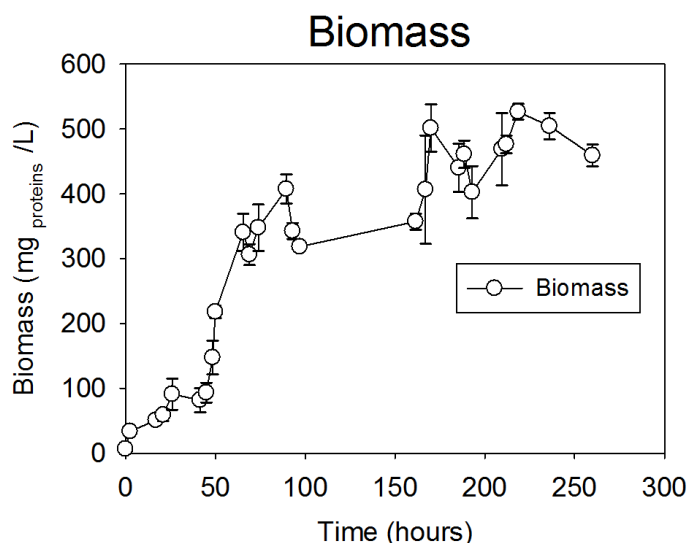


**Figure 5 3:** Protein concentration estimated by Lowry's method in the membrane - coupled biohydrogen production test

All the tests were performed in triplicate. In the exponential phase the amount of total protein raised from 93,3 mg/L to a maximum value of 406,6 mg/L, and remains in a stationary state (with a little increasing) until 218,5 hours where the lysis becomes prevalent.

The key part of the experiment was the coupling of the membrane module. As reported in the appropriate description paragraph in the material and methods chapter, the module was coupled during all the exponential phase of the fermentation (from 48,5 to 97 hours).

The results of the membrane performance (gently provided by the Diffusion in Polymers and Membrane Separation Group of Prof. M. G. Baschetti and G. C. Sarti), are reported in table 5.1.

***Membrane separation performances***

	Feed	Permeate
$H_2$ (%)	79,9	94,7
$CO_2$ (%)	12,4	5,3
$P H_2$ (barrer)	8,2	
$P CO_2$ (barrer)	3,7	
Selectivity	2,2	

***Table 5.1: Membrane performances during the biohydrogen production test in the integrate bioreactor***

The values are calculated on the average hydrogen and  $CO_2$  feed, and in the permeate of the membrane, during the exponential phase. The estimated permeability coefficient (in Barrer unit) are calculated with this expression:

$$P = q * \frac{t}{A} * \Delta p$$

where q is the mass flux of gas through a membrane of area A and thickness t, under a partial pressure gradient  $\Delta p$  across the membrane (Stern, 1968).

The selectivity is the ratio between the two permeability ( $P H_2/P CO_2$ ). This coefficient is lower respect to the theoretical one (3,1), reported in previous experiments of the Diffusion in Polymers and Membrane Separation Group with pure gases. Probably, the humidity of the biogas (despite the condenser), and the non – constant flow rate of the biogas in the feed of the membrane causes a swelling of the membrane resulting in altered membrane mechanical process, and lower efficiency. Anyway the purity of hydrogen was improved until c.ca 95 % (with a 14,8% increased) with a halved  $CO_2$  percentage in the permeate, suggesting a good starting point for further optimization of the process.

### 5.1.2 Co – feeding tests

In previous works (Cappelletti et.al., 2012) and (Dario Frascari, 2013), different experiments using molasses and cheese whey are performed. The aim of those tests was to determine the most fitting kinetic model for hydrogen production, estimating the principal kinetic parameters. Moreover, with 10 g/L of total sugar, bioproduction test in microcosms with separate molasses and cheese whey, were developed in order to determine the maximum  $H_2$  productivity (mmol/L/h) and the  $H_2$  / substrate yield (mmol  $H_2$  / g sugar).

Starting from these data, different co – feeding tests with molasses and cheese whey were performed both in microcosms, both in 19 L bioreactor, as described in sections 4.3.3 and 4.3.4. The ratio between molasses and cheese whey was 75% - 25%, 50% - 50% and 25% - 75%, with 10 g/L as total starting sugars, to maintain the same line as previous tests. In the graphs below are reported for every co – feeding ratio, the profiles of hydrogen productivity, total sugars and the biogas composition.

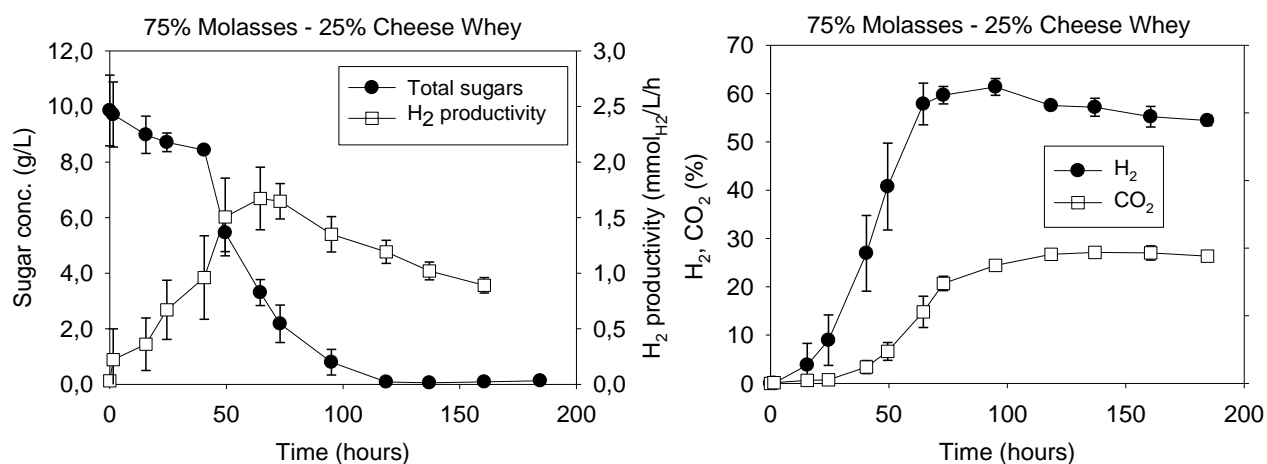


**Figure 5.4:** Main fermentation parameters in the molasses 75% - cheese whey 25% co-feeding microcosm test

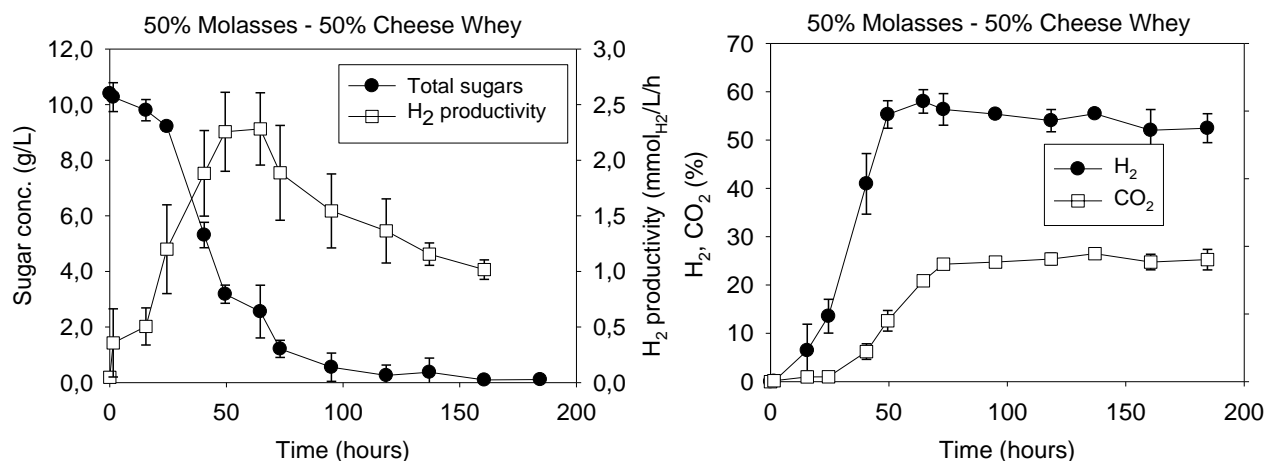


**Figure 5.5:** Main fermentation parameters in the molasses 50% - cheese whey 50% co-feeding microcosm test

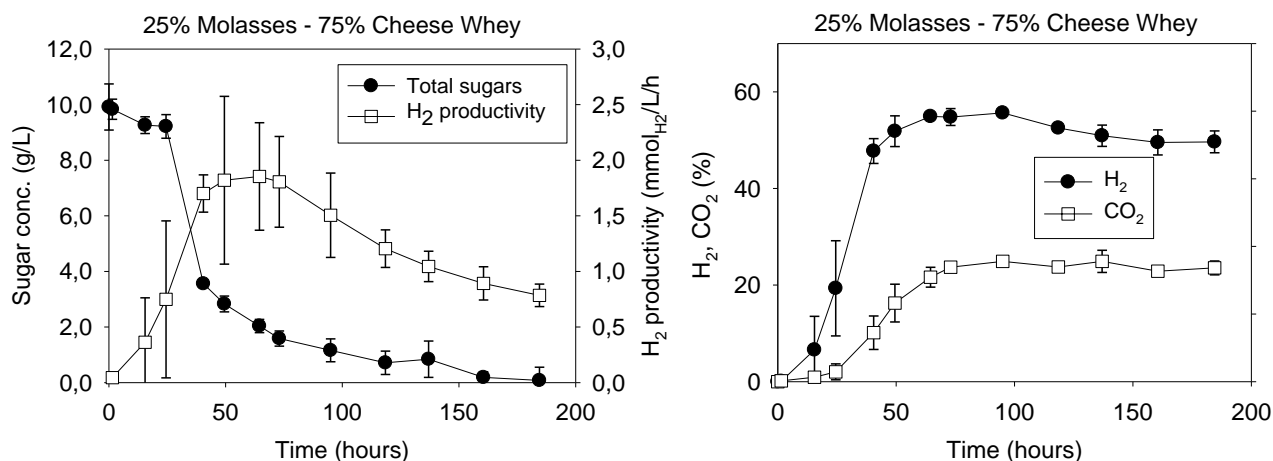


**Figure 5.6:** Main fermentation parameters in the molasses 25% - cheese whey 75% co-feeding microcosm test

All the considered tests were performed in triplicate, and starts from 10 g/L of total sugars, completely depleted after 185 hours. As it clearly evident from the graph the fermentation profiles are very similar between the experiments, demonstrating that the co – feeding between these two by – products it's absolutely feasible.

The carbohydrates conversion was 98,7%, 98,9% and 99,2% for respectively the 75% - 25%, 50% - 50% and 25% - 75% co-feeding ratios, and the carbohydrate consumption rates were similar between the experiments, corresponding to 0,053, 0,056 and 0,053 g/L/h respectively. The exact concentrations of initial and final carbohydrate in the medium, the final amount of organic acids and the maximum biomass concentration are reported in table 5.2:

***Sugars, biomass and acids observed in the microcosms co-feeding experiments***

	Initial total carbohydrates concentration (g/L)	Final total carbohydrates concentration (g/L)	Final acetic acid concentration (g/L)	Final lactic acid concentration (g/L)	Maximum biomass concentration (mg/L)
<i>75% molasses- 25% milk whey</i>	(9,86 ± 1,27)	(0,13 ± 0,02)	(4,55 ± 0,42)	(1,88 ± 0,40)	(739,06 ± 24,40)
<i>50% molasses- 50% milk whey</i>	(10,40 ± 0,11)	(0,11 ± 0,03)	(3,16 ± 0,07)	(3,30 ± 0,39)	(730,83 ± 35,21)
<i>25% molasses- 75% milk whey</i>	(9,91 ± 0,83)	(0,08 ± 0,05)	(3,07 ± 0,19)	(3,99 ± 0,22)	(689,22 ± 30,84)

**Table 5.2:** *Sugars, biomass and acids observed in the co-feeding tests*

The lactic acid concentration is increasing as the increase of milk whey in the feed. This is normal due to the waste sugar composition. 1 g/L of molasses contains 0.48 g/L of total sugars (0.095 g/L of glucose, 0,140 g/L of fructose and 0,245 g/L of sucrose), whereas 1 g/L of cheese whey contains 0.80 g/L of total sugars (only lactose). Every tests reached the higher biomass concentration after 95 hours of fermentation with comparable values. The hydrogen percentage in the biogas is included in the range between 50% and 60%, with a lower value of carbon dioxide, near 20% in every experiments.

In the following table are evident the hydrogen yield and productivity obtained in these tests and compared to the experiments reported in Dario Frascari, 2013, with pure molasses (first row) and pure cheese whey (last row). In the second, third and fourth rows are respectively shown the value for 75% molasses and 25% cheese whey, 50% molasses and 50% cheese whey, and 25% molasses and 75% cheese whey.

Maximum H <sub>2</sub> productivity (mmol L <sup>-1</sup> h <sup>-1</sup> )	H <sub>2</sub> /substrate yield (mmol <sub>H2</sub> g <sub>sugar</sub> <sup>-1</sup> )
1.3 ± 0.2	9.9 ± 0.2
1.6 ± 0.1	14 ± 1
1.7 ± 0.2	12 ± 1
1.6 ± 0.1	9.7 ± 0.8
0.42 ± 0.05	5.8 ± 0.3

**Table 5.3:** *H<sub>2</sub> productivity and yield in the microcosms co – feeding experiments. Rows 1 and 5 represent bioproduction tests with only molasses and cheese whey respectively. In rows 2 – 3 – 4 are reported co – feeding tests with respectively 75% molasses 25% cheese whey, 50% molasses 50% cheese whey and 25% molasses 75% cheese whey*

It's evident that all the 3 co-digestion tests led to an improvement of both  $H_2$  productivity and  $H_2$ /substrate yield, and the best performances were obtained in the two tests characterized by the highest molasses concentrations (row 2 and 3). The attainment of higher performances in co-digestion tests in comparison with single-substrate tests is in agreement with numerous other studies of both  $bioH_2$  and  $bioCH_4$  production (Mata-Alvarez, 2000), (Dario Frascari, 2013).

## 5.2 BIO – CH<sub>4</sub> PROJECT: ANAEROBIC DIGESTION

As reported in section 4.4 and sub – paragraphs related, different types of experiments were performed, both in small 116 ml microcosms scale, both in 29,7 L bioreactor. The aim of those tests (conducted in collaboration with different private companies), was to evaluate the biomethane potential of different agro – industrial waste, using different consortia without performing expensive pretreatment. In literature is extensively reported that lignocellulosic biomass needs appropriate pretreatment procedure in order to obtain free cellulose and hemicellulose for further fermentation (see paragraph 1.5.2.). In these tests, grape pomace in particularly but also tomato peels, maize silage (alone or in co-feeding between them), were tested to determine the best obtainable yield, performing a cheaper thermal pre-treatment like only 3 days at 55 °C.

### *5.2.1 Batch, fed – batch and continuous bioreactor test*

In these experiment, extensively described in section 4.4.2, three different approach were used, in order to investigate the biomethane production from red grape pomace in a 29,7 L CSTR bioreactor (described in paragraph 4.4.1), using an already acclimatized inoculum called “DICAM”, described and characterized in sections 4.2 and 4.4.2.

In previous work, (unpublished results) a series of three acclimatized microcosms were prepared as reported in the 4.4.2 section with 10% w/w of DICAM inoculum and 20% w/w of red grape pomace. These microcosms were anaerobically incubated for 78 days at 55 °C and 150 rpm/min stirring velocity, with an initial pH corrected in the range between 7,5 – 8 with 2 M NaOH, and monitored periodically (11 total samples were taken) to determine the biogas quantity, composition and the VFA concentration. The obtained methane yield, expressed in terms of NL CH<sub>4</sub> / Kg SV are kept as base data to compare the results of the first batch reactor test, described in section 4.4.2 (table 4.9). This first reactor test was performed in the same experimental condition as the preliminarily microcosms test, in terms of inoculum and substrate percentage (respectively 10% w/w and 20% w/w), and physico – chemical characteristics e.g. pH and T °C.



In figure 5.7 is reported the comparison between the preliminary microcosm test and the first bioreactor test.

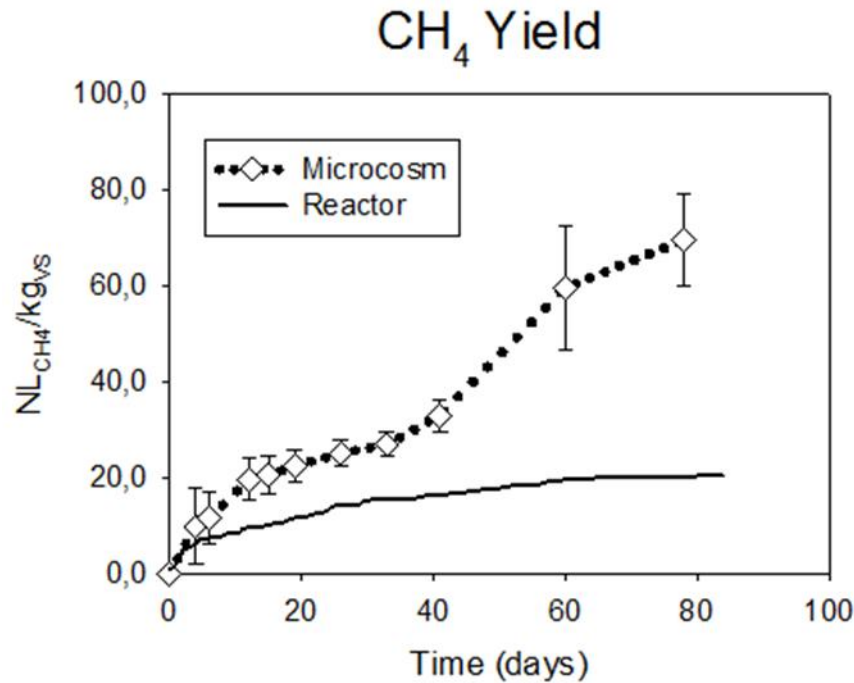


**Figure 5.7:** Methane yield comparison between preliminary microcosms test and first batch bioreactor experiment. Black dotted line with diamond symbol represent the microcosms yield trend and sampling point. The continuous black line represents the methane yield in the bioreactor. For the sake of clarity, daily reactor sampling points are omitted, only yield trend is reported.

From the graph is evident, that the yield of both the process are very low. E. Dinuccio 2010 reports an average yield value of 116 NL CH<sub>4</sub> /Kg vs for grape pomace. Moreover, the reactor yield is lower than microcosms, with a maximum value of 20,4 NL CH<sub>4</sub> /Kg vs, compared to a maximum value of (69,5 ± 9,6) NL CH<sub>4</sub> /Kg vs in the microcosm experiments. Regarding the methane production velocity, a maximum of (0,18 ± 0,04) NL CH<sub>4</sub> /L/d was reached after 55 days of fermentation, whereas negligible methane velocity was observed in the bioreactor test.

In both experiments, the value of volatile solid fed at the beginning was the same (139,1 g/L vs), and a good conversion was founded in both test. In fact, the final value of volatile solids at the end of the two studies were 9,57 g/L and 1,81 g/L for reactor and microcosms test respectively, with a total percentage conversion of 92% and 98%. This is a strong indication that the hydrolytic, acidogenic and

acetogenic phases of the process is well – established, but the methanogenic step is clearly inhibited in the reactor.

This theory is supported by the methane percentage detected in the biogas. Microcosm tests reached a maximum methane percentage of  $(85,88 \pm 1,66) \%$ , in the last sample at 78 days, with a maximum methane velocity production rate of  $(0,62 \pm 0,12) \text{ Nml}_{\text{CH}_4} / \text{L} / \text{d}$ . Moreover, the final percentage  $\text{CO}_2$  value represented less than 14% in the same sample, in each single study.

In the reactor, instead, the maximum amount of methane was reached after 38,9 days and represented only the 48% of total biogas, with c.ca 50% of  $\text{CO}_2$  in the same sample, and remained stable till the end of the test, with a negligible methane velocity production rate.

These results are explainable analyzing the concentration of short chain fatty acids in the culture medium, and in particular of the acetic acid. In literature is clearly reported that higher amount of acetic acid is one of the principal inhibition source of the methanogenic activity, whereas a minimum amount of this VFA is necessary to ensure the acetoclastic activity of the methanogenic archaea. Besides that, is difficult to estimate the exact inhibition range, due to the higher phylogenetic variability inside the consortia, and to the continuously acclimatization of the selected consortia to acetic acid. Anyway, some articles (Aguilar, 1995), (Ye Chen, 2008), reports that up to 4 g/L of total acid concentration, no inhibition of AD is generally detected, while 10 g/L or higher values of total VFA are generally associated to higher inhibitory state. In the next figure is reported the profile of the principal volatile fatty acids (acetic, propionic and butyric), during the microcosm and reactor tests.

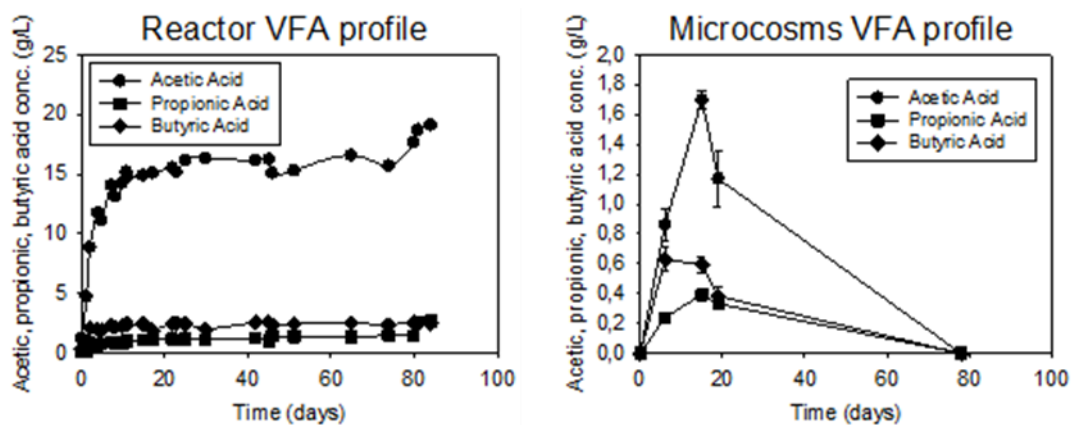


*Figure 5.8: Comparison of the VFAs profiles in bioreactor batch test and in the microcosm experiments*

In the microcosms the amount of acetic acid reached a maximum of  $(1,70 \pm 0,06)$  g/L after 15 days of fermentation, with a total VFAs concentration of 2,69 g/L, that is below the inhibition range reported by Aguilar, 1995 and Ye Chen, 2008. Moreover, from this point the concentration of acetic acid rapidly decreasing to values near zero until the end of fermentation with an average consumption rate of 0,027 g/L/d of  $\text{CH}_3\text{COOH}$ ; this trend is in line with the hypothesis that the acetic acid is converted to  $\text{CH}_4$  from the acetoclastic part of the archaea population.

In the reactor, instead, a rapid accumulation of mainly acetic acid was observed in the first ten days of fermentation reaching more than 15 g/L of only  $\text{CH}_3\text{COOH}$  and an amount of total VFA higher than 18,5 g/L. According to Aguilar, 1995 and Ye Chen, 2008, this concentration leads to a deep inhibition of anaerobic digestion process; in fact, no increasing of methane percentage in the produced biogas was detected, and no decreasing in acetic acid concentration was observed till the end of the test. According to the stoichiometry of the disproportionation of acetic acid and carbon dioxide, if all the 15 g/L of acetic acid accumulated in the first ten days of process, was converted to methane, 110,5  $\text{NL}_{\text{CH}_4}$  were produced, that means other 40,93  $\text{NL}_{\text{CH}_4} / \text{Kg vs.}$  Adding this value to the 20,4  $\text{NL}_{\text{CH}_4} / \text{Kg vs}$  already produced, a yield of 61,33  $\text{NL}_{\text{CH}_4} / \text{Kg vs}$  are obtained, very close to value reached in the microcosms, confirming the previous hypothesis.

Due to this negative results, the second bioreactor test used a fed-batch approach as described in section 4.4.2, in order to diluate the digestate with a solution of demi  $\text{H}_2\text{O}$  and 20% w/w grinded red grape pomace, and limit  $\text{CH}_3\text{COOH}$  inhibition. According to the data reported in literature, and to the result obtained from an inhibition test made with our “DICAM” consortium (see description in paragraph 4.4.4, and results in 5.2.3.), 8 g/L was chosen as maximum tolerated acetic acid concentration. Besides that, a maximum limit of 73 g/L of volatile in the feed was set, in order to avoid rapid acetic acid accumulation. In the graphs reported in figure 5.9, are shown the principal results.

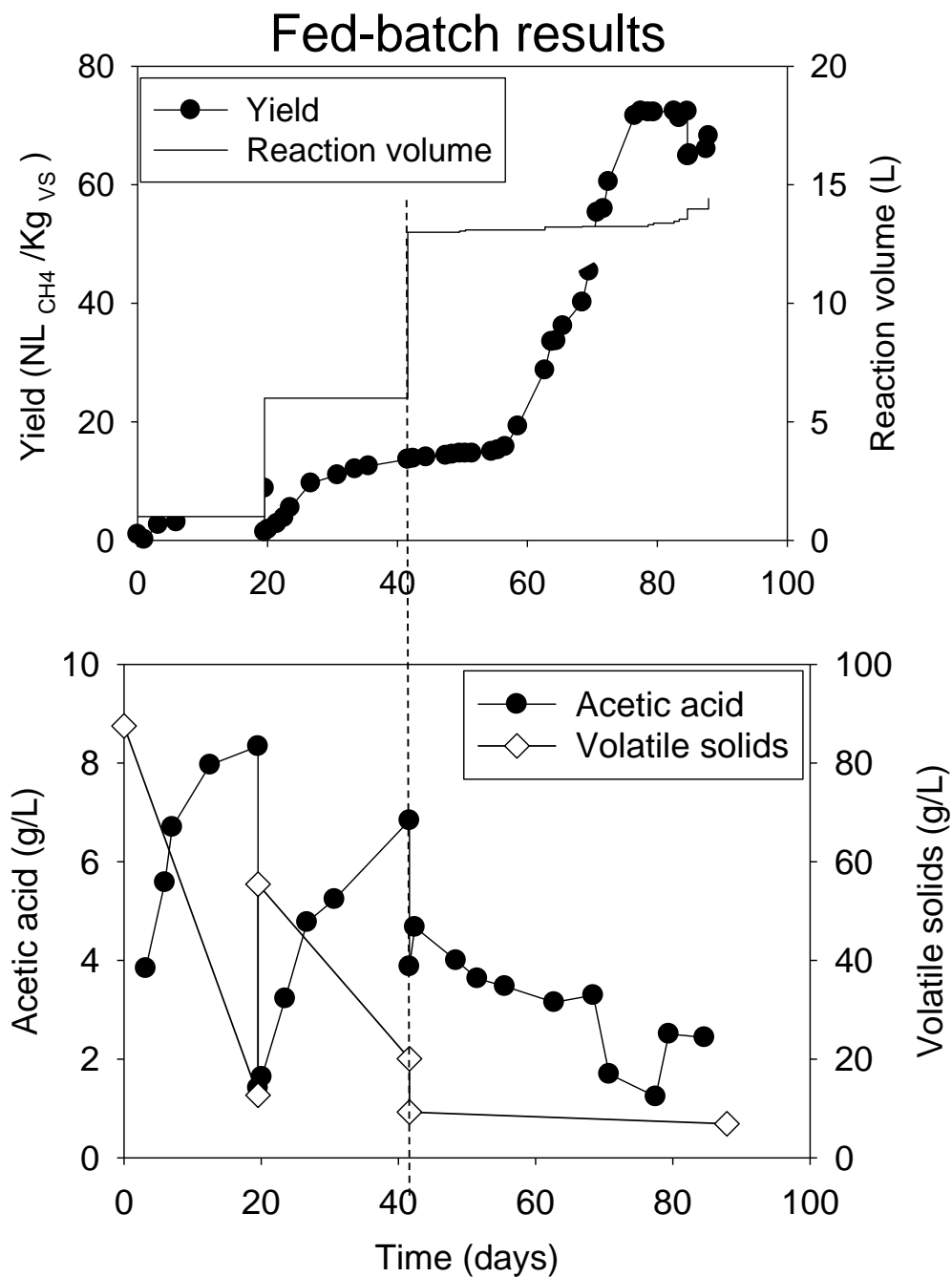


**Figure 5.9:** Principal result of red grape pomace anaerobic digestion in fed – batch experiment. In the left side of the black dotted line the experiment was conducted in a 1 Lt and 6 Lt bottle equipped as reported in figure 4.10. In the right side, the test was shifted in the fermenter.

As reported in the caption, the vertical dotted line represents the shift of the experiment from the 1 Lt and 6 Lt bottles to the reactor. In the first graph, the continuous line is referred to the volume increasing, up to 15 L. Every volume change was decided in function of acetic acid concentration (black circles in the second graph). When the  $\text{CH}_3\text{COOH}$  concentration was near 8 g/L, a dilution step

was performed with demi water and 20% w/w of grinded red grape pomace, in order to lower the VFA concentration. The values of propionic and butyric acid are not reported in the graph, because their concentrations stay below 0,5 g/L for all the tests, far below the estimated inhibitory concentration (Ingrid H. Franke-Whittle, 2014). Every dilution procedure was performed in order to results in a final acetic acid concentration between 2 g/L and 4 g/L, a non – inhibitory concentration, according to Aguilar, 1995 and Ye Chen, 2008. Moreover, before and after every dilution step, a sample for volatile solids (VS) analysis was taken (white diamonds in the second graph), to ensure that the value doesn't exceed the maximum concentration, set at 73 g/L.

This fed – batch approach leads to a better results compared to the first batch test.

From a starting value of 3,8 g/L and 87,5 g/L of volatile solids, from the first 19,5 days, a huge increasing of acetic acid concentration (up to 8,3 g/L) was detected, with a VS reduction to 12,7 g/L. This result is in line with the trend reported for the batch experiment where after 15 days, an accumulation of more than 15 g/L of acetic acids, led to a complete inhibition of the process. In this case, a lower acetic acid accumulation velocity was detected in the first seven days of fermentation, respect to the batch test: 0,72 g/L/d, and 1,73 g/L/d. This is probably due to a progressive acclimatization of the “DICAM” consortium during the first bioreactor experiment. The low volatile solids concentration, is a further confirmation that the hydrolytic, acidogenesis and acetogenic phases of anaerobic digestion are well – established, as reported also in the previous test, with a 85,5% of VS conversion. The final yield of this first step was 8,8 NL  $\text{CH}_4$  /Kg  $\text{VS}$  after 19,5 days, in line with the value of 13,2 NL  $\text{CH}_4$  /Kg  $\text{VS}$  obtained after 18,5 days of fermentation. After 19,5 days, a first step dilution was performed from 1 Lt to 6 Lt bottle, with an increasing of VS from 12,7 g/L to 55,5 g/L (due to the grape pomace fed together with water), and a decreasing of acetic acid concentration from 8,3 g/L to 1,4 g/L. This stage was prolonged for other 22 days, and the trend observed from all the considered parameters was the same as reported from the previous part of the experiment. The acetic acid value was increased from 1,4 g/L to 6,8 g/L but with a lower daily increment respect to 1 Lt phase: only 0,25 g/L/d respect to 0,72 g/L/d of the previous phase. Also the VS concentration followed the same trend. From the initial concentration of 55,5 g/L, a final value of 20,1 g/L was reached, with

a 63,8% conversion; this percentage is lower respect to the value calculated in the first part of the experiment. It's possible to speculate that the lower acetic acid daily accumulation rate, and the lower VS conversion, are strong indicators of a switching in the consortium prevalent metabolism, from the first three phases of anaerobic digestion towards methanogenesis. Anyway the methane yield is still very low, only 13,7 NL  $\text{CH}_4$  /Kg  $\text{VS}$ , in line both with the microcosms test (14,5 NL  $\text{CH}_4$  /Kg  $\text{VS}$  after 22 days). For this reason, another dilution step was performed, shifting the experiment from agitated bottles to the reactor, with an increasing working volume from 6 L to 13 L, only with demi water, without adding grape pomace as substrate. In this way, the amount of initial VS concentration was kept below 10 g/L (in particularly 9,3 g/L), to facilitate the instauration of methanogenic activity. Also the  $\text{CH}_3\text{COOH}$  concentration passed from 6,8 to 3,9, maintaining the value in the range set before starting this test. These condition was maintained for 35,9 days.

After 15 days of lag phase where both the yield value and the acetic acid concentration remained constant, the fermentation trend completely changed. A rapid and exponential increasing in methane yield was observed reaching a maximum value of 72 NL  $\text{CH}_4$  /Kg  $\text{VS}$  after 77,5 days of total process, and a production velocity of 0,25 NL  $\text{CH}_4$  /L/d and an acetic acid consumption velocity of 0,09 g/L/d from the acetoclastic part of the consortium. Moreover, the final methane percentage in biogas represents the 63% with a 34% of  $\text{CO}_2$ . This yield is absolutely comparable with the value of  $(69,5 \pm 9,6)$  NL  $\text{CH}_4$  /Kg  $\text{VS}$  obtained in the first microcosms test (figure 5.7). Moreover, the methane production velocity was higher respect to the value calculated for microcosm tests (0,18 NL  $\text{CH}_4$  /L/d), indicating a complete shift towards acetoclastic methanogenic activity. This result is also confirmed from the decreasing of the acetic acid concentration, from 3,9 to 1,7 g/L with a daily consumption rate of 0,08 g/L/d. If all the remained acetic acid was completely converted in methane according to the equimolar stoichiometry of the reaction the yield would increase by others 50,0 NL  $\text{CH}_4$  /Kg  $\text{VS}$  reaching a maximum value of 122 NL  $\text{CH}_4$  /Kg  $\text{VS}$ , comparable to the methane yield reported by E. Dinuccio 2010 (116 NL  $\text{CH}_4$  /Kg  $\text{VS}$ ). Besides that, the concentration of VS in this last part of the test remained quite constant, only a small decreasing from 9,3 g/L to 6,9 g/L was observed. This is another indication that support the completely shift of the consortium metabolism towards the methanogenic

activity. In fact, the consuming of the VS is directly related to the first anaerobic digestion phase, the hydrolysis of complex organic matter to the respectively simple units.

From the methanogenic part of the graphs, it's evident that the exponential phase of the methane yield starts when the  $\text{CH}_3\text{COOH}$  concentration was below 4 g/L; this value was in accordance with the data reported by Aguilar, 1995 and Ye Chen, 2008, and was kept as maximum limit of this VFA during all the subsequent continuous experiment. The best yield, instead, was reached when the acetic acid concentration value was 1,7 g/L. Probably below this limit the substrate became limiting in the methanogenic acetoclastic reaction. No equilibrium was founded between the hydrolytic-acid-acetogenic bacteria of the consortium and the methanogenic archaea, but only a complete shift from one type of metabolism to another.

According to these results, in the last part of the fed – batch test, the reaction volume was stepwisely increased from 13 L to 13,7 L, and the experiment was shifted from a fed – batch approach, to a continuous test described in section 4.4.2. In fact, due to the difficulty to ensure a full methanogenic activity with this consortium, it was decided to maintain this evolved consortia, changing the grape pomace feed modality from periodically fed – batch to a daily continuous (according to the company), without restarting a new test with pre-culture and reactor inoculation procedures. The long dead time in set-up the reactor and the pre-culture step, the evolution of the consortium on a methanogenic phase, the higher (only supposed) tolerance of the archaea to acetic acid concentration, and the long lag phase (up to 15 days) of this methanogenic population, were determinant criteria considered in taking this decision.

As reported in the appropriate description section, different organic loading rates were tested in collaboration with the company partner of the project. The volumetric flow rate (Q) was set at 0,22 L/day, that leads to a 68 days of HRT and the acetic acid concentration was kept lower than 4 g/L. According to the company partner of the project, the objective of the experiment was to increase

systemically the Organic Loading Rate feed (OLR) (keeping constant the HRT), from very low value (i.e. 0,4 g<sub>sv</sub>/L/day) to, at least, 1 g<sub>sv</sub>/L/day, and evaluate the performance of the plant.

In this long test (246 days), the OLR was increased only when the acetic acid concentration in the culture broth was below 1 g/L, or if the reactor reached a steady - state where the acetic acid concentration remained stable. In the latter case, in fact, all the produced acetic acid in the preliminary stages of anaerobic digestion, is immediately converted in methane by the acetoclastic archaea, leaving apparently constant the resulting CH<sub>3</sub>COOH concentration.

A long preliminary phase was performed where the OLR was initially stepwisely increased from 0,1 g<sub>sv</sub>/L/day to 0,3 g<sub>sv</sub>/L/d, in order to further acclimatize the consortium to the desired starting OLR value. In this period, the organic loading rate was increased only when the acetic acid was lower than 1 g/L, to avoid inhibition risk.

As soon as the reactor was stable, the OLR was raised to 0,4 g<sub>sv</sub>/L/d and maintained constant for 56 days. Then, was increased to 0,6 g<sub>sv</sub>/L/d for other 67 days for a total test duration of 123 days for these two OLR values. In the next graph, is reported the trend of the experiment during this period, in terms of acetic acid accumulation, biomethanization velocity and organic loading rate.

Moreover, in the graph is also reported the maximum yield obtained for every OLR range.



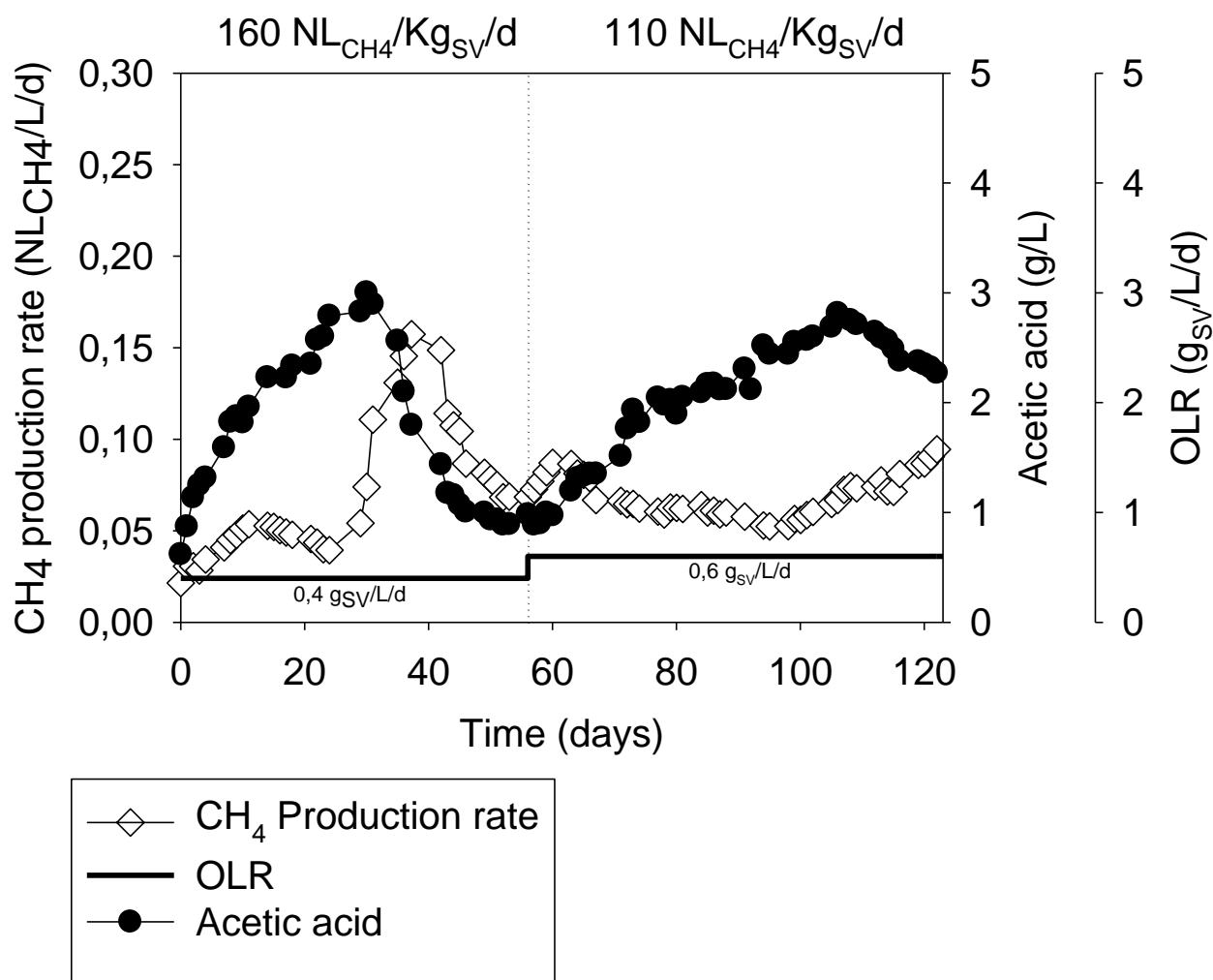


**Figure 5.10:** Continuous biomethanization tests performed with 0,4 g<sub>SV</sub>/L/d and 0,6 g<sub>SV</sub>/L/d.

In the left axis, the CH<sub>4</sub> production rate (white diamonds) expressed in NL<sub>CH<sub>4</sub></sub> /L/d, is related to the acetic acid profile (black circle) expressed in g/L, for every OLR (black continuous line), expressed in g<sub>SV</sub>/L/day.

To ensure a continuous daily feed, every day from the reactor was discharged 0,220 L of digestate, and immediately fed with the appropriate anaerobic mixture of grinded red grape pomace and demi water, as detailed in table 4.10. After the equilibration phase where the OLR was stepwisely increased (data not shown) until 0,3 g<sub>SV</sub>/L/day, the acetic acid concentration was 0,62 g/L, with a final CH<sub>4</sub> percentage in the biogas of 37% and 21% of CO<sub>2</sub>. The remained gas was nitrogen, used to flux the reactor in order to establish anaerobic condition prior the experiment set-up.

In the graph a black vertical dotted line represent the OLR shift, from 0,4 g<sub>sv</sub>/L/day to 0,6 g<sub>sv</sub>/L/day. It's evident that both of two part of the graph are characterized by a cyclical trend, both for CH<sub>3</sub>COOH concentration and both for biomethanization rate.

Analyzing the left part of the graph (where the OLR was set at 0,4 g<sub>sv</sub>/L/day), the acetic acid value in fermenter immediately raised from 0,62 g/L to a maximum concentration of 3 g/L at 30 days of continuous experiment, with a quite linear increment of 0,071 g/L/d, in line with the first stage of fed – batch approach. This is an indication that in response to an increasing of substrate feed, the preliminary stages of the anaerobic digestion are immediately active, since the first days of the process. In fact, the genera responsible for the hydrolytic (*Streptococcus* or *Enterobacterium*), acidogenic (*Pseudomonas*, *Bacillus*, *Clostridium*, *Micrococcus*, or *Flavobacterium*) and acetogenic (*Syntrophomonas* or *Syntrophobacter*) steps of anaerobic digestion, are characterized by a fast duplication rate, like few hours (Fayyaz Ali Shah, 2014).

Moreover, also in a bioreactor completely oriented to ensure the best methanogenic conditions, those type of bacteria are able to produce acetic acid, confirming the high tolerance to environmental changing, reported also in literature (Delbes, 2000). This characteristic is one of the key that justify the broad spectrum of anaerobic digestion industrial application, and the large number of study present in literature to determine the best reactor configuration that ensures high activity of both the archaea and bacteria population (J. Guendouz, 2010), (Joseph G. Usack, 2012), (Kim M, 2002).

Together with the acetic acid accumulation, in the first month of experiment a very small increasing of biomethanization rate was observed, from initial 0,048 to a maximum value of 0,074 NL<sub>CH<sub>4</sub></sub> /L/d. This is probably related to hydrogenotrophic methanogenesis extensively reported in paragraph 3.2 and in table 3.3. This type of methanogenic activity uses only 4 H<sub>2</sub> to reduce 1 CO<sub>2</sub> producing 1 CH<sub>4</sub> and 2 H<sub>2</sub>O, and is mediated by different types of archaea. It's usually a low efficient contribution to the overall process, because the most abundant methanogenic activity is represented by acetoclastic part of the consortia. It's hard to estimate the contribution of the hydrogenotrophic methanogenic activity, because a lot of factor influences this process (e.g., partial pressure, phylogenetic composition), and represent one of the most variable parameters in different anaerobic digestion tests.

In the first part of the process that is considered now, the yield of this hydrogenotrophic part is very low (less than 15 NL  $\text{CH}_4$  /Kg vs), leading to a smaller increasing of methane percentage in the produced biogas, from 37% to 48%. This type of methanogenic activity is not related to a consumption of acetic acid, so this can explain the contemporary increasing of both acetic acid concentration and both biomethanization velocity. Thus, is possible to speculate that in this phase of the process only the hydrogenotrophic archaea are active. Some confirmation of our hypothesis are represented by a negligible amount of hydrogen founded in biogas composition (always less than 0,5%), and some literature studies that reports that hydrogenotrophic methanogens have a faster duplication velocity that acetoclastic methanogens, and usually represents (in a temporary scale), the first detected biomethanization activity in a mixed consortium (Burak Demirel, 2008). The volatile solids conversion oscillates in this period between 57% and 78% with a concentration in the fermenter kept in the range between 5,99 g/L and 11,55 g/L, paying attention to not exceed over 10 – 15 g/L.

Then, after 30 days of continuous feeding the trend was completely inverted. Acetic acid was consumed with a 0,14 g/L/d consumption rate from day 30 to day 43, reaching a final concentration of 1,18 g/L. It's important to notice, that this acetic acid consumption velocity is higher that the value calculated for the methanogenic phase in the fed – batch experiment (0,091 g/L/d). This represent an ulterior evidence of the continuous acclimatization of the acetoclastic part of the used consortium to a continuous exposition to  $\text{CH}_3\text{COOH}$ . Together to the acetic acid consumption, a huge increasing in the biomethanization rate was detected, reaching a maximum value of 0,16 NL $\text{CH}_4$  /L/d after 37,3 days of fermentation. In that day, the daily amount of produced methane was to 3,1 NL $\text{CH}_4$  (4,1 NL biogas with a methane composition of 85% of  $\text{CH}_4$  ad only 14% of  $\text{CO}_2$ ). It's evident the shifting towards a full acetoclastic methanogenic condition, where the acetic acid is disproportionate to  $\text{CH}_4$  and  $\text{CO}_2$ . The maximum yield was reached in the middle of exponential phase (day 37) and was 160 NL $\text{CH}_4$  /Kg vs, a value more than doubled respect to the previous fed – batch experiment (72 NL $\text{CH}_4$  /Kg vs), and higher also respect the maximum yield reported in literature by E. Dinuccio, 2010 (116 NL $\text{CH}_4$  /Kg vs). This is absolutely an astonishing result, if is considered the absence of specific pretreatment of the lignocellulosic initial raw material. It's good to remember that this result is a combination of the

acetoclastic pathway, but also of the hydrogenotrophic activity, that is still ongoing from the first days of fermentation. Moreover, at day 37, 1,8 g/L of acetic acid was present in the fermentation broth, it means other 9,4 NL<sub>CH<sub>4</sub></sub> /Kg<sub>VS</sub> of theoretical biomethane. Considering the overall potential, a maximum yield of 169,4 NL<sub>CH<sub>4</sub></sub> /Kg<sub>VS</sub> was obtainable from this process.

According to the results observed in the fed – batch experiment, during the methanogenic exponential phase, the concentration of the volatile solids in the fermenter remains stable, due a completely imbalance of the consortium towards methanogenic metabolism. Thus, if there are no consumption of volatile solids, practically no acetic acid was produced in this phase. In this part of the continuous experiment, anyway, the concentration of VS slowly decreases, from 11,44 g/L immediately present before the methanogenic phase, to 7,83 g/L and 5,99 g/L at the end of exponential phase (day 37). This is a strong indication that the acetoclastic methanogenic is the prevalent metabolic activity present in the consortium in this moment, but also the hydrolytic-acidogenic-acetogenic bacteria are still active, and there is a continuous consuming of organic matter. This is an important metabolic improvement in the equilibrium of the consortium. Probably the continuous feeding had a positive effect on the overall stability of the integrated mixed culture. So probably the total acetic acid consumption can be higher respect to the observed 0,14 g/L/d, because this value is a resulting balance between the real acetic acid consumption rate, and the basal acetic acid production rate, due to the bacterial part of the inoculum.

Besides this qualitative value, if this hypothesis is correct, after this exponential methanogenic phase, the system should reach a steady state, where both biomethanization rate, both acetic acid concentration are stable. In this condition, the system can reach an equilibrium where the bacterial part of the consortium hydrolyze the complex organic matter and transform the simple biochemical units (monosaccharides, aminoacids, and VFAs) in acetic acid, H<sub>2</sub> and CO<sub>2</sub>, and the archaeal part of the inoculum that converts these products in methane and carbon dioxide through both hydrogenotrophic and both acetoclastic pathway.

In fact, after a short period where the velocity decreased, together the acetic acid (day 42 – day 47), both biomethanization rate, both acetic acid concentration reached a constant value (day 47 – 56). The

biomethanization rate settled on average value of  $(0,073 \pm 0,006)$  NL<sub>CH<sub>4</sub></sub> /L/d, and the CH<sub>3</sub>COOH concentration remained on the average value of  $(0,937 \pm 0,044)$  g/L, for ten days.

From this desired steady – state, the OLR was increased from 0,4 g<sub>sv</sub>/L/day to 0,6 g<sub>sv</sub>/L/day from day 57, to day 123, as reported in the right side of previous graph.

It's immediately recognizable the cyclic trend, similar to the previous one both for acetic acid concentration, both for the biomethanization rate. It's also evident from the graph that the shape of this cyclic trend is different from that one observed during the previous OLR. In fact, after 57 days, a steady state was reached in the previous phase, now in 66 days of 0,6 g<sub>sv</sub>/L/day as OLR, not only the steady state was not detectable, but all the velocity of the process seems to be slowly, from the acetic acid accumulation and subsequent consumption, to the biomethanization rate. Probably some substrate – related inhibition is the cause for this slow process.

Anyway, for the first week of experiment (day 57 to day 64), a small increasing of biomethanization rate was detected, from 0,069 to 0,081 NL<sub>CH<sub>4</sub></sub> /L/d, together with acetic acid accumulation. This effect is probably connected to the hydrogenotrophic methanogenesis. In fact, the acetic acid accumulation is an indication of high bacterial activity in the consortium, and H<sub>2</sub> is the main product (together with CH<sub>3</sub>COOH) of this anaerobic metabolism. But hydrogen is also the main substrate for hydrogenotrophic methanogens, and this can explain this small increasing in the CH<sub>4</sub> production velocity. Also in this case, in fact, no hydrogen accumulation was founded in the produced biogas (less than 0,5%). From day 57 to day 106, acetic acid concentration increased from 0,98 g/L to 2,81 g/L, with an average accumulation rate of 0,037 g/L/d, that is halved from the previous accumulation velocity during previous OLR (0,071 g/L/d). This is another indication of some transversal inhibition process on all the bacterial and archaeal part of the consortium. This hypothesis is also confirmed from the analysis of the volatile solids. In fact, higher amount of volatile solids was founded in the fermenter, ranging from 10,98 g/L to 19,30 g/L during the acetic acid accumulation phase, with a percentage conversion in line with the data reported for previous OLR. Probably some synergic inhibition effects were the responsible for this slow process e.g. higher amount of VS (in the batch experiment the acetoclastic methanogenesis started when the concentration of VS was lower than 10

g/L), and some grape pomace related compounds (like lignocellulosic derived compounds) that can have inhibitory effect. Like the previous OLR, negligible methane yield was obtained (less than 20 NL<sub>CH<sub>4</sub></sub> /Kg vs), and low CH<sub>4</sub> formation velocity was detected, in the range between 0,05 – 0,06 NL<sub>CH<sub>4</sub></sub> /L/d.

From day 103 to day 123, as previously reported, the trend the trend was completely inverted. Acetic acid was consumed passing from 2,81 g/L to 2,18 g/L, with a 0,035 g/L/d. This value is absolutely not comparable with the same calculated for previous OLR (0,14 g/L/d), giving another indication of some inhibitory effect. Together to the acetic acid consumption, an increasing in the biomethanization rate was detected, reaching a maximum value of 0,09 NL<sub>CH<sub>4</sub></sub> /L/d after 123 days of fermentation. Again, this value is not comparable to the previous biomethanization rate (0,16 NL<sub>CH<sub>4</sub></sub> /L/d). The maximum yield was reached in days 123 and was 110 NL<sub>CH<sub>4</sub></sub> /Kg vs. It's obviously lower respect to the 160 NL<sub>CH<sub>4</sub></sub> /Kg vs obtained with 0,4 g<sub>sv</sub>/L/day, but anyway comparable with the data reported in literature (E. Dinuccio, 2010). Another data that can confirm the inhibition theory is that, if all the remained acetic acid was converted in methane, according to the reaction stoichiometry, the total yield should lead to 167,5 NL<sub>CH<sub>4</sub></sub> /Kg vs, completely in line with the previous exponential phase.

Also in this case, a small consumption of volatile solids was detected during this methanogenic activity. In fact, the concentration passes from 19,30 g/L at the end of VFA accumulation phase, to 9,34 detected at day 122. This represent a confirmation of the previous theory that during acetoclastic methanogenic phase, also the hydrolytic-acidogenic-acetogenic bacteria are still active. As previously reported, probably the continuous feeding had a positive effect on the overall stability of the integrated mixed culture. So, also in this case probably the total acetic acid consumption can be higher respect to the observed 0,035 g/L/d, because this value is a resulting balance between the real acetic acid consumption rate, and the basal acetic acid production rate, due to the bacterial part of the inoculum. Anyway, also considering this effect, no comparison is possible with the previous detected acetic acid consumption rate, and a possible inhibition of the whole process remain the most accredited theory. From the graph is also evident, that no data is reported after day 123, while the methanogenic phase was not concluded.

After external analysis of the culture broth that revealed a lack of nitrogen, due to the high Carbon-to Nitrogen content of the grape pomace. According to M.A. Bustamante, 2007 that screened different types of winery by-product in his work, the C/N ratio of grape pomace can fluctuate between 13:1 and 19:1. Microorganisms are able to metabolize substrates with a C/N ratio up to 40:1, but the ideal carbon-to-nitrogen ratio in the feed for an efficient anaerobic digestion process should be less than 10:1 (Alastair J. Ward, 2008), (Mata-Alvarez, 2000). According to preliminary estimation of our grape pomace, the C/N ratio should be around 16:1. Moreover, in industrial digesters, the C/N ratio in the digestate is usually kept between 5:1 – 10:1, when external analysis revealed that in our fermenter broth the C/N ratio was 14:1

For this reason, in order to obtain a C/N ratio in the digestate of 7,5:1, at day 123, 78 grams of ammonium nitrate ( $\text{NH}_4\text{NO}_3$ ) was added as nitrogen source in the reactor, paying attention to avoid ammonia inhibition (a concentration of 0,81 g  $\text{NH}_4\text{-N/L}$  was detected).

Different articles, in fact, reported that ammonia accumulation is one of the most inhibitory effect on anaerobic digestion. In particularly early literature related the inhibition of AD process to total ammonia nitrogen (TAN) concentration, (Hansen, 1998), (Nakakubo, 2008), (Procházka, 2012), which is a combination of free [unionized] ammonia nitrogen (FAN) and ionized ammonium nitrogen ( $\text{NH}_4$ ). As the end – product of anaerobic digestion of nucleic acid and protein, ammonia is essential at low concentration, but also very toxic at higher concentration. It's very difficult to estimate the threshold level, because a lot of physiological and chemical factor are related to ammonia inhibition. Primarily, two types of inhibition are detected. TAN – related inhibition occurred when total ammonia concentration exceed 1,5 g/L (Melbinger NR, 1971), (OE., 1961), but with the microflora acclimatization, different examples of well – established process are present in literature with TAN concentration up to 6 g/L (Soto, 1991), (Calli, 2005). It's evident that inoculum composition, plays a key role in this inhibitory process. Besides that, it should be noted that the prevalent inhibition effect on AD by ammonia should be related directly to the FAN levels, due to the high permeability across the cell membrane (Müller, 2006). FAN concentration primarily depends on three parameters such as TAN, pH and temperature, and can be estimated using this empirical relationship:

$$\text{NH}_3 (\text{Free}) = \text{TANX} \left( 1 + \frac{10^{-\text{pH}}}{10^{-(0.09018 + \frac{2729.92}{T(\text{K})})}} \right)^{-1}$$

**Figure 5.11:** Relationship between FAN (Free Ammonia Nitrogen) and TAN (Total Ammonia Nitrogen), pH and T °C (Rajinikanth Rajagopal, 2013)

Different studies (Hafner, 2009), (Nielsen, 2008), (Ho, 2012) demonstrated that for the anaerobic digesters operated at pH 7 and 35 °C, FAN represents less than 1% from the total ammonia, while, at the same temperature, but pH 8 the FAN increases to 10%. In a similar study (Kayhanian, 1999), showed that FAN concentration at thermophilic (55 °C) temperatures is expected to be six times higher than under mesophilic conditions at the same pH.

An increase in pH from 7 to 8 will lead to an eightfold increase of the free ammonia levels in mesophilic conditions and even more at thermophilic temperatures, because temperature influences the dissociation constant of ammonia nitrogen based on the equation in figure 5.11. Anyway, according to Rajinikanth Rajagopal, 2013, a maximum FAN concentration of 1,2 g/L leads to a complete inhibition of AD process, but also level below 0,2 g/L can lower the methane yield (Massé, 2003).

Knowledge of how ammonium toxicity occurs is limited and few studies with pure cultures have shown that ammonia may affect methanogenic bacteria in two ways: (i) ammonium ion may inhibit the methane producing enzymes directly and/or (ii) hydrophobic ammonia molecule may diffuse passively into bacterial cells, causing proton imbalance or potassium deficiency.

A fraction of  $\text{NH}_3$  that enters into the cells causes a pH change due to its conversion into ammonium ( $\text{NH}_4^+$ ), while absorbing protons in the process. The cells must then consume energy in proton balancing, using a potassium ( $\text{K}^+$ ) pump to maintain the intracellular pH, thus increasing maintenance energy requirements and potentially causing inhibition of specific enzyme reactions (Rajinikanth Rajagopal, 2013).

After this long excursus of ammonia inhibition, it's clear that is impossible defining a threshold limit because a plethora of different parameters are involved, and our nitrogen addition approach was based on the estimated C/N ratio in the feed, the desired C/N ratio in the digestate, and these ammonia inhibition data reported in literature.



Immediately after the ammonium nitrate addition, unfortunately, a complete block of the methanogenic process was observed, with a deep collapse of biogas production from an average 2/3 L/d with an average 60% - 70% of CH<sub>4</sub>, to less than 0,1 L/day with a negligible methane percentage. Besides that, a complete inversion of acetic acid trend was observed; from the acetoclastic methanogenesis and a slow but continuous CH<sub>3</sub>COOH consuming (0,035 g/L/d), to an increasing concentration from 2,3 g/L to 4,7 g/L in 35 days with an average acetic acid bioproduction velocity of 0,07 g/L/d. Besides a possible ammonia inhibition as previously depicted (while the g NH<sub>4</sub>-N/L concentration remained lower than 1,5 g/L for all the 35 days), it's also possible to speculate a nitrate – related inhibition. Hydrogenotrophic methanogens, in fact, can also use nitrate as electron acceptor instead of CO<sub>2</sub>, resulting in an alternate use of produced hydrogen in place of methanogenesis, and a competition between these two alternative routes. In figure 5.12 is detailed this possible mechanism:

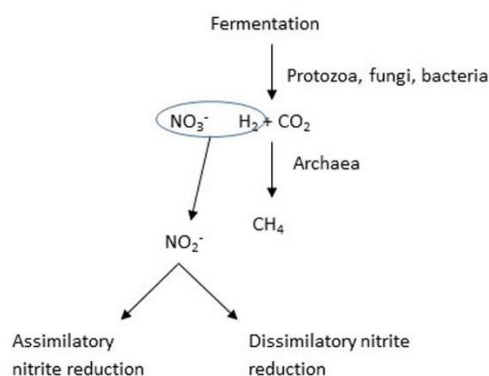


**Figure 5.12:**

*Possible alternative pathway of hydrogen utilization in presence of nitrate in a methanogenic fermenter (Chengjian Yang, 2016).*

This alternative pathway has a higher – energy metabolic content respect to the hydrogenotrophic methanogenic route (H. Detlef Klüber, 1998). Besides that, nitrogen – related compounds, increase the redox potential, from – 200 mV (typical for the methanogenic reaction), to more than + 400 mV (J. C. Akunna, 1998), producing a non – favorable environment for methane production, and major sensitivity to FAN inhibition. For all of these reason, in presence of nitrate, the methanogenic pathway is unfavored.

Anyway, this type of inhibition affects only the hydrogenotrophic part of the consortia, thus, other type of inhibition processes must be involved. It's evident that the nitrate present in the culture broth, stimulate the growth of the nitrate reducing bacteria, that are involved in the dissimilative nitrate

reduction. This process leads to the formation of toxic by - products nitrogen oxides ( $\text{NO}$ ,  $\text{N}_2\text{O}$ ), that may directly suppress also acetoclastic methanogenic activity. Probably, more than a competition between denitrifying and methanogenic bacteria, a direct inhibition due to N-oxides compound derived from nitrate reduction, is the major responsible for the complete block of methanogenic activities (Ungerfeld, 2015). In fact, 50 mM of nitrate concentration is enough to inhibit the 65% of acetoclastic methanogenesis, whereas, only 0,18 mM and 0,32 mM of respective  $\text{N}_2\text{O}$  and  $\text{NO}$ , are able to be completely inhibitory (T. Scheper, 2003). Again, other type of studies reports that this inhibition process is completely reversible; when all electron acceptors were reduced, the methanogenic activity is completely restored (H. Detlef Klüber, 1998).

The nitrate concentration in the fermenter, (measured spectrophotometrically) in the first days after ammonium nitrate addition was in the range between 107,1 mM and 74,3 mM, higher than 50 mM indicated by T. Scheper, 2003, so probably this concentration (together with  $\text{NO}$  and  $\text{N}_2\text{O}$  as by - products) is the major responsible for methanogenic activity inhibition. To lower this high nitrate and N-oxides concentration, the digestate was diluted 1:1 with demi water, reducing the nitrate concentration to 50,2 mM. After this procedure, in a couple of days the methane productivity gradually increased again, and the cyclic trend was re-instaurated again.

After 1 month where the OLR was kept again at 0,6  $\text{g}_{\text{sv}}/\text{L}/\text{day}$ , the steady state was reached again with values in line with the previous part of the experiment (0,07  $\text{NL}_{\text{CH}_4}/\text{L}/\text{d}$ ), with an average VS concentration of 13 g/L and a restored VS conversion of c.ca 70%. The total yield was 165  $\text{NL}_{\text{CH}_4}/\text{Kg}$  vs, in line with the data reported for 0,4  $\text{g}_{\text{sv}}/\text{L}/\text{day}$  as OLR (160  $\text{NL}_{\text{CH}_4}/\text{Kg}$  vs), with a 2,2 g/L of residual acetic acid and an average  $\text{CH}_3\text{COOH}$  consumption velocity of 0,15 g/L/d.

At this point, the OLR was increased to 0,9  $\text{g}_{\text{sv}}/\text{L}/\text{day}$ , and subsequently as last step to 1,2  $\text{g}_{\text{sv}}/\text{L}/\text{day}$ , as required by the company. The results are reported in figure 5.13

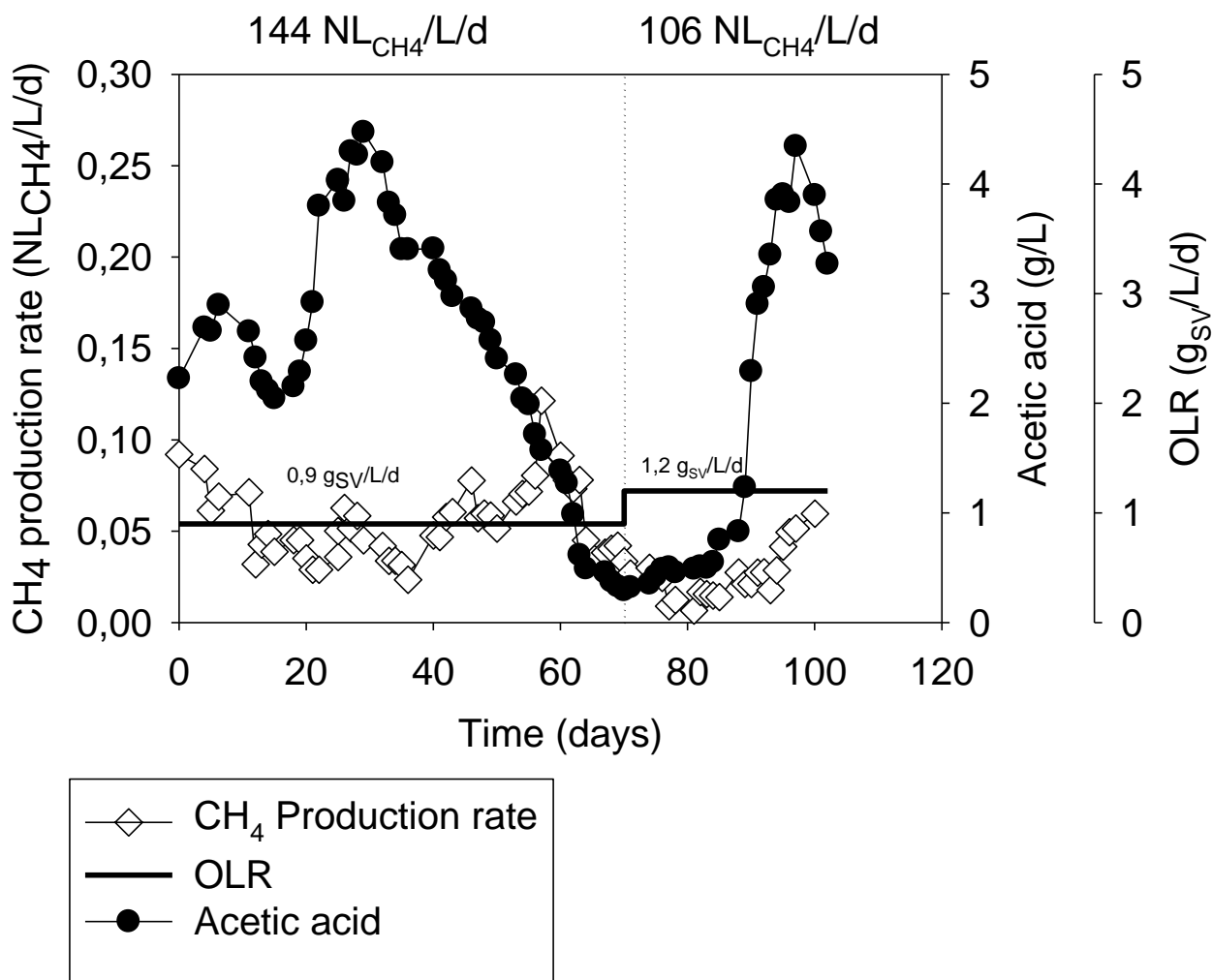


**Figure 5.13:** Continuous biomethanization tests performed with 0,9 g<sub>sv</sub>/L/d and 1,2 g<sub>sv</sub>/L/d.

Also in this graph (as previously reported for OLR: 0,4 g<sub>sv</sub>/L/day and OLR: 0,6 g<sub>sv</sub>/L/day), the acetic acid shows a cyclic trend for each OLR.

During the 70 days of 0,9 g<sub>sv</sub>/L/day as OLR, from 2,2 g/L, the maximum acetic acid concentration was reached after 29 days (4,8 g/L), but the increment was not constant as the previous tests. Anyway, a decreasing in the concentration from 4,8 g/L to 0,29 g/L (day 70) and an interesting consuming velocity rate (0,10 g/L/d) were detected. Together to the acetic acid consumption, an increasing in the biomethanization rate was detected, reaching a maximum value of 0,12 NL<sub>CH<sub>4</sub></sub> /L/d after 57 days of feeding with this OLR. In that day, the daily amount of produced methane was to 1,6 NL<sub>CH<sub>4</sub></sub> (1,7 NL<sub>biogas</sub> with a methane composition of 70% of CH<sub>4</sub> and 27% of CO<sub>2</sub>). The maximum yield was 144

$N_{LCH_4}$  /Kg vs, a value a little bit lower respect the previous phases, but still higher respect the maximum yield reported in literature by E. Dinuccio, 2010 (116  $N_{LCH_4}$  /Kg vs).

According to the results observed in the fed – batch experiment, during the methanogenic exponential phase, the concentration of the volatile solids in the fermenter remains stable, due a completely imbalance of the consortium towards methanogenic metabolism. In this part of the continuous experiment, anyway, the concentration of VS increases due to a higher feed rate up to 21,7 g/L, probably higher respect an optimal value (in the fed – batch exponential phase the value was lower than 10 g/L), but the conversion was still high, in the range between 60% and 70%.

The steady state was reached after 70 days with a biomethanization rate settled on average value of  $(0,026 \pm 0,002)$   $N_{LCH_4}$  /L/d, and the  $CH_3COOH$  concentration remained on the average value of  $(0,396 \pm 0,073)$  g/L, for ten days.

With this OLR, is evident the difficulty to maintain an equilibrium between the two different phases. In fact, the cyclic trend, especially for the biomethanization velocity, is not so clear, probably due to an instability of the consortia after more than 190 days of total experiment. Probably some inhibition of methanogenic activity (maybe related to the accumulate of some toxic by – product related to lignocellulosic hydrolyzation), or higher amount of VS in the fermenter are two of the main causes of this results.

Anyway, after this steady state, the OLR was increased again to 1,2  $g_{sv}$ /L/day for 33 days, as required by the company partner of the project, and (after a week of assessment to the new OLR), a huge increasing in acetic acid concentration was observed up to 4,41 g/L from 0,39 g/L of the previous steady – state in less than 10 days. This is probably related to a higher feeding rate respect to the methane production kinetic, because also volatile solids in the reactor increased their concentration, from 21,7 g/L of the previous phase, to a maximum value of more than 30 g/L. This is probably the principal effect of an overload, due a higher OLR, that leads to an inhibitory VS concentration. In fact, the acetic acid accumulation velocity was 0,24 g/L/d, a value never reached in all of this tests. This can be a sign or an indication of a non - equilibrium of the consortium, probably due to a methanogenic inhibition effect (some lignocellulosic derived compounds or VS, as previously

hypnotized). Anyway after reached a maximum after 97 days of this test, the acetic acid concentration decreased with a consumption rate of 0,18 g/L/d. Also in this case the consumption velocity from the acetoclastic archaea is very high respect all the previous phase, but the velocity (apart from a small increasing), never reached again an interesting value, with a maximum biomethanization rate less than 0,06 NL<sub>CH<sub>4</sub></sub> /L/d, and a yield of 106 NL<sub>CH<sub>4</sub></sub> /Kg vs. Those value of velocity and yield were the lowest obtained until now, and for this reason, this long experiment, was stopped, after a total 246 days of total fermentation. In table 5.4 are reported an overview of the principal parameters obtained in all of these fermentation tests, compared to the initial microcosm experiment, and to the values reported in literature (E. Dinuccio, 2010).

***Principal fermentation parameters obtained during the biomethane production tests with  
grinded red grape pomace***

	Yield (NL <sub>CH<sub>4</sub></sub> /KgSV fed)	Velocity (NL <sub>CH<sub>4</sub></sub> /L/d)	OLR (gsv/L/day)	Note well (NB)
<i>Batch</i>	20,4	< 0,05	/	
<i>Fed – Batch</i>	72,0	0,25	/	(Optimal parameters estimated: ✓ Acetic acid < 8 g/L ✓ VS concentration < 80 g/L in the feed and < 10 g/L in the exp. phase)
<i>Continuous</i>	160	0,16	0,4	
<i>Continuous</i>	110 / 165	0,09 / 0,14	0,6	(the values on the right are obtained without supposed ammonia/nitrate inhibition)
<i>Continuous</i>	144	0,12	0,9	(probable inhibition by higher VS concentration – 21,7 g/L, or by accumulation of lignocellulosic derived compounds)
<i>Continuous</i>	106	0,06	1,2	(probable inhibition by higher VS concentration - > 30g/L, or by accumulation of lignocellulosic derived compounds)
<i>Microcosms</i>	(69,5 ± 9,6)	(0,18 ± 0,04)	/	
<i>Literature</i>	116	/	/	

**Table 5.4:** Principal parameters estimated in the bioreactor anaerobic digestion tests with grinded red grape pomace, compared to microcosm experiments and literature yield.

From this summary, some conclusion can be made.

- The batch approach is feasible only in small scale fermentation (116 ml microcosms), because in the reactor leads to an inhibitory accumulation of volatile fatty acids.
- In the fed – batch conduction a methanogenic phase was reached keeping the acetic acid concentration below 8 g/L and in particularly below 4 g/L, reaching a methane yield comparable with the microcosms experiment. Moreover, less than 80 g/L of VS in the feed is necessary to maintain acetic acid below the set concentration, and exponential methane phase is reached when VS concentration is below 10 g/L. Probably some substrate – inhibition effect is involved
- In the continuous experiment, a very good yields are reported, higher than the maximum reported in literature, for this kind of red grape pomace, but different parameters need to be optimized:
  - ✓ With this type of consortium, it's harder to maintain an equilibrium between the preliminarily stages of anaerobic digestion and the methanogenic step → intrinsic difficulties to reach a steady – state.
  - ✓ The continuous grape pomace feed leads to a nitrogen shortage, due to the high C/N ratio of this substrate. Moreover, an external addition of nitrogen needs to be very carefully evaluated, in order to avoid ammonia, or nitrate inhibition processes.
  - ✓ With higher OLR, (0,9 g<sub>SV</sub>/L/day – 1,2 g<sub>SV</sub>/L/day), an accumulation of VS is reported, that can lower the overall yield of the process.
  - ✓ After a prolonged feed, probably some toxic compounds derived from lignocellulosic degradation accumulates in the fermenter. They can alter the stability of the consortia, and inhibit completely the methanogenic activity. A lot of different studies reported in literature confirms this theory, where phenolic compounds and furans are characterized as the influent inhibitory compounds in fermentations processes (see paragraph 5.2.3. for the lignocellulosic inhibition tests, and the molecular details of the possible

mechanisms inhibition). This is probably the motivation for the decreasing trend of methanization rate and yields when the OLR was incremented.

- Generally speaking, it's possible to affirm that without a specific pre-treatment, this process is an innovative, feasible, with interesting yields, higher respect to the value reported in literature. Anyway, the higher C/N ratio of the substrate, the prolonged lag phase of the methanogens and the instability of the consortium are the most limiting parameters. Probably a co-digestion with a high nitrogen content substrate can resolve the nitrogen limitation.

Besides that, the acclimatization of the consortium is a factor that is not to underestimate. A further acclimatization, in fact, can enhance the methanogenic activity, and also the tolerance to the inhibitory effects.

### *5.2.2 White pomace BMP experiment*

During the long continuous tests extensively described previously, the discharged digestate was sometimes used as inoculum, to perform different types of studies. For example, (as reported in paragraph 4.4.3), at days 43,94 of fermentation at 0,4 g<sub>SV</sub>/L/day as OLR, a battery of microcosms was prepared, with the inoculum taken from the reactor, to test if white pomace were able to produce biomethane. In fact, due to the high polyphenols content, white pomaces are less used into anaerobic digestion process (Field J. A., 1989), (Field J. A., 1987). For this reason, one of the triplicate was supplemented with a mixture of microelements and vitamins (described in 4.4.3.), to enhance microbial growth. Besides that, to compare the yield and the biomethanization rate, a triple positive control was prepared in the same conditions, but fed with red grape pomace. Besides that, a double negative control was also investigated, without any grape pomace supplementation.

In order to make comparable the yield results, all the microcosms must have the same amount of volatile solids (VS) concentration. For this reason, a preliminarily analysis of VS of the digestate / inoculum used, was performed, and in that period, the reactor has 10,98 g/L of VS, corresponding to 0,44 grams of VS in each microcosm. Thus, in order to maintain the OLR used in the reactor at that

time, calculations reported in 4.4.3. section shown that 1,346 g of grape pomace was necessary for each 116 ml – microcosms (liquid volume 40 ml), and according to the percentage of VS of each type of pomace (table 4.1, section 4.1.2.), 1,12 grams of VS was added to the positive controls as red grape pomace, and 1,17 grams of VS was added to the microcosms fed with white pomace.

The total amount of VS, was respectively 1,61 grams in the microcosms with white pomace, 1,56 grams in the microcosms with red pomace, and 0,44 grams in the negative controls (only inoculum). In figure 5.14, and in table 5.5. are reported the methane volume production, and the maximum values of yields and velocity obtained, compared to those reported from the first microcosms experiment in figure 5.7 with red grape pomace. It's important to notice that the test was interrupted before the complete consumption of all the VS; in fact, the main monitored parameters are the yields and the initial velocity. This one must be determine in the first part of the fermentation, when the substrate is in excess respect to the inoculum (zero order and exponential phase).

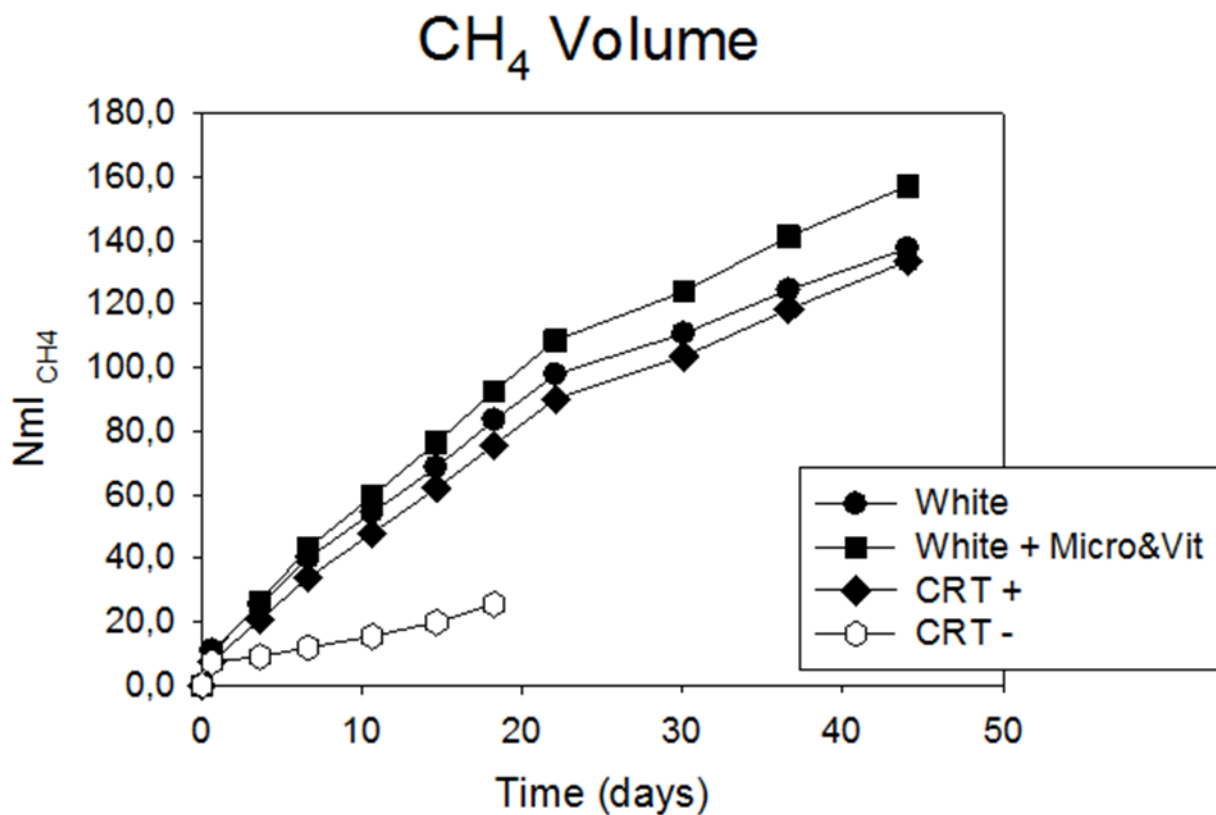


**Figure 5.14:** Nml of methane produce in the BMP of white pomace. Only white pomace supplemented with microelements and vitamins is a single test. All the other are triplicates (except negative control that is in duplicate)



### *Yields and biomethanization rates*

	Max. yield (NL <sub>CH4</sub> /KgSV fed)	Max. velocity (NL <sub>CH4</sub> /L/d)
<i>White</i>	(84,09 ± 16,43)	(0,44 ± 0,05)
<i>White + micro&amp;vit</i>	96,10	0,39
<i>Ctr +</i>	(84,48 ± 1,49)	(0,30 ± 0,01)
<i>Ctr -</i>	> 20	(0,11 ± 0,02)
<i>Microcosm test (figure 5.7)</i>		
	(69,50 ± 9,16)	(0,18 ± 0,04)

**Table 5.5:** Yields and CH<sub>4</sub> production rates of white pomace, compared to the controls and the previous microcosms experiment

From the graph it's evident that also the white pomaces are able to produce biomethane using "DICAM" inoculum. Moreover, the produced volume is very comparable with the red pomace (Ctr +), considering the standard deviation: (137,50 ± 26,87) Nml<sub>CH4</sub> for the white pomace, and (133,56 ± 2,35) Nml<sub>CH4</sub> for the red. Only the supplementation of microelements and vitamins leads to a small increasing in production, 157 Nml<sub>CH4</sub>, but due to the single analysis, it's impossible to make any consideration. Anyway, different literature articles reviewed the beneficial effect of the supplementation of trace elements and vitamins on the methanogens activity (Demirel, 2011), (Nel, 1985), (Osuna, 2003).

Regarding the biomethanization rates, seems that white pomace anaerobic digestion is faster than the treatment of the red pomace. Probably this value, in reality, are comparable confirming that polyphenols are not inhibitory, at least in this condition and with this inoculum. Moreover, is interesting compare the positive controls (with red pomace) with the first experiment before reactor tests with the same red grape pomace (figure 5.7.). Both yield and both CH<sub>4</sub> production velocity are higher, confirming that the acclimatization of the inoculum to the substrate, in one of the principal key to obtain a high – yield anaerobic digestion process. One interesting parameters to consider is the acetic acid concentration.

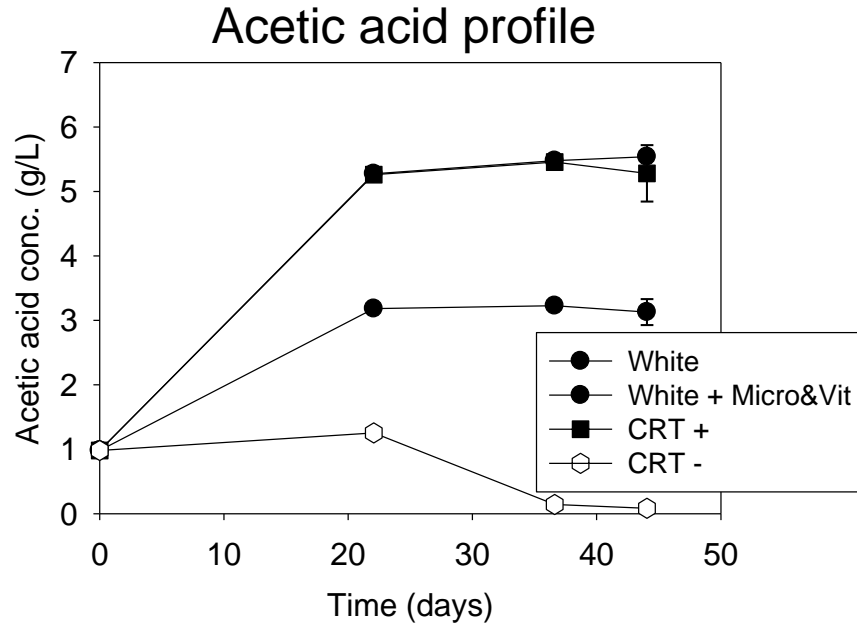


*Figure 5.15: Acetic acid profile in the biomethanization experiment of white pomace*

Starting from the same amount of volatile solids and the same inoculum, white pomace releases more acetic acid than red pomace. This can be an issue during a possible scale up of the process, due to the inhibitory effect of acetic acid on the methanogen activity, but also a key point to improve the yield. Thus, a carefully control of OLR and consequently on VFA concentration, seems essential to establish a high – yield process.

### 5.2.3 Inhibition assays

Oxygen and acetic acid are the most common inhibitory compounds of anaerobic digestion. Besides that, also lignocellulosic – derived compounds, (HMF, syringaldehyde and ferulic acid), are recognized as major sources of inhibition when the in the feed lignin – rich raw materials are present, as grape pomace. (Ye Chen, 2008), (Barakat et.al., 2012).

#### ✓ Oxygen toxicity

O<sub>2</sub> toxicity on methanogenic activity is universally claimed in different literature works, but conversely improved hydrolysis, acidogenic and acetogenic activities are improved in presence of small amount of oxygen (J. E. Johansen, 2006), (L. Hao, 2009), (P. S. Jagadabhi, 2009). The molecular

basis of oxygen toxicity is based on the inhibition of the methyl coenzyme M reductase (MCR), the last enzyme involved in the methanogenesis pathway (indicated from the black arrows in figure 5.16).

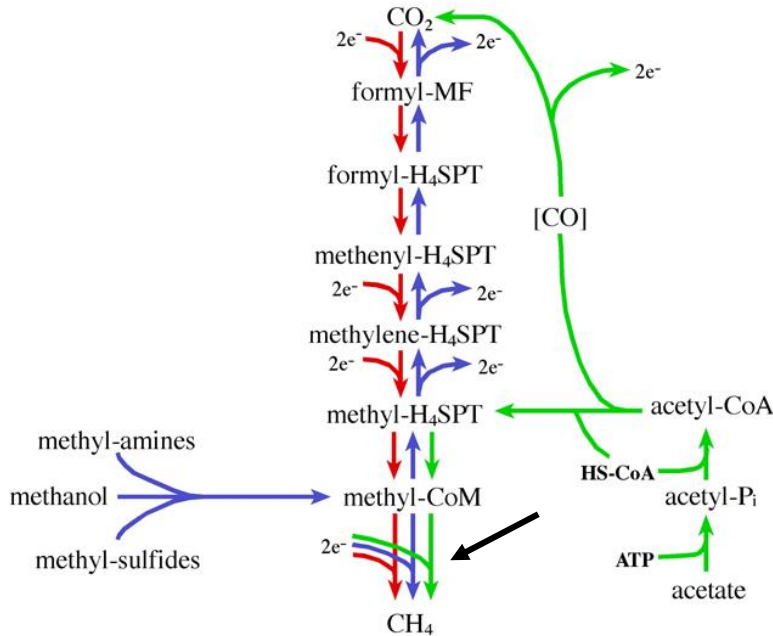


**Figure 5.16:**

*Different metabolic paths of methanogenesis in "Methanosarcina". The hydrogenotrophic (red), the methylotrophic (blue), and the acetoclastic (green).*

(Rother, 2005)

This enzyme is the principal methanogenic protein that undergoes in rapid inhibition in the presence of oxygen (Nagle DP Jr, 1983). Oxygen exposure for this specific enzyme results in the reversible inactivation of the reduced nickel (Ni (I))- tetrapyrrole activation center (Cedervall PE, 2010). The loss of MCR function completely inhibits the growth of methanogenic communities and halts methane production. In addition to this, the principle electron acceptor of methanogenesis,  $\text{CO}_2$ , generates less energy per mol compared to all other commonly used electron acceptors. For this reason, archaeal methanogens are energetically outcompeted by almost all other microbial species (Hedin, 1998), (Canfield, 2005). Besides this sensibility, however, there is increasing evidence that methanogenic archaea can survive prolonged periods of oxygen stress in both pure culture and environmental conditions. Moreover, this inhibition is reversible. Upon the re-establishment of anoxic conditions, methanogens that have undergone oxygen stress can also rapidly grow and produce methane (Brioukhanov, 2006). This resilience was first observed by Yuan Y., 2011 via qPCR that demonstrate the reduction of methanogens abundance after 24 hours of oxygen stress but that the community

persistence after 72 hours of oxygen stress. The molecular defense mechanisms against oxygen stress in strict anaerobic microbes is unclear but there is mounting genomic evidence that complex antioxidative defense enzymes associated with aerobes may play a major role (e.g. superoxide dismutase - SOD), (Brioukhanov, 2006). In fact, only few species of methanogens can synthesize SOD enzyme (for example *Methanosarcina* but not *Methanococcus*), but in mixed culture, the action of facultative anaerobic microorganism can rapidly reduce the oxygen content in the reactor.

In practical application, the most evident effect of oxygen presence in the reactor, is a prolonged lag phase prior methanogenic step. According to D. Botheju, 2010, initial aeration of an anaerobic inoculum resulted in a three times longer lag period before gas generation started, compared to an unaerated inoculum. Similar results are also highlighted by J. Gerritse, 1990. The same author reports also that when the cultures were exposed to O<sub>2</sub> over a period of time, the same oxygen levels which were previously inhibitory, were not inducing any inhibition effect anymore. In fact, acclimatization of the consortium is a key aspect that can improve oxygen tolerance.

After this small overview, it's clear that in the "DICAM" consortium was necessary a complete estimation of oxygen sensitivity. This test was performed at the end of the fed – batch conduction, when the consortium is in a complete – methanogenic phase, prior switching to continuous mode, with a VS concentration of 25,3 g/L.

As reported in the appropriate part of the section 4.4.4, up to 4% of oxygen is tested in triplicate, in a small 116 ml scale microcosms, and parameters like yield and lag phase are evaluated. In figure 5.17, are reported the results.

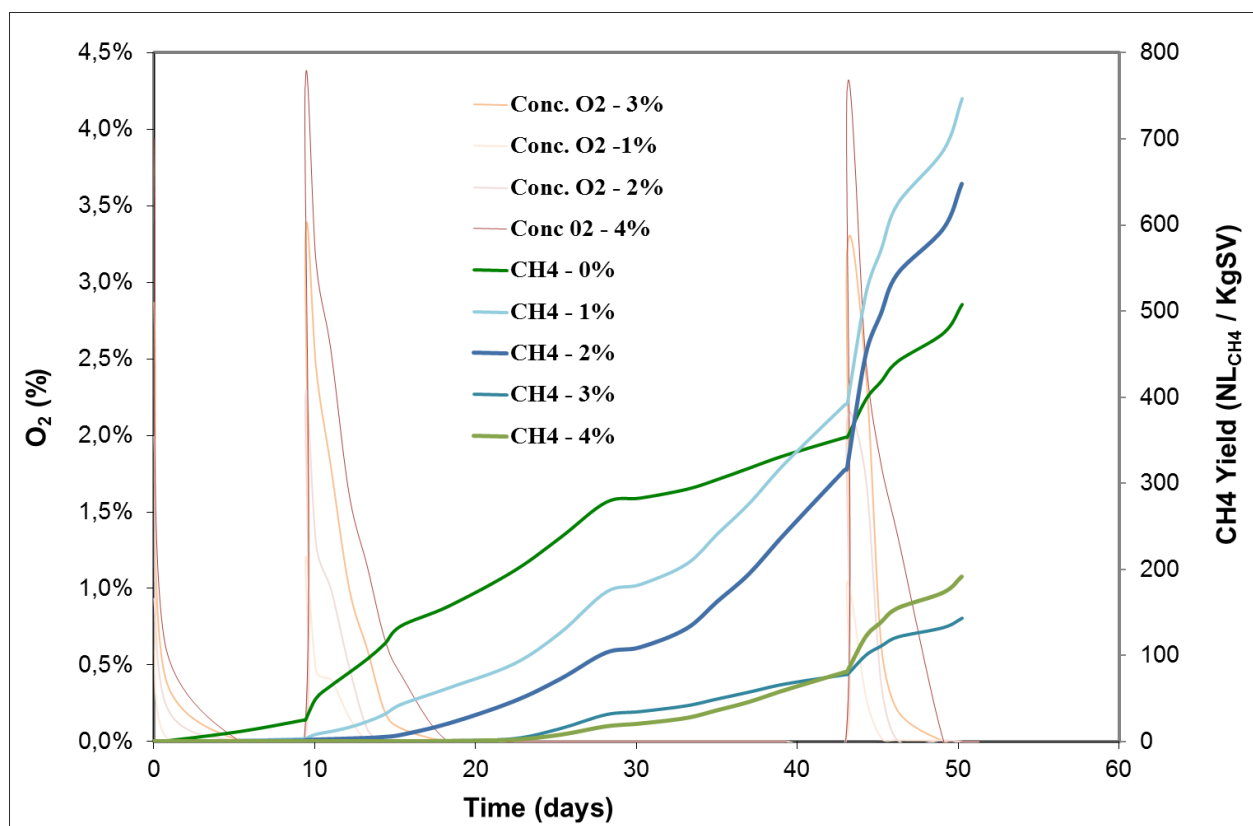


**Figure 5.17:** Oxygen inhibition test results. Standard deviations are not reported for the sake of clearance, anyway all the data have less than 15% of standard error.

In this complex graph are reported the obtained yields and the oxygen consumption rates in the tested microcosms. In the red color scale (from the clear that represents 1% to the darkness that is used for 4%) are reported the oxygen percentages used in each bottle test, and in the other green – blue colors are reported the yields, in terms of  $NL_{CH_4} / Kg$  vs of each microcosm. As reported in the description section, three oxygen injection are performed, one at the beginning of the experiment to investigate the  $O_2$  consumption velocity, the second one immediately thereafter to evaluate the influence on the lag phase, and the last one during the exponential phase, to check if the oxygen presence can affect the already established methane production. In the first three days, for every considered test, all the oxygen was consumed. This is an evidence that in the mixed consortia, facultative anaerobic bacteria, are actively consuming the present oxygen. Due to the low oxygen concentrations tested, only 4% as maximum concentration, no kinetic studies are provided. In fact, the main focus of this test, was to evaluate the oxygen effect on the methanogenic part of anaerobic digestion. During the first 9 days of test, only in the control assay (dark green line in the graph) with no oxygen, a small biomethanization

activity was detected with a partial yield of  $(24,67 \pm 10,68)$  NL<sub>CH<sub>4</sub></sub>/ Kg vs, in line with the hydrogenotrophic yield of the biomethanization process. In all the other microcosms, while the oxygen was consumed in the first three days, no biomethane production was detected, in line with the data reported by R. I. Scott, 1983, that indicates a complete methane production inhibition at below 30 nM of oxygen concentration. In the 1% microcosm (lowest concentration), a 35,7 mM of oxygen are present, higher than the inhibitory value reported by R. I. Scott 1983. Besides that, due to the generation of highly reactive oxidizing agents such as peroxides and superoxides in the liquid medium during AD (G. Gottschalk, 1992), it is suggested that not only functional inhibition but also rapid cell lysis (Jarrell, 1985) of obligatory anaerobic species can occur. As demonstrated by J. H. Martin, 1988 oxygen (and the derived radicals) can damage the chromosomal DNA of strict anaerobic microorganisms, in particularly methanogens without SOD enzyme. For all of this reason, no methane was detected in all the tests (except control, in the first 9 days of fermentation).

Another oxygen spike was, then performed after 9 days to check how the oxygen influences the lag phase. Also in this case, the oxygen was completely depleted, but slower than previous time. Only the microcosm with 1% of oxygen in the 40 ml headspace consumed the oxygen after 3 days, with 2 % of oxygen 5 days are required, and with 3% and 4%, 9 days are necessary to ensure again anaerobic conditions. This data confirms again the possibility to DNA damage and cell lysis reported by J. H. Martin, 1988 and Jarrell, 1985, and the difficulty of the methanogens to sustain multiple oxygen injection. Anyway, as previously reported, in all the microcosms, the methanogenic activity was established again, confirming the resilience of the population, and the reversibility of the inhibition process. Again, our data confirms the experiment reported by D. Botheju, 2010, and also in our case the lag phase was two times higher respect to the non – spiked microcosm (18 days respect to 9 days for 1% and 2% microcosms), and three times higher respect to the non – spiked microcosm (26 days respect to 9 days for 3% and 4% microcosms).

During the full methanogenic phase, instead, no inhibition of CH<sub>4</sub> was detected, and in 3 – 4 days all the microcosms depletes all the oxygen content. Moreover, seems that in full methanogenic phase, small quantity of oxygen leads to an increasing of the global yield, as previously reported by few

studies (M. T. Kato, 1997), (D. Botheju B. L., 2010), (S. J. Pirt, 1983). No molecular explanation for this behaviour is still identified yet. In conclusion, is also evident, in according to possible DNA damage and cell lysis, that the overall yield reported for the higher oxygen content (3% and 4%) are lower than the values obtained in the negative control and in the 1% - 2% microcosms. Thus, no more than 2% of oxygen in the headspace is tolerate by this consortium, at this fermentation stage, in order to re – establish again a full methanogenic state.

#### ✓ Acetic acid toxicity

High volatile fatty acids concentration is one of the most reported reason for anaerobic digestion failure (Ahring, 1995). It's hard to estimate a unique limit for VFA because, the tolerance towards different types of organic acid is function of the physiology of each microorganism, and of the acclimatization of the consortia. Different type of fatty acids can be found in anaerobic digestion, due to the plethora of metabolism involved (table 5.6).

Formic acid	HCOOH
Acetic acid	CH <sub>3</sub> COOH
Propionic acid	CH <sub>3</sub> CH <sub>2</sub> COOH
Butyric acid	CH <sub>3</sub> CH <sub>2</sub> CH <sub>2</sub> COOH
Valeric acid	CH <sub>3</sub> CH <sub>2</sub> CH <sub>2</sub> CH <sub>2</sub> COOH
Hexanoic acid	CH <sub>3</sub> CH <sub>2</sub> CH <sub>2</sub> CH <sub>2</sub> CH <sub>2</sub> COOH
Heptanoic acid	CH <sub>3</sub> CH <sub>2</sub> CH <sub>2</sub> CH <sub>2</sub> CH <sub>2</sub> CH <sub>2</sub> COOH
Octanoic acid	CH <sub>3</sub> CH <sub>2</sub> CH <sub>2</sub> CH <sub>2</sub> CH <sub>2</sub> CH <sub>2</sub> CH <sub>2</sub> COOH

**Table 5.6:**

*Main VFA present in anaerobic digestion process (Aguilar, 1995)*

Usually, in industrial consolidated bioprocess, the amount of total short chain fatty acids is limited to less than 1 g/L, but this value is typical of every process, and needs to be optimized, and monitored constantly during the whole test. Moreover, due to the acetogenic phase of anaerobic digestion, different type of microorganism (as reported in 3.2), converts and transforms this VFA mixture in only acetic acid, with small traces of propionic and butyric acids. For this reason, the accumulation of acetic acid is considered the principal candidate for anaerobic digestion failure (Ingrid H. Franke-Whittle, 2014). Different studies on the inhibitory effect of acetic, propionic and butyric acid on the biomethanization process, are made. For example, Y. Wang, 2009 reports that up to 2,4 g/L of acetic

acid and 1,8 g/L of butyric acid, no inhibition was detected, instead, only 0,9 g/L of propionic acid was necessary to provide a significant inhibition of the methanogenic activity. On the contrary, Xiao K, 2016, in a very recent article (february 2016), reports that in a 2 – stage anaerobic digestion experiment, after a 27 days acclimatization of methanogenic population, up to 8,2 g/L of acetic acid was tolerated without affecting the biomethane yield. Moreover, both propionic and butyric acid with a concentration higher than 1,5 g/L, doesn't cause any detectable inhibition. So, it does not appear to be possible to define VFA levels to indicate the state of an anaerobic process, as different systems have their own levels of VFAs that can be considered 'normal' for the reactor, and conditions that cause instability in one reactor do not cause problems in another reactor (Ingrid H. Franke-Whittle, 2014). There are different principal mechanisms reported for the short – chain fatty acid (SCFA) inhibition. The most accepted idea is related to the accumulation of those compounds in the fermentation broth; if the process has a low buffering capacity, the accumulation of the dissociated form of the acid can lower the pH, and leads to a complete inhibition of the process. In fact, due the their weak acid nature, the accumulation of the anionic form of the SCFA depends from their dissociation constant ( $K_a$ ), and thus, from the pH with the Henderson-Hasselbalch relationship. Besides that, another inhibition source is recently reported, and is related to the direct effect of the undissociated form of the carboxylic acid to the microorganism cells. Undissociated weak acids are liposoluble and can diffuse across the plasma membrane of the cells. The growth-inhibiting effect on microorganisms has been proposed to be due to the inflow of undissociated acid into the cytosol (Axe, 1995), (Stouthamer, 1979), (Verduyn C. P., 1990). In the cytosol, dissociation of the acid occurs due to the neutral intracellular pH, thus decreasing the cytosolic pH. At this point, two toxicity mechanism are possible. The anionic form of the acid is captured in the cell and undissociated acid will diffuse into the cell until equilibrium is reached (Rottenberg, 1979); this lower pH leads to a rapid cell death, probably by apoptotic mechanism (D. Lagadic-Gossman, 2004). According to the another theory, the drop in intracellular pH resulting from the inflow of weak acids is neutralised by the action of the plasma membrane ATPase, which pumps protons out of the cell at the expense of ATP hydrolysis, (Verduyn C. P., 1992), (Stouthamer, 1979). At high acid concentrations, the proton pumping capacity



of the cell is exhausted, resulting in depletion of the ATP content, dissipation of the proton motive force, acidification of the cytoplasm and consequent cell death (Eva Palmqvist, 2000). Lastly, Liam A. Royce, 2013 reports also that short chain fatty acids accumulation in fermentation broth up to 2,4 g/L results in reduction of cell membrane fluidity, accompanied by a change in membrane lipid composition and a decrease in cell surface hydrophobicity in *E. coli*. The overall result is a lower growth rate on glucose.

It's evident that the pH is crucial, because from the regulation of this parameters depends the amounts of dissociated/undissociated ratio of SCFA and thus the toxicity of this compounds. Besides that, also a strict control on the organic loading rate in the feed, and the determination of maximum tolerated concentration of short – chain fatty acids is necessary to ensure a high – yield biomethanization process. As reported several time, also the acclimatization of the consortium is a key parameter, as depicted by Xiao K, 2016.

For all of these motivation, an acetic acid inhibition test was performed with DICAM inoculum during the continuous experiment, starting from the digestate taken from the bioreactor at the interface between 0,4 g<sub>sv</sub>/L/day and 0,6 g<sub>sv</sub>/L/day (55 days of continuous experiment). It's evident that the only hypothesis for an inhibition related to acetic acid can derived from the external accumulation. In fact, the automatic pH control of the reactor maintains the value between 7,6 and 7,8. At those value the acetic acid is completely deprotonated (pK<sub>a</sub> 4,76), and the CH<sub>3</sub>COO<sup>-</sup> can't pass the membrane cell. Anyway, to detect how the acetic acid accumulation in the fermenter can leads to a inhibition of the process, as reported in the appropriate section of paragraph 4.4.4. a set of 21 microcosms were prepared in order to screen six acetic acid concentrations plus negative control: 0,79 g/L, 1,95 g/L, 4,81 g/L, 5,98 g/L, 7,85 g/L, 10,63 g/L and 12,51 g/L. The negative control was a triplicate taken from the reactor without any addition of acetic acid (0,79 g/L of acetic acid in the reactor). In all the experiments, an initial concentration of 11,75 g/L of volatile solids was determined. The experiment was performed for 20,6 days, but only the initial velocity in the first 10,6 days was considered, in order to avoid complete volatile solids consumption, and remain in the linear phase of the kinetic model. In fact, at the end of the experiments only a little variation of VS concentration was detected,

and respective analysis reported that all in all the tests, the VS concentration remained in the range between 9 g/L and 12 g/L.

Plotting the Nml of produced methane against time, the biomethanization rate ( $NL_{CH_4}$  /L/d) was estimated with a linear regression in the first 10,6 days (the coefficient of determination was in the range between 0,97 and 0,99 for all the equation).

To better point out the results, the initial velocity (the slope of the  $Nml_{CH_4}$  /time graph) and the obtained yield, were plotted again versus the respective acetic acid concentration with the appropriate standard error (figure 5.18).

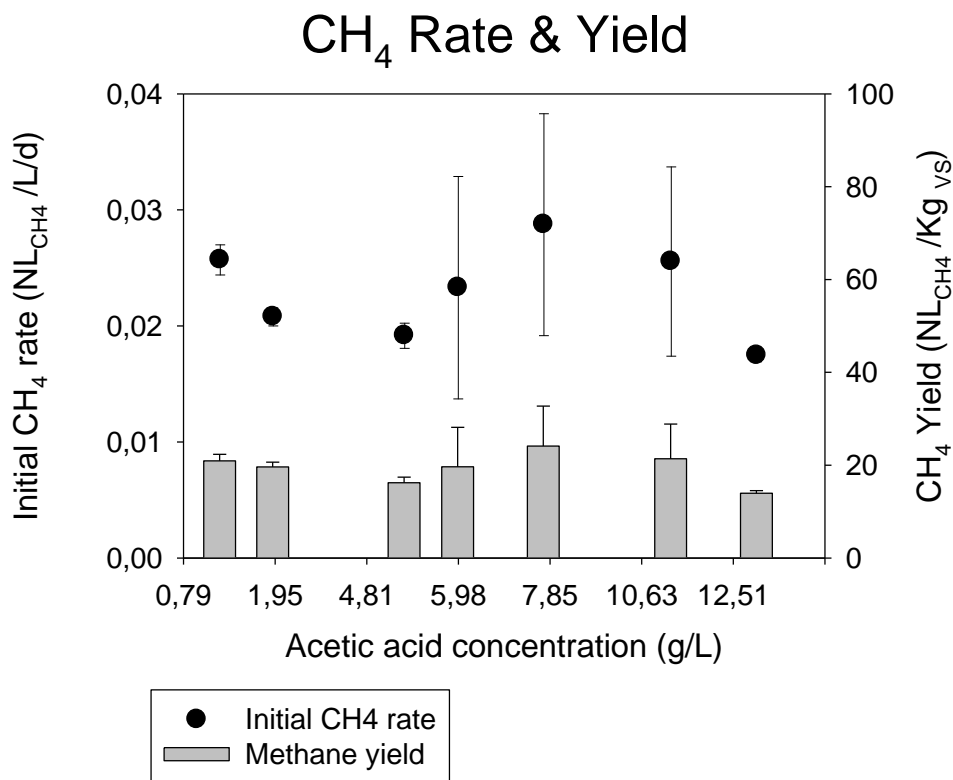


**Figure 5.18:** Initial biomethanization rates and yields plotted against each acetic acid concentration used in the tests.

As it clearly evident from the graph, no appreciable differences in the biomethanization rates and yields can be noted, from the negative control at 0,79 g/L of CH<sub>3</sub>COOH (first point on the left) until 12,51 g/L, without any influences on the methanogenic activity. This result is in line with the data of Xiao K, 2016 that reports that after 27 days of acclimatization the methanogenic population can tolerate up to 8,2 g/L without affecting the methane yield. In this case, also up to 12,51 g/L, no

inhibition traces were founded, confirming that the acclimatization of a mixed culture is a fundamental key of the anaerobic digestion process. Probably this results can be limited only to the hydrogenotrophic part of the consortium, because the experiment was started at day 55 of the continuous test, where the OLR was just increased from at 0,4 g<sub>sv</sub>/L/day to at 0,6 g<sub>sv</sub>/L/day, and the system was in acetic acid accumulation phase. In this condition, previous tests demonstrate that the only biomethane production derives from the hydrogenotrophic archaea. This hypothesis is also suggested from the low yield observed, in line with Avery G. B., 1999 that reports that only 30% (average value) of the global methane yield are produced by the hydrogenotrophic pathway. The average biomethanization rate was about 0,22 NL CH<sub>4</sub> /L/d, with a yield in the range between 16,22 NL CH<sub>4</sub> /Kg VS and 24,13 NL CH<sub>4</sub> /Kg VS, in line with the values obtained in the reactor when only the hydrogenotrophic part of the consortium was active.

No conclusion can be made for the acetoclastic part of the community, but besides that, it's evident that no one of the toxic mechanisms explained before are active on the hydrogenotrophic part of the consortia. The accumulation of acetic acid up to 12,51 g/L in the fermentation broth shown no toxic effects. Moreover, all the tests were performed in a pH range between 7,5 and 8. At those values, the acetic acid is completely deprotonated and the anionic form can't enter in the cells.

#### ✓ Lignocellulosic inhibition

Different types of compounds derived from the bioconversion of lignocellulosic matrix, are recognized as inhibitors on anaerobic digestion process (figure 5.19):

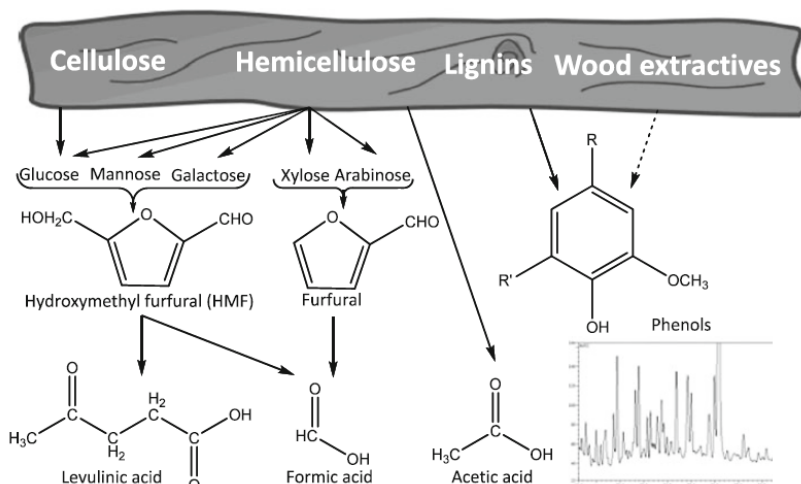


**Figure 5.19:** Scheme indicating main routes of inhibitor formation during the anaerobic digestion of lignocellulosic matrix (Leif J Jönsson, 2013)

When hemicellulose is degraded, xylose, mannose, acetic acid, galactose, arabinose and glucose are liberated; cellulose is hydrolyzed instead to only glucose. Xylose and arabinose are further degraded to furfural, similarly, 5-hydroxymethyl furfural (HMF) is formed from hexose degradation. Formic acid is further formed when furfural and HMF are broken down, and acetic acid is liberated from the hydrolysis of acetyl groups of hemicellulose. Besides that, levulinic acid is also formed by HMF degradation (Dunlop, 1948), (Ulbricht, 1984). Phenolic compounds are generated from partial breakdown of lignin (Bardet, 1985), (Lapierre, 1983), in particular, vanillin and ferulic acids, are formed by the degradation of the guaiacyl-propane units of lignin, whereas syringic acid, are formed from the degradation of syringyl-propane units (Jonsson, 1998), (Tran, 1985).

Anyway, the most representative phenolic compound is 4-hydroxybenzoic acid, that constitutes a large fraction of the lignin-derived compounds in hydrolysates from both hardwoods and softwoods raw materials, (Ando, 1986), (Bardet, 1985), (Jonsson, 1998).

The inhibition mechanism of weak acetic acids as formic, levulinic and acetic, was previously reported; in addition to those data, total inhibition of yeast growth was detected at concentrations exceeding 100 mM (Larsson S, 1999). Furfural is metabolised by *S. cerevisiae* under anaerobic conditions to furfuryl alcohol with high yields during fermentation processes (Diaz de Villegas, 1992), (Taherzadeh, 1998), as and HMF is reduced to 2,5-bis-hydroxymethylfuran (Taherzadeh MJ, 2000). NADH-dependent alcohol dehydrogenase (ADH) is believed to be responsible for furfural and HMF

reduction (Weigert, 1998). Furfural has been shown to reduce the specific growth rate, the cell-mass yield on ATP, the volumetric and specific ethanol productivities. In particular, concentration of 0,02 g/L (0.1 mM) was enough to inhibit ethanol production using *S. cerevisiae* (Azhar, 1981). Anyway, the adaptation process is again a key parameter. Boyer, 1992, was able to demonstrate that the ADH activity in anaerobic fermentation increased by 78%, tolerating up to 2 g/L of total furfural.

Inhibition details of furfural and HMF are not completely clear, but different studies report that affects energy metabolism while changing the TCA and glycolytic fluxes de-activating key enzymes such as alcohol dehydrogenase, aldehyde dehydrogenase and pyruvate dehydrogenase, (Modig T, 2002) (Sarvari Horvath I, 2003). In addition, furfural and HMF induces the ROS accumulation in *Saccharomyces cerevisiae* causing cellular damage to mitochondria, vacuolar membranes and nuclear chromatin, inducing apoptotic processes (Allen SA, 2010).

Lignin – derived phenolic compounds inhibition is not clear up to now. Anyway, those compounds seem able to reduce membranes fluidity and integrity, thereby affecting the ability to serve as selective barriers and enzyme matrices (Heipieper, 1994). Lack of studies characterize this scientific aspects, due to the practical difficulty to solubilize those aromatic compounds. Few results, for example, Larsson, 2000 founded that ferulic acid was inhibitory to *S. cerevisiae* at 0.20 g/L (1.0 mM), whereas 0.02 g/L (0.1 mM) of coniferyl aldehyde was enough to reduce of 50% the ethanol production. Besides that, a large number of metabolic studies reports that not only yeast, but also methanogenic population are inhibited by lignocellulosic compounds. Zhenming Zhou, 2011, for example reports that methanogenic activity was reduced in the range between 71% and 99% in presence of 50 mM of furans, or concentration of 0,76 g/L of vanillin can seriously affect the methanogens growth rate (Amlan K. Patra, 2014).

After this brief review on possible inhibition due to lignocellulosic derived compounds, it's easy to imagine that after 246 days of continuous experiment with an increasing organic loading rate, of only lignocellulosic biomass without any specific pretreatment, the descendant trend of both yield and both biomethanization velocity, can be due to an increasing of metabolic inhibition from those compounds on methanogenic archaea.

To have a preliminary confirmation of this hypothesis, a BMP – BioMethanization Test, was performed at the end of the continuous test, as described in the last section of paragraph 4.4.4. According to the procedure reported in Angelidaki, M. et.al., 2009, from the exasusthed digestate of the reactor, one ngative control and one sample,(each in triplicate), were prepared. In the negative control, the microcosms were simply incubated without any treatment with reactor digestate, whereas, in the test, the biomass was centrifuged and resuspended in rich medium with 2 g/L of glucose as only carbon source, to evaluate the metabolic status of all the consortium, from hydrolytic bacteria to he methanogens archaea. It's evident that also negative control was supplemented with 2 g/L of glucose. In figure 5.20 and 5.21 are reported the results of the test.

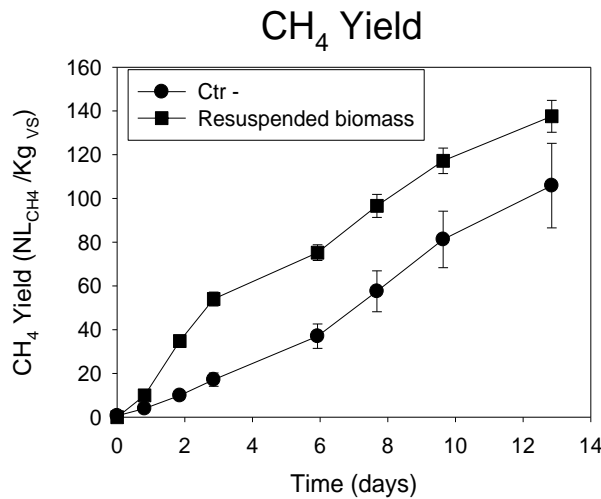


**Figure 5.20**

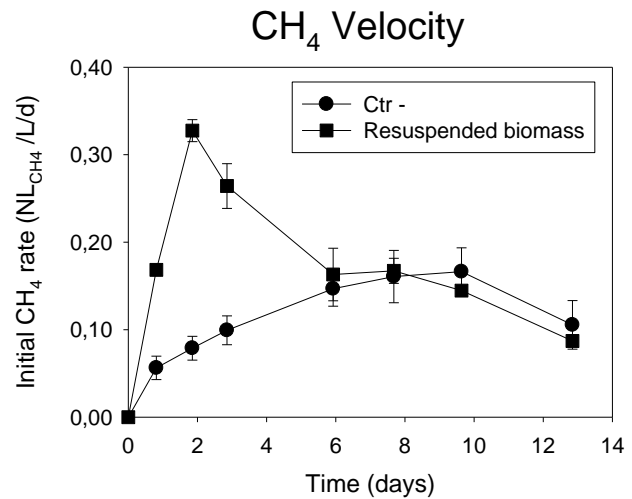


**Figure 5.21**

**Figure 5.20:** Obtained yield in microcosms BMP test with negative control and resuspended biomass

**Figure 5.21:** Biomethanization rates in microcosms BMP test with negative control and resuspended biomass

All the microcosms started with 13,75 g/L of volatile solids, and after the 12,85 days of test, the final concentration remained quite stable, around 10 g/L. In fact, the experiment was stopped when the glucose was finished in the media, and the produced acetic acid derived from glucose was completely depleted.

The differences are evident. Besides the yield improvement,  $(105,89 \pm 19,33)$  NL<sub>CH<sub>4</sub></sub> /Kg vs for the negative control and  $(137,56 \pm 7,92)$  NL<sub>CH<sub>4</sub></sub> /Kg vs for the BMP test probably due to a higher

exploitation of the energy of pure sugar respect to a raw biomass, the most relevant result is the parallel between the two initial velocity in figure 5.21. The maximum value for the BMP test was reached after 1,8 days and  $(0,32 \pm 0,01)$  NL<sub>CH<sub>4</sub></sub> /L/d, a doubled value respect to the  $(0,16 \pm 0,03)$  NL<sub>CH<sub>4</sub></sub> /L/d obtained for the negative control. Inasmuch as the only difference between the two set of microcosms was only the fermentation medium, but with the same carbon source, it's possible to speculate that something present in the fermentation medium of negative control microcosms (and so of the reactor), was responsible for this low yield. The principal candidates, thus, are some lignocellulosic – derived compounds.

#### *5.2.4 Co – digestion results*

The numerous results obtained with “DICAM” inoculum and grape pomace highlighted that the major issues are related to the inoculum instability, and to the high lignocellulosic content of this raw materials. For these reasons, according to the company partner of the project, different BMP tests in small 116 ml microcosms are performed (see paragraph 4.4.5), using an already acclimatized industrial inoculum called “SEBIGAS” (see table 4.15), provided by the company from a tomato peels digester. In fact, the idea of this experiment, was to perform a grape pomace BMP to compare the results obtained from the “DICAM” inoculum, but moreover, to screen other matrix as maize silage, tomato peels and olive mill wastewater, alone or in co – digestion between them and grape pomace. All these raw materials were characterized in terms of %TS, %VS and other physical parameters in table 4.1.

Maize silage is the most used dedicated crop in the anaerobic digestion, due to the high disponibility and the high yields. A large number of studies are reported in literature where maize silage is used as only carbon sources with very interesting yields values, like  $(296 \pm 31)$  NL<sub>CH<sub>4</sub></sub> /Kg vs and  $(307 \pm 21)$  NL<sub>CH<sub>4</sub></sub> /Kg vs (M. Luna-del-Risco, 2011), 338 NL<sub>CH<sub>4</sub></sub> /Kg vs (M. Neureiter, 2011), 295 NL<sub>CH<sub>4</sub></sub> /Kg vs (Vilis Dubrovskis, 2009) and in the range between 335 – 370 NL<sub>CH<sub>4</sub></sub> /Kg vs (Herbert Pobeheim, 2010). Due to its nature of dedicated crop, maize silage is used often in co-digestion to ensure an interesting

final yield, or as a reference in the screening of new raw by – products. One of the most interesting matrix for anaerobic digestion are the tomato residues. In fact, due to the optimal C/N ratio (15:1, average value) reported by Amalendu Chakraverty, 2014, and the nature of by – product and not as dedicate crop, can represent one of the major application field for AD process. In literature, E. Dinuccio, 2010 report a global yield of 218 NL<sub>CH4</sub> /Kg vs without any kind of pre-treatment for tomato skins and seeds, higher respect but only few studies focused properly on tomato peels. R. Sarada, 1993 reports a yield for a batch test with 24 days of HRT in a semicontinuous process of 325 NL<sub>CH4</sub> /Kg vs, a value absolutely in line with the treatment of maize silage. Moreover, recently, a final yield of 353 NL<sub>CH4</sub> /Kg vs, were reached with untreated tomato peels in a single batch test (Paolo S. Calabro', 2015). Also olive mill wastewater (OMW) represents an interesting option for anaerobic digestion, depending on the residual COD and polyphenols content. In fact, only OMW with high chemical oxygen demand can be suitable for a high – yield AD process, but usually high polyphenols concentration is inhibitory for bacteria growth. For this reason, only a few studies where OMW are used alone in AD can be founded in literature. Anyway an interesting global yields are reported, for examples, 122 NL<sub>CH4</sub> /Kg COD (A. Gianico, 2013) or a range between 168 NL<sub>CH4</sub> /Kg COD and 245 NL<sub>CH4</sub> /Kg COD (Nuri Azbar, 2008).

In this test different BMP experiments were performed in small scale using maize silage, tomato peels, grape pomace and OMW, alone or in co-digestion between them. The principal co-digestion tested were: tomato peels – maize silage, tomato peels – grape pomace and grape pomace – maize silage.

As reported in section 4.4.5., two main rules are followed in order to compare the final results:

- ✓ In all the tests, the ratio between the grams of volatile solids of the inoculum and the total grams of volatile solids of the substrates must be: 4:1

Equation 1:

$$\frac{g\ VS_{inoculum}}{g\ VS_{substrate\ 1} + g\ VS_{substrate\ 2}} = 4$$

**Figure 5.22 (a):** Fundamental equations for anaerobic co – digestion processes

- ✓ The co-digestion ratio between the two substrates in terms of volatile solids must be 1:1:



Equation 2:

$$g VS_{substrate 1} = g VS_{substrate 2}$$

**Figure 5.22 (b):** Fundamental equations for anaerobic co – digestion processes

Due to the high content of VS of the new “SEBIGAS” inoculum, 58,5 g/L (2,37 g in 40 ml of fermentation broth in each microcosm), all the yields are reported net to the inoculum yield, estimated by a negative control test performed as a BMP in the same condition without any external feed. As reported in table 4.16, the total VS provided in each microcosm by the substrate was 0,59 g in 40 ml, with a total amount in each microcosms (including inoculum) of 2,96 grams. The experiment was carried until all the VS was consumed and the biomethanization was completely stopped. Here are highlighted the principal results in terms of yields, maximum biomethanization rate, total amount of CH<sub>4</sub> produced and biogas composition.

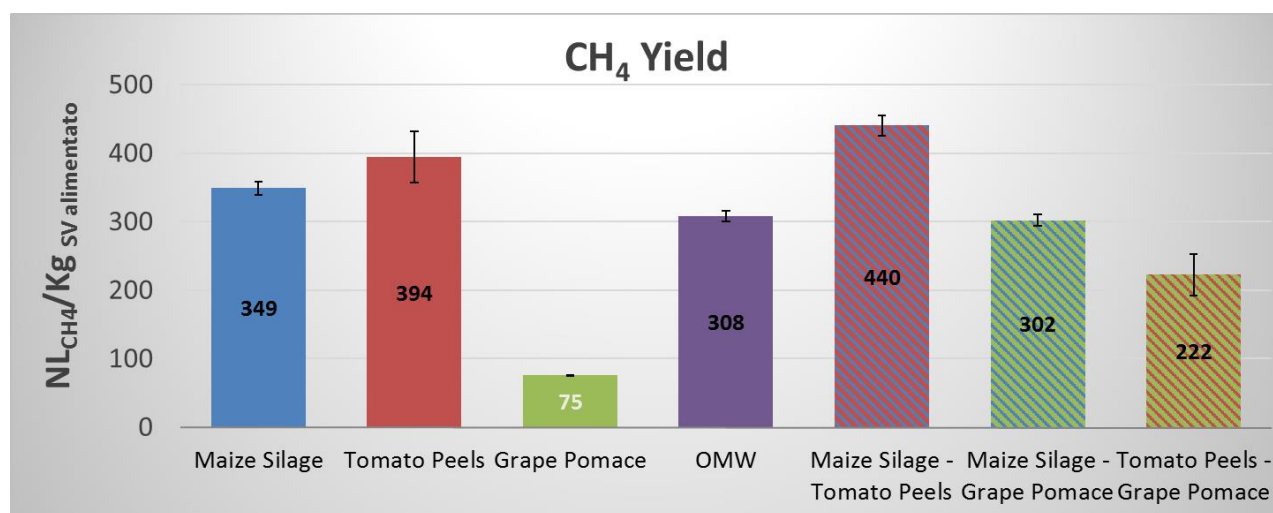


**Figure 5.22:** Biomethane yield obtained with “SEBIGAS” inoculum and different substrates, alone or in co – digestion in microcosm BMP batch test.

From these results, different conclusion can be made. For instance, the anaerobic digestion of maize silage leads a final yield of  $(349 \pm 10)$  NL CH<sub>4</sub> /Kg vs, in line with the literature values. In fact, the high starch content of this plant (up to more than 40% of the total solids according to Emiliano Bruni, 2010, can explain this high yield when used as only carbon source. Tomato peels yield, instead was higher than expected. Fresh biomass without any thermal pre-treatment, leads to  $(394 \pm 37)$  NL CH<sub>4</sub>

/Kg vs, a value higher than the best yield reported in literature by Paolo S. Calabro', 2015 (353 NL<sub>CH4</sub> /Kg vs) for a single batch test with tomato peels as only carbon source. Probably continuous acclimatization of the “SEBIGAS” consortium to this waste was key element for this results; in fact, as previously reported, this inoculum was provided by the company from a tomato peels anaerobic digester. The grape pomace yield, that was in line (75 ± 1) NL<sub>CH4</sub> /Kg vs with the yield obtained with “DICAM” inoculum in the first batch microcosm experiment in figure 5.7 – dotted line (69,5 ± 9,6) NL<sub>CH4</sub> /Kg vs, confirming that the high C/N ratio and the high lignin content can represent the main limits for the exploitation of this raw material, at least in a batch test. Probably, with a further acclimatization of the “SEBIGAS” consortium to the grape pomace, and a continuous anaerobic digestion process, the yield should have been higher as previously reported in table 5.4, but the same inhibition problems should have represented again a problem. During olive mill wastewater BMP, a final yield of (308 ± 7) NL<sub>CH4</sub> /Kg vs was obtained, higher than all the values reported in literature. Anyway it's necessary to highlights that this OMW has a high COD value estimated in 31,5 g/L, whereas the yield of 122 NL<sub>CH4</sub> /Kg COD reported by A. Gianico, 2013 was obtained by a OMW with only (4,8 ± 0,3) of total COD, and the yields between 168 NL<sub>CH4</sub> /Kg COD and 245 NL<sub>CH4</sub> /Kg COD reported by Nuri Azbar, 2008 were obtained in a continuous reactor changing the HRT, with a total COD of 10 g/L. Despite this consideration, also this OMW, can represent a good alternative for an AD process.

From these results obtained with single substrate, three different co-digestions were performed. Grape pomaces were tested with both maize silage and tomato peels, in order to enhance yield and digestibility. In the last one, tomato peels and maize silage were co-digested, to determine the maximum performance obtainable from these two wastes.

To evaluate the co-digestion results it's necessary to keep in mind that, every tests was performed with the same amount of initial VS concentration, and the ratio between the VS of the two substrates was 50% - 50%. Following this relationship, in every co-digestion, the global yield is derived half from the firs substrate and half from the second one. This value needs to be compared with the half value of global yield for each BMP test with the single substrate, to maintain the same amount of

volatile solids concentration. For example, considering the maize silage – tomato peels co-digestion the global yield is  $(440 \pm 14)$  NL<sub>CH<sub>4</sub></sub> /Kg COD with 0,59 grams of initial VS in the microcosms (all the value are reported net to the inoculum). Thus, it's possible to estimate that 220 NL<sub>CH<sub>4</sub></sub> /Kg SV are derived maize from 0,295 g of VS of maize silage and 220 NL<sub>CH<sub>4</sub></sub> /Kg VS are derived from 0,295 g of VS of tomato peels. To compare this value to each single substrate digestion, the total yield of the BMP of each single substrate needs to be divided by two, to maintain the same amount of VS. In fact, the  $(349 \pm 10)$  NL<sub>CH<sub>4</sub></sub> /Kg VS total yield of maize silage yield with 0,59 g of VS, corresponds to 174,5 NL<sub>CH<sub>4</sub></sub> /Kg VS with 0,295 g of VS. This is lower than the 220 NL<sub>CH<sub>4</sub></sub> /Kg SV calculated from the co-digestion. This lead, to an enhancement of the yield of 45,5 NL<sub>CH<sub>4</sub></sub> /Kg SV from single substrate to the co-digestion for maize silage. Same calculations are made for the tomato peels in this co-digestion, and an improvement of 23 NL<sub>CH<sub>4</sub></sub> /Kg SV.

Making the same consideration for the two co-digestion with the grape pomace, the major increase in grape pomace yield was obtained in the co-digestion with maize silage, with an increment of 113,5 NL<sub>CH<sub>4</sub></sub> /Kg VS respect to the single grape pomace digestion process. In the latter co-digestion of grape pomace with tomato peels, anyway, a 73,5 NL<sub>CH<sub>4</sub></sub> /Kg VS of yield improvement was noticed. A preliminarily synergic effect can be detected in every process, representing an interesting option to improve biomethane yield from grape pomace. In the next table are reported the maximum velocity, the global amount of methane production and the biogas composition of each test.

***Biomethanization rates, methane volume and biogas composition for each co-digestion***

	Max. velocity (NL <sub>CH4</sub> /L/d)	CH <sub>4</sub> volume (NmL <sub>CH4</sub> )	Biogas composition (%)
<i>Maize silage</i>	(0,66 ± 0,16)	(207,44 ± 8,13)	CH <sub>4</sub> : (60,60 ± 1,03) CO <sub>2</sub> : (35,50 ± 0,36)
<i>Tomato peels</i>	(0,47 ± 0,05)	(233,87 ± 9,94)	CH <sub>4</sub> : (61,98 ± 1,55) CO <sub>2</sub> : (33,45 ± 1,12)
<i>Grape pomace</i>	(0,32 ± 0,02)	(173,73 ± 6,90)	CH <sub>4</sub> : (58,26 ± 1,55) CO <sub>2</sub> : (29,74 ± 1,12)
<i>OMW</i>	(0,21 ± 0,03)	(114,94 ± 1,49)	CH <sub>4</sub> : (70,04 ± 1,70) CO <sub>2</sub> : (29,81 ± 0,37)
<i>Maize silage – Tomato peels</i>	(0,50 ± 0,07)	(261,25 ± 11,20)	CH <sub>4</sub> : (63,91 ± 2,47) CO <sub>2</sub> : (33,36 ± 0,97)
<i>Maize silage – Grape pomace</i>	(0,54 ± 0,13)	(179,26 ± 4,77)	CH <sub>4</sub> : (63,23 ± 0,22) CO <sub>2</sub> : (31,64 ± 0,24)
<i>Tomato peels – Grape pomace</i>	(0,42 ± 0,16)	(130,41 ± 16,55)	CH <sub>4</sub> : (62,90 ± 1,53) CO <sub>2</sub> : (37,33 ± 1,73)

***Table 5.7: Biomethanization rates, methane volume and biogas composition for each co-digestion***

From this table is evident the methane percentage in the biogas remains in the range of 60% - 70% and CO<sub>2</sub> between 30% and 35%, values in line with a normal AD process for every tests. Regarding the biomethanization rate of the single substrate digestion, maize silage showed the best value, confirming that is the best dedicated crop for anaerobic digestion. AD of grape pomace with “SEBIGAS” inoculum demonstrate a biomethanization rate of (0,32 ± 0,02) NL<sub>CH4</sub>/L/d that is practically double respect to the value obtained with “DICAM” inoculum in the first batch test (0,18 ± 0,04) NL<sub>CH4</sub>/L/d. We can speculate that “SEBIGAS” inoculum can represent a better mixed consortium for anaerobic digestion respect to the “DICAM” one, probably due to a better balance between bacteria and archaea population. Another interesting consideration on the biomethanization rate of the co-digestion is that all the co-

digestion velocities are higher (or at least equal) to the single substrate BMP tests, excluding maize silage. This is another hint towards the synergic effect of the co-digestion, respect to the single substrate anaerobic digestion experiment. Looking at the volume of biomethane production, the maize silage – tomato peels co – digestion shown the higher volume,  $(261,25 \pm 11,20)$  Nml  $\text{CH}_4$ . This was a predictable data, because this co-digestion was the one with the higher yield. For the single substrate digestions, it's important to notice that tomato peels can produce more biomethane in terms of Nml, respect to the maize silage. This can be a focus point for the exploitation of this raw material for further anaerobic digestion scale – up.

Looking to the volatile fatty acids (and in particularly to the acetic acid), no-one of those tests showed a VFAs concentration higher than 4 g/L, thus, no inhibitory effect can be hypothesized. It's interesting to notice that all the experiments with maize silage, (both single, both double substrate digestions), reported the higher values of acetic acid. At days 2,8 of fermentation, single anaerobic digestion of maize silage showed the higher acetic acid value:  $(3,54 \pm 0,74)$  g/L. Respective co-digestion of maize silage with tomato peels and grape pomace highlighted acetic acid values of  $(2,70 \pm 0,76)$  g/L and  $(2,06 \pm 0,14)$  g/L. This results fits perfectly with the composition of the maize silage: the higher percentage of starch, leads obviously to a higher acetic acid production during the preliminarily stages of anaerobic digestion process and, thus, to a higher biomethane production in the methanogenic step. Moreover, in according to the yield trend, anaerobic digestion of grape pomace shows the lowest amount of acetic acid, only  $(0,94 \pm 0,69)$  g/L, that derived to the low concentration of fermentable biomass inside this raw material.

### 5.3 BIO – PROPANOL PRODUCTION: SCREENING RESULTS

As reported in section 4.5 and sub – paragraphs related, this project was strictly related to the anaerobic digestion biorefinery. The main idea was to enrich this biorefinery using the VFAs originated by the action of hydrolytic, acidogenic and acetogenic bacteria, as a “platform” for the production of bio-alcohols. In particularly, propionic acid was chosen because after acetic acid, is the most abundant VFA in anaerobic digestion, and the reduction of this acid can lead to n – propanol, that is one of the major promising compounds for engine – fuels. Besides that, n – propanol is also

used as chemical intermediate for a lot of industrial application, but is hardly produced by fermentation from native strain, due to low yields of the process. Anyway, Kirsten J.J. Steinbusch, 2008, reports that is feasible reduce 50 mM of acetic, propionic and butyric acid in the respective alcohols using mixed culture isolated from a UASB reactor from wastewater treatment. For this reason, the aim of this project is to evaluate the feasibility of the reduction of propionic acid to n – propanol, screening three different consortia present in our laboratory, and find the best condition for propanol production.

As reported in section 4.5.1., the experiment starts screening 3 different inocula, called “DICAM”, “OMW”, and “MAIS” extensively described and characterized in section 4.2.

The growth, selection and acclimatization phase, were conducted as described in 4.5.1, and no sample were taken, only before growth phase, 5 ml of each “mother” culture was taken for the PCR – DGGE analysis.

In the next figures, are reported the results of the production phase, where only 2 g/L of propionic acid was used as carbon source. Moreover, in the test phase, the microcosms headspace was replaced with pure hydrogen as electron donor, and finally pressurized to 1.5 bar. The 36 microcosms tested were derived from the three different consortia, pasteurized or not in the selection phase, and tested in presence / absence of sodium molybdate in the acclimatization phase, each one screened in triplicate. To summarize, 4 consortia are derived from each mother culture:

- ✓ Non - Pasteurized (NP)
- ✓ Pasteurized (P)
- ✓ Non – pasteurized + sodium molybdate (NP + S.M)
- ✓ Pasteurized + sodium molybdate (P + S.M)

each one tested in triplicate.

In figure 5.24 and 5.25, a comparison between all the consortia without supplementation of sodium molybdate are reported, in terms of mg/L of n – propanol produced, and percentage yield. For the sake of clearance, no standard deviations are reported in the graph, but only the average values of the triplicates. Anyway, in table 5.8, the higher production and yield values are reported with standard

error, together with the average n – propanol production velocity (in mmol/L/d) and the respective propionic acid and hydrogen consumption rates (both of them also in mmol/L/d) in the first 15,9 days, corresponding to the exponential phase of the process:

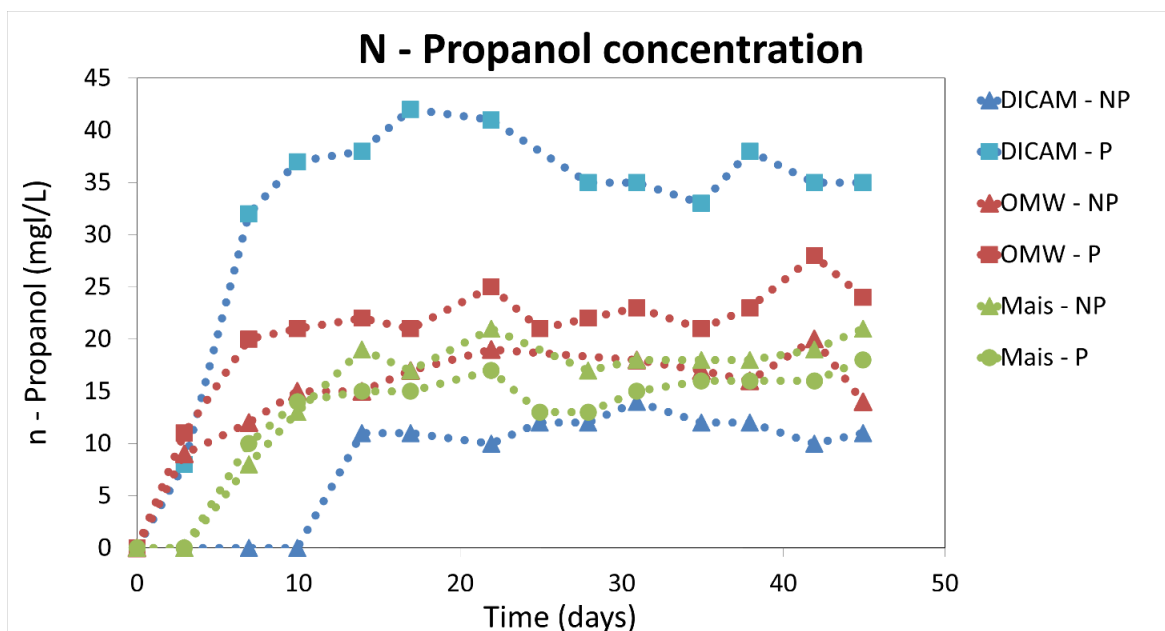


**Figure 5.23:** *N* – propanol production in each consortium, pasteurized or not, without  $\text{Na}_2\text{MoO}_4$  supplementation

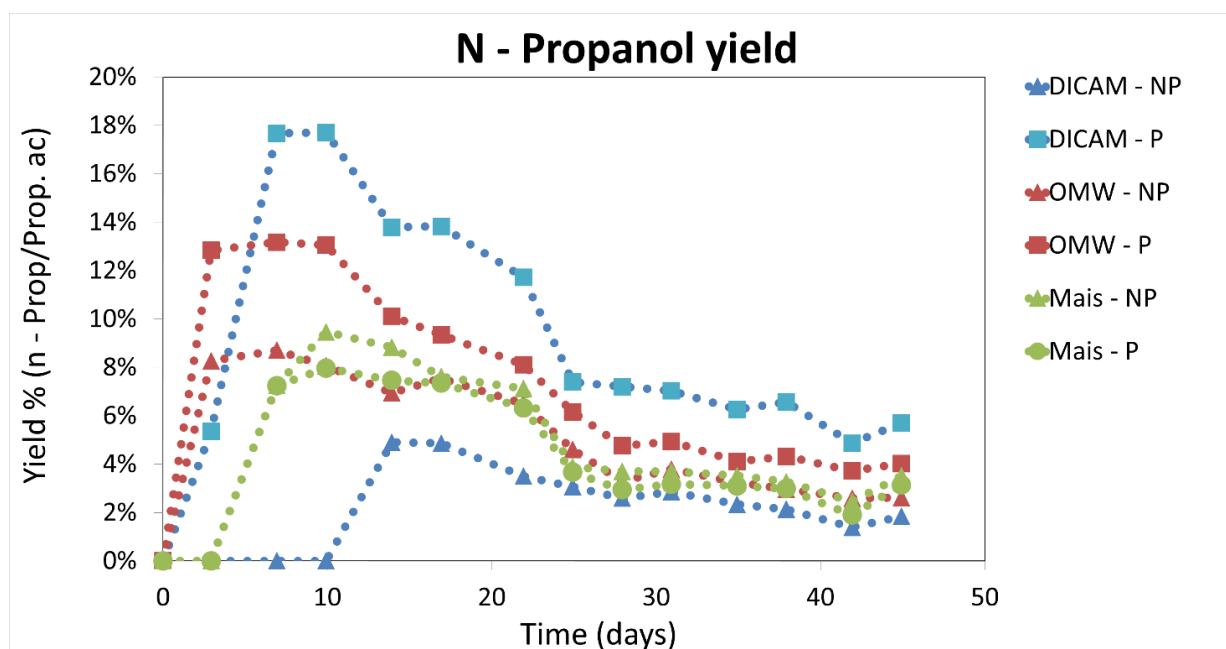


**Figure 5.24:** *N* – propanol yield in each consortium, pasteurized or not, without  $\text{Na}_2\text{MoO}_4$  supplementation

In these graphs, the blue lines represent the DICAM consortium, the red lines represent the OMW consortium, and the green lines the “Mais” consortium. Moreover, triangle indicators are used for non-pasteurized consortia, whereas square indicators are used for pasteurized consortia.

***Main parameters estimated for each consortium without Na<sub>2</sub>MoO<sub>4</sub>.***

	N – propanol production rate (mmol/L/d)	Propionic acid consumption rate (mmol/L/d)	H <sub>2</sub> consumption rate (mmol/L/d)	Max. production (mg/L)	Max. yield (%)
“DICAM” – NP	(0,014 ± 0,008)	(0,305 ± 0,035)	(1,117 ± 0,585)	(14,0 ± 0,9)	(5,0 ± 0,3)
“DICAM” – P	(0,027 ± 0,002)	(0,279 ± 0,048)	(1,606 ± 0,090)	(42,0 ± 0,8)	(18,1 ± 2,0)
“OMW” – NP	(0,019 ± 0,003)	(0,291 ± 0,069)	(1,665 ± 0,660)	(19,3 ± 1,4)	(9,1 ± 4,8)
“OMW” – P	(0,020 ± 0,007)	(0,295 ± 0,084)	(2,161 ± 0,062)	(28,9 ± 9,1)	(13,2 ± 5,0)
“Mais” – NP	(0,021 ± 0,001)	(0,238 ± 0,006)	(1,861 ± 0,61)	(13,7 ± 3,2)	(9,7 ± 3,6)
“Mais” – P	(0,014 ± 0,002)	(0,249 ± 0,026)	(2,032 ± 0,249)	(21,3 ± 2,6)	(7,8 ± 0,9)

**Table 5.8:** Main fermentation parameters estimated for each consortium, pasteurized or not, without Na<sub>2</sub>MoO<sub>4</sub> supplementation

From the graphs and the table reported, is evident that all the consortia screened without sodium molybdate supplementation, are able to reduce propionic acid, and produce n – propanol with different production rates and yields. This is a good result because can represent a good base result to screen the best conditions to increase productivity. From the other side, no – one of the consortia were able to conclude the fermentation. From 1,59 mmol of propionic acid fed (corresponding to 2 g/L), only a small amount, in the range between 0,5 mmol/ and 0,7 mmol, were consumed, with a propanol production of 0,03 – 0,04 mmol (30 mg/L – 40 mg/L) as maximum productivity. It’s evident, that as reported in literature by different studies depicted in section 3.3, the yield and the productivity are very low, but in line with those studies. Moreover, the utilization a mixed pure culture instead of a single recombinant strain is an advantage in terms of costs, security and adaptability of the fermentation.

Unfortunately, around day 20 the fermentation stopped with no further increasing of propanol production. Due to the innovative nature of the process, no literature hint was founded regarding this



factor, anyway it's possible to speculate that is not related nor to substrate or product inhibition, neither to phylogenetic composition of the consortia. In fact, in all the microbial cultured tested the same behavior was detected, and also Kirsten J.J. Steinbusch, 2008, in her work, from 50 mmol of propionic acid, leads to a production of 8,08 mmol of propanol, a concentrations at least 10 times higher respect to the values used in this work. Probably the phylogenetic composition of the consortium and the acclimatization efficiency are key parameters to explain this different results. Anyway, also in her work, after 27 days of fermentation, the process was stopped and an incomplete conversion of propionic acid was observed (only 11,08 mmol of propionic acid was consumed respect to the 50 mmol fed). In this case, our results were in according with our work, but with a better propionic acid conversion, 37,7% in our case respect to a 22,1% in her work. The problem is probably related to different thermodynamic factors. In fact, in these experimental condition, the Gibbs free energy change of this conversion is only – 9,4 KJ/mol:

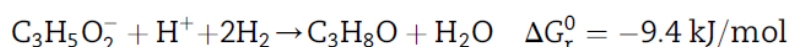


**Figure 5.25:** Thermodynamic calculation for the conversion of propionic acid in n - propanol (Kirsten J.J. Steinbusch, 2008)

Moreover, going deeper to this thermodynamic aspects, Kirsten J.J. Steinbusch, 2008, speculate also that in these conditions only a small amount of electron equivalents are distributed from reagent to products, and in order to reach a value of – 20 KJ/mol for  $\Delta G$ , more hydrogen must be used, or lower pH (4,87), must be set to achieve a more favourable reaction, going towards a obvious microbial growth related problems. It's possible to speculate that the non – continuous hydrogen supply in the microcosms can leads to a inconvenient thermodynamic environment, and a inhibition of the process. According to this limit, the yield of all the processes (figure 5.25), reached a maximum around day 10, and the obviously decreases, because no propanol was further produced (figure 5.24). Thus, all the calculation reported in table 5.8 are related only to the first fifteen days of process.

Figure 5.24, shows that no appreciable differences (net to the standard deviation reported in table 5.8) in n – propanol production were detected with an average maximum production of 15 mg/L - 20 mg/L, except for one consortium, the pasteurized “DICAM” mixed culture, that leads to a maximum production more than double: 42 mg/L at day 14,92. Same trend was reported for the yield, where the

pasteurized “DICAM” culture reports after 6,92 and 9,92 days of process an 18% of conversion, respect to all the other microcosms where the maximum yields were lower than 13,2%. According to the other parameters estimated in table 5.8, only propanol formation rate of pasteurized “DICAM” is higher respect to all the other consortia, whereas substrates consumption rates (propionic acid and hydrogen) are line with the other mixed cultures. Maybe, the higher amount of n – propanol production, can be related to a higher biomass concentration in the consortia. In fact, looking to the graph in figure 5.28, the second column from the left that represents the pasteurized “DICAM” inoculum, at the end of the test, showed a higher biomass concentration respect to all the other mixed culture. Interestingly, the pasteurized “OMW” inoculum reported the second higher biomass concentration, and not by chance, this consortium had the second best yield and the second best n – propanol quantity at the end of the experiment, after only the pasteurized “DICAM” culture.

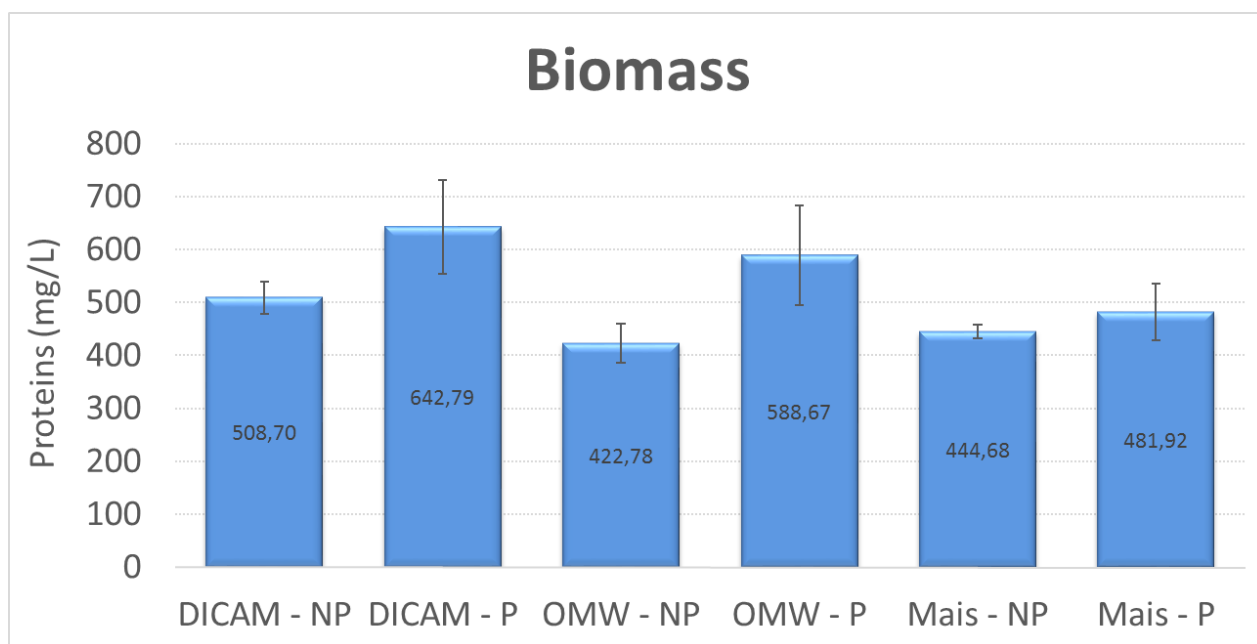


**Figure 5.26:** Biomass estimation with Lowry’s method in each consortium for n – propanol production without sodium molybdate

When all the consortia were supplemented with 15 mM of sodium molybdate in the acclimatization phase, the results were worst for all the consortia, in terms of both yield and both for n – propanol concentration. In figure 5.27 and 5.28, a comparison between all the consortia with supplementation of sodium molybdate are reported, in terms of mg/L of n – propanol produced, and percentage yield.

In this case only single test were performed. In table 5.9, the higher production and yield values are reported, together with the average n – propanol production velocity (in mmol/L/d) and the respective propionic acid and hydrogen consumption rates (both of them also in mmol/L/d) in the first 9,8 days, corresponding to the exponential phase of the process:

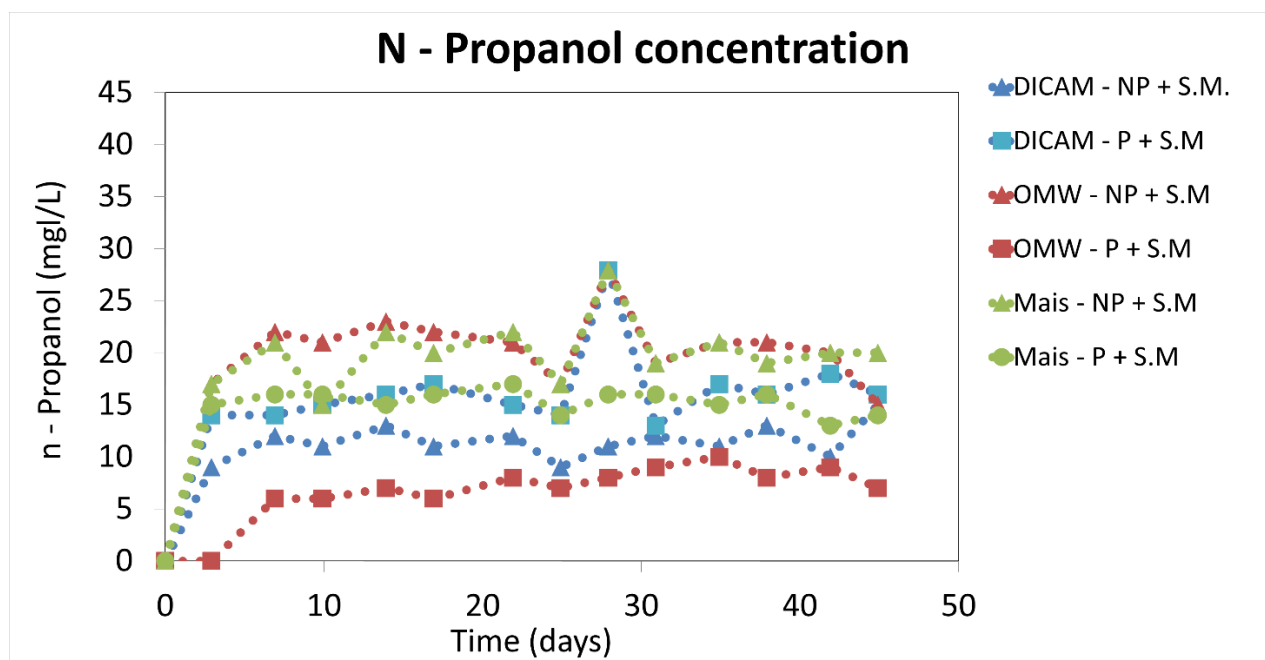


Figure 5.27: N – propanol production in each consortium, pasteurized or not, with  $\text{Na}_2\text{MoO}_4$  supplementation

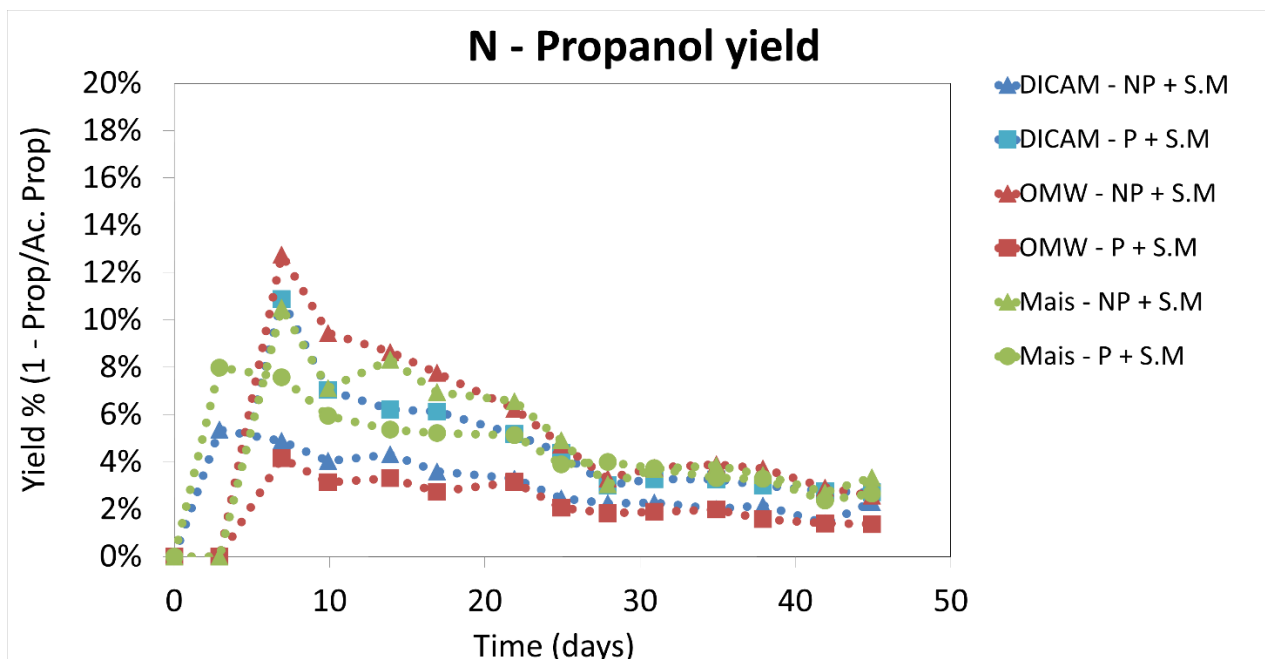


Figure 5.28: N – propanol yield in each consortium, pasteurized or not, with  $\text{Na}_2\text{MoO}_4$  supplementation

Differently from graph in figures 5.24 and 5.25, in this case no observable differences are reported in terms of n – propanol production rates and respective yields. The parameters detail in the following table, confirms this first impression.

***Main parameters estimated for each consortium with Na<sub>2</sub>MoO<sub>4</sub>.***

	N – propanol production rate (mmol/L/d)	Propionic acid consumption rate (mmol/L/d)	H <sub>2</sub> consumption rate (mmol/L/d)	Max. production (mg/L)	Max. yield (%)
“DICAM” – NP + S.M.	0,019	0,274	0,797	11,1	5,3
“DICAM” – P + S.M.	0,019	0,327	0,947	17,9	10,5
“OMW” – NP + S.M.	0,031	0,261	0,364	24,7	13,1
“OMW” – P + S.M.	0,007	0,251	0,906	6,3	4,1
“Mais” – NP + S.M.	0,038	0,252	1,092	20,3	11,1
“Mais” – P + S.M.	0,014	0,303	1,545	15,3	8,2

**Table 5.9:** Main fermentation parameters estimated for each consortium, pasteurized or not, with Na<sub>2</sub>MoO<sub>4</sub> supplementation

Comparing table 5.9 with the table 5.8, where the same parameters are reported without sodium molybdate, besides low yield and production, the only quantifiable difference is in the hydrogen consumption rate. For all the tested consortia, in presence of sodium molybdate the hydrogen consumption was markedly lower respect to the same condition without Na<sub>2</sub>MoO<sub>4</sub>. On the contrary to what one might expect, the biomass concentration in presence of sodium molybdate, is comparable to the values reported without this compound (figure 5.30):

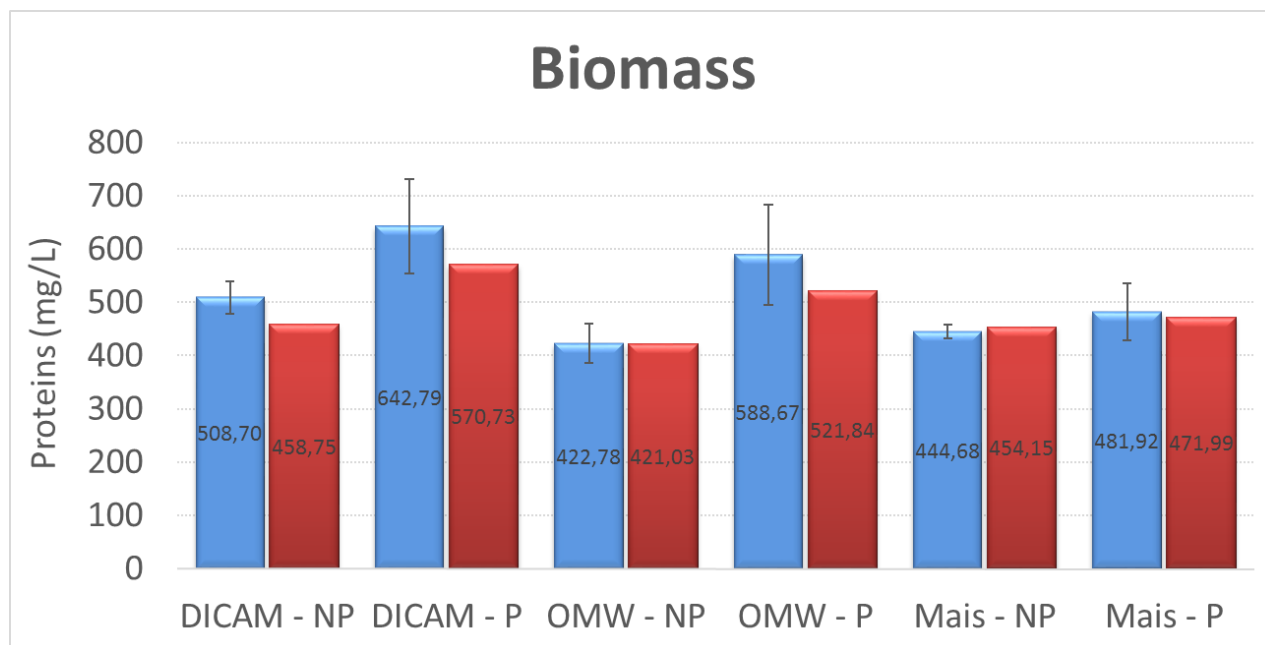


**Figure 5.29:** Biomass estimation with Lowry's method in each consortium for *n* – propanol production with (red) and without (blue) sodium molybdate

The blue bars of the histogram are the same reported in the respective graph, (figure 5.27) and represents the biomass estimated with Lowry's method without sodium molybdate, whereas the red bars represent the same analysis with the same consortia with sodium molybdate. It's evident that no growth inhibition is detected.

Probably the lower performances of the process in presence of 15 mM of sodium molybdate can be ascribed to the syntrophic activity of all the bacteria classes within the consortia. Is extensively reported in literature that sulphate reducing bacteria forms syntrophic interactions with different type of microorganisms, like methanogenic archaea (Li Y.-Y. S., 1996), (Stams, 1994), (Harada, 1994), (Raskin, 1996) and *Clostridium* species (Stieb, 1985), (Schnürer, 1996). Moreover, electron transfer (hydrogen in particularly) was recently demonstrated between methanogens or homoacetogenic bacteria (e.g. *Clostridium*), and sulphate reducing bacteria in syntrophic metabolism (Alfons J. M. Stams, 2009). In addition to that, Michael J. McInerney, 2008 reported that different types of gram-positive, spore-forming, thermophilic, sulfate-reducing bacteria from the genus *Desulfotomaculum* and other closely related genera have also been shown to degrade a variety of compounds (i.e.

saturated fatty acids, unsaturated fatty acids, alcohols, and hydrocarbons) in syntrophic association with specific microorganisms as *Clostridia*, with a fermentative metabolism.

So probably, the lower hydrogen consumption velocity reported in presence of sodium molybdate is the consequence of a metabolism changes in the consortia. Probably, in presence of  $\text{Na}_2\text{MoO}_4$  (but is only a hypothetic approach and no evidences are reported to support this hypothesis), the microorganisms belonging to the *Clostridium* species are not completely responsible anymore for the reduction of propionic acid to n – propanol, but they syntrophically deliver parts of provided hydrogen to the sulphate – reducing bacteria (in a lower efficiency, and this can explain the lower consumption rate), to permit the metabolization of the propionic acid from the action of sulphate reducing bacteria. In fact, in presence of sodium molybdate, the inhibition of sulphate reducing bacteria is related only to metabolic pathway, and not to the growth (as reported in paragraph 4.5.1 and demonstrated in graph 5.30). So maybe SRB can't reduce the sulphate in presence of sodium molybdate, but can growth syntrophically with *Clostridium* species, consuming hydrogen as electron donor, and small amount of VFAs as carbon source.

Looking to the overall results of this combined experiment, it's evident that no definitive conclusions can be made. In fact, the selection and acclimatization phases needs to be better evaluated, and a further insight is necessary. Anyway, the principal objective has been achieved, because with no doubts, the pasteurized “DICAM” consortium with no supplementation of sodium molybdate shows the best performances in terms of production, and yield.

This results fits perfectly with the related theory. Solventogenic carboxydutrophic bacteria belonging to *Clostridium* genus, e.g. *C. ljundgalhi*, *C. ragsdalei*, *C. coskatii*, *C. autoethanogenum*, *C. acetobutylicum*, *C. beijerinckii*, *C. saccharolyticum*, *C. thermocellum* are able to use Wood–Ljungdahl pathway using hydrogen as an electron donor and different types of compounds as VFAs, syngas or carbon dioxide as an electron acceptor as well as a carbon source for building block biosynthesis, as reported in section 3.3. (Perez et.al., 2012), (Papoutsakis ET., 2008).

Moreover, the bacteria belonging to *Clostridium* genus are involved (as reported by extensive literature – see section 3.2) in the preliminary stages of anaerobic digestion, as hydrolytic, acidogenesis and acetogenic phases (Heike Sträuber, 2012), (Fayyaz Ali Shah, 2014).

The DICAM consortium was isolated from the reactor during the preliminary phase of the continuous biomethanization test in bioreactor, where the organic loading rate (OLR) was initially stepwisely increased from 0,1 g<sub>sv</sub>/L/day to 0,3 g<sub>sv</sub>/L/d. In that moment, the mixed culture was already acclimatized to anaerobic digestion, after 84 days of batch test, and other 90 days of fed – batch experiment, plus all the microcosms initial test and the acclimatization phase to AD process, performed by our colleagues (Lorenzo Bertin research group - Bertin, et al., 2012). It's absolutely conceivable that different types of bacteria belonging to *Clostridium* genus (with high probably also some solventogenic carboxydophilic strains) were already enriched in this mixed culture at the times of the isolation from the anaerobic digestion reactor. This factor can represent (together with the further selection by pasteurization treatments) a phylogenetic advantage of this consortium respect to the others, that can explain the higher performances of this culture.

To confirm the presence of solventogenic carboxydophilic bacteria in the pasteurized “DICAM” consortium, a PCR – DGGE (*Polymerase Chain Reaction – Denaturing Gradient Gel Electrophoresis*) approach was used to identify the main bacteria present in the consortium, responsible for the conversion of propionic acid into propanol, followed by sequencing of the main bands detected. All of the analysis were performed in duplicate. The samples were taken at the beginning from the non – selected mother cultures prior selection and acclimatization steps, and at the end of the production phase. Due to the lower yields, no samples for the PCR – DGGE analysis were taken from the consortia supplemented with sodium molybdate.

In the first six lanes of the gel in figure 5.31, is clearly evident the phylogenetic differences of the three mother inoculum, whereas from lane seven to eighteen, the phylogenetic composition of the three selected and acclimatized consortia (pasteurized or not in duplicate) are reported. In table 5.10 the name of the consortia, the code and the respective line of each sample in the DGGE gel are shown:

***Samples names, codes and respective lines in DDGE gel***

		Samples code	Lines in DGGE gel
Mother consortia	“DICAM”	$D_{1-t.0} / D_{2-t.0}$	1 – 2
	“OMW”	$O_{1-t.0} / O_{2-t.0}$	3 – 4
	“Mais”	$M_{1-t.0} / M_{2-t.0}$	4 – 5
Acclimatized consortia	“DICAM” – NP	$D_{1-NP t.f} / D_{2-NP t.f}$	7 – 8
	“DICAM” – P	$D_{1-P t.f} / D_{2-P t.f}$	9 – 10
	“OMW” – NP	$O_{1-NP t.f} / O_{2-NP t.f}$	11 – 12
	“OMW” – P	$O_{1-P t.f} / O_{2-P t.f}$	13 – 14
	“Mais” – NP	$M_{1-NP t.f} / M_{2-NP t.f}$	15 – 16
	“Mais” – P	$M_{1-P t.f} / M_{2-P t.f}$	17 – 18

**Table 5.10:** Sample names, codes, and respective lines in the DGGE gel of the consortium for propanol production

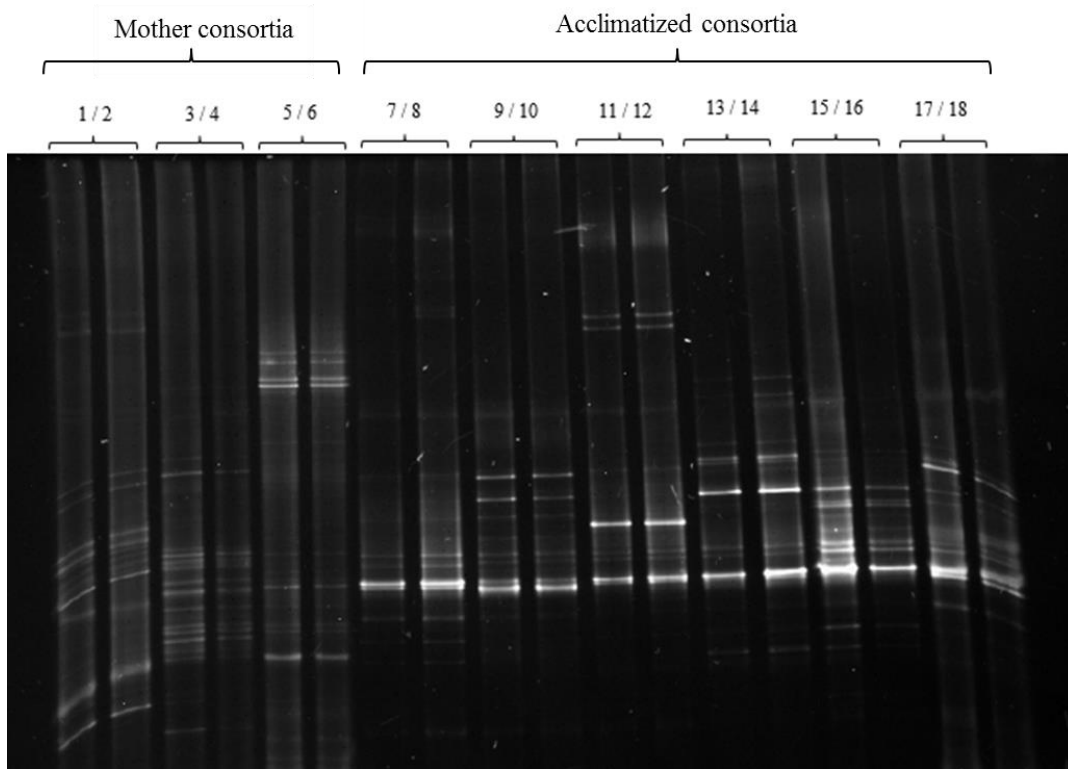


**Figure 5.30:** Overview of the DGGE gel of the selected consortia for propanol production



In the first six lanes, as previously reported, are evident the phylogenetic diversity of the three mother inocula (respectively, lanes 1/2 “DICAM”, lanes 3/4 “OMW” and lanes 5/6 “Mais”). After the growth, selection, acclimatization and production phase, the derived mixed cultures (all without sodium molybdate) were analyzed in DGGE, from lane 7 to 18. In lanes 7/8 the non-pasteurized “DICAM” inoculum at the end of production phase is showed, and next to these lanes, the phylogenetic composition of the pasteurized “DICAM” inoculum is represented (lanes 9/10). The same scheme is followed for “OMW” consortium (lanes 11/12 for non-pasteurized “OMW” after production phase, and lanes 13/14 for pasteurized “OMW” after production phase) and “Mais” consortium (lanes 15/16 for non-pasteurized “Mais” after production phase, and lanes 17/18 for pasteurized “Mais” after production phase). It's clearly evident that from the diversity of the mother inoculum, all the phylogenetic profiles shifted towards a unique band pattern. It's possible to speculate that the selection and acclimatization phases were effective in order to enrich the microbial population in the desired microorganisms. Moreover, the restrictive incubation conditions (i.e. 100% H<sub>2</sub> in the headspace, and pH 6), favored the growth of the few selected species.

From this complex pattern it's possible to highlights some evidences (see the same gel of figure 5.31, reported in figure 5.32, for more clarity).

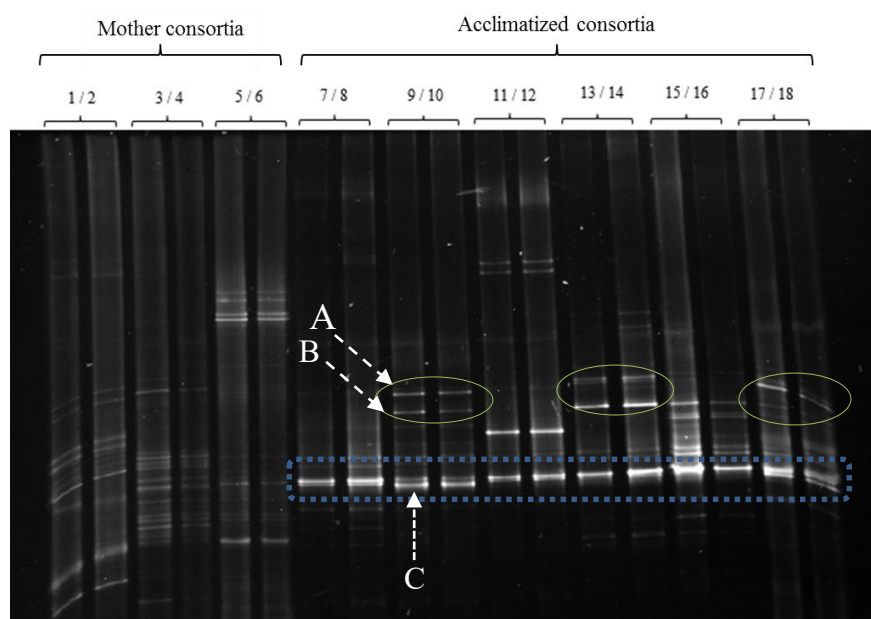


**Figure 5.31:** Same DGGE gel reported in figure 5.31 with additional graphic conclusions.

In the blue dotted rectangle, is now graphically evident the conclusion made before. The constant presence of those bands with this intensity, all along the acclimatization consortia, and the contemporary absence in the respective mother consortia, is the proof that the restrictive conditions (i.e. 100% H<sub>2</sub> in the headspace and pH 6) leads to a deep selection in the phylogenetic composition of all the screened mixed culture. Moreover, the bands present in the blue dotted rectangle are ubiquitous along pasteurized and non – pasteurized consortia. This is another evidence that the main enrichment procedure is made by the restrictive incubation conditions and not, probably from the selection / acclimatization phases. Anyway, those phases contribute to select and acclimatize the desired bacteria to the propionic acid, and moreover to perform a further step of enrichment. In fact, as is clear from the green arrows and circles, in all the three pasteurized consortia a couple of bands for each line are present only in these mixed cultures and not in the respectively non – pasteurized tests. With high probabilities, those bands represent some sporigen microorganisms (maybe *Clostridia*) that were selected only with thermic treatments.

Due to the higher performances demonstrated by pasteurized “DICAM” consortium (lanes 9/10), the bands A – B – C represented by the white dotted arrows in figure 5.32. were cut from the gel with a sterile scalpel and the DNA was eluted, re-amplified and resolved in another DGGE, to confirm the purity. Then, the DNA was purified and sent to a private company for sequencing procedure. Each 16S rRNA gene sequence obtained, was aligned to Ribosomal Database Project-II (RDP, release 11, <http://rdp.cme.msu.edu>) using “Seqmatch” tool. The phylogenetic affiliation of every sequence was obtained from the same website through the “Classifier” tool. The results are reported in the following table:

Band	Phylogenetic group	Closet match [accession #]	Identity
A	<i>Clostridia</i>	<i>Clostridium pasteurianum</i> (T); JCM 1408; AB536773	99 %
B	<i>Clostridia</i>	<i>Pseudoflavonifractor capillosus</i> (T); ATCC 29799; AY136666	96 %
C	<i>Clostridia</i>	<i>Clostridium celerecrecens</i> (T); DSM 5628; X71848	99 %

**Table 5.11:** Sequencing of the predominant DGGE bands highlighted in the most performing propanol production consortium

Confirming the initial hypothesis, the phylogenetic analysis demonstrates that the sequence of the 16S rRNA gene is typical of three specific microorganisms belonging to the genus *Clostridia*, with a higher percentage of similarity.

*Clostridium celerecrescens*, is an anaerobic, Gram +, sporigen and motile bacterium with an optimal temperature growth at 37 °C and pH 6,5, isolated by M. LL. Palops, in 1989. Is a cellulotic microorganism and can ferment a plethora of different carbohydrates to produce alcohols, volatile fatty acids, hydrogen or CO<sub>2</sub>. Recently was also used in two different patensts (Germany Patent n. WO2014135633 A1, 2014), (U.S.A. Patent n. US20080311640 A1, 2008), for the production of butanol and other chemical compounds.

*Pseudoflavonifractor capillosus*, knows also as *Clostridium orbiscindens* (Carlier JP, 2010) is a well know sporigen bacterium with a high genome similarity with the saccharolytic bacteria *C. difficile* involved in the metabolism of several flavonoids (Schoefer L1, 2003). Besides this well-established characteristic, recently Venessa Eeckhaut, 2011 phylogenetically identified *Pseudoflavonifractor capillosus* together with other 15 species belonging to the *Firmicutes* phylum in the caecal content of chickens, that are able to ferment and metabolize small amount of VFAs as propionic and butyric acid.

*Clostridium pasteurianum*, is a saccharolytic and spore-forming obligate anaerobe bacterium, usually used as a classic acid producer from a plethora of raw material (Gottschalk, 2006), (M. Heyndrickx, 1991). Anyway, different literature studies report the ability to switch from acid to solventogenic metabolism as ABE fermentation (Harris, 1986) or 1,3-propanediol production (Nakas, 1983), under specific conditions, as the presence of electron source.

## 5.4 SUCCINIC ACID – VITO RESULTS

### 5.4.1 Batch results with CSTR reactor: lactose VS milk whey

To perform preliminary tests in order to evaluate the fermentation performances with both lactose and both milk whey, a simple batch approach was used. As reported in section 4.6.1., the tests were conducted in a 5 L bioreactor (3,4 L as working volume), with 1,5 filled with liquid medium, and 1,9 L of headspace. The fermenter was kept at pH 6,6 with a sterile solution of NaOH 10M, because according to Ke-Ke Cheng, 2012, at this pH the PEP – carboxykinase demonstrates the maximum efficiency in fixing the CO<sub>2</sub> molecule. In fact, as reported in detail in section 3.4 (and graphically explained in figure 3.11), after the glycolytic or pentose – phosphate pathways, the carbon source is converted to pyruvate and then to phosphoenolpyruvate (PEP). At this point the metabolic pathway is divided in two separate branches: the “C3 pathway”, and the “C4 pathway”. The “C4 pathway” leads to the succinate production and involves as a first step the transformation of PEP into oxalacetate through the action of phosphoenolpyruvate carboxykinase (PEP – K). It’s evident that the PEP – K enzyme is the key for achieve and high yield of succinate. A. succinogenes, in fact, fix 1 mol of CO<sub>2</sub>, for every mol of succinic acid formed (Cheng K, 2012). For this reason, to provide enough CO<sub>2</sub>, the fermenter was constantly kept in a small overpressure of 350 mbar of pure and sterile - filtered carbon dioxide. The fermenter was inoculated with 20% v/v from two subsequent steps of pre – cultures, described in details in paragraph 4.6.2.

Prior showing the results, some calculation needs to be explained: to consider also the contribution of sodium hydroxide addition in the yield of the process, a new parameter reported as theta ( $\theta$ ) was introduced, and defined as:

$$\theta * \text{batch initial volume} = \text{base volume}$$

thus,

$$\theta = \frac{\text{base volume}}{\text{batch initial volume}}$$

where base volume and batch initial volume are respectively the liters of sodium hydroxide added, and the initial liquid working volume in the fermenter. In this way,  $1 - \theta$ , can be considered as a corrective factor derived from the addition of NaOH 10M.

The carbohydrates (as a sum of glucose, lactose and galactose concentrations) consumption rate (g/L/h), defined as  $S_{\text{carbohydrates}}$  can be calculated as:

$$S_{\text{carbohydrates}} = \frac{((1 - \theta) * C_{\text{carbohydrates initial}} - C_{\text{carbohydrates final}})}{t}$$

where  $C_{\text{carbohydrates}}$  are the initial and final concentrations of the total sugars present in the liquid medium and detected by HPLC (g/L),  $t$  is the time of fermentation (h), and  $1 - \theta$  is the corrective factor.

The succinate productivity ( $P_{SA}$ ) expressed in grams of succinic acid/L/hour (g/L/h), is defined, as usual, as

$$P_{SA} = \frac{C_{SA}}{t}$$

where  $C_{SA}$  is the concentration of succinic acid (g/L), reported at a certain time of fermentation, and  $t$  is obviously the time of the process.

Similarly, the total acid productivity ( $P_{\text{Total acids}}$ ) that is one of the main parameters to compare to the succinic acid productivity ( $P_{SA}$ ), is defined as

$$P_{\text{total acids}} = \frac{C_{\text{total acids}}}{t}$$

where  $C_{\text{Total acids}}$  is the summary of concentration of all the organic acids produced in the fermentation in grams/L (pyruvate, succinate, formate, acetate), reported at a certain time of fermentation, and  $t$  is obviously the time of the process.

At this point, the succinic acid (SA) yield (expressed in g<sub>SA</sub> / g<sub>carbohydrates</sub>) and known formally as  $Y_{P/S}$  can be calculated as the ratio of SA productivity to carbohydrates consumption rate:

$$SA \text{ yield } (g \cdot g^{-1}) = Y_{P/S} = \frac{P_{SA}}{S_{\text{carbohydrates}}}$$

Substituting in the  $Y_{P/S}$  equation the respectively relationship for succinic acid productivity and  $S_{\text{carbohydrates}}$  expressed in the previous page, the results is:

$$SA \text{ yield } (g \cdot g^{-1}) = Y_{P/S} = \frac{C_{SA}}{((1 - \theta) * C_{\text{carbohydrates initial}} - C_{\text{carbohydrates final}})}$$

Following this scheme for the total acids, it's possible to define the total acid yield (expressed in g  $\text{Total acids} / \text{g carbohydrates}$ ) can be calculated as the ratio of total acids productivity to carbohydrates consumption rate

$$Total \text{ acid yield } (g \cdot g^{-1}) = Y_{P/S} = \frac{P_{\text{total acids}}}{S_{\text{carbohydrates}}}$$

Substituting again in the total acids yield equation the respectively relationship for total acids productivity and  $S_{\text{carbohydrates}}$  expressed in the previous page, the results is:

$$Total \text{ acid yield } (g \cdot g^{-1}) = Y_{P/S} = \frac{C_{\text{total acid}}}{((1 - \theta) * C_{\text{carbohydrates initial}} - C_{\text{carbohydrates final}})}$$

Finally, the carbohydrates utilization percentage is calculated as:

$$\text{Carbohydrates utilization} = \left( 1 - \frac{C_{\text{carbohydrates, final}}}{(1 - \theta) * C_{\text{carbohydrates, initial}}} \right) * 100$$

In the following graphs and tables is reported the comparison between the performances of the two batch fermentations.

Both of them are conducted with 40 g/L of lactose, or lactose equivalent when milk whey is used, in the same condition (1,5 L as working volume. 20% v/v as inoculum, pH 6,6, 0,35 bar of pure CO<sub>2</sub> overpressure and 2'' rpm/min as stirring velocity).

In figure 5.33 and table 5.12 are reported the data for the lactose fermentation, whereas in figure 5.34 and table 5.13, are reported the results obtained with milk whey. In the graphs are reported the concentrations of sugars and acids on the left axes, and the moles of sodium hydroxide added in the fermenter on the right side of the graphs.

In the tables, instead, the calculations for kinetic parameters (previously described) are reported in terms of concentrations, yields, productivities and carbohydrates utilization.

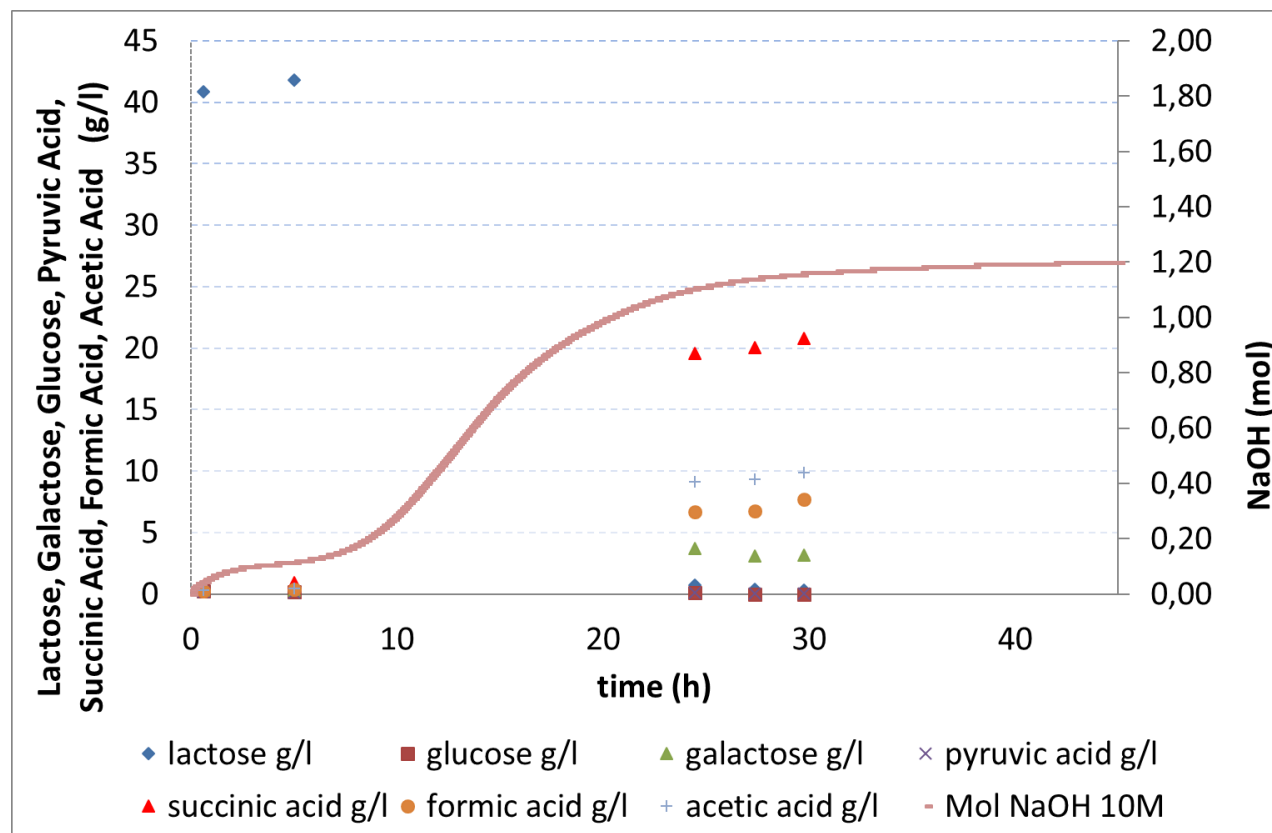


Figure 5.33: Batch fermentation results of succinic acid production with lactose.

In blue triangles, red squares, and green triangles are reported respectively the concentrations of lactose, glucose and galactose during this 30 - hours experiment. On the same left axis, the concentration of pyruvic, succinic, formic and acetic acids are reported, respectively with purple crosses, red triangles, orange circles and light blue plus.

With the continuous pink line, instead on the right axis the moles of sodium hydroxide added to the fermenter were reported. Every 15 seconds, in fact, the system registered the values, making feasible to relate graphically the sodium hydroxide addition to the bacteria growth, and obviously to the fermentation trends.

As it clear from the moles added to the fermenter, the shape of the curve fits perfectly with a batch fermentation, with an initial lag phase of more or less 8 hours, an exponential phase from hour 8 to

hour 25, followed by a stationary phase. Reached the stationary phase, after 30 hours the experiment was stopped. The lactose, in fact, was completely converted after 24,4 hours, and the glucose was immediately consumed because no accumulation is observed. Only small amount of galactose accumulation was detected, up to 3,7 g/L after 24,4 hours of fermentation and then slowly consumed until a final residual concentration of 1,8 g/L. This is obviously in line with the classic diauxic lactose consume model. When lactose is hydrolyzed to glucose and galactose, the first is immediately consumed, whereas the latter is accumulated until the glucose is completely depleted, and only at this point, the bacterium start consuming the accumulated galactose (William F. Loomis, 1967).

As reported in section 3.4., the overall reaction is stoichiometric: 1 mol of glucose and 1 mol of carbon dioxide leads to 1 mol of succinate, 1 mol of acetic acid and 1 mol of formate (Van der Werf MJ, 1997). According to Cheng K, 2012 the maximum theoretical yield (in grams, excluding growth and maintenance) is 1,31 g of succinic acid for 1 g of glucose consumed. Moreover, M.F.A. Bradfield, 2014, reports that in a continuous succinic acid production by *A. succinogenes* in a biofilm reactor, the optimal succinic acid/acetic acid ratio (SA/AA) must be maintained in the range between 2,3 and 3, whereas succinic acid/formic acid ratio (SA/FA) must be kept around 1,8. As a consequence, formic acid/acetic acid ratio must be lower than 1.

t (h)	Carbohydrates (g.L <sup>-1</sup> )	SA (g.L <sup>-1</sup> )	S <sub>carbohydrates</sub> (g.L <sup>-1</sup> .h <sup>-1</sup> )	P <sub>SA</sub> (g.L <sup>-1</sup> .h <sup>-1</sup> )	SA yield (g.g <sup>-1</sup> )	Carbohydrates utilization (%)	SA/AA	SA/FA	FA/AA
0,6	41,4	0,7					2,2	2,9	0,7
5,0	42,3	1,0	1,5	0,2	0,1	14,7	2,1	2,7	0,8
24,4	4,5	19,6	1,7	0,8	0,5	90,2	2,1	2,9	0,7
27,4	3,5	20,0	1,6	0,7	0,5	92,4	2,2	3,0	0,7
29,8	3,5	20,8	1,4	0,7	0,5	92,4	2,1	2,7	0,8

**Table 5.12:** Production of succinic acid from lactose using batch fermentation. Parameters and calculations

From this table and also from the graph, it's evident that succinic acid is a growth – related product. In fact, when the fermentation reached the stationary phase, the succinic acid production never increased anymore. As previously reported, the total sugars were practically depleted (only small amount of galactose was founded in the fermentation medium), with a constant carbohydrates consumption rate in the range between 1,4 and 1,7 g/L/h.



After 30 hours of fermentation, the final SA concentration was 20,8 g/L, with a maximum productivity of 0,8 g/L/h of succinic acid after 24,4 hours and a yield of 0,5 g<sub>SA</sub> / g<sub>carbohydrates</sub>. Those values are a little bit lower respect to the yields and productivity reported in section 3.4 (table 3.9) of the main literature works, but the ratio numbers (SA/AA, SA/FA, FA/AA), are absolutely constant with the values reported by M.F.A. Bradfield, 2014.

In the following figure and table, are reported the same data for the equivalent milk whey fermentation.

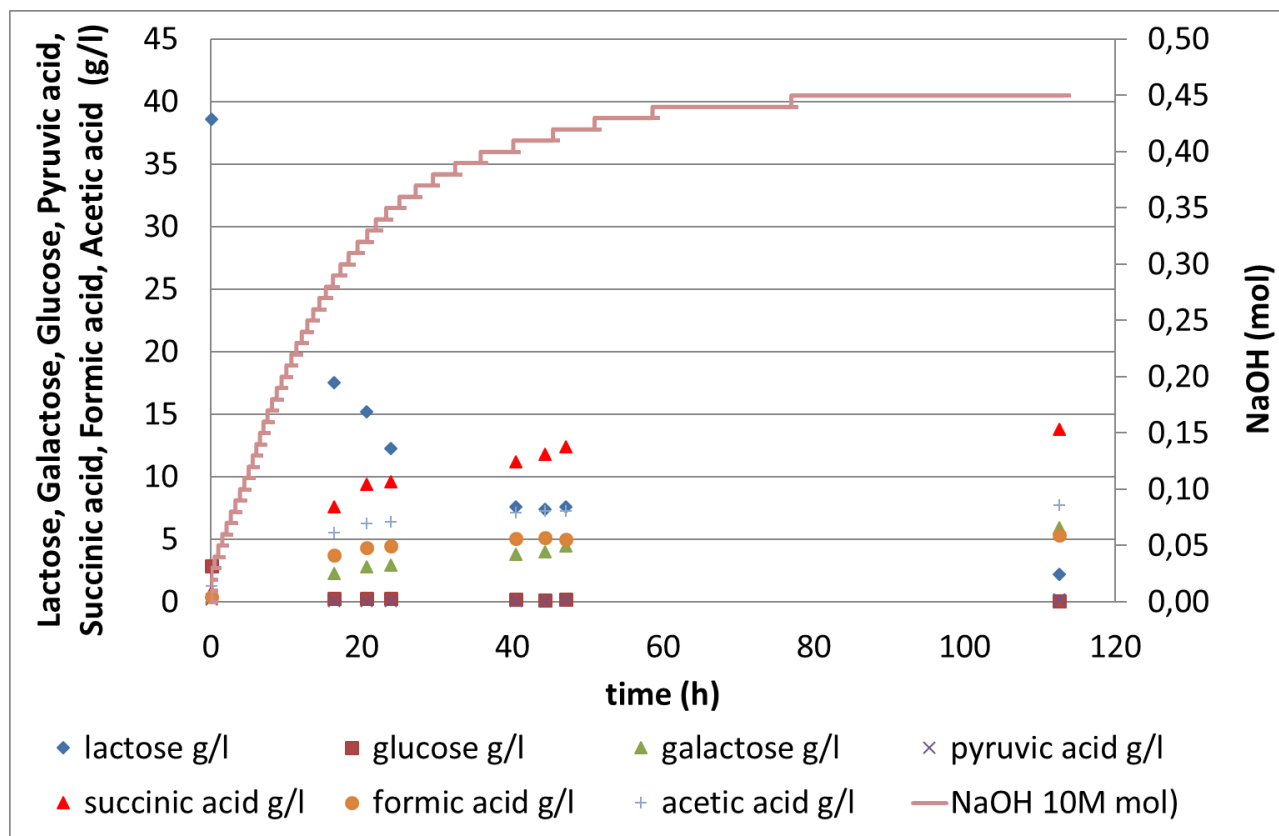


Figure 5.34: Batch fermentation results of succinic acid production with milk whey.

t (h)	Carbohydrates (g.L <sup>-1</sup> )	SA (g.L <sup>-1</sup> )	S <sub>carbohydrates</sub> (g.L <sup>-1</sup> .h <sup>-1</sup> )	P <sub>SA</sub> (g.L <sup>-1</sup> .h <sup>-1</sup> )	SA yield (g.g <sup>-1</sup> )	Carbohydrates utilization (%)	SA/AA	SA/FA	FA/AA
0,1	41,8	0,8					0,6	2,1	0,3
16,4	20,0	7,6	1,3	0,5	0,4	51,5	1,4	2,0	0,7
20,7	18,3	9,4	1,1	0,5	0,4	55,6	1,5	2,2	0,7
23,9	15,5	9,6	1,1	0,4	0,4	62,4	1,5	2,2	0,7
40,5	11,6	11,2	0,7	0,3	0,4	71,8	1,6	2,2	0,7
44,4	11,5	11,8	0,7	0,3	0,4	71,8	1,6	2,3	0,7
47,2	12,2	12,4	0,6	0,3	0,4	70,1	1,7	2,5	0,7
112,6	8,2	13,8	0,3	0,1	0,4	79,9	1,8	2,6	0,7

**Table 5.13:** Production of succinic acid from milk whey using batch fermentation. Parameters and calculations

According to the graph reported in figure 5.34, no lag phase was observed using milk whey. This is an unusual result, and in literature no evidences are reported. Only Amir Hussain, 2015, reported that in a packed bed bioreactor lowering the glucose concentration from 10 g/L to 4 g/L, no lag phase was detected. Anyway in this case, probably the composition of milk whey reported in section 4.1.2, and specifically in table 4.5, plays a key role. Maybe the high proteins concentration, equivalent as 2,2 g/L, or the presence of 0,4 g/L of total nitrogen and phosphorous, can improve the growth efficiency reducing lag phase of this microorganism. Anyway, no evidences are reported about that speculation. Using a by – product as milk whey, more time is necessary to complete the fermentation, and to hydrolyze all the lactose: 112 hours respect to the 24 hours using pure lactose. Moreover, also in this case, no glucose was detected, but at the end of fermentation higher amount of galactose was detected (8,2 g/L respect to 3,5 g/L using pure lactose), that leads to a lower carbohydrate utilization efficiency, 79,9% compared to 92,4% using pure lactose. This is also reported by Daniel Pleissner, 2015 when in his work reported all the principal fermentation processes present in literature for SA production using pure sugars or by - products. The carbohydrates consumption reached a maximum of 1,3 g/L/h after 16,4 hours, and then slowly but constantly decreased until the end of the fermentation. This value is obviously lower respect to the maximum value detected using pure lactose (1,7 g/L/h). After 112,6 hours of fermentation, the final SA concentration was 13,8 g/L, with a maximum productivity of 0,5 g/L/h of succinic acid after 20,7 hours and a yield of 0,4 g<sub>SA</sub> / g<sub>carbohydrates</sub> across the overall fermentation process. Those values are a little bit lower respect to the concentration and productivity reported with pure lactose, but the obtained yield and productivities, are in line with the principal literature studies, for example, 0.58 g/L/h as productivity and 0,44 g<sub>SA</sub> / g<sub>carbohydrates</sub> as yield

(Wan C, 2008). The ratio numbers (SA/AA, SA/FA, FA/AA), are reproducible from the previous fermentation, only the SA/AA is lower, that probably an indication of a little unbalance between the C3 and C4 metabolic pathway.

It's possible to conclude that these value represented a good starting point for the integrated experiment described at the end of the chapter 5.4.

#### 5.4.2 Electrodialysis outcomes: LCD and parameters determination

As described in section 4.6.1., the pre-pilot ED plant is formed from three independent storage tanks (concentrate, diluate, electrolyte solution) connected by separates loops to a multi – layer membrane stack, formed by alternate layer of anionic and cationic membranes. Three peristaltic pumps recirculate continuously the liquid between the compartments and the membranes, and the ions is separated under the influences of an electric field.

ED principle is reported in figure 5.35:

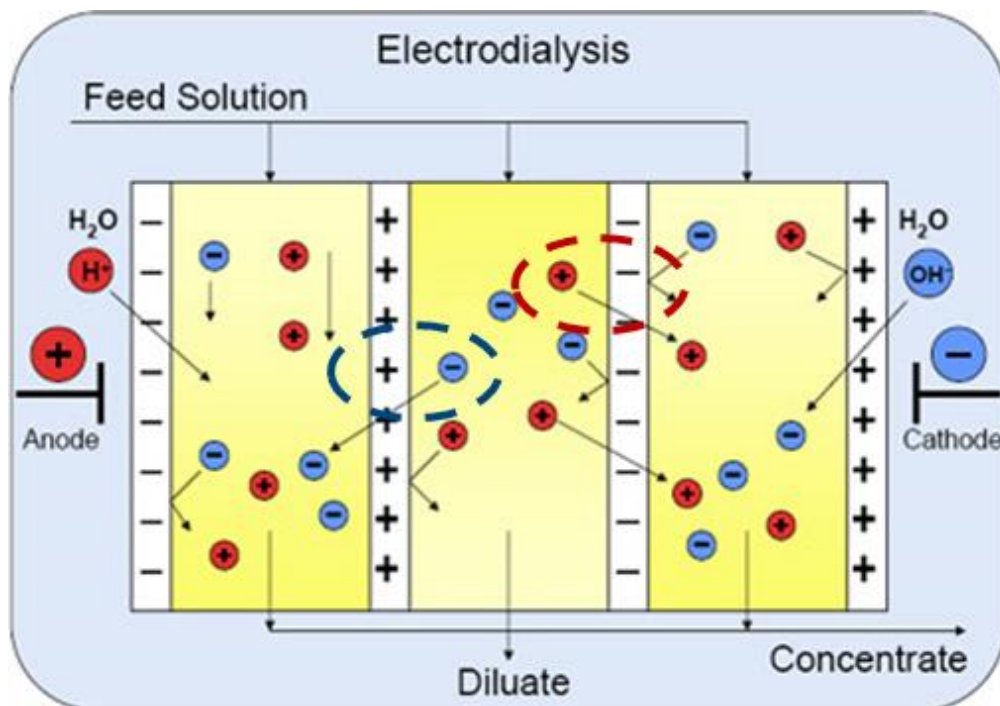
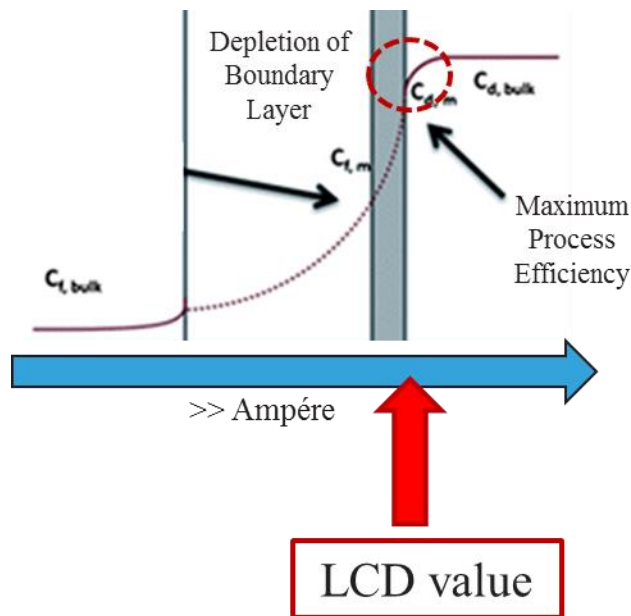


Figure 5.35: Electrodialysis concept.

When an electric pulse is applied through the membrane stack, the negative ions (blue dotted line) present in the feed solution in the dilute compartment migrates toward the positively charged anode. These ions pass through the positively charged anion exchange membrane, but are prevented from further migration toward the anode by the negatively charged cation exchange membrane present in the stack, and therefore stay in the concentrate stream, which becomes concentrated with the anions. The positively charged species (red dotted line) migrate in the same manner toward the negatively charged cathode and pass through the negatively charged cation exchange membrane. These cations also stay in the concentrate stream, prevented from further migration toward the cathode by the positively charged anion exchange membrane. The overall result of the electrodialysis process is an ion concentration increase in the concentrate stream with a depletion of ions in the dilute solution feed stream (AWWA, 1995). ED is industrially applied in the desalination of seawater, and numerous studies and patents are present in literature (Mohtada Sadrzadeh, 2008), (Banasiak, 2007), (Kalogirou, 2005), (Van der Bruggen, 2002), (Kim Y. B., 2011), (U.S.A. Patent n. US8999171 B2, 2015), (U.S.A. Patent n. US4539088 A, 1985). Recently, another interesting application of ED is the integration as downstream process in a fermentation plant for the production and separation of organic acid from culture broth. In fact, after a middle – cell retention steps (as ultra or micro filtration units), ED was successfully used for the separation of lactic acid (Věra Hábová, 2004), (P. Boyaval, 1987), (Y.H Kim, 2001), citric acid (Senad Novalic, 1996), (Xu Tongwen, 2002), small chain carboxylic acids from C1 (formic) to C6 (caproic), (Alberto Vertova, 2009), or other type of charged compounds as for example 1 – 3 propanediol (Yan Gong, 2004). Also for succinic acid recovery electrodialysis process was used (DA. Glassner, 1995), (Kurzrock, 2010) after numerous pre-treatment steps as microfiltration, ultrafiltration, and active charcoal adsorption. The most promising results is reported by Zeikus JG, 1999 where a 60% of global purification yield was achieved after cell – retention step and two subsequent stage of ED desalination.

The main parameter that needs to be characterized in a ED plant, is the LCD, the limiting current density of the system. LCD value, is defined as the current value applied to the membranes to ensure

the maximum transportation efficiency. The maximum efficiency is reached when during the transport across the membranes, the ion concentration becomes zero on the surface of ion exchange membranes. In figure 5.36, this concept is clearly explained as a graphical scheme:



**Figure 5.36:** Limiting current density concept.

When the bulk concentration ( $C_{bulk}$ ) of a certain species in the feed solution is transported towards a suitable ion exchange membrane, the boundary layer is continuously depleted with higher efficiency as higher is the applied current. When the concentration on the surface of the exchange membrane is approaching to zero (red dotted line), the process reached the maximum efficiency. This current value represents the desired LCD parameter.

Two side – effects needs to be considered in ED experiments:

❖ Osmosis

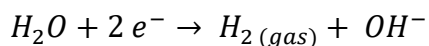
This is an unavoidable effect. In fact, when an ionized species from a concentrate compartment is transferred to a diluate compartment, is well known that water is transferred in the opposite way (from diluate, to concentrate compartment). In this case, the diluate compartment has a lower concentration of succinic acid (max 30 g/L) respect to the concentrate compartment (usually 60 g/L), and the transfer of SA is forced from diluate to the concentrate. It's evident, thus, that water migrates from diluate to

the concentrate compartment together with succinic acid, leading to a continuous volume decreasing in the diluate compartment, and a continuous volume increasing in the concentrate. This is an undesired effect, because the volume increasing the concentrate is the cause of a dilution of the compartment, and a lower SA final concentration with a huge impact on the efficiency and on the yield of the process.

In the process optimization, is absolutely important to consider that after a while, lowering too much the concentration in the diluate compartment, leads to a drastic increase of the osmotic effect (due to a higher concentration difference between the two compartments), with a drastic performances reduction. An equilibrium needs to be founded in order to maintain a balance between costs and process efficiency.

#### ❖ Water splitting

This occurs only when the current is higher respect the LCD value. Water splitting results in the ionization of water, and the formation of  $\text{OH}^-$ , due to this reaction



When the operation is conducted above LCD value, detrimental effects on the process occurs with a high probability of a complete failure of the test. The first effect is the immediate pH raising in the concentrate compartment, because the  $\text{OH}^-$  ions migrates toward the positively charged anode through ions exchange membranes from diluate to the concentrate compartment (due, in this case to the higher water concentration in the diluate respect to the concentrate). This can lead to a precipitation at the membrane interfaces of pH – sensitive substances as calcium carbonate.

Besides that, the resistance is higher than normal when water splitting occurred. In fact, when water dissociation starts, the  $\text{OH}^-$  start migrating across the anionic membranes, demanding more and more voltage to continue the dissociation of water molecules. Also, a thin film of highly depleted solution forms at the depleting sides of the membranes. These films have high – specific resistances which are in series with the other resistances in a ED stack. Both the increased voltage needed for continuous ionization of water, both the high specific resistances of the depleted layers, contributes to increase stack total resistance (Rousseau, 1987).

The ED plant for the LCD offline tests is described in section 4.6.1, whereas in section 4.6.3, is reported the specific of the experiments.

In the graph reported in figure 5.37 is reported the integrated Cowan plot for the experiment performed with the 5 diluted synthetic solutions (table 4.23) that simulates 5 different fermentation broth with different succinic acid concentrations: 30 g/L, 20 g/L, 10 g/L, 5 g/L, 2,5 g/L. A Cowan plot is the classical plot for the LCD determination in ED processes (Goldberg, 1997). When the supplied current was stepwisely increased every minute of 60 mA, the corresponding voltage was registered by the software. Using Ohm's law, the resistance in the stack was calculates as a ratio, between Voltage and the supplied Ampère. Plotting for every minute the reciprocal of the current ( $1/\text{Ampère}$ ) in function of the calculated resistance, the resulting curve exhibits a typical upward concavity with the minimum value corresponding to the desired LCD.

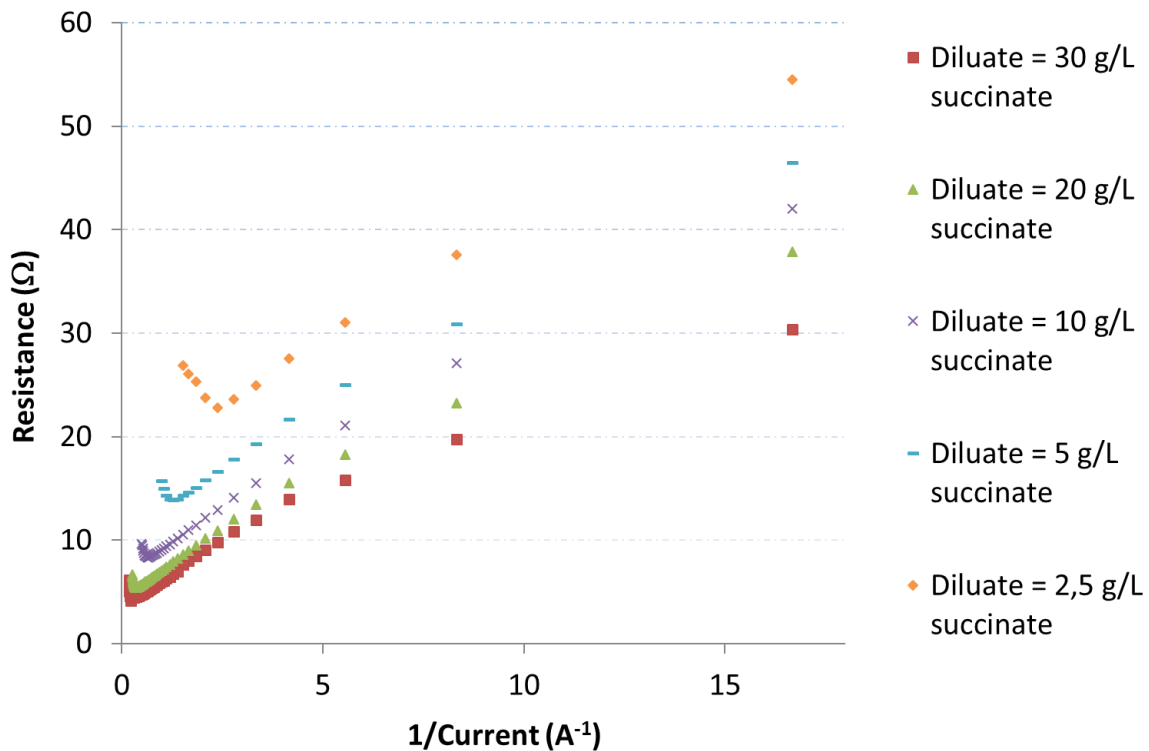


Figure 5.37: LCD determination graph.

In the graph, red squares, green triangles, purple crosses, blue lines and orange rhombus represents respectively the diluted solution with respectively 30 g/L, 20 g/L, 10 g/L, 5 g/L and 2,5 g/L of succinic

acid. The minimum value of the curve on the x – axis is the 1/LCD, and from the reciprocal the LCD is calculated, as reported in table 5.14;

Succinate (g/L)	Acetate (g/L)	Initial conductivity (mS/cm)	Final Conductivity (mS/cm)	LCD value (A)	0,80*LCD	Voltage (V)
29,52	8,42	37,70	26,80	4,41	3,53	18,32
19,20	6,36	27,50	22,20	2,88	2,30	15,66
10,63	3,64	17,27	16,11	1,50	1,20	12,50
5,82	1,85	9,34	9,22	0,78	0,62	10,81
3,17	1,12	6,28	5,64	0,42	0,34	9,56

*Table 5.14: LCD determination table. Parameters and calculations*

Is evident that with the decreasing of the S.A. concentration, the LCD value is decreasing, because less energy is required for the ions transportation. Working at LCD value leads to the maximum efficiency, but is tricky because a little instability of the current input can cause the shift the process above the LCD, with detrimental consequences. For this reason, usually the plants work at 80% of the LCD value, in order to maintain a safety level of security. Conductivity is the main operational parameters that can be monitored in the ED procedure. The lowering of the conductivity in the diluted compartment is usually a sign of ions transportation, in fact the final conductivity at the end of the experiments is always lower respect to the initial value reported in the table 5.14.

Plotting the final conductivity in function of the LCD (blue line), or in function of 80% of LCD (red line), a very fitting 3° grade polynomial regression (figure 5.38) is estimated in the next graph.



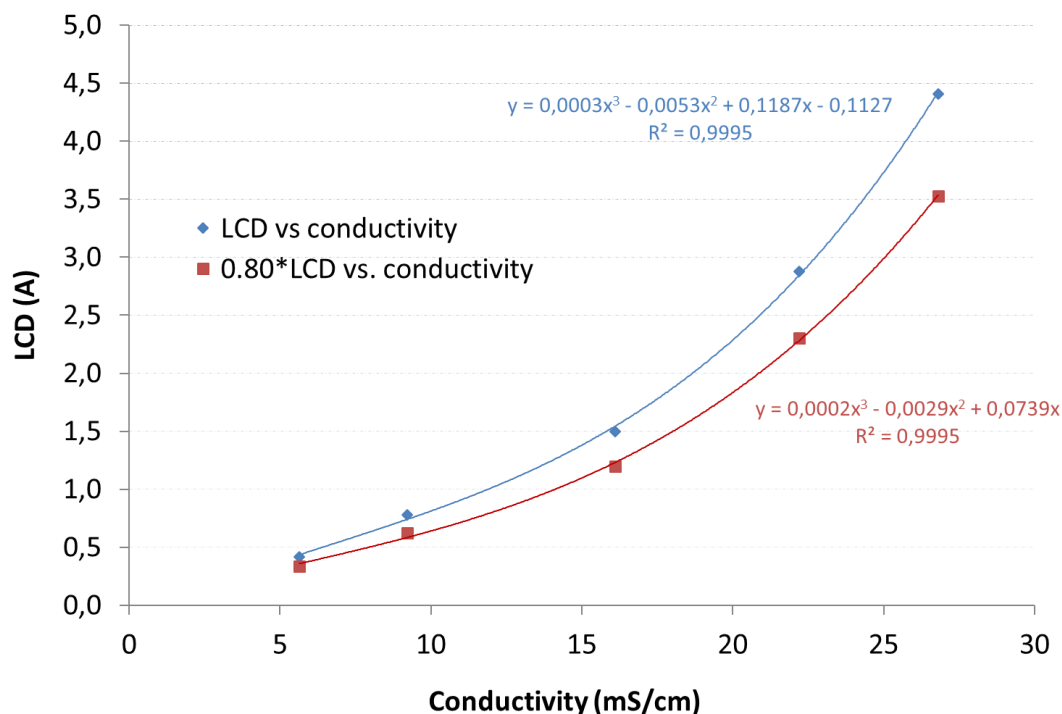


**Figure 5.38:** Experimental relationship between conductivity and LCD.

Following the red equation, it's possible to adapt the LCD value input in function of the conductivity in the diluted solution, that can be monitored online every 15 seconds.

#### 5.4.3 ED results with synthetic broth

Following the relationship established in the LCD experiment between LCD and conductivity, a separation test was performed using a synthetic solution in the diluate compartment. In this test, described in section 4.6.4, in the diluate compartment was used a synthetic solution with the same composition as the solution reported in the first row of table 5.14 (30 g/L of succinic acid), and 60 g/L in the concentrate. After 20,43 hours until the diluate conductivity was below 7 mS/cm, the diluate compartment was refilled with another solution with the same composition of the previous one, without change neither the concentrate, nor the electrolyte compartment. The current supplied was lowered in function of the conductivity measured online.

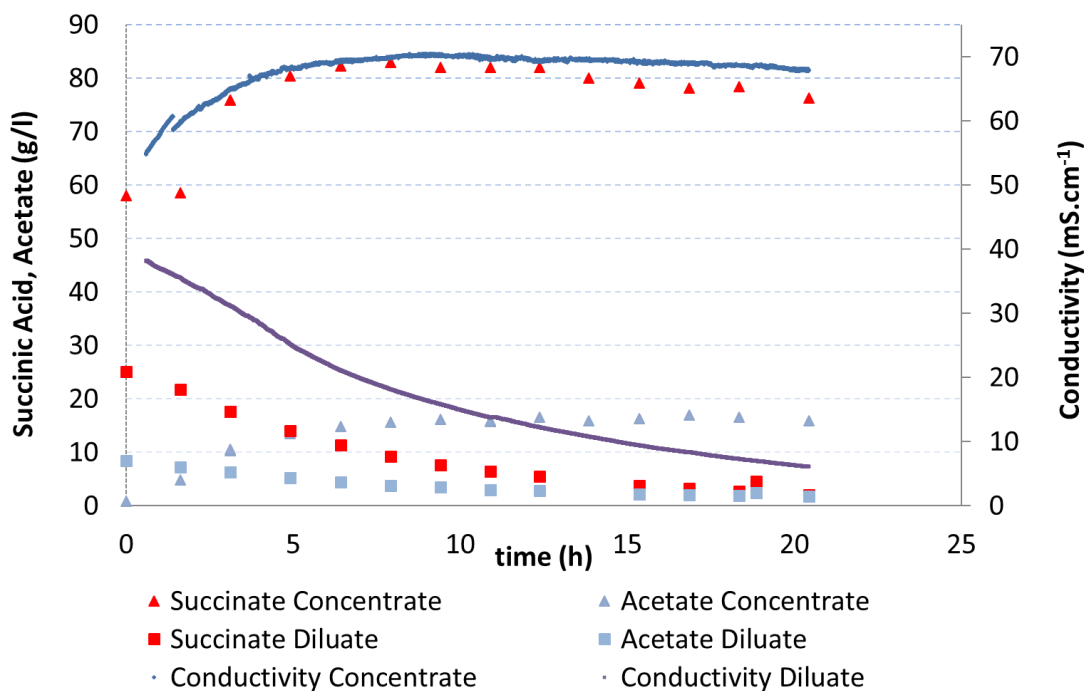


**Figure 5.39:** Conductivity and concentration profiles of succinic and acetic acid in both diluate and concentrate compartment.

In figure 5.39 are reported the results. In red is reported the succinic acid concentration (squares in the diluate, and triangles in the concentrate), whereas in light blue is reported the acetic acid concentration (again, squares in the diluate, and triangles in the concentrate). The continuous lines are the conductivity profile measured online. Dark blue in the concentrate, and purple in the diluate. At the starting point, the initial values of succinic acid were 58,05 g/L in the concentrate and 25,15 g/L in the diluate, whereas for the acetic acid the values were 0 g/L in the concentrate and 8,41 in the diluate. Succinic acid is rapidly increased from 58.05 g/L to 81.95 g/L in the first 9.40 h of process, following the raising profile of conductivity. From 9.40h to 20.43 h there is an osmotic effect prevalent because the ions concentration in the diluate compartment was very low. For this reasons the final concentration of S.A. is slowly decreased from 81.95 g/L to 76.28 g/L.

The same profile is observed for Acetic acid that is transported from diluate to concentrate. In the first 9.40h from 0 g/L to 16.19 g/L, and then is decreased due to the osmotic effect to 15.87 g/L

Following the red equation in figure 5.38, the resulting profile of Ampère and Voltage in the stack are reported in the following graph. Following the decreasing of the conductivity, the current was adapted to remain in the condition of 80% of LCD value during the whole process.

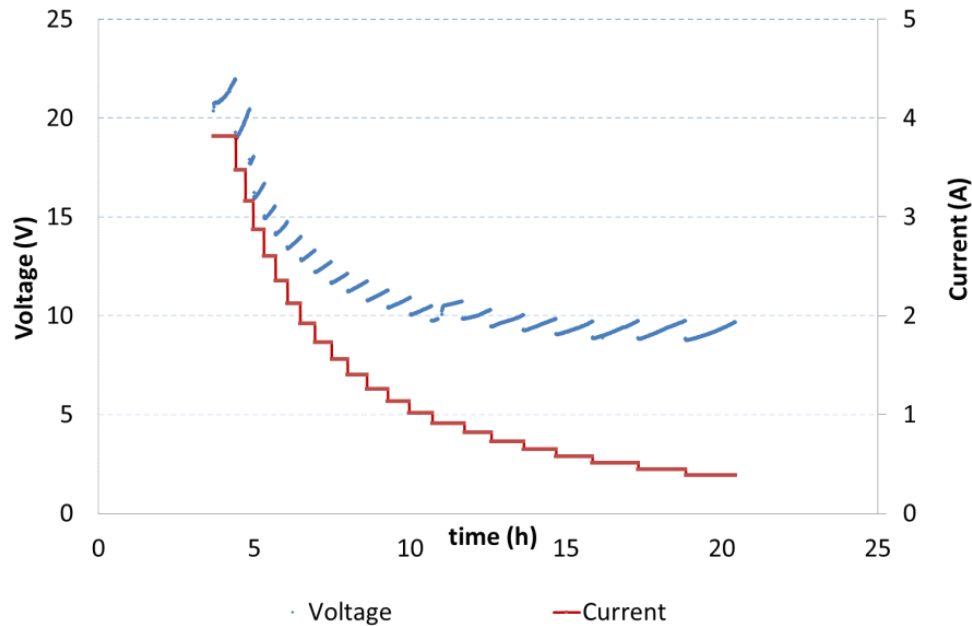


**Figure 5.40:** Current and voltage profiles.

The Ampère were stepwisely lowered from 3,89 A to 1,19 A. It's evident that, keeping constant the value of the current in every "steps" leads to a temporary increasing of the resistance (due to the ions transportation), and thus to an increasing of the resulting voltage for the Ohm's law.

Considering the behavior after 9,40 hours, osmotic transport is observed in this last phase of the test. Since the supplied current was kept below the LCD value for every step of current decreasing, electrosmotic transport and water splitting can be considered negligible, and the water transport from diluate to the concentrate compartment can be ascribed only to the unavoidable osmotic effect coupled to ions transportation. In fact, a huge water transport from diluate to concentrate was detected, and the level of the concentrate solution raised from 2,00 Lt to 5,73 Lt after 20,43h of process. In the same manner, a decreasing of the volume of the diluate compartment was detected, from 10 Lt, to 6,46 Lt. Both pH of diluate and concentrate are constant. This is a confirmation that no electro-osmotic effect is detectable in this process.

From this raw data, some calculation can be made, dividing this test in two parts on the bases of osmotic effect, from 0 to 9,4 hours, and from 9,4 hours to the end of the experiment.

Water transport number (TW number) is calculated as follow, and relates the quantity of transported ions to the quantity of transported water.

$$TW \text{ number} = \frac{\text{mol H}_2\text{O transported}}{\text{mol ion transported}}$$

This value is practically constant during the first 9,4 hours of the experiment (average 57,7 CV=17,29%; N= 4). This equals a transport of 231,6 g of water per g of SA transported. The same principle is applied for acetic acid. The water transport number is constant in the first 9,4 hours (average 86,43; CV = 12,7%; N=4). With this transport rate, the maximum SA concentration is 116,17 g/l (CV 17%, N=4) in the first 9,40 hours, whereas during the last period (9,4 h – 20,43 h) with the osmotic effect, the maximum concentration in the membrane was lower (61,55 g/l SA, CV = 20,04% N=4).

Moreover, some calculation regarding the current efficiency (CE) and energy use are determined.

All the values are determined only for the first 9,4 hours of the experiment (transportation from 58,05 -81,95 g/l SA).

$$\text{Coulomb} = \text{Ampere} * \text{Second}$$

$$CE = \frac{\frac{\text{mol ion transported} * \text{ion charge}}{\text{cell pairs number}}}{\frac{\text{Coulomb}}{\text{Faraday number}}} * 100$$

$$\text{Power usage (Joule)} = \text{Volt} * \text{Ampere}$$

$$\text{Energy used (KWh)} = \frac{(\text{Power usage} * \text{Time})}{3600 * 1000}$$

$$\text{Specific power consumption} \left( \frac{\text{kWH}}{\text{kgSA}} \right) = \frac{\text{Energy used}}{\text{Grams of ion transported} * 1000}$$

$$\text{Transpotrt rate} \left( \frac{\text{Kg ion}}{\text{m}^2 * \text{h}} \right) = \frac{\left( \frac{\frac{\text{grams of ion transported}}{1000}}{\frac{\text{time (h)}}{3600}} \right)}{\text{cell pairs number} * \text{surface (m}^2\text{)}}$$

In the following table are summarized the principal results for the first 9,4 hours:

Parameter	Avg	CV	unit
SA C.E.	61	25%	%
Specific power consumption	2,2	13%	kWh/kg SA
Specific water transport	57	17%	mol H <sub>2</sub> O/ mol SA
Maximum transported SA conc	116	17%	g SA/L
Transport rate	0,3	27%	Kg/m <sup>2</sup> h

**Table 5.15:** Calculation of the most prominent parameters only for the first 9,4 hour of test, prior refilling the diluate compartment

After 20,43 hours the diluate compartment was refilled with another solution with the same composition of the previous one, and the same graphs and calculations were made.

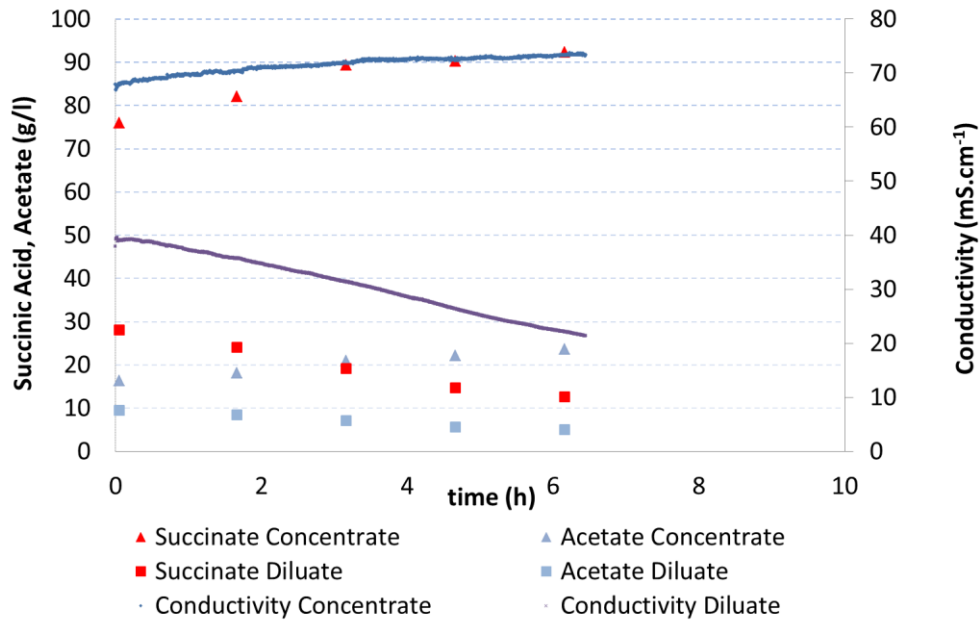


**Figure 5.41:** Conductivity and concentration profiles of succinic and acetic acid in both diluate and concentrate compartment, after refilling.

It can be seen from the conductivity graph that the transport started again due to the ions refilling in the diluate compartment. This test is ended after 6,16 h of process, in order to avoid high osmotic effect as previously reported. At this second starting point, the initial values of succinic acid were 75,93 g/L in the concentrate and 28,22 g/L in the diluate, whereas for the acetic acid the values were 16,38 g/L in the concentrate and 9,54 in the diluate. After 6,16 h the conductivity passed from 39,1 mS/cm to 21,7 mS/cm and succinic acid rapidly increased from 76,28 g/L reached in the test 1 to 92

g/L, following the raising profile of conductivity. The same profile is observed for the acetic acid that is transported from diluate to concentrate. In 6,16 h from 15,87 g/L of the test 1 to 23,57 g/L at the end of the process.

Same trend is reported for current and voltage:

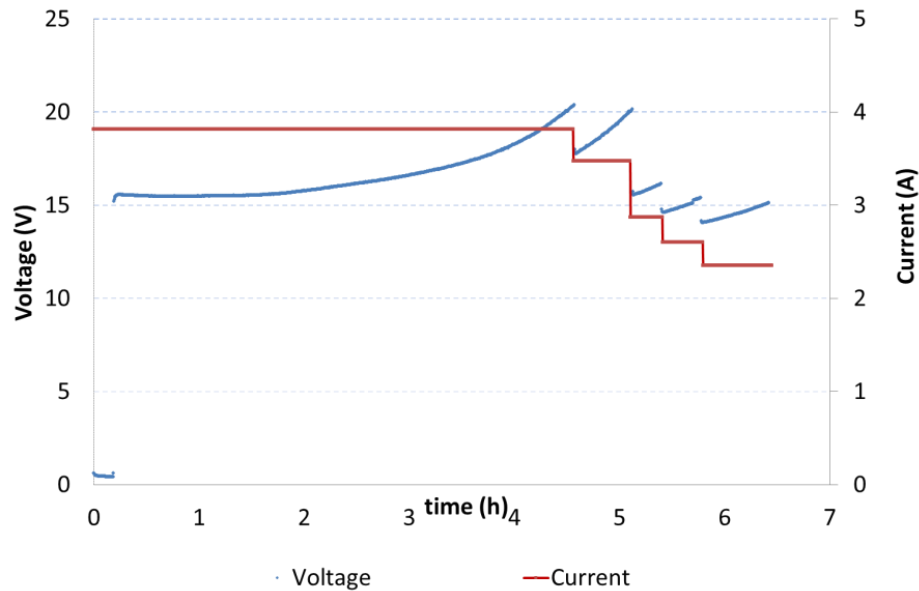


**Figure 5.42:** Current and voltage profiles after refilling.

The Ampère were stepwisely lowered from 3,89 A to 2,35 A. Since the supplied current was again kept below the LCD value for every step of current decreasing, electrosmotic transport and water splitting can be considered also in this case negligible, and the water transport from diluate to the concentrate compartment can be ascribed only to the unavoidable osmotic effect coupled to ions transportation. The level of the concentrate solution raised from 2,00 Lt to 3,3 Lt with a decreasing of the volume of the diluate compartment was detected, from 10 Lt, to 8,57 Lt. Also in this case no pH variations were observed.

The same calculations regarding the water transport are made. Transport water number (TW number) prior and after refilling were constant, ensuring the replicability of the tests (57,7 CV=17,29%; N= 4 prior refilling and 56.52 CV=17.62%; N= 4 after refill). Constant was also the acetic acid related transport number: (average 86,43; CV = 12,7%; N=4 prior refilling and 95.73; CV = 21.67%; N=4

after refill). With this transport rate and without osmotic effect, the maximum SA concentration is 116,17 g/l (CV 17%, N=4) in the first 9,40 hours prior refilling, and this value was confirmed after refilling with a maximum achievable SA concentration of 118,59 g/l (CV 16.74% N=4), completely comparable with the previous value.

Again, same calculation regarding current efficiency, specific power consumption and transport rate, were made. In table 5.16 is reported the results

Parameter	Avg	CV	unit
SA CE	56	18%	%
Specific power consumption	2,2	20%	kWh/kg SA
Specific water transport	56	17%	mol H <sub>2</sub> O/ mol SA
Maximum transported SA conc	118	16%	g SA/L
Transport rate	0,46	27%	Kg/m <sup>2</sup> h

**Table 5.16:** Calculation of the most prominent parameters only for the first 9,4 hour of test, after refilling the diluate compartment

Looking to the results in table 5.15 and 5.16, it's evident that they are absolutely comparable. The process, thus, can be considered optimized (at least with synthetic broth). Further experiment with real broth are described in the next chapter.

#### 5.4.4 ED results with real broth

After the experiments with synthetic broth, both for LCD determination, both for a proper separation test, a real – centrifuged fermentation broth was used in another LCD test. All the characteristics were exactly the same of the previous LCD determination, only the diluate compartment was filled with a real exhausted fermentation broth with a concentration of 10,1 g/L of succinic acid and 4,3 g/L as acetic acid as main products. The culture broth was previously centrifuged for 30' at 4 °C at 8000 rpm/min to remove the cells, and the supernatant was used as diluate solutions. According to the LCD table 5.14 in the previous paragraph, a concentration of c.ca 10 g/L of succinic acid leads to a limiting current density value around 1,5 A (1,2 A as 80% of LCD). In the next table, the same 5.14 table is reported with at the bottom line, the parameters derived from the real – centrifuged broth.

	Succinate (g/L)	Acetate (g/L)	Initial conductivity (mS/cm)	Final Conductivity (mS/cm)	LCD value (A)	0,80*LCD	Voltage (V)
Synt	29,52	8,42	37,70	26,80	4,41	3,53	18,32
	19,20	6,36	27,50	22,20	2,88	2,30	15,66
	10,63	3,64	17,27	16,11	1,50	1,20	12,50
	5,82	1,85	9,34	9,22	0,78	0,62	10,81
	3,17	1,12	6,28	5,64	0,42	0,34	9,56
Real centrifuged	10,10	4,30	24,10	20,80	2,28	1,82	17,02

**Table 5.17:** LCD determination table with real centrifuged broth. Parameters and calculations

Also in this case, the conductivity passed from 24,10 mS/cm to 20,80 mS/cm that is an indirect confirmation of the ions passage. The LCD value was 2,28 Ampère, a higher value respect to the 1,50 Ampère determined for the same concentration in the synthetic broth. Also the applied voltage was higher (17,02 V respect to 12,5 V for the synthetic broth), that leads in a similar resistance value, according to Ohm's law, 7,46  $\Omega$ , and 8,3  $\Omega$  respectively for real and synthetic broth. These discrepancies in the Ampère values, are probably related to the presence of other ionic compounds in the culture broth, as calcium, potassium, sodium, chlorine or other ionic molecules that are transferred together with the succinate and the acetate, requiring more energy. The resistances, in fact, were comparable and this is the most important parameters, because increasing of stack resistance is strictly related to an over limiting current process. To qualitatively estimates that if the relationship founded between conductivity and LCD was applicable also with real centrifuged broth, the final conductivity value determined with this real – non centrifuged broth was plotted in function of the LCD, as in figure 5.38.

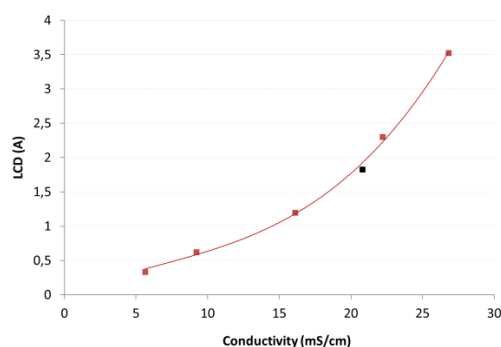


**Figure 5.43:** Experimental relationship between conductivity and LCD including the value for real centrifuged broth.



The red points are the same reported in figure 5.38 for the synthetic analysis, whereas the black one is that one estimated for real non centrifuged broth LCD test. It's evident that fits with the equation estimated between conductivity and 80% of LCD value, reported in the graph in figure 5.38, so it's possible to conclude that the composition of the real culture medium doesn't affect the separation performances.

In section 5.4.3, an integrated separation test with synthetic broth was described following the relationship between conductivity and LCD. The same principle was followed performing another separation test using a real broth without centrifugation. In this case the initial concentration of succinic acid and acetic acid were respectively 18,19 g/L, and 3,36 g/L. The concentrate compartment, was formed by a synthetic succinic acid solution of 50,79 g/L, and the experiment was continued for 11,91 hours. Similarly to figure 5.39, in the following is reported the trends of the succinic acid concentration (red squares in the diluate, and red triangles in the concentrate), whereas in light blue is reported the acetic acid concentration (again, squares in the diluate, and triangles in the concentrate). The continuous lines are the conductivity profile measured online. Dark blue in the concentrate, and purple in the diluate.

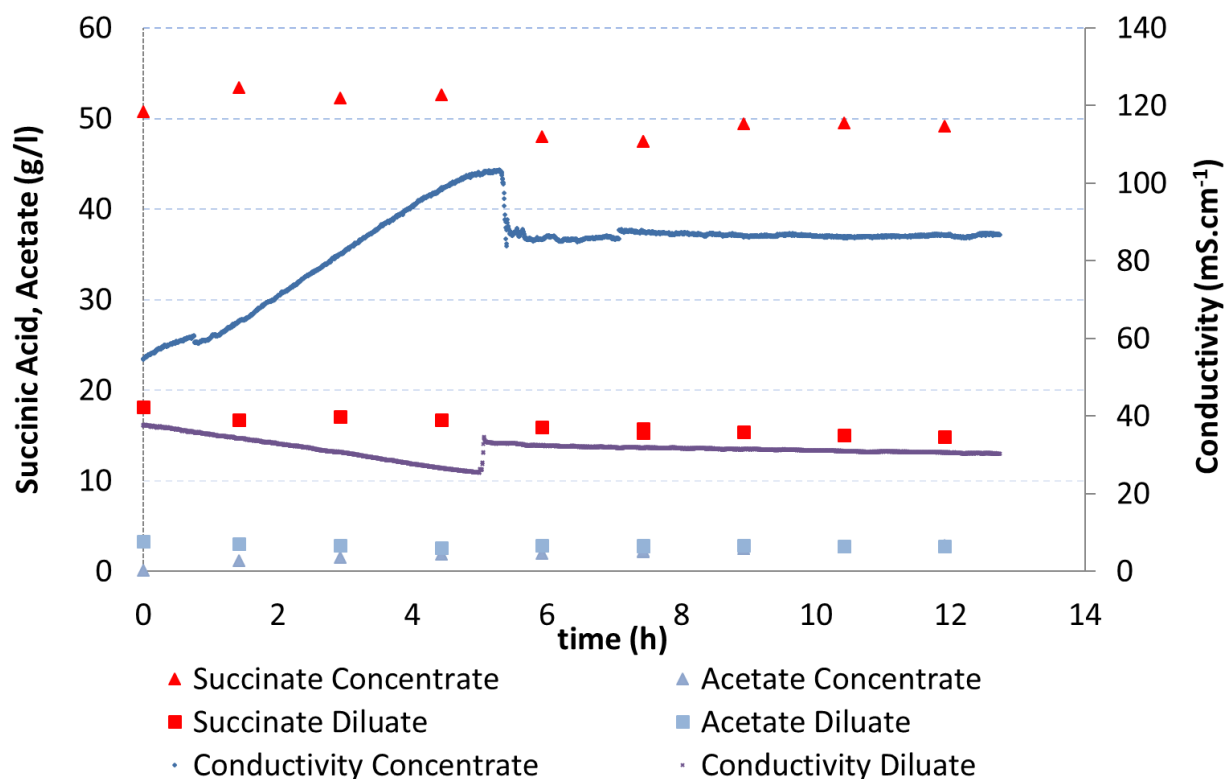


**Figure 5.44:** Conductivity and concentration profiles of succinic and acetic acid in both diluate and concentrate compartment using a real non centrifuged broth.

The differences between figure 5.44 (real non centrifuged broth) and figure 5.39 (synthetic broth), are evident. Besides the initial increasing of the conductivity of the concentrate compartment, the succinic acid concentration remained constant, around 50 g/L in the concentrate, and no decreasing was observed in the diluate. Thus, is evident that no transfer between the stack occurred, though the increasing in conductivity; something else is obviously involved. Looking to the other parameters of the process, starting with the same amount of current input (3,82 A derived from the equation between conductivity and LCD previously determined), for both the experiments, the registered voltage was doubled in the real test (c.ca 40 V) respect to the 21 V determined for the synthetic experiment. This means a doubled resistance between the stack, and as a consequence a lower LCD value respect to the values previously determined, probably due to the cell - derived fouling on the membrane. In this way, the process was working above the real limiting current density. This hypothesis was verified by the drastically raising of the pH in the concentrate compartment, from 6,9 to more than 12.

The pH raising was one of the major effect of the overcoming of LCD value. Moreover, the raising of the conductivity can be ascribed on the migration of  $\text{OH}^-$  through the anionic membrane. It's obvious that fouling derived from the cells in the broth is the main responsible of this inconvenient.

Estimating the crossflow velocity of the liquid medium through each membrane layers was about 0,15 m/s, whereas in literature an ultrafiltration plant with a crossflow velocity below 3 m/s was already susceptible by reversible fouling (Hyeok Choi, 2005).

Due to this high fouling of the membranes, from 5,92h to 11,91 (end of the test), the approach was shifted from a constant current input, to a constant voltage input of 8 V. According to Ohm's law, in fact, if a constant Ampère were supplied, the increasing of the resistance in the stack leads to an increasing of the resulting voltage, whereas, if a constant voltage was supplied and the resistance is increased in the stack, the resulting current is lower. In the latter case the transfer process was slower (because less energy is provided), but there is no risk to work above the limiting current density. The results were obviously lower than expected: anyway, a small increasing in S.A. concentration, from 48 g/L to 49,14 g/L was detected with a reduction of S.A. concentration in the diluate from 15,95 g/L to 14,85 g/L. To confirm our hypothesis, another LCD test was performed with the "dirty" and "fouled stack" with another synthetic 30 g/L solution of succinic acid as previously reported in the first line of table 5.14 (real S.A. concentration was 29,15 g/L). The obtained LCD value was only 0,94 A, respect to the 4,41 A detected with the clean stack. This confirms that the fouling causes an increasing of the resistance in the stack, and the uselessness of the previous relationship founded in order to carry out the bioreactor – ED integrated test. Moreover, with a supplied constant voltage of 8 V, the resulting current lowered from 0,93 A to 0,71 A, that were lower respect to the new "fouled" LCD founded values. For this reason, in the integrated test (see next paragraph) in the integrated test, a constant supply of 8 V was used to perform the separation, assuming that the fouling process is constant between different tests carried out in the same conditions.

#### 5.4.5 Integrated test

As described in section 4.6.5, the innovative part of this activity performed at VITO, was the realization of an integrated ISPR plant without cell retention steps thanks to an improved stack design. In particular, the fermenter at steady – state phase was directly coupled to the optimized ED plant, to perform a direct separation.

The fermenter was prepared as described in materials and methods section, using 5,7 g/L of initial lactose concentration, and conducted in batch phase for 23,78 hours, achieving a succinic acid concentration of 18 g/L, and 7 g/L of acetic acid. In this initial part of the test, the residual lactose concentration was 31,6 g/L with a 0,27 g/L/h of carbohydrate consumption rate, and a 17,8% of utilization efficiency. The S.A. productivity and yield were respectively 0,37 g<sub>SA</sub> /L/h, and 1,38 g<sub>SA</sub> \* g Carbohydrates<sup>-1</sup>. Then, a 118,30 hours of continuous phase was performed, using a previously optimized 16,8 hours as residence time, with a 1,49 ml/min as feed rate of a 50 g/L of lactose medium solution, with a resulting dilution rate (“D”) of 0,059 h<sup>-1</sup>. The steady state was reached with an average succinic acid composition in the fermenter around 10,4 g/L, and acetate concentration of 4,0 g/L. The residual carbohydrates in the culture broth were about 28 g/L, with a higher consumption rate respect to the batch phase 1,2 g/L/h of carbohydrate consumption rate, and a 41,6% of utilization efficiency. The S.A. productivity was higher respect to the batch phase (0,62 g<sub>SA</sub> /L/h) but the yield was lower, only 0,52 g<sub>SA</sub> \* g Carbohydrates<sup>-1</sup>, respect to the batch period.

After 149,67 hours of total fermentation, the ED plant was coupled, and the culture broth started flowing through the membrane, and back to the fermenter. As demonstrated from the separation test with real broth, is evident that a huge fouling affects the plant performance in the first hours of test, lowering the LCD value from the hypothetical value of 4,41 A to a real value of 0,94 A, using the same stack, and the same synthetic 30 g/L S.A. solution in the diluate compartment. For this reason, a constant voltage supply through the stack was provided, in order to achieve an 80% of the real LCD value (0,94 A) previously determined, that is 0,75 A. With a constant supply of 4,2 V through the membrane was 0,78 A, that was used as initial value for the separation. As described in section 4.6.4, in this real integrated test, only 1 membrane layer was used instead of 6 layers, because the estimated

removal rate of the ED plant, needs to be maintained lower respect to the estimated S.A. production in the fermenter.

Based on the final part of the separation graph reported in figure 5.44 (from 5,92h to 11,91), where the input was switched from constant Ampère to constant voltage, some calculations were made.

At 5,92 hours the concentration of S.A. in the diluate was 15,95 g/L and the volume in the tank was 9,63 L, resulting in a 153,61 total grams of succinic acid. In the same way, at the end of the test (11,91 h), the amount of succinic acid in the diluate was 14,85 g/L, in 8,41 L, that leads to 124,83 grams of S.A. in the compartment, with a reduction in this 5,99 hours of separation conducted with constant 8 V, of 28,78 grams of succinic acid, and a removal rate of 4,81 g<sub>SA</sub>/h. The feed flow in the fermenter was set to 1,49 ml/min; estimating a 5% more considering the 10 M NaOH to maintain the pH, the total amount of feed flow is 1,56 ml/min (0,094 L/h). Considering also an estimated concentration of S.A. of 15 g/L it's possible to calculate a productivity of 0,89 g<sub>SA</sub>/L/h and a production rate of 1,34 g<sub>S.A.</sub>/h. This value needs to be higher respect to the removal rate previously calculated, that was 4,81 g<sub>SA</sub>/h with 6 membrane layer. Dividing by 6 the removal rate, it's possible to estimate that every membrane layer can remove 0,8 g/h of succinic acid, whereas using 2 layers 1,6 g<sub>S.A.</sub> will be removed, that is higher of the estimated production rate (1,31 g<sub>S.A.</sub>/h). Thus, only one layer of membrane was used in the integrated experiment, in order to ensure that the production rate (1,31 g/h) is higher to the estimated removal rate (0,8 g/h), with an estimated water transport using one layer of 0,068 L/h.

In figure 5.45 is reported the final graph regarding the fermenter. “0” phase corresponds the batch phase, “1” corresponds to the continuous mode, and “2” represents the ED – coupled phase.

For the sake of clarity, only lactose (blue square), succinic acid (red triangles) and lactic acid (orange triangles) are reported. Moreover, in table 5.18, are summarized, the main operational parameters used in this experiment.

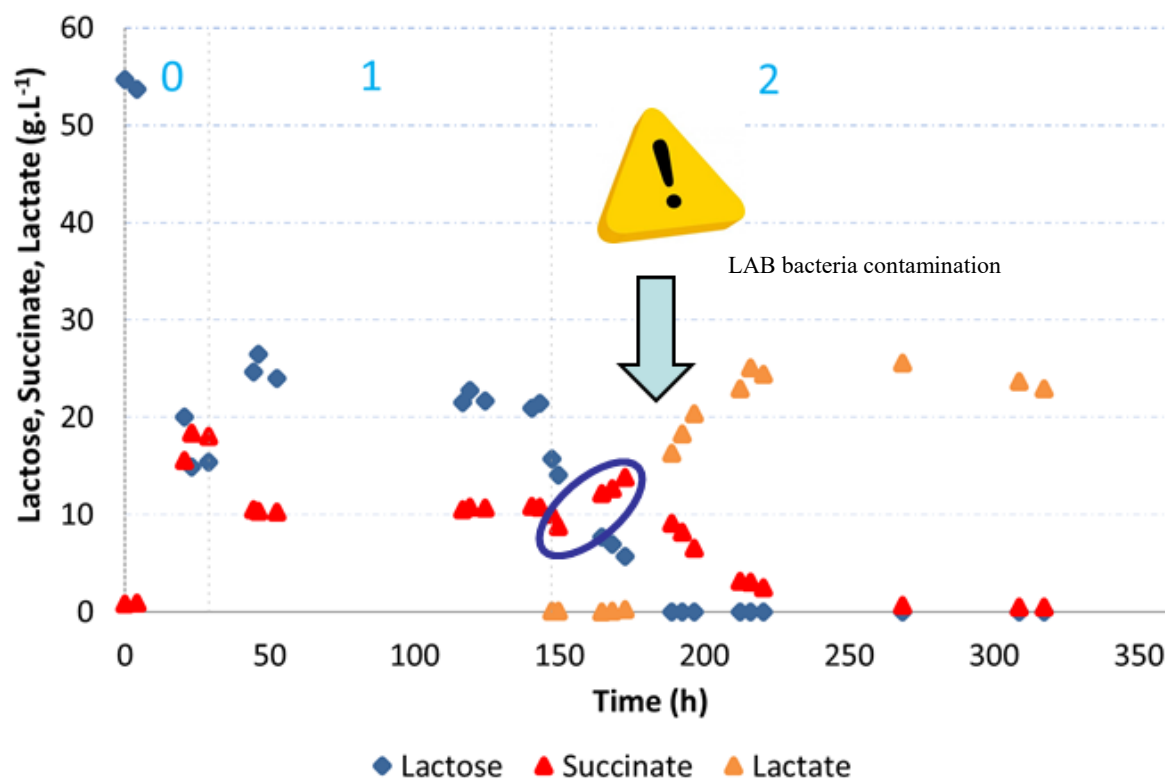


Figure 5.45: ED – coupled test. Fermentation results.

0	BATCH PHASE	54,7 g/L Lactose fed 18 g/L S.A achieved
1	CONTINUOUS PHASE	Feed flow 1,49 ml/min (Lactose 50 g/L) Residence time 16,8 h D (h <sup>-1</sup> ): 0,059 10 g/L S.A achieved
2	CONTINUOUS PHASE + ED COUPLING	Estimated “fouled stack” LCD: 0,94 A Estimated production rate fermenter (g <sub>SA</sub> /h): 1,31 Estimated removal rate stack (g <sub>SA</sub> /h): 0,8  Applied voltage: 4,2 V Resulting initial current: 0,78 A

Table 5.18: Main plant parameters during ED – coupled experiment

Unfortunately, after 41,42 hours of integrated tests (188,7 hours of total fermentation), a lactic acid bacteria (LAB) contamination was found in the plant. This is one of the major problem in these types of experiments. The contamination was confirmed through metagenomics analysis.

In figure 5.45, in fact, lactic acid was rapidly accumulated in the fermenter up to 25,28 g/L, at the expense of S.A., due to the higher growth velocity and high metabolic adaptability of the LAB

bacteria respect to *A. succinogenes* (Makarova, 2006). LAB, in fact, can win the competition with other type of microorganism also because they are able to produce different types of toxic peptides, as bacteriocins, that kills all the other microbial species in the environment (Parada, Caron, Medeiros, & Soccol, 2007).

Anyway, some interesting conclusion can be made looking to the behavior of the plant in the first 41,42 hours of integrated plant. Looking to the fermentation results in figure 5.45, in the blue circle is highlighted the increasing of the concentration of S.A. in the fermenter, from an average concentration of 10 g/L at the end of the continuous phase, to 12,83 g/L prior contamination, with an increment of 0,17 g/L/h ( $R^2 = 0,966$ ), and an estimated production rate of 1,33 g<sub>SA</sub>/h, that was absolutely in line with the value reported for the continuous phase. This is probably related to the in situ continuous removal of the product from the fermenter, and the consequent lower effect of product inhibition on the microorganism metabolism. Moreover, an increasing in the optical density (OD<sub>600 nm</sub>), passed from 5,95, to 6,71 can be another hint of the positive effect of this in situ product recovery effect. Lactose was consumed from 15,75 g/L to 5,72 g/L with an average consumption rate of 0,39 g/L/h.

In the next figure, the graph reports the trend in the ED plant during the coupled experiment:

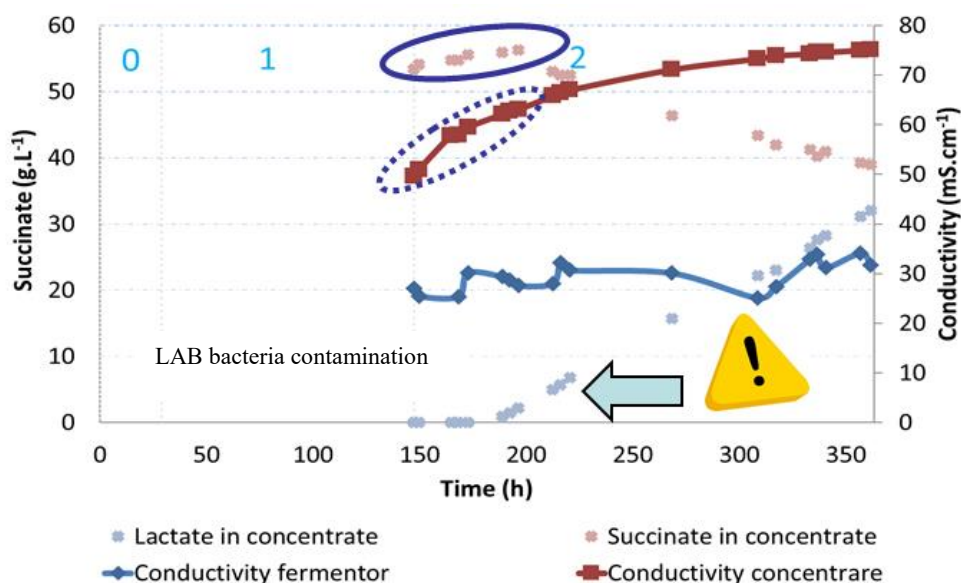


Figure 5.46: ED – coupled test. Electrodialysis plant results.

In this figure, pink cross represents the succinic acid concentration in the concentrate compartment, and red continuous line, the conductivity profile in the concentrate. Moreover, the dark blue continuous and dotted line highlights the hours of tests prior LAB contamination. Light blue cross are the symbols for lactic acid in the concentrate, whereas continuous blue line is the conductivity profile in the diluate / fermenter.

Prior contamination, the S.A. concentration increased in the concentrate compartment from an initial value of 53,36 g/L to 55,52 g/L, with a removal rate of 0,15 g<sub>SA</sub> / h, lower than the expected 0,8 g<sub>SA</sub> / h. This is confirmed from the low water transport, only 0,0008 L/h, respect to the estimated 0,068 L/h, probably due to a lower current efficiency. No pH variation was observed, and the current passed from the initial value of 0,74 A, to 0,71 after 44,41 hours with a final resistance value of 5,77  $\Omega$  through the stack, that was halved respect to the 10,8  $\Omega$  determined in the real separation offline test, again confirming a low current efficiency.

Obviously, during the LAB contamination, the lactic acid was transferred in the concentrate, and the S.A. was contemporary depleted due to the only lactic acid produced in the fermenter.

Regarding the fouling process, three LCD determination was performed, after 167,21 h (18 h of coupled test), after 215,07 h (65,5 hours of coupled test) and the third one after 311,23 h (260,62 hours of coupled test). During the first one, prior LAB contamination, the resulting LCD was 2,4 A with a succinic acid concentration in the diluate / fermenter of 12,2 g/L. According to table 5.17, with the real non centrifuged broth, a succinic acid concentration of 10,1 leads to a LCD value of 2,28 A, that is in line with this value. Thus, it's possible to estimate, that the fouling level is comparable between different integrated tests, and the LCD determination made with an offline test using real non centrifuged broth is reliable. The other two LCD value during LAB contamination were both 1,86 A, that are lower than the previous one, due to the higher fouling between the stack for the increased biomass quantity (OD<sub>600 nm</sub> more than 12 the end of the test), but besides the real current resulting through the stack. In fact, starting from 0,74 A, derived from a constant supply of 4,2 V, the current was kept for all the duration of the test below 0,8 A, adapting only the voltage



supply. The previous LCD tests, confirms that all the experiment was conducted below LCD limiting value.

It's possible to conclude that this direct ISPR process without cell retention is feasible, and represents a major innovation in this research field, strongly reducing complexity and costs. Prior contamination, in fact, the succinic acid was transferred from the fermenter to the concentrate, and this process improved the S.A. production in the fermenter, reducing product inhibition. The feasibility is also demonstrated from the fact that during the LAB contamination the lactic acid was anyway transferred from the diluate to the concentrate compartment.

It's evident that different parameters need to be optimized. In particular sterility of the ED plant is the major challenge. Besides that, transfer optimization, increase current efficiency, and limiting the fouling are other aspects that are suitable for a better and deep study.

## 5.5 SUCCINIC ACID – DICAM RESULTS

After the period at Flemish Institute For Technology (VITO), a strong collaboration was established between VITO and DICAM laboratory (Department of Civil, Chemical, Environmental, and Materials Engineering) in Bologna, in order to evaluate different aspect of the bioproduction of succinic acid. In this last part of the project (see section 4.7 and related sub – paragraph), a new procedure for biofilm fermentation was developed, screening different types of commercial carriers in order to statistically evaluate the best in terms of biofilm development and fermentation performances. Then, a kinetic approach was followed in order to estimate the principal kinetic parameters ( $\mu_{max}$  and  $K_s$ ) for the biofilm fermentation, using both pure lactose, both milk whey. Finally, a mini scale – up in 1 L column plant (PFR type) filled with the chosen carrier was developed, and preliminary studies were made to evaluate the performances in repeated batch experiments.

### 5.5.1 *Choosing the best carrier: screening and statistical evaluations*

As extensively described in section 4.7.2, five commercial carriers were purchased and used in *A. succinogenes* fermentation, in order to evaluate the biofilm development, and the succinic acid production using 116 ml microcosm tests. In table 4.24 and in figure 4.20 are reported and described the principal characteristics of each carrier. In the same section was also reported the detailed procedure, entirely developed in DICAM laboratory, for the biofilm development and subsequent bioproduction tests with only attached biomass.

In a preliminary phase, a triplicate test with suspended biomass, was performed, using 7 g/L as only carbon source, to avoid drastic pH reduction in the microcosms, following the test for 29,67 hours, sampling four times. The suspended tests were necessary in order to compare and assess the reliability of the fermentation process between DICAM and VITO laboratories (in terms of biomass growth, final S.A. concentration, and by – product amount).

The data is reported in the Appendix section (figure 7.3), and showed that S.A. production was comparable with the VITO batch test, and the same by – products as acetic and formic acids were founded, confirming the metabolic pathway of the bacterium, and the possibility to compare the DICAM results with VITO results.

Then, initial five different tests (conducted in triplicate, every triplicate for each carrier), were performed using the same lactose concentration (7 g/L) and followed for 29 hours sampling once an hour. With these tests the procedure for biofilm development was evaluated in terms of sterility and reliability, and a preliminary evaluation of the process was performed, considering the total fermentation time, or the amount of by - products. Each graph for each carrier is reported in the Appendix section, (figures 7.4 – 7.5 – 7.6 – 7.7 – 7.8) and is possible to make some preliminary conclusion.

- Each carrier leads to a biofilm formation, and a consequent lactose consumption and S.A. production.
- The biofilm is developed in the “biofilm growth phase” (see section 4.7.2). Only small amount of growth can be reported in the “bioproduction phase” (see section 4.7.2)

- The composition and stoichiometry of by – products are comparable with the suspended test conducted both at DICAM, both at VITO.
- Glucose is detected in negligible concentration for all the tests, thus is obvious to hypnotize that is consumed as soon as produced from the hydrolysis of lactose. This results fits perfectly with the VITO results, and confirms the idea that the lactose hydrolysis is the slow step of the overall bioconversion.
- Galactose is accumulated (as also reported in batch VITO fermentation), confirming the diauxic behavior, and is only consumed when lactose concentration leads to zero.
- Interestingly short lag phase respect to the 8 hours of VITO suspended test was observed, from 0 to maximum 2 hours in the worst case. If confirmed, this is a huge improvement of the process. Conflicting and no clear evidences are reported in literature regarding the connection between biofilm development and lag phase, and only some speculations were made. Prieto MB, 2002, in fact, speculates that immobilization technology can help microorganism to resist the inhibition from the toxic substrates or products and decrease the lag phase. This results are confirmed by Ming-Der Bai, 2008 that reports a 65% - 70% lag phase reduction in batch biohydrogen production tests using immobilized cells. Moreover, using *L. casei* for lactic acid production using attached cells on PCS – Plastic Composite Supports, also Kai-Lai G. Ho, 1997 reports a lag phase reduction from c.a 5 hours, to c.ca 1 hour. Anyway, no clear explanations were provided.

Qualitatively assessed that all the supports lead to a biofilm development, and to succinic acid production, to start a quantitative evaluation of each carrier, the first step in to determine the absolute velocity of lactose consumption ( $-r_{Lac}$ ) and succinic acid production ( $r_{SA}$ ) that are represented from the slope of the linear part (first 9 hours of tests) of the previous graphs (substrate and product concentration in function of time) reported in the Appendix section. Figure 5.47, reports the slope of the linear part of those graphs in terms of lactose consumption and succinic acid production, whereas in table 5.19 are highlighted the numerical value of the slope (g/L/h), that are the production – consumption rate, and their ratio, that represent the  $g_{SA} / g_{Lac}$ , together with the maximum S.A. concentration reached at the end of the fermentation tests

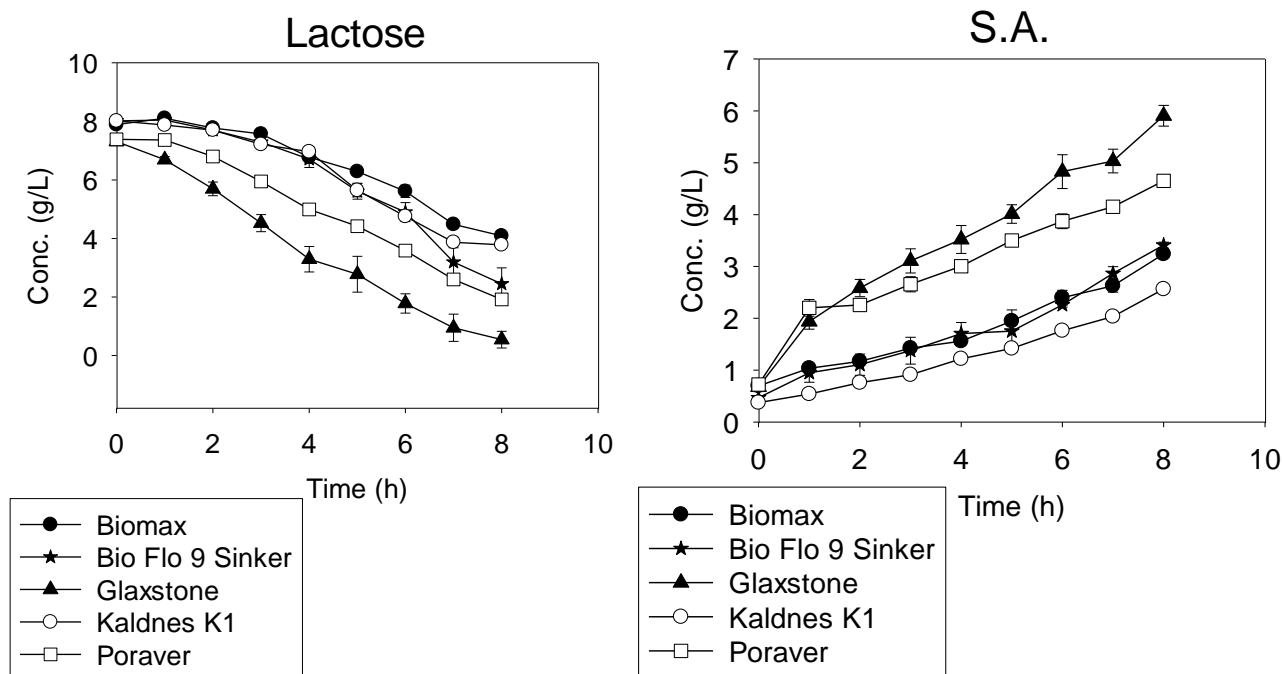


**Figure 5.47:** Absolute velocity graph of lactose consumption and succinic acid production for each carrier with attached biomass

	$r_{Lac}$ ( $g\ L^{-1}\ h^{-1}$ )	$r_{SA}$ ( $g\ L^{-1}\ h^{-1}$ )	$r_{SA}/-r_{Lac}$ ( $g_{SA}\ g_{Lac}^{-1}$ )	Final S.A. concentration ( $g\ L^{-1}$ )
<b>Biomax ®</b>	$-0,71 \pm 0,05$	$0,30 \pm 0,01$	0,42	$5,82 \pm 0,06$
<b>Kaldnes K1 ®</b>	$-0,80 \pm 0,04$	$0,26 \pm 0,01$	0,33	$4,83 \pm 0,22$
<b>Bio-Flo 9 Sinker ®</b>	$-0,73 \pm 0,07$	$0,34 \pm 0,01$	0,47	$5,47 \pm 0,48$
<b>Poraver ®</b>	$-0,82 \pm 0,06$	$0,39 \pm 0,01$	0,48	$5,82 \pm 0,17$
<b>Glaxstone ®</b>	$-0,94 \pm 0,13$	$0,54 \pm 0,01$	0,57	$6,72 \pm 0,15$

**Table 5.19:** Absolute velocity values of lactose consumption and succinic acid production for each carrier with attached biomass.

Firstly, it's important to underline that the S.A. yields are comparable, or higher (in the case of Glaxstone ®) respect to the value reported in section 5.4.1 for a single suspended batch test.

From a simple preliminary analysis seems that in absolute terms, Poraver ® and Glaxstone ® reports higher lactose consumption rates and higher final S.A. concentrations.

To statistically confirm this speculation, an ANOVA test, followed by a t – test, were performed:

## ➤ ANOVA

The analysis of variance (ANOVA) of the desired parameters (absolute velocities in this case) was performed with a significance level of 0,05 to the ratio  $s^2_{between}/s^2_{within}$  where  $s^2_{between}$  is the variance between the screening carrier experiments and  $s^2_{within}$  instead is the variance within each triplicate. The test was applied with  $k-1$  degrees of freedom for  $s^2_{between}$ , and with  $2k$  for  $s^2_{within}$  (DF\_within);  $k$  is the number of screened carriers.

As every hypothesis test, the main idea is to compare the “null” hypothesis (as the difference of the average values needs to be ascribed to a small and unavoidable fluctuation in the experimental conditions between one measure and the next one), with the hypothesis that the difference of the average values is related instead to the diversity of the used carriers. The result of the test is a measure of the probability to observe the examined difference assuming that is true the hypothesis that the analyzed cases are not different. If the value of this probability is lower respect to the significance level (5% in this case), rather than believe that a rare event is observed and ascribed the difference to a statistical fluctuation, the difference is attribute to the diversity of the tested carriers.

In this case, if the results of the test lead to refuse the hypothesis of the equality of the average value, another statistical analysis was performed in order to compare all the possible couple of values to identify possible “statistical cluster carriers” that are not significantly different between them. Every comparison is a t – test (see later) performed with a significance level of  $0,05/n$  where  $n$  is the number of the comparison made (10 in this case).

In the following table, the ANOVA results are reported:

	DF between	DF Within	S <sup>2</sup> between	S <sup>2</sup> within	$s^2_{between}/s^2_{within}$	P – value	Significance level	Results
r <sub>SA</sub>	4	10	3,6E-02	1,2E-04	3,1E+02	2,0E-10	0,05	Statistically different
r <sub>Lac</sub>	4	10	5,1E+00	2,1E+00	2,5E+00	1,1E-01	0,05	Not statistically different

**Table 5.20:** ANOVA test for the absolute velocity of lactose consumption and succinic acid production.

The  $p$  – value (the probability to observe at least the difference between the reported average values), is the result of the test. If this probability is lower respect the significance level, the hypothesis of the equality of the average values of the velocities observed is refused, considering these value statistically different. This is the case of the absolute velocity of succinic acid production ( $r_{SA}$ ).

For the lactose consumption velocity, instead, the  $p$  – value is higher respect the significance level. In this case the probability that the “null” hypothesis is true (in this case that the performance of the biomass doesn’t affect each carrier) is higher than 0,05 and the velocity values are considered not statistically different.

For this reason, the main parameter considered for the choice of the best carrier was the S.A. production rate, and a  $t$  – test was performed.

➤  $T$  – test

The  $t$  – test was performed in order to compare the 10 possible carrier couple on the basis of S.A. production rate, see results in table 5.21:

<i>Significance level: 0,05/10</i>	<b>Kaldnes K1</b>	<b>Bio-Flo 9 Sinker</b>	<b>Poraver</b>	<b>Glaxstone</b>
<b>Biomax</b>	1,5E-02 *	2,0E-02 *	7,8E-04	2,2E-05
<b>Kaldnes K1</b>		3,4E-04	4,5E-05	2,9E-06
<b>Bio-Flo 9 Sinker</b>			2,5E-03	2,0E-05
<b>Poraver</b>				8,4E-05

**Table 5.21:**  $T$  - test results considering only the succinic acid production rates.

The couple marked with an asterisk (Biomax ® - Kaldnes K1 ® and Biomax ® - Bio Flo 9 Sinker) are not statistically different, whereas all the other couple can be considered statistically different.

The carriers that (according to table 5.19) showed the higher S.A. velocity value were Glaxstone ®, Poraver ® and Bio Flo 9 Sinker ® (that is not statistically different from Biomax ®).

In order to choose the best carrier, also the final concentration of succinic acid achieved (reported in the last column of table 5.19) was considered, and the three higher concentrations were achieved in the experiments with Glaxstone ®, Poraver ® and Biomax ®.

After these consideration, from now, only Glaxstone ®, Poraver ® and Biomax ® were considered. For sure, is not a coincidence that both of the HDPE (High Density Poly Ethylene) carriers were excluded; probably this material is not suitable for the immobilization of *A. succinogenes*.

In all of the previous test regarding the absolute velocity, no attention was paid to the distinction between suspended and attached biomass. In fact, the velocity performance can be ascribed to the sum of the contribution of both attached and both suspended biomass. However, this represent a key parameter in order to establish which is the best carrier. For this reason, in each of the three carriers (Glaxstone ®, Biomax ® and Poraver ®) the Lowry's method was used in order to estimate the biomass concentration. Three types of biomasses were categorized: “suspended biomass”, “strongly attached biomass” and “weakly attached biomass” (see section 4.8.4 for the description). The weakly biomass can be imagined as the biomass present in external dynamical part of the biofilm at the interface between liquid and solid carrier material, that can be removed with a little increasing of the turbulence or variation in shears stress. Practically, this biomass is derived from the preliminary wash of the carrier with 7 ml of NaCl 0,9% solution for 1 hour at 90 rpm/min stirring at room temperature. In the next graph, and table is reported the trend in the biomass composition:

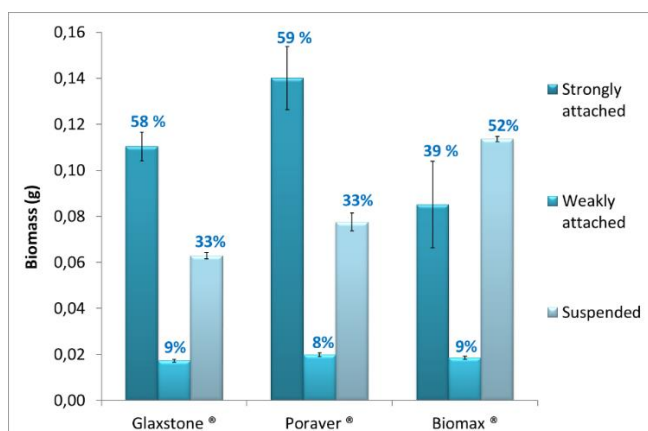


**Figure 5.48:** Biomass composition graph (in grams) for Biomax ®, Poraver ®, and Glaxstone ®.

	Strongly attached biomass (grams)	Weakly attached biomass (grams)	Suspended biomass (grams)
<b>Biomax ®</b>	0,11 ± 0,01	0,0173 ± 0,0007	0,063 ± 0,001
<b>Poraver ®</b>	0,14 ± 0,01	0,0198 ± 0,0008	0,078 ± 0,004
<b>Glaxstone ®</b>	0,085 ± 0,019	0,0185 ± 0,0007	0,114 ± 0,001

**Table 5.22:** Biomass composition table (in grams) for Biomax ®, Poraver ®, and Glaxstone ®.

From graph in figure 5.48 and related table, it's evident that Glaxstone ® and Poraver ® supports lead to a similar biomass composition (c.ca 60% of strongly attached, c.ca 30% of suspended and c.ca 10% of weakly attached), whereas Biomax ® results are completely opposite. The large amount of biomass is suspended (more than c.ca 50%), and only less than c.ca 40% was strongly attached. Instead, the percentage of weakly attached biomass was constant, about 10%.

For this reason, Biomax ® was excluded, and the kinetic study was performed only with Glaxstone ® and Poraver ® supports.

### 5.5.2 Poraver ® or Glaxstone ®? Monod model with lactose

In the previous paragraph, Glaxstone ®, Poraver ®, were selected as most suitable candidate for biofilm growth. For both of them, a kinetic study in order to determine the kinetic parameters  $\mu_{max}$  and  $K_S$  with lactose as only carbon source was performed. With this quantitative results, the best carrier was chosen, and the same kinetic study was repeated using milk whey as substrate.

To estimate the kinetic parameters, the “initial velocity method” was applied. Different substrate concentrations were tested in the bioproduction phase, in order to determine the initial absolute velocities of substrate consumption and S.A. ( $r_{Lac}$ ,  $r_{SA}$ ). From these values, the specific velocities were calculated for lactose ( $q_{Lac}$ ) and S.A. ( $q_{SA}$ ) making the ratio between absolute velocity and biomass quantity (X) estimated by Lowry's method. At this point, the tested concentrations (reported in table 4.26 – section 4.7.3), were plotted in function of the initial specific velocity ( $q_{Lac}$ ,  $q_{SA}$ ), and related



with a Monod model, using a best-fit procedure minimizing the mean square deviation for every parameter.

Similarly to the previous experiment, only the linear part of the reaction was considered in the determination of the absolute velocity. Besides that, in the determination of the specific velocity, the absolute velocity (calculated as the slope of the linear part of the time/concentration graph of lactose consumption or S.A. production), needs to be divided by the biomass value. Anyway, differently from the suspended biomass tests, with attached biomass only a small cell growth was detected in the bioproduction phase (see Appendix graphs). For this reason, a medium value between the initial and the final biomass was chosen for the calculation of the specific velocities. Moreover, the total initial and final biomass values were considered (as the sum of suspended, weakly attached and strongly attached) to make the average, supposing that all the biomass typology shares the same kinetic behavior.

In the same manner as before with 7 g/L as initial lactose concentration, in the following table (5.23), are reported the values of the absolute velocities of lactose consumption and S.A. production ( $r_{Lac}$ ,  $r_{SA}$ ), interpolated from the slope of the linear part of each time/concentration graphs. (See Appendix section figures 7.9 – 7.10 – 7.11 – 7.12 + figure 5.48 for 7,3 g/L concentration for Glaxstone ®. See Appendix section figures 7.13 – 7.14 – 7.15 – 7.16 + figure 5.48 for 7,3 g/L concentration for Poraver ®).

	S.A.		Lactose		
Lactose conc. (g L <sup>-1</sup> )	Slope (g L <sup>-1</sup> h <sup>-1</sup> )	St. dev (g L <sup>-1</sup> h <sup>-1</sup> )	Slope (g L <sup>-1</sup> h <sup>-1</sup> )	St. dev (g L <sup>-1</sup> h <sup>-1</sup> )	r <sub>SA</sub> / <b>-r<sub>Lac</sub></b> (g <sub>SA</sub> g <sub>Lac</sub> <sup>-1</sup> )
<b>Glaxstone ®</b>					
<b>1,8</b>	0,15	0,00	-0,36	0,02	0,42
<b>2,4</b>	0,13	0,04	-0,39	0,02	0,33
<b>4,7</b>	0,42	0,03	-0,62	0,01	0,68
<b>7,3</b>	0,54	0,01	-0,94	0,13	0,57
<b>9,3</b>	0,48	0,03	-0,86	0,10	0,56
<b>11,5</b>	0,45	0,02	-0,91	0,06	0,49
<b>Poraver ®</b>					
<b>2,2</b>	0,02	0,01	-0,24	0,03	0,08
<b>4,6</b>	0,39	0,01	-0,64	0,07	0,61
<b>7,4</b>	0,39	0,01	-0,82	0,06	0,48
<b>9,4</b>	0,37	0,07	-0,70	0,04	0,53
<b>11,7</b>	0,36	0,02	-0,65	0,06	0,55

**Table 5.23:** Absolute velocities (slope) values of lactose consumption and succinic acid production for Glaxstone ® and Poraver ® with different lactose concentrations using attached biomass.

Looking at the table, comparing the absolute velocity (slope) of S.A. production is evident that for all the tested concentrations, the values for Glaxstone ® are higher respect to the value determined for Poraver ®. This can be a preliminary hint that can focus the attention more on Glaxstone ® support respect to the Poraver ®. Anyway, it's necessary to consider also the biomass values, in order to definitively develop a kinetic model, and thus, choose the best carrier. In the next table, the biomass values (expressed in g/L) are reported for each lactose concentrations both for Glaxstone ® and both for Poraver ®. In blue are highlighted the average values used for the calculation of specific velocities.

<b>Lactose conc.</b> (g L <sup>-1</sup> )	<b>Initial total biomass</b> (g L <sup>-1</sup> )	<b>Initial total biomass error</b> (g L <sup>-1</sup> )	<b>Final total biomass</b> (g L <sup>-1</sup> )	<b>Final total biomass error</b> (g L <sup>-1</sup> )	<b>Average biomass</b> (g L <sup>-1</sup> )	<b>Average biomass error</b> (%)	<b>Growth variation</b> (%)
<b>Glaxstone ®</b>							
<b>1,8</b>	2,07	0,23	2,92	0,31	<b>2,49</b>	11%	41%
<b>2,4</b>	2,66	0,11	2,73	0,17	<b>2,69</b>	5%	3%
<b>4,7</b>	2,45	0,10	2,01	0,15	<b>2,23</b>	5%	39%
<b>7,3</b>	2,44	0,00	3,28	0,13	<b>2,86</b>	2%	-18%
<b>9,3</b>	2,42	0,21	3,06	0,93	<b>2,74</b>	21%	35%
<b>11,5</b>	2,55	0,21	2,77	0,40	<b>2,66</b>	11%	26%
<b>Poraver ®</b>							
<b>2,2</b>	2,02	0,20	4,32	1,40	<b>3,17</b>	25%	114%
<b>4,6</b>	1,94	0,20	5,31	0,88	<b>3,62</b>	15%	173%
<b>7,4</b>	2,16	0,21	4,44	0,34	<b>3,30</b>	8%	106%
<b>9,4</b>	1,87	0,20	3,26	0,53	<b>2,57</b>	14%	74%
<b>11,7</b>	1,85	0,20	3,69	0,80	<b>2,77</b>	18%	99%

**Table 5.24:** Biomass values (g/L) for Poraver ®, and Glaxstone ® with different lactose concentrations. The values are the sum of strongly attached, weakly attached and suspended

A particularly behavior can be noticed. In the bioproduction phase using Glaxstone ®, small amount of growth is detected, with an average difference percentage value of 19%. With Poraver ® instead, a huge increasing of the total biomass was detected for all lactose concentration between the initial and final time, with an average increasing of 113%. No explanations were given for this trend, probably the biofilm dynamics and the interactions between material support and biofilm are involved.

Making the ratio between the absolute velocities of lactose consumption and S.A. production (g/L/h) with the biomass values (g/L), the specific velocities (h<sup>-1</sup>) were obtained (q<sub>Lac</sub>, q<sub>SA</sub>).

Those values were plotted in function of the used lactose concentration, and related to a Monod model with a best fit for the minimization of the main square error for this equation:

$$q = q_{max} \frac{S}{k_s + S}$$

In the next table are reported the specific velocities (with their percentage errors), for lactose consumption and S.A. production for both Glaxstone ® and Poraver ®

Lactose conc. (g L <sup>-1</sup> )	q <sub>Lac</sub> (h <sup>-1</sup> )	q <sub>Lac</sub> err (%)	q <sub>SA</sub> (h <sup>-1</sup> )	q <sub>SA</sub> err (%)
<b>Glaxstone ®</b>				
1,8	0,14	15%	0,06	14%
2,4	0,30	31%	0,07	20%
4,7	0,28	7%	0,19	13%
7,3	0,33	16%	0,19	4%
9,3	0,31	33%	0,17	27%
11,5	0,34	18%	0,17	15%
<b>Poraver ®</b>				
2,2	0,08	39%	0,01	40%
4,6	0,18	25%	0,11	27%
7,4	0,25	15%	0,12	16%
9,4	0,27	20%	0,15	27%
11,7	0,23	27%	0,13	29%

**Table 5.25:** Specific velocity values of lactose consumption and succinic acid production for Glaxstone ® and Poraver ® with different lactose concentrations using attached biomass.

And in the following graphs, are reported the interpolation with the Monod model:

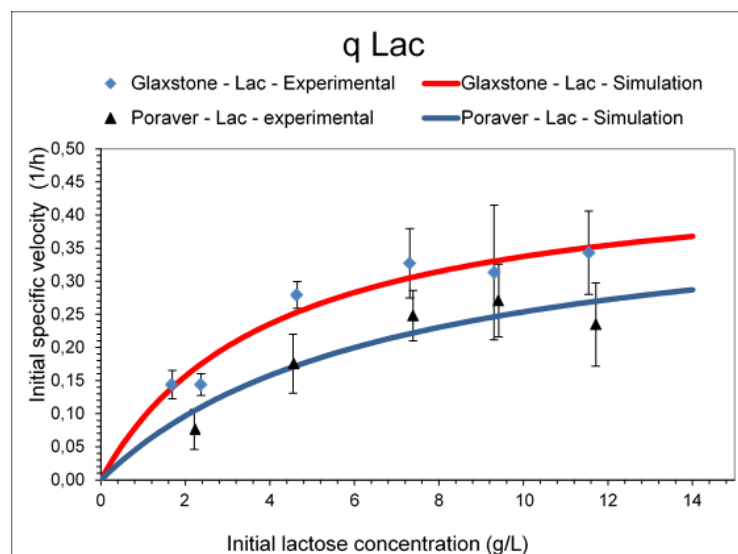


**Figure 5.49:** Interpolation with the Monod model for the substrate of Poraver ®, and Glaxstone ®

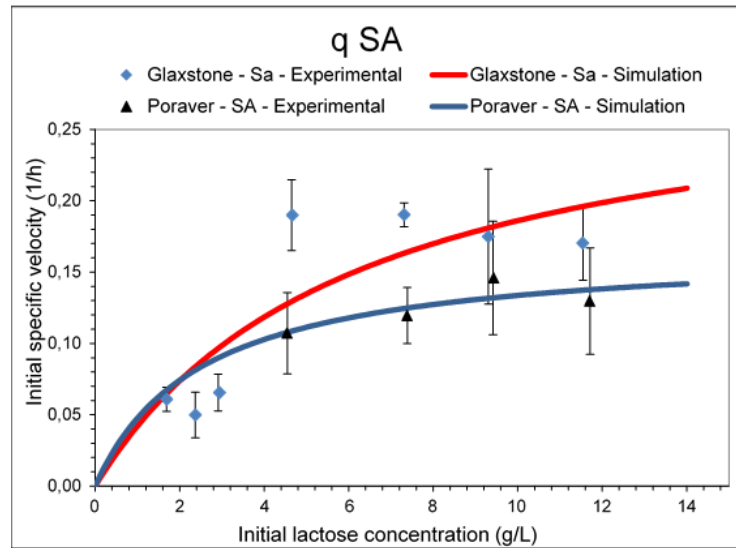


**Figure 5.50:** Interpolation with the Monod model for the product of Poraver®, and Glaxstone®.

Figure 5.49 reports the interpolation results for lactose. In blue square and in black are evident the experimental points for Glaxstone® and Poraver® respectively, whereas the red (for Glaxstone®) and blue (for Poraver®) lines are the interpolation with the model. Same scheme was adopted for the interpolation of S.A. To complete the analysis, in table 5.26 are reported the estimated  $\mu_{\max}$  and  $K_s$  with their error for both the carriers:

	$\mu_{\max}$ ( $h^{-1}$ )	$\mu_{\max}$ st. error	$K_s$ (g/L)	$K_s$ st. error	Correlation
<b>Glaxstone®</b>					
<b>q<sub>Lac</sub></b>	0,474	0,06	4,050	1,28	0,94
<b>q<sub>SA</sub></b>	0,300	0,13	6,135	5,92	0,97
<b>Poraver®</b>					
<b>q<sub>Lac</sub></b>	0,427	0,14	6,831	5,03	0,98
<b>q<sub>SA</sub></b>	0,167	0,03	2,506	1,95	0,97

**Table 5.26:**  $\mu_{\max}$  and  $K_s$  estimation for Poraver® and Glaxstone® for both substrate and product using lactose for both carriers.

From all these results different types of conclusions can be made. The Monod model is a good model for these data range, because fits with a higher correlation values. Besides that, from the last table it's

possible to notice that the standard error for  $\mu_{\max}$  is relatively small, because the asymptotic values of the curves are evident in the graphs. This is due to the large number of tests performed with high substrate concentrations, that gave good specific velocity results that are in proximity of the  $\mu_{\max}$  value. This results are in according with the hypothesis that for the most of the time the trends in function of time are linear, that means a zero order for the large parts of the reaction. For the same reason  $K_s$  is affected by a large standard error, due to small amount of experiments conducted with low substrate concentration (in particularly with Poraver®).

Besides this data, it's possible to affirm that with this quantitative analysis, in the same conditions, the specific velocities observed with Glaxstone® are higher respect to the values detected with Poraver®, both in terms of lactose consumption, both in terms of S.A. production. For this reason, Glaxstone® was chosen as the definitive support for the subsequent kinetic tests with milk whey, and the preliminary experiments in the 1 L plant.

### 5.5.3 *Monod model with milk whey*

After the identification of the best carrier for biofilm development, Glaxstone® was used to perform another kinetic study to estimate the kinetic parameters with the “initial velocity method” using milk whey as substrate (milk whey characteristics are described in section 4.1.2). Besides the objective to determine the kinetic parameters, in this case a higher lactose concentration was tested, to evaluate some substrate or product inhibition, for the subsequent plant tests. Again, different substrate concentrations were tested in the bioproduction phase, in order to determine the initial absolute velocities of substrate consumption and S.A. ( $r_{\text{Lac}}$ ,  $r_{\text{SA}}$ ). From these values, the specific velocities were calculated for lactose ( $q_{\text{Lac}}$ ) and S.A. ( $q_{\text{SA}}$ ) making the ratio between absolute velocity and biomass quantity ( $X$ ) estimated by Lowry's method. At this point, the tested concentrations (reported in table 4.26 – section 4.7.3), were plotted in function of the initial specific velocity ( $q_{\text{Lac}}$ ,  $q_{\text{SA}}$ ), and related with a Monod model, using a best-fit procedure minimizing the mean square deviation for every parameter. Similarly to the previous experiment, only the linear part of the reaction

was considered in the determination of the absolute velocity, and the average total biomass values were used in the calculations of the specific velocities. In the Appendix section, the starting graphs (concentration/time) of both lactose consumption and both succinic acid production were reported. In the same manner of the results exposed in table 5.23 for lactose as substrate tested with Poraver<sup>®</sup> and Glaxston<sup>®</sup>, in the following table (5.27), are reported the values of the absolute velocities of milk whey consumption and S.A. production ( $r_{\text{Milk whey}}$ ,  $r_{\text{SA}}$ ), interpolated from the slope of the linear part of each time/concentration graphs (see Appendix section figures 7.17 – 7.18 – 7.19 – 7.20 and 7.21).

	<b>S.A.</b>		<b>Equivalent lactose</b>		
<b>Lactose equivalent conc. in milk whey</b> (g L <sup>-1</sup> )	Slope (g L <sup>-1</sup> h <sup>-1</sup> )	St. dev (g L <sup>-1</sup> h <sup>-1</sup> )	Slope (g L <sup>-1</sup> h <sup>-1</sup> )	St. dev (g L <sup>-1</sup> h <sup>-1</sup> )	<b><math>r_{\text{SA}}/-r_{\text{Milk whey}}</math></b> (g <sub>SA</sub> g <sub>Lac</sub> <sup>-1</sup> )
<b>Glaxstone<sup>®</sup></b>					
<b>1,8</b>	0,36	0,08	-0,44	0,08	0,81
<b>5,5</b>	0,33	0,03	-0,59	0,05	0,56
<b>8,6</b>	0,30	0,07	-0,57	0,18	0,53
<b>11,8</b>	0,58	0,05	-1,08	0,37	0,54
<b>14,7</b>	0,56	0,03	-1,05	0,13	0,53

**Table 5.27:** Absolute velocities (slope) values of lactose consumption and succinic acid production for Glaxstone<sup>®</sup> with different lactose equivalent concentrations present in milk whey, using attached biomass.

Comparing the absolute velocities (slope) of S.A. production and lactose consumption of Glaxstone<sup>®</sup> biofilm fermentation using milk whey (this table) and lactose (table 5.23) is evident that no differences (net to the standard deviations) were detected for all the similar tested concentrations. Moreover, increasing the equivalent lactose concentrations from 11,8 g/L to 14,7 g/L, the absolute velocities remained stable, both for lactose consumption both for milk whey, suggesting that the asymptotic zone of the Monod model was reached.

In order to evaluate the specific velocity, in the next table, the biomass values (expressed in g/L) are reported for each lactose concentrations both for Glaxstone ® and both for Poraver ®. In blue are highlighted the average values used for the calculation of specific velocities (see later).

<b>Lactose equivalent conc. in milk whey</b> (g L <sup>-1</sup> )	<b>Initial total biomass</b> (g L <sup>-1</sup> )	<b>Initial total biomass error</b> (g L <sup>-1</sup> )	<b>Final total biomass</b> (g L <sup>-1</sup> )	<b>Final total biomass error</b> (g L <sup>-1</sup> )	<b>Average biomass</b> (g L <sup>-1</sup> )	<b>Average biomass error</b> (%)	<b>Growth variation</b> (%)
<b>Glaxstone ®</b>							
<b>1,8</b>	6,34	1,40	10,77	2,42	<b>8,55</b>	22%	70%
<b>5,5</b>	6,63	1,38	11,56	2,55	<b>9,09</b>	21%	74%
<b>8,6</b>	6,54	1,23	12,75	3,24	<b>9,65</b>	19%	95%
<b>11,8</b>	8,23	2,73	11,56	2,61	<b>9,89</b>	33%	40%
<b>14,7</b>	8,61	2,71	10,88	2,72	<b>9,74</b>	32%	26%

**Table 5.28:** Biomass values (g/L) for Poraver ®, and Glaxstone ® with different lactose concentrations. The values are the sum of strongly attached, weakly attached and suspended

Comparing this table with the table 5.24 where are reported the biomass data using pure lactose using Glaxstone ® as carrier, is evident that this values are higher. In fact, comparing the similar lactose concentrations (e.g. 1,8 g/L for both tests, and 11,5 g/L with pure lactose / 11,8 g/L with equivalent lactose), the resulting biomass are completely different. With 1,8 g/L of pure lactose an average value of 2,49 g/L ± 11% of total biomass was reached, whereas using 1,8 g/L of equivalent lactose in milk whey, an average value of 8,55 g/L ± 22% was obtained. Same trend for the 11,5 g/L of pure lactose that leads to an average biomass of 2,66 g/L ± 11%, respect to 11,8 of equivalent lactose in milk whey that reported 9,74 g/L ± 32%. It's possible to speculate that other elements present in milk whey (as proteins, nitrogen and phosphorous compounds, see table 4.5), can leads to a beneficial effect on the microorganism.



Making the ratio between the absolute velocities of equivalent lactose consumption and S.A. production (g/L/h) with the biomass values (g/L), the specific velocities ( $h^{-1}$ ) were obtained ( $q_{\text{Milk whey}}$ ,  $q_{\text{SA}}$ ).

Those values were plotted in function of the used lactose concentration, and related to a Monod model with a best fit for the minimization of the main square error for this equation, in the same manner as made for pure lactose:

$$q = q_{\max} \frac{S}{k_s + S}$$

In the next table are reported the specific velocities (with their percentage errors), for equivalent lactose consumption and S.A. production using Glaxstone ® as carrier.

Lactose equivalent conc. in milk whey ( $g L^{-1}$ )	$Q_{\text{Milk whey}}$ ( $h^{-1}$ )	$Q_{\text{Milk whey err}}$ (%)	$q_{\text{SA}}$ ( $h^{-1}$ )	$q_{\text{SA err}}$ (%)
<b>Glaxstone ®</b>				
<b>1,8</b>	0,05	22%	0,04	31%
<b>5,5</b>	0,06	23%	0,04	23%
<b>8,6</b>	0,06	36%	0,03	29%
<b>11,8</b>	0,11	48%	0,06	34%
<b>14,7</b>	0,11	34%	0,06	32%

**Table 5.29:** Specific velocity values of equivalent lactose consumption and succinic acid production for Glaxstone ® with different equivalent lactose concentrations using attached biomass.

Comparing to table 5.25 (where are reported the same specific velocities for pure lactose), these values are lower, because starting from a similar absolute velocity, divided for a higher biomass quantity (see previous table), the resulting specific velocities are obviously lower.

In the following graphs, are reported the interpolation with the Monod model:

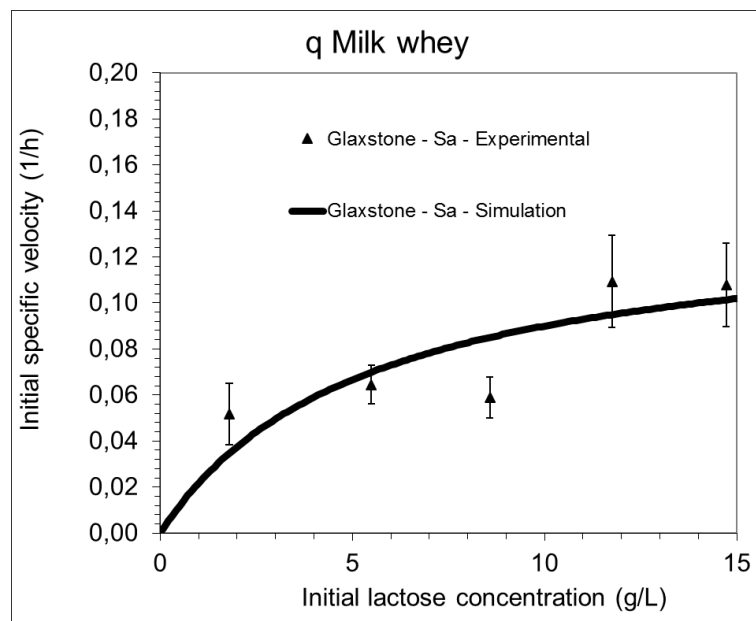


**Figure 5.51:** Interpolation with the Monod model for the substrate (milk whey) using Glaxstone® as carrier

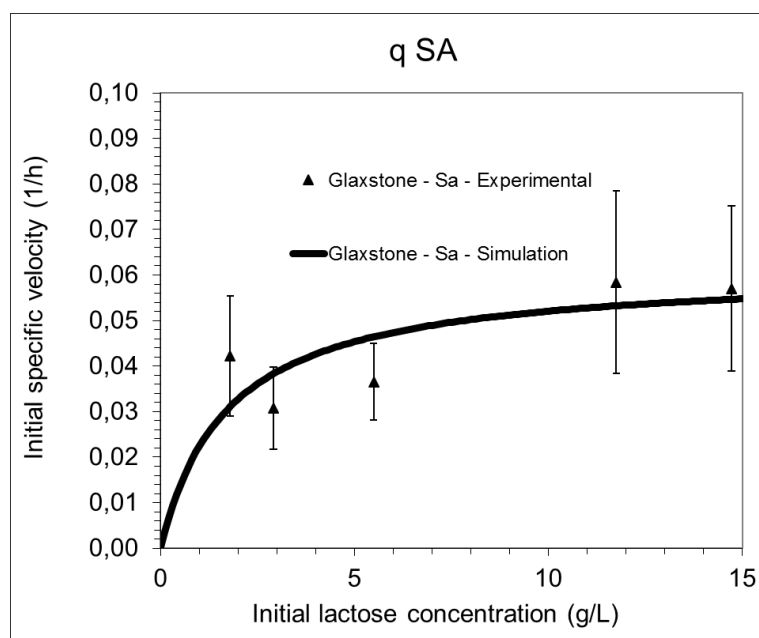


**Figure 5.52:** Interpolation with the Monod model for the product using milk whey and Glaxstone® as carrier.

Figure 5.51 reports the interpolation results for the equivalent lactose concentrations present in milk whey. In black triangles are evident the experimental points, whereas the black lines are the interpolation with the model. Same scheme was adopted for the interpolation of S.A. To complete the analysis, in table 5.30 are reported the estimated  $\mu_{max}$  and  $K_S$  with their error for both the carriers:

	$\mu_{\max}$ ( $h^{-1}$ )	$\mu_{\max}$ st. error	$K_s$ (g/L)	$K_s$ st. error	Correlation
<b>Glaxstone ®</b>					
<b>qMilk whey</b>	0,138	0,111	5,37	11,75	0,96
<b>qSA</b>	0,061	0,025	1,73	3,23	0,85

**Table 5.30:**  $\mu_{\max}$  and  $K_s$  estimation for Glaxstone ® for both substrate and product using equivalent lactose in milk whey.

Comparing this table with the table 5.26, that estimates the same value using the same carrier for pure lactose, it's evident that this values are lower, that is in according for the utilization of a by – product and not a pure sugar. Anyway, the higher errors that affect these measure, require a deep study, in particularly using low milk whey concentrations in order to better estimate the  $K_s$ .

Anyway, looking to these data, no inhibition seems to be reported using high lactose concentrations, up to c.ca 15 g/L, that is in according with the VITO results, where batch fermentations were conducted using 50 g/L of lactose in the feed, both using pure sugars, both using equivalent lactose derived from milk whey.

#### 5.5.4 Biofilm plant: preliminary results with repeated batch tests

In the last phase of this project, a 1 L plant was developed as a PFR column type, as extensively described in section 4.7.1. The column was packed with Glaxstone ®, (the chosen carriers that leads to higher fermentation performances in the previous microcosm tests), sterilized, vacuumed and connected to the plant.

This bioreactor operated in condition of “perfectly mixed phase” as extensively detailed in section 4.7.4. For this reason, a preliminary fluidodynamic test was executed in order to determine the filling time of the vacuum – packed column ( $\tau_{\text{column}}$ ). This value represents, the minimum amount of time necessary to change completely the medium inside the PFR. As already detailed, a perfectly mixed phase is defined when the total residence time of the plant (HRT), is, at least, 1 order of magnitude less of the characteristic time of the reaction (Fogler, 2014). In this experiment, the characteristic time

of the reaction was considered when the 75% of lactose conversion to S.A. was reached in the microcosms tests with Glaxstone ® and pure lactose 7 g/L. Assuming that the ratio between the liquid volume in the column and the liquid volume in the bottle (considering negligible the dead volume of the tubes) will be 1,5, it's possible to estimate the column residence time ( $HRT_{column}$ ) as the ratio between  $1/10$  characteristic reaction time / 1,5. Dividing the total liquid volume in the column and the estimated  $HRT_{column}$ , the desired minimum flow rate to obtain a perfected mixing phase in the glass column, was calculated.

In figure 5.53, the results of the fluidodynamic test are reported:

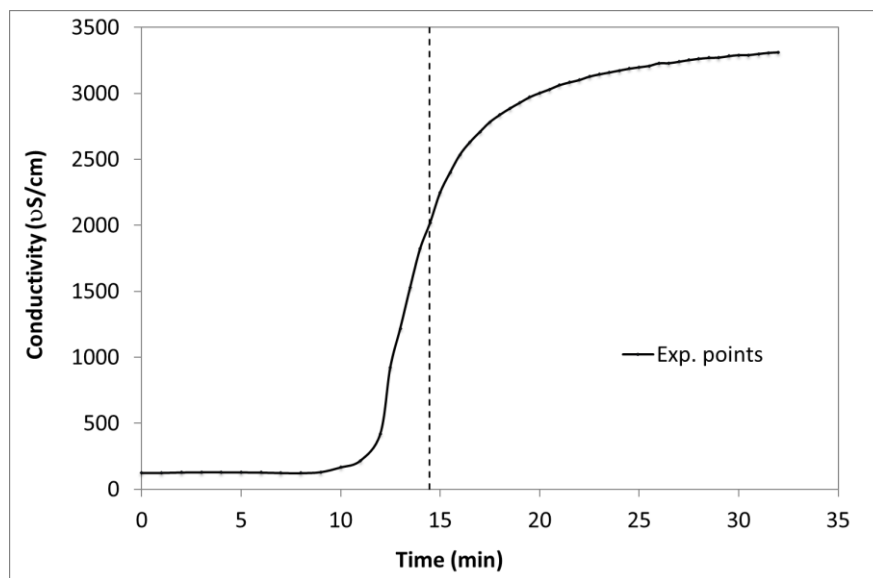


**Figure 5.53:** Fluidodynamic test results of the 1 L column plant vacuum – packed with Glaxstone ®.

From the reported dotted black line, the characteristic  $\tau$  time of this plant is 14,8 minute. From the calculation previously reported, the minimum flow rate in order to maintain a perfectly mixed phase was 24,12 ml/min with a surface velocity of 1,22 cm/min. Maintaining a large safe value, the set flow rate was 40,00 ml/min with a surface velocity of 2,12 cm/min. In a further step will be necessary to evaluate if this flow rate can influence the biofilm development and behavior, in terms (for example) as increased shear stress, that can lead to a low biofilm development. In table 5.31, are listed the principal parameters estimated for this PFR plant:

<b>Reactor volume (ml)</b>	<b>579,00</b>
<b>Estimated <math>\tau</math> (min)</b>	<b>14,47</b>
<b>Fermentation characteristic time* (min)</b>	<b>360,00</b>
<b>Desired system residence time - HRT (min)</b>	<b>36,00</b>
<b>Ratio between liquid total volume in the plant and liquid volume in the column</b>	<b>1,50</b>
<b>Desired column residence time - HRT (min)</b>	<b>24,00</b>
<b>Desired flow rate (ml/min)</b>	<b>24,12</b>
<b>Surface velocity of the desired flow rate (cm/min)</b>	<b>1,22</b>
<b>Real set flow rate (ml/min)</b>	<b>40,00</b>
<b>Surface velocity of the set flow rate (cm/min)</b>	<b>2,12</b>

\*Corresponding to a 75% of lactose conversion

*Table 5.31: Principal plant parameters estimated for the PFR plant used for succinic acid production.*

As reported in section 4.7.4, five repeated batch tests were performed.

The main objectives of these experiments were to evaluate the repeatability of this process, paying attention to the optimization of immobilization and production phases in the reactor. In fact, from an industrial point of view, the biofilm development phase is a dead time. The most important variable is the number of bioproduction batch phases that can be made without repeating a growth phase.

A first 48-hour growth phase was initially performed, prior the test with 8 and 12 g/L of pure lactose. Subsequent, another 48-hour biofilm development step was made, and immediately thereafter three repeated bioproduction phases with 16 g/L of lactose were performed.

In the next figure, the produced S.A. concentration in function of time is plotted for all the five total tests:

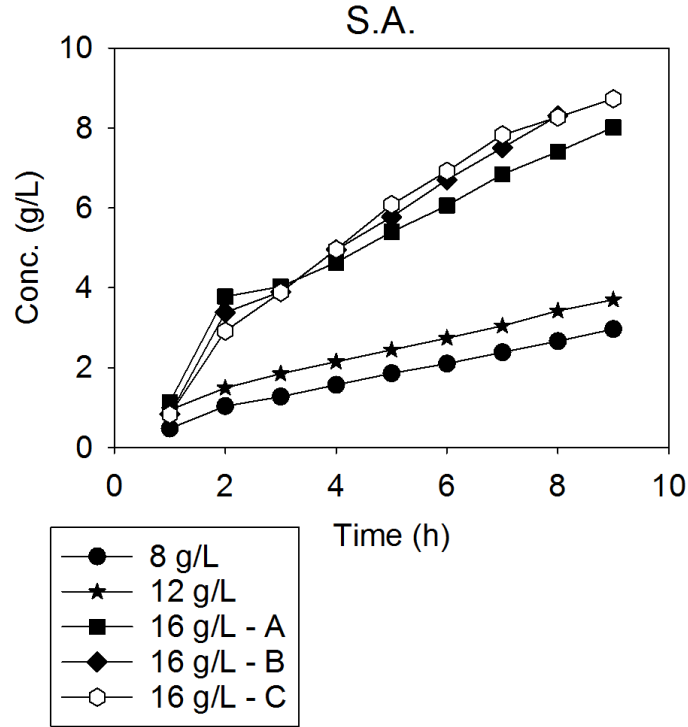


**Figure 5.54:** Succinic acid concentrations obtained in the five bioproduction tests in the 1 L column plant.

Moreover, in table 5.32, are reported the absolute velocities of S.A. production ( $g_{SA}/L/h$ ), and lactose consumption ( $g_{lac}/L/h$ ), with the calculated yields ( $g_{SA}/g_{lac}$ ), for each test.

	S.A.	Lactose		
Lactose conc. ( $g L^{-1}$ )	Slope ( $g L^{-1} h^{-1}$ )	Slope ( $g L^{-1} h^{-1}$ )	Final S.A. conc ( $g L^{-1}$ )	$r_{SA}/-r_{Lac}$ ( $g_{SA} g_{Lac}^{-1}$ )
<b>1 L Column plant (Glaxstone ®)</b>				
<b>7,4</b>	0,29	-0,39	2,97	0,75
<b>11,2</b>	0,33	-0,89	3,70	0,37
<b>15,2</b>	0,76	-1,63	8,02	0,46
<b>13,5</b>	0,98	-1,90	8,30	0,52
<b>13,9</b>	0,96	-1,88	8,73	0,51

**Table 5.32:** Absolute velocities (slopes) values of lactose consumption and succinic acid production for 1 – L plant packed with Glaxstone ®

From a first qualitatively analysis, passing from the first test with c.ca 8 g/L of lactose, to the three final experiments with c.ca 16 g/L of lactose, the S.A. increased from 2,97 g/L up to more than 8 g/L

in the last tests. The yield was maintained (in particularly in the last experiments), in the range around  $0,5 \text{ g}_{\text{SA}}/\text{g}_{\text{lac}}$  that is in line both with the microcosms tests, both with the results obtained in the VITO batch fermentations.

It's also evident that the slope of the graph (the absolute S.A. production rate in the table), are similar with the experiments with  $7,4 \text{ g/L}$  and  $11,2 \text{ g/L}$  of substrate, and increased in the last three tests. Moreover, with the increasing of the lactose concentrations, an increasing in the lactose consumption rate was observed. These behaviors can be related to the biomass present in the column. Due to the nature of subsequent repeated batch tests, and to the dynamic structure of the biofilm, probably the maintenance factor becomes higher and higher from batch to batch, requiring more substrate in order to maintain the same biomass population.

The drastic increase of S.A. production rate, between the two initial tests and the three final tests, is surely related to the two separates biofilm development phase. It's harder to make accurate considerations regarding the biomass, due to the intrinsic nature of the tests. Was impossible, in fact, to sample the carrier between one experiment and the following ones, thus, only the trend of the suspended biomass was monitored. Only at the end of the last experiment, three carriers from the bottom, middle and upper side of the column were sampled in order to determine the final biofilm development, and the quantity of entrapped biomass. As reported in section 4.8.4, the entrapped biomass represents those cells that remained entrapped between the dead space of the carrier during the experiments (and for this reason are not detected in the analysis of suspended sample), without contributing to the biofilm development.

In the next table, the trend of the suspended biomass during the two biofilm development phases are reported:

Phase 1		Phase 2	
Time (h)	Suspended biomass (g)	Time (h)	Suspended biomass (g)
0	0,278	0	0,093
4,7	0,421	4,3	1,010
21,8	0,482	20,8	1,800
28,7	0,258	28,8	0,555
44,5	0,258	43,8	0,569

**Table 5.33:** *Suspended biomass trend during the two phase of biofilm development*

From this table, two conclusions can be made. For both of the phases, a maximum biomass growth (expressed in grams of proteins) was reached after about c.ca 20 hours of immobilization (21,8 hours in the first step, and 20,8 in the second one). Then, the total amount of biomass rapidly decreased. If is assumed that the trend of the suspended biomass follows the biofilm development, only 20 h of biofilm immobilization are enough to ensure the maximum biomass development. In the second phase, also, the values are higher respect to the first step. In the second growth phase, two previous batch were performed, and probably a cumulative effect is observed. The higher biomass values can explain the increasing in the S.A. production rate, observed in the graph reported in figure 5.55. Obviously, more biomass in the plant can leads to a higher S.A. production.

The suspended biomass was also monitored at the beginning, and at the end of each bioproduction tests. Differently from the microcosm tests where the accumulation of the total biomass from the beginning to the end of the kinetic phase (see graphs in the Appendix) was negligible, in the plant, an increasing in the suspended biomass was observed (+ 59% as average value considering all the tests) was observed, with a standard error of 33%.

Despite to the high error value, it's evident that a different behavior is observed, and is probably related to the conformation of the plant. The feed bottle, in fact, is the ideal place for the growing of the suspended biomass, and despite the low volume kept, an increasing in the suspended biomass concentration is unavoidable.



Lastly, a consideration on the composition of the biomass all along the column can be made, after the last experiment and the sampling of the carrier. In the next graph are reported the trend of the attached biomass (strongly and weakly attached), at the bottom, in the middle and in the upper side of the column.

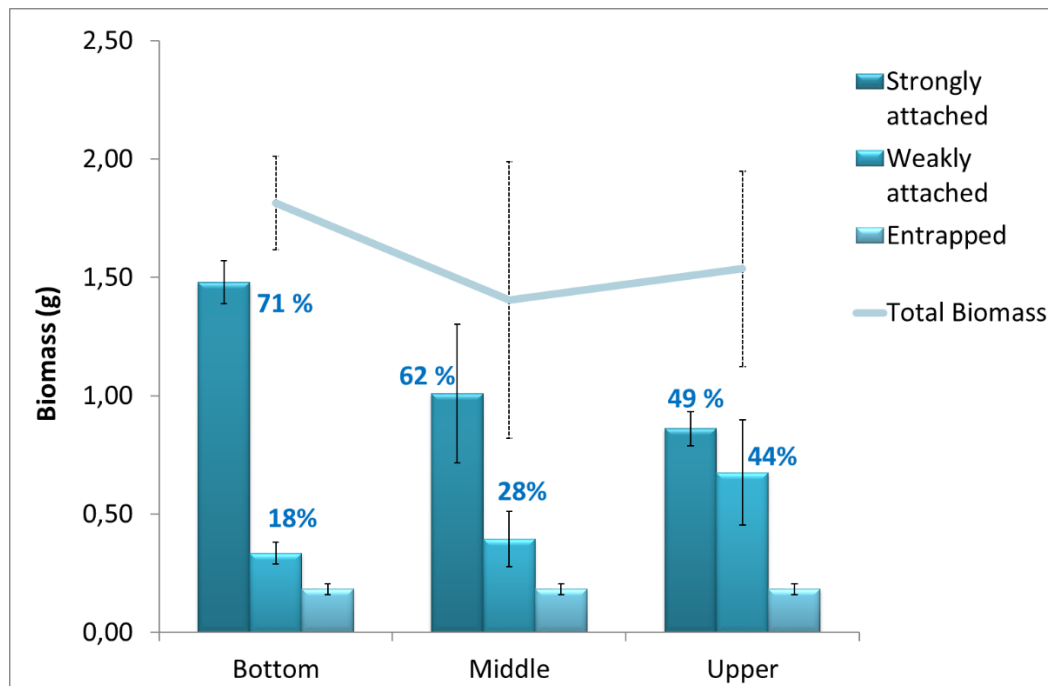


*Figure 5.55: Biomass distribution along the column at the end of the repeated batch test*

All along the column, the entrapped biomass remained practically constant, between 7% and 11% of the total. The total biomass value (net to the standard deviation) is constant around 1,7 grams of proteins, and is represented from the light blue continuous line in the last figure. The composition of the attached biomass drastically changes along the column. In particularly going from the bottom to the upper side, the percentage of the biofilm decreases from  $71\% \pm 6\%$  to  $49\% \pm 9\%$ , whereas the weakly attached biomass has the opposite trend, from  $18\% \pm 3\%$ , up to  $44\% \pm 14\%$ . This behavior is related to the flow direction in the plant, that pass from the bottom to the upper side of the column. In this way, the carriers present in the lower part of the column were colonized from the biomass, and represent the most suitable part of the column for the establishment of a biofilm.

It's evident that that these preliminary data can represent a good starting point for further optimization of the process. In particular, a better distribution of biofilm to ensure high productivity, and an optimized immobilization phase are required.

## 6 CONCLUSIONS

---

According to the IEA Bioenergy Task 42 released by European Commission, biorefinery processes are defined as a “*sustainable processing of biomass into a spectrum of marketable products and energy*” (Jungmeier G, 2013).

Biorefineries are facilities where raw biomass conversion processes are performed in order to produce fuels, power, heat, and value-added chemicals. Biorefineries represent a key element for the developing and the establishment of the circular economy strategy (Ellen MacArthur Foundation, 2012), that is the only sustainable environmental economic model in the future. As reported in section 1.4.1 (figure 1.23) different types of biorefinery are strictly interconnected one to the others, in order to establish a network where different types of platforms are used to convert different types of feedstocks in a plethora of products through numerous industrial processes.

Recently, numerous studies were focused on the exploitation of lignocellulosic biomasses for the production of biogas and bio-based chemicals (U.S. Department of Energy, 2014), (Sudip Chakraborty, 2012). The high impact of lignocellulosic residues on the global wastes production (N.S. Bentsen, 2014), and, the high lignin content of those residues (D. Pleissner, 2014), represent a big challenge in the management of this type of by – products.

In this dissertation, different types of biorefinery process were considered from different points of view.

- In partnership with different private companies, biogas – related biorefinery processes were used in order to produce biomethane from lignocellulosic by – products (as white and red grape pomaces), alone or in co – digestion with other types of substrates (e.g. olive mill wastewaters, tomato peels or maize silage), without any specific pre-treatments in order to reduce the fixed costs of the plant. Moreover, two different types of mixed consortia were used, and the performances were evaluated in different types of process (batch, fed – batch and continuous biomethanization tests). To complete the results, and to highlights the principal advantages and

the limits of the considered processes, numerous inhibition experiments were performed, in order to assess the effect of substrates, product and oxygen on the fermentative biochemical pathway.

- Due to the low literature studies, and to the highly – innovative nature of the process, a bio – alcohol production process was established from the mixture of volatile fatty acids produced in the first stages of anaerobic digestion process. The main idea was to enrich the biogas biorefinery, providing an alternative biochemical route switching from the normal biomethanization process to a n – propanol bioproduction phase, starting from propionic acid originated from the acidogenic phase of the anaerobic digestion.

After a long literature studies, in this biorefinery approach, three different consortia were acclimatized and screened in order to evaluate the possibility for n - propanol production.

- Milk whey was used and tested as a principal by – products in two different biorefinery approaches. In the first ones, biogas biorefinery was again exploited in order to produce biohydrogen from milk whey alone (or in co – feeding with molasses), using pure culture of *Thermotoga neapolitana*. In particularly, integrated experiments were performed, coupling the 19 L bioreactor, to an external membrane module for biohydrogen enrichment. No studies were identified in literature with this type of reactor - membrane configuration.
- Succinic acid (S.A.) is one of the Top 12 building blocks reported by the U.S.A. Department of energy (DOE) in 2014, produced from biomass transformation (U.S. Department of Energy, 2014). Is one of the most promising chemical intermediate for the production of a plethora of different industrial – related compounds, is used as neutralizer agent (E363) and in the new generation bioplastic production e.g. PBS, Poly – Butylene Succinate (see figure 3.10) (Zeikus JG, 1999). Moreover, the fermentation process fix 1 mol of CO<sub>2</sub>, for every mol of succinic acid formed. For all of these reasons, the establishment of high – yield succinic acid fermentation, represents one of the most promising bioengineering challenges for our society. Numerous S.A. production studies are reported in literature (table 3.8 and 3.9), both with natural production strains (using *Actinobacillus succinogenes* in particularly), both with engineered microorganisms (*E. coli*).

In collaboration with the Flemish Institute For Technological Research (VITO), in this project the C5 – C6 fermentation biorefinery was used in order to perform different fermentation studies for the bioproduction of S.A. using *A. succinogenes* from both pure lactose, both from milk whey. At VITO, the main idea was to study the feasibility of an innovative integrated plant coupling the reactor with an ISPR (In Situ Product Recovery Process), using electrodialysis for the separation of S.A., without any cell retention step in between. Again, no clear evidences were founded in literature regarding the set – up of this innovative type of plant.

Back to Bologna, the collaboration continued, and a reliable method for biofilm fermentation with attached biomass was established. The main work was related to the development a new procedure for the biofilm growth, evaluating 5 different commercial carriers, both in terms of succinic acid production, both in terms of biofilm growth. Besides that, a deep statistical analysis with ANOVA and t – test was applied to identify the best carrier. Then, a kinetic study both with lactose, and both with milk whey was performed, relating the results with a Monod model and estimating the principal parameters ( $\mu$  max and  $K_s$ ). Finally, preliminary repeated batch tests in 1 L plant were executed, and the performances were evaluated in terms of S.A. production and biomass development, in order to understand the possible future improvements.

### **Biomethane tests**

E. Dinuccio 2010 was the only literature study that reports an average yield value of 116 NL  $\text{CH}_4$  /Kg vs for the biomethanization of the grape pomace.

In this project, an already acclimatized mixed consortium called “DICAM” (Bertin, et al., 2012) isolated from OFMSW (Organic Fraction Of Municipal Solid Waste), was used the digestion experiment. After a preliminary microcosms screening, a first batch test was performed with 10% w/w of DICAM as inoculum, and 20% w/w of red grape pomace as substrate. This test leads to only 20,4 NL  $\text{CH}_4$  /Kg vs with a negligible biomethanization velocity (figure 5.7). The main cause was the accumulation of the acetic acid up to more than 15 g/L (figure 5.8). Some articles in fact, (Aguilar, 1995), (Ye Chen, 2008), reports that 10 g/L or higher values of total VFA are generally associated to

higher inhibitory state. For this reason, a fed – batch approach was used, diluting the fermentation broth with demi H<sub>2</sub>O and 20% w/w when the acetic acid reached the maximum set value of 4 g/L. After a long lag phase, an exponential increasing in methane yield was observed reaching a maximum value of 72 NL CH<sub>4</sub> /Kg vs after 77,5, and a production velocity of 0,25 NL CH<sub>4</sub> /L/d, with a maximum methane percentage of 63% with a 34% of CO<sub>2</sub> (figure 5.9). Then, according to the company, a long continuous biomethanization test was performed, increasing the feed (expressed as organic loading rate – OLR in g<sub>sv</sub>/L/d) from 0,4 to industrial interesting values (up to 1 g<sub>sv</sub>/L/d). This test was prolonged for 246 days, and the results are reported in figures 5.10 – 5.13 and summarized in table 5.4. The maximum achieved yields were in the range between 106 NL CH<sub>4</sub> /Kg vs and 165 NL CH<sub>4</sub> /Kg vs, that are in line and also higher respect to the value reported by E. Dinuccio 2010, with a maximum biomethanization rate of 0,16 NL CH<sub>4</sub> /L/d. This process represents an innovative and interestingly possibility for the valorization of grape pomaces with high yields without performing any specific pre-treatment. Moreover, the high methane percentage (up to 70%), and the low intrinsic costs (e.g. no sterility required, no specific pre – treatment involved), represent attractive factors for the valorization of these winery by – product. Anyway, some limiting factors needs to be highlighted. In particular, the intrinsic difficulty (probably due to the phylogenetic composition of the mixed culture) to maintain an equilibrium between the preliminarily stages of anaerobic digestion and the methanogenic step, leads to the impossibility to reach a stable steady – state. Besides that, the continuous grape pomace feed leads to a nitrogen shortage, due to the high C/N ratio of this substrate (Alastair J. Ward, 2008), (Mata-Alvarez, 2000) causes a yield reduction and leads to a necessity of nitrogen supply. Another aspect that lead to a reduction in the performances, is the accumulation of volatile solids (VS) at higher OLR. During the fed – batch, in fact, was estimated that a VS concentration higher than 72g/L cause an inhibition of the acetoclastic part of the methanogens population. Anyway, the main concern is represented from the accumulation of some toxic compounds derived from lignocellulosic degradation in the fermenter after a prolonged feed. Inhibition test, in fact, confirms that re-suspending the consortia in a rich medium, the performances of the process returns to the initial performances (figures 5.20 – 5.21). Another interesting aspect is

represented from the versatility of the process, and the higher adaptability of the consortia. In fact, at the end of the continuous test, oxygen and acetic acid inhibition experiments shows that 5% of oxygen was tolerated by the mixed culture (figure 5.17), and up to 12 g/L of  $\text{CH}_3\text{COOH}$  no inhibition of the methanogenic activity was detected (figure 5.18). “DICAM” consortium was also tested for the digestion of white pomaces, that are recalcitrant to the anaerobic digestion (AD) process, due to the high polyphenols content (Field J. A., 1987). Anyway, “DICAM” consortium shows high biomethanization performance also with this types of pomaces (figure 5.14), leading also (with the same concentration of VS in the feed) to a comparable methane yield with the red ones:  $(84,09 \pm 16,43)$  for the white, and  $(84,48 \pm ,49)$  for the red (table 5.5). This is an astonishing result, that can enrich the potential of this biorefinery.

Finally, to improve the nitrogen content, grape pomaces were co – digested with different types of raw materials (Olive Mill Wastewater – OMW, maize silage and tomato peels), using an industrial acclimatized consortium isolated from a tomato peels digester, called “SEBIGAS” (figure 5.23). Initially, same performances in terms of yield and velocity are detected with a simple AD process with only grape pomace, also with this type of consortium, confirming that the unbalance in the C/N ratio is one of the main issues in this process. Then, grape pomaces co – digestion with maize silage and tomato peels lead to an improvement of the methane yields, in particularly  $+ 113,5 \text{ NL}_{\text{CH}_4} / \text{Kg}$  vs using maize silage, and  $+ 73,5 \text{ NL}_{\text{CH}_4} / \text{Kg}$  vs in presence of tomato peels. Also in this case no pretreatments were effectuated on those raw agro – industrial products. This result is another attractive aspect, that can represent an optimal solution to valorize different types of wastes, exploiting in a more profitable and environmental friendly manner this type of biorefinery.

### **Biohydrogen tests**

In figures 5.1, 5.2 and in table 5.1 are reported the results of the integrated bioreactor – membrane biohydrogen production test. During the exponential phase (after 40 h of lag phase), the hydrogen productivity reached a maximum value of  $0,31 \text{ mmol H}_2 / \text{L/h}$ , corresponding to  $8,4 \text{ mmol H}_2 / \text{mol}$  glucose consumed, with volumetric flow rate of  $7,5 \text{ L/d}$ . A maximum hydrogen percentage of 79,9 %

prior membrane coupling was detected, and the biomass concentration (expressed in  $\text{mg}_{\text{proteins}}/\text{L}_{\text{reactor}}$ ), determined by Lowry's method, reached the maximum value (406,6  $\text{mg}/\text{L}$ ) after 97 hours of fermentation. In collaboration of the "Diffusion in Polymers and Membrane Separation Group" (thanks to Prof. Giulio Cesare Sarti, and Prof. Marco Giacinti Baschetti), after 41,5 hours of integrated coupling test, the hydrogen purity was improved until c.ca 95 % (with a 14,8% increased) with a halved  $\text{CO}_2$  percentage in the permeate (from 12,4% to 5,3%), suggesting a good starting point for further optimization of the process, for a future fuel cells applications.

Co-feeding tests of milk whey with molasses represent an interesting perspective, in order to contemporary valorize different types of agro – industrial wastes. The co - feeding ratios between molasses and cheese whey were respectively 75% - 25%, 50% - 50% and 25% - 75%, maintaining 10  $\text{g}/\text{L}$  as total starting sugars. In table 5.3 are reported the co – feeding results in terms of productivity ( $\text{mmol}_{\text{H}_2}/\text{L}/\text{h}$ ) and in terms of yield ( $\text{mmol}_{\text{H}_2}/\text{g}_{\text{consumed sugar}}$ ), compared with single molasses/cheese whey test. Both in terms of yield and productivity, all the 3 co-digestion tests led to an improvement of the process, and the best performances were obtained in the two tests characterized by the highest molasses concentrations. These results represent an improvement of the state-of-the-art of this biorefinery, leading to a better exploitation of the process combining two different wastes. Moreover, the integrated membrane test can focus a fix point of a further improvement of hydrogen in electricity production with fuel cell. Deeper studies can be made in order to optimize the membrane module to increase hydrogen purity.

### **N - propanol tests**

In this project, three different mixed consortia were screened in order to identify the best for the n – propanol production. 1) "DICAM" consortium was the same used in the biomethanization experiments, "OMW" inoculum was gently provided by Lorenzo Bertin research group (Bertin, et al., 2010). The "Sebigas" company collected and provided to us the third inoculum (called "MAIS" inoculum), from a CSTR anaerobic reactor fed with maize silage. A long literature documentation allowed us to identify some particularly characteristic of this bioprocess. For instance, thermodynamic



calculations reported by Kirsten J.J. Steinbusch, 2008, revealed for the first time that the reduction of volatile fatty acids in presence of hydrogen as electron donor is feasible from mixed culture, only if 0,5 bar of overpressure was applied. Despite low yields (only few mg/L), this process represents an improvement of the state-of-the-art, because up to now, only engineered microorganisms (*E. coli* as the most used) were used to produce n – propanol (Kajan Srirangan, 2013), (R. Jain, 2011), (Shota Atsumi, 2008). Moreover, solventogenic carboxydophilic bacteria (*Clostridium* as the main genus), are able to use Wood–Ljungdahl pathway using hydrogen as an electron donor and different types of compounds as VFAs, syngas or carbon dioxide as an electron acceptor for the biosynthesis of numerous compounds, including alcohols (e.g. ABE fermentation). (Perez et.al., 2012), (Papoutsakis ET., 2008), (Day, 1970), (Peralta-Yahya, 2012), (Isom, 2015). Due to the sporigen nature of the *Clostridia* (W.-W. Yang, 2009), the main idea of this project was to develop different steps of growth, selection, acclimatization and bioproduction, in order to identify the best mixed consortium. After the identification, a PCR – DGGE – SEQUENCING approach was used in order to characterize phylogenetically the microbial population in the culture. After a growth phase on glucose of all the three consortia, a selection procedure characterized by 3 subsequent pasteurization phases was performed and six total consortia were obtained. During the acclimatization, only propionic acid was used as a carbon source at pH 5, whereas in the bioproduction phase, propionic acid and hydrogen overpressure in the headspace at pH 5 were used as incubation conditions. In this phase, the effect of sulphate - bacteria inhibitory compound as sodium molybdate (D.R. Ranade, 1999) was investigated for all the six consortia, leading to a total of 12 consortia. In figure 5.24 and 5.25 are reported the results, quantitatively reported in table 5.8, in terms of percentage yield, n – propanol production velocity, propionic acid and hydrogen consuming rate. The pasteurized DICAM consortium without sodium molybdate supply was identified as the best consortium with higher yield of n – propanol production with a  $(0,027 \pm 0,002)$  mmol/L/d production rate and a  $(0,279 \pm 0,048)$  mmol/L/das propionic acid consumption rate. The maximum final percentage yield was around 18% with a final n – propanol titer of  $(42,0 \pm 0,8)$  mg/L. This titer is absolutely comparable with the values reported in the literature studies with engineered microorganism, representing an alternative methodology for 1 –

propanol production without using a GMO culture. Moreover, the “DICAM” consortium was already acclimatized to the AD process, and in literature numerous evidences reports the *Clostridia* is one of the most represented genus involved in the acidogenic and acetogenic steps of anaerobic digestion process (Fayyaz Ali Shah, 2014). Thus, it's possible to speculate that this mixed culture started with an already selective advantages respect to the other consortia, because the probability of the presence of some specific microorganism belonging to the *Clostridia* genus was higher respect to the OMW and “MAIS” culture. The phylogenetic analysis reported in table 5.11 demonstrate that *Clostridium pasteurianum* JCM 1408, *Pseudoflavonifractor capillosus* ATCC 29799 and *Clostridium celerecrescens* DSM 5628 are three of the main microorganisms involved in this biochemical reduction, identified with a 16S rRNA gene sequence homology of 99%, 96% and 99% in the Ribosomal Database Project-II (RDP, release 11, <http://rdp.cme.msu.edu>).

This study represents a solid starting point for the production of 1 – propanol from mixed culture. The individuation an acclimatized mixed consortia and its characterization is a key point for further studies, in order to increase the adaptability, and thus the yield, of the process. Moreover, the possibility of a fully integration on the biomethane biorefinery, represent a powerful mechanism to adapt the biorefinery to multiple situations, changing only physical parameters (as pH and temperature).

### **Succinic acid (S.A.) tests**

#### **- VITO results**

In order to evaluate and compare the results of preliminary batch tests with the performances reported in numerous literature studies (table 3.9), some batch tests were performed both with lactose and both with milk whey. In figure 5.33 and table 5.12 are reported the results for the test executed with 40 g/L of pure lactose, whereas in figure 5.34 and table 5.13 are reported the results for the test executed with the same amount of equivalent lactose present in milk whey. With lactose, 20 g/L of final titer of S.A. was reached, with a productivity of 0,8 g<sub>SA</sub> /L/h, and a final yield of 0,5 g<sub>SA</sub> / g consumed lactose. With the milk whey, the performances are obviously lower, but absolutely in line with the literature. A final

titer of 13,8 g/L, a productivity of 0,5 g SA /L/h, and a final yield of 0, g SA / g consumed equivalent lactose. Obviously, also the carbohydrate utilization was lower with milk whey (72,9%) respect to lactose (92,4%).

After these tests, the work focused deeply on the optimization of the electrodialysis (ED) plant, in order to perform the final integrated experiment, coupling ED to the fermenter as ISPR technique without any steps of cell retention in between. An accurate set of LCD (Limiting Current Density) determination tests were conducted to establish the maximum current value to apply in order to drag the ions separation within the membrane stack (see the detailed explanation in section 5.4.2). The results are reported in figure 5.37 and table 5.14. With the increasing of the S.A. in the diluate compartment, the LCD value raises, because more current needs to be applied to trigger the transportation of the ions from the diluate to the concentrate compartment. Interestingly, figure 5.38 shows the very fitting 3 ° grade exponential relationship founded between the LCD value and the conductivity of the solution. This equation is important, because following online (every 15 seconds) the conductivity profile in the diluate, it's possible to determine the amount of current that needs to be applied to work at the maximum efficiency. Practically, the system worked with an 80% of this LCD value, in order to maintain a safety step in case of process instability, avoiding problems related to the overcoming of limiting current (increasing of pH and resistance, water splitting) that often lead to a complete failure of the test. In paragraph 5.4.3 are reported the results of the simulations of a separation test using a synthetic broth that mimes the real fermentation medium. Figures 5.39 and 5.41 reports the profile of the concentration of succinate and acetate together with the conductivity profile both in diluate, both in the concentrate compartment, prior and after the refilling of the diluate compartment with another fresh synthetic solution. In figure 5.39, starting from a 58,05 g/L of S.A. in the concentrate and 25,15 g/L in the diluate, the acid concentration rapidly increased to 81,95 g/L in the first 9.40 h of process, following the raising profile of conductivity. From 9.40h to 20.43 h there is an osmotic effect prevalent because the ions concentration in the diluate compartment was very low, and for this reason a refill of the diluate was performed and reported in figure 5.41. Again, the concentration of S.A. started raising again following the conductivity profile from 76,28 g/L reached

in the test 1 to 92 g/L. The current was manually lowered following the previously determined equation, and in figures 5.40 and 5.42 are reported the profiles. Finally, in table 5.15 and 5.16, some calculation regarding the current efficiency (%), the specific water transport number (adimensional), the transport rate ( $\text{Kg}_{\text{SA}}/\text{m}^2 \cdot \text{h}$ ) and the maximum transported S.A. concentration were made, in order to preliminary estimates some parameters that are not only fundamental for the quantitatively valuation of a classic ED process, but also for a possible scale – up.

Moreover, the relationship between LCD and conductivity was validated using a real centrifuged broth (black point reported in figure 5.43), but was completely useless when a preliminary test was conducted with real not – centrifuged broth as reported in figure 5.44. Huge fouling problems were detected (due to a low crossflow velocity estimated respect to the normal values reported for industrial processes fouling (Hyeok Choi, 2005)), that increases the resistance within the stack, leading to a drastic reduction in LCD value. Thus, working with previous relationship would lead the plant to work above the new LCD value, with detrimental effect on the whole test. In fact, an LCD determination was performed with the “fouled stack”, and the new value was 0,94 A respect to the 4,41 A reported for a clean stack with 30 g/L of succinic acid in the diluate compartment.

For this reason, in the subsequent coupled test, the operational parameter was switched from constant current to constant voltage, in order to maintain the derived current value below this new LCD. In fact, according to the Ohm’s law, if a constant voltage was supplied, when the resistance increased duo to the fouling, the resulting Ampère decreases, avoiding all the problems related to the overcoming of limiting current density.

In the integrated test, after 150 hours of batch and continuous conduction, the coupling was developed for 50 hours. The results are reported in figure 5.45 and table 5.18, with a deep focus on the ED plant efficiency in figure 5.46. Unfortunately, after 50 hours, a contamination derived from LAB (lactic acid bacteria) was observed, but in the 2 days of continuous test an increasing of S.A. concentration in the concentrate compartment was observed, passing from an initial value of 53,36 g/L to 55,52 g/L, with a removal rate of 0,15  $\text{g}_{\text{SA}}/\text{h}$ . Besides that, no pH variation was observed, and the current passed from the initial value of 0,74 A, to 0,71 after 44,41 hours, confirming that the plant worked below the

LCD limit. Moreover, looking to the fermentation results in figure 5.45, in the blue circle is highlighted the increasing of the concentration of S.A. from an average concentration of 10 g/L at the end of the continuous phase, to 12,83 g/L prior contamination, with an increment of 0,17 g/L/h ( $R^2 = 0,966$ ), and an estimated production rate of 1,33 g<sub>SA</sub>/h, that was absolutely in line with the value reported for the continuous phase. This is probably related to the in situ continuous removal of the product from the fermenter, and the consequent low effect of product inhibition on the microorganism metabolism.

#### - DICAM results

Back to Bologna, a strict collaboration between VITO and DICAM department was established, and other aspects regarding the development of a procedure for a biofilm fermentation, and a deep kinetic study were conducted, both with lactose and both with milk whey.

Different carriers (figure 4.16 and table 4.24) were screened in order to determine the best in terms of S.A. production (figure 5.47) and biofilm growth (figure 5.48). In order to statistically evaluate the performances of the most two promising carriers, an ANOVA test (table 5.20), and a subsequent t – test (table 5.21), were conducted.

Then, with the “initial velocity method”, a kinetic study was performed, relating the fermentation results with the Monod model, using a best-fit procedure that minimize the mean square deviation for every considered parameter ( $\mu$  max and  $K_S$ ). From this test, the main kinetic variables, as  $\mu$  max and  $K_S$  were estimated, for the two most promising carriers. After this long quantitatively, and statistically validated screening phase, the choice was made between the two carriers. The initial velocity method involves the set – up of different fermentation tests using different substrate concentration (table 5.23). Then, from the initial linear part of the time/concentration graphs (both for substrate, both for product) where the substrate is in excess, the slope was determined (that is the absolute velocity expressed in g/L/h). This value was related to the biofilm concentration (in g/L - table 5.24), and the resulting specific velocity (expressed in  $h^{-1}$  – table 5.25) values were plotted in function of the substrate

concentration. Then, the resulting graphs are interpolated with a Monod model, and  $\mu_{\max}$  and  $K_S$  are estimated (figure 5.49 – figure 5.50 – table 5.26).

After the choice of the best carrier, same kinetic study was performed using milk whey, that leads to the same Monod model (tables 5.27 – 5.28 – 5.29, and figures 5.51 and 5.52) with the estimation of  $\mu_{\max}$  and  $K_S$  (table 5.30).

Finally, a preliminary tests using a 1 L plant formed by a glass column packed with the chosen carrier were performed, increasing the lactose concentration from 8 g/L to 16 g/L. The main objective of these tests was to evaluate the performance of the immobilization on the column and verify the reliability of subsequent repeated batch tests (figure 5.54). Three consequent production phase with 16 g/L of substrate were performed with reliable results, without the necessity to develop a growth step.

This C5 – C6 biorefinery was extensively studied from different point view. In particularly the integration of the ISPR recovery techniques represent a stable base for a further industrial processes. From the other side, the development of a stable and reliable procedure for *A. succinogenes* immobilization, and the kinetic characterization are focus points that can be combined with the ISPR coupled plant, in order to face the high demand of this building block.

## 7 APPENDIX

Microorganism	Genotype	Substrate	Ethanol yield (g/L)	Time (h)	References
<b>Cellulolytic</b>					
<i>Clostridium cellulolyticum</i> H10	Wild type	Cellulose MN301	0.51	460	195,196
<i>Clostridium cellulolyticum</i> CC-pMG8	pdc adhB	Cellulose MN301	0.83	460	195
<i>Clostridium japonicus</i> Ueda107	Wild type	Avicel	0.0002	48	197
<i>Clostridium japonicus</i> MSB280	pdc adhB	Avicel	0.0035	48	197
<i>Clostridium thermocellum</i> ATCC 27405	Wild type	Crystalline cellulose	2.66	240	198
		Sugarcane bagasse	3.5	240	199
		Paper pulp sludge	14.1	240	199
<i>Clostridium thermocellum</i> DSM 1313	Wild type	Avicel	1.3	72	69
<i>Clostridium thermocellum</i> M1570	$\Delta$ ldh $\Delta$ pta	Avicel	5.6	72	69
<i>Clostridium phytofermentans</i> ATCC 700394	Wild type	Filter paper	2.9	672	200
		AFEX corn stover	2.8	234	201
<i>Geobacillus</i> sp. R7	Wild type	Prairie cord grass	0.035	168	202
<i>Trametes hirsuta</i>	Wild type	Rice straw	3	96	203
<b>Hemicellulolytic</b>					
<i>Thermoanaerobacterium saccharolyticum</i>	Wild type	Xylose	3.4	10	166
<i>Thermoanaerobacterium saccharolyticum</i> ALK2	$\Delta$ ldh $\Delta$ pta $\Delta$ ack	Xylose	5.5	10	166
<i>Thermoanaerobacterium saccharolyticum</i> M1442	$\Delta$ ldh $\Delta$ pta $\Delta$ ack	Hardwood hydrolyzate	7.4	68	204
<i>Geobacillus thermoglucosidarius</i> TM242	$\Delta$ ldh $\Delta$ pfl pdh-unreg	Xylose	9.6	12	205
<i>Clostridium phytofermentans</i> ATCC 700394	Wild type	Birch wood/Xylan	0.46	24	200
<i>Thermoanaerobacterium aotearoense</i> SCUT27	Wild type	Xylose	1.5	24	206
<i>Thermoanaerobacterium aotearoense</i> $\Delta$ ldh Mutant	$\Delta$ ldh	Xylose	3.5	24	206
<i>Thermoanaerobacter mathranii</i> BG1	Wild type	Xylose	2.3	48	207
<i>Thermoanaerobacter mathranii</i> BG1LI	$\Delta$ ldh	Xylose	2.2	48	207

Table 7.1: Principal consolidated bioprocess for large-scale ethanol production (Mbaneme-Smith V, 2014)

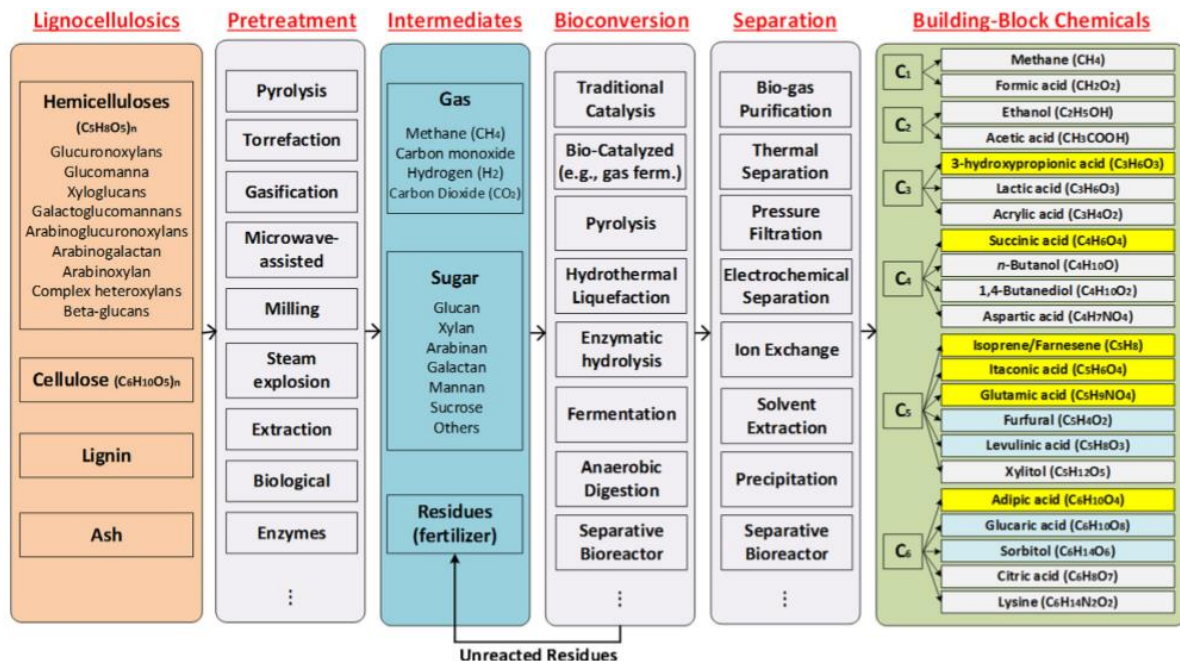
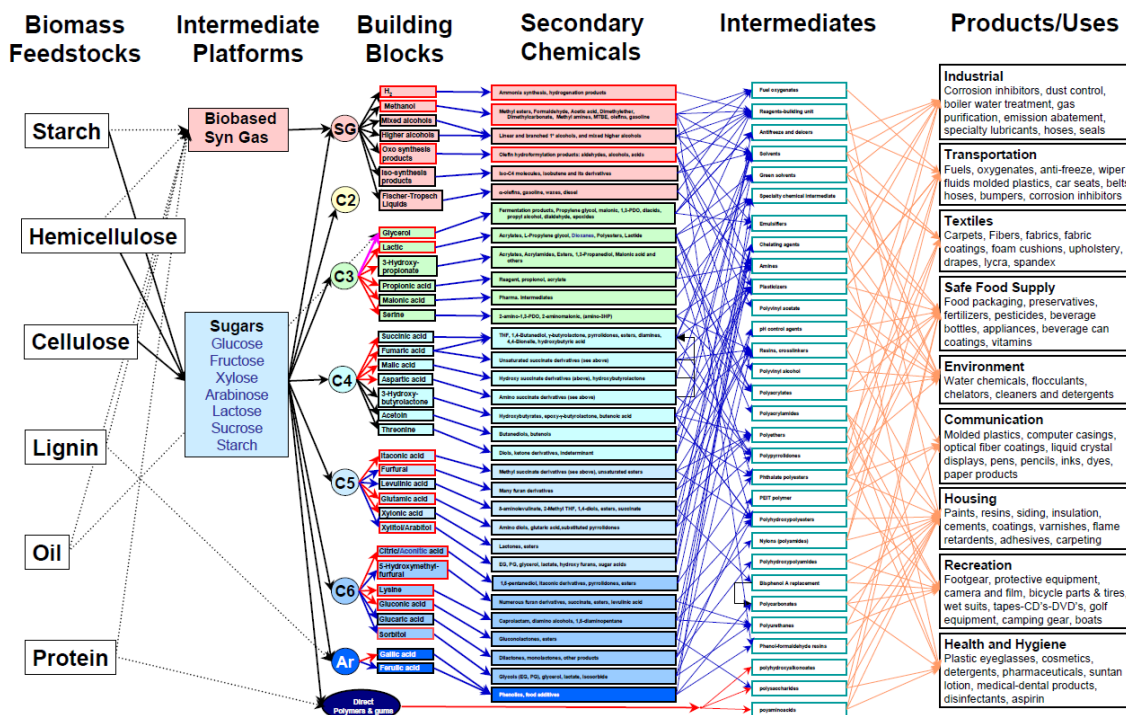


Figure 7.2: Industrial-scale processes for building block production from lignocellulose derived raw materials (Shu-Yuan Pan, 2015)

	Fermentation product	Ref.
<i>Rhodospirillum rubrum</i> <i>Rhodobacter sphaeroides</i> <i>Methanobacterium thermoautotrophicum</i> <i>Methanosarcina barkeri</i> <i>Clostridium thermoaceticum</i> <i>Rhodopseudomonas gelatinosa</i> <i>Rhodopseudomonas capsulate</i> <i>Rhodopseudomonas palustris</i> <i>Rubrivivax gelatinosus</i> <i>Bacillus simithii</i> ERIH2 <i>Rhodopseudomonas palustris</i> P4 <i>Citrobacter amalonaticus</i> Y19 <i>Rhodocyclus gelatinosus</i> <i>Carboxydotherrmus hydrogenoformans</i>	Hydrogen $\text{CO} + \text{H}_2\text{O} \rightarrow \text{CO}_2 + \text{H}_2$	[14,21,23–33]
<i>Clostridium autoethanogenum</i> <i>Clostridium ljungdahlii</i> <i>Moorella</i> sp. HUC22-1 <i>Acetobacterium kivui</i> <i>Peptostreptococcus productus</i> <i>Alkalibaculum bacchi</i>	Mixture of acetic acid and ethanol $6\text{CO} + 3\text{H}_2\text{O} \rightarrow \text{CH}_3\text{CH}_2\text{OH} + 4\text{CO}_2$ $2\text{CO}_2 + 6\text{H}_2 \rightarrow \text{CH}_3\text{CH}_2\text{OH} + 3\text{H}_2\text{O}$ $6\text{CO} + 6\text{H}_2 \rightarrow 2\text{CH}_3\text{CH}_2\text{OH} + 2\text{CO}_2$ $4\text{CO} + 2\text{H}_2\text{O} \rightarrow \text{CH}_3\text{COOH} + 2\text{CO}_2$ $2\text{CO}_2 + 4\text{H}_2 \rightarrow \text{CH}_3\text{COOH} + 2\text{H}_2\text{O}$	[14,22,34–38]
<i>Eubacterium limosum</i> <i>Clostridium carboxidivorans</i> <i>Butyribacterium methylotrophicum</i>	Mixture of ethanol, butanol, acetic acid and butyric acid $6\text{CO} + 3\text{H}_2\text{O} \rightarrow \text{CH}_3\text{CH}_2\text{OH} + 4\text{CO}_2$ $4\text{CO} + 2\text{H}_2\text{O} \rightarrow \text{CH}_3\text{COOH} + 2\text{CO}_2$ $12\text{CO} + 5\text{H}_2\text{O} \rightarrow \text{C}_4\text{H}_9\text{OH} + 8\text{CO}_2$ $10\text{CO} + 4\text{H}_2\text{O} \rightarrow \text{C}_4\text{H}_9\text{OH} + \text{CO}_2$ $12\text{H}_2 + 4\text{CO}_2 \rightarrow \text{C}_4\text{H}_9\text{OH} + 7\text{H}_2\text{O}$	[14,39–46]
<i>Peptostreptococcus productus</i> <i>Eubacterium limosum</i> <i>Acetobacterium woodii</i> <i>Acetobacterium wiewingae</i> <i>Clostridium thermoaceticum</i>	Acetic acid $2\text{CO}_2 + 4\text{H}_2 \rightarrow \text{CH}_3\text{COOH} + 2\text{H}_2\text{O}$ $4\text{CO}_2 + \text{H}_2\text{O} \rightarrow \text{CH}_3\text{COOH} + 2\text{CO}_2$	[14,21,47–49]
<i>Methanospirillum hungatii</i> <i>Methanobacterium formicicum</i> <i>Methanobrevibacter smithii</i> <i>Methanosarcina barkeri</i> <i>Methanobacterium thermoautotrophicum</i>	Methane $4\text{H}_2 + \text{CO}_2 \rightarrow \text{CH}_4 + \text{H}_2\text{O}$ $4\text{CO} + 2\text{H}_2\text{O} \rightarrow \text{CH}_4 + 3\text{CO}_2$	[21,35]

**Table 7.2:** Principal consolidated bioprocess for large-scale bio – H<sub>2</sub>, Bio – CH<sub>4</sub>, and bioalcohols (ethanol and butanol) production from syngas (Maedeh Mohammadi, 2011)



**Figure 7.1:** Network of principal relationship established between biorefineries for the production of bio – based products, and principal application sectors (U.S. Department of Energy, 2014)



Strain	Growth conditions				Products					Efficiency				References
	Substrate	Medium	Temp (°C)	pH	Ethanol (g/L)	Acetate (g/L)	Lactate (g/L)	Propionate (g/L)	CO <sub>2</sub> (g/L)	H <sub>2</sub> (g/L)	Carbon Recovery	Yield	Economic feasibility	
27405	0.3 % wt/vol Milled Filter Paper	EM	60	7.0	0.80	0.54	ND	ND	ND	ND	ND	ND	Low	Lv and Yu, 2013
	Microcrystalline Cellulose (1% wt/vol)	BM7	60	6.0–7.5	1.09	1.49	2.43	0.25	ND	ND	ND	ND	Low	Tachaapaikoon et al., 2012
	<sup>15</sup> N Cellulose (5 g/L)	MTC	58	6.8	1.34	1.17	ND	ND	ND	ND	ND	0.50 (g/g)	Low	Raman et al., 2009
	<sup>14</sup> N Cellulose (5 g/L)				1.27	1.16						0.49 (g/g)		
	Cellobiose (5 g/L)				1.02	1.43						0.49 (g/g)		
	Z-Trim® (5 g/L)				0.54	0.81						0.45 (g/g)		
	Cellulose-Xylan (5 g/L)				0.62	0.71						0.44 (g/g)		
	Cellulose-Pectin (5 g/L)				0.49	0.69						0.39 (g/g)		
	Cellulose-Pectin-Xylan (5 g/L)				0.54	0.60						0.38 (g/g)		
	Pretreated Switchgrass (5 g/L)				0.32	0.60						0.37 (g/g)		
	Pretreated Switchgrass (5 g/L)	MTC	58	6.8	0.20	0.50	ND	ND	ND	ND	ND	ND	Low	Wilson et al., 2013a
	Pretreated Populus(5g/L)				0.30	0.80							Low	
DSM 1313	Cellulose	CM3	60	7.8	0.96	0.75	0.38	ND	1.20	0.04	0.88	ND	Low	Weimer and Zeikus, 1977
	Avicel (19.5 g/L)	MTC	55	7.0	1.32	2.74	2.49	ND	ND	ND	0.72	ND	Low	Argyros et al., 2011
	Cellobiose (5 g/L)	Rich media	55	7.0	0.68	1.10	0.25	ND	ND	ND	ND	ND	Low	Tripathi et al., 2010
	Avicel (5 g/L)				0.70	1.10	0.05							
CS7	0.3 % wt/vol Milled Filter Paper	EM	60	7.0	0.79	0.32	ND	ND	ND	ND	ND	ND	Low	Lv and Yu, 2013
CS8	0.3 % wt/vol Milled Filter Paper				0.83	0.43	ND	ND	ND	ND	ND	ND	Low	Lv and Yu, 2013
S14	Microcrystalline Cellulose (1% wt/vol)	BM7	60	6.5–7.0	1.90	3.72	0.74	1.23	ND	ND	ND	ND	Low	Tachaapaikoon et al., 2012
YS	Cellulose	CM3	60	7.3	1.40	1.90	ND	ND	ND	0.10	ND	ND	Low	Lamed et al., 1988
	Cellobiose				1.20	1.80				0.10				
LQRI	0.4% wt/vol Cellulose	GS	60	7.0	0.71	0.96	0.31	ND	1.33	0.05	≥0.80	ND	Low	Ng et al., 1981
	0.4% wt/vol Glucose				0.75	0.89	0.22		1.21	0.04				
	0.4% wt/vol Cellobiose				0.72	0.74	0.21		1.52	0.06				
	Cellulose	CM3	60	7.3	0.90	2.90	ND	ND	ND	0.20	ND	ND	Low	Lamed et al., 1988
	Cellobiose				0.90	3.00				0.20				
JW20	1% (wt/vol) Cellulose	Minimal Media	58–61	6.1–7.5	0.61	1.21	0.43	ND	2.38	0.14	0.87	ND	Low	Freier et al., 1988
BC1	Cellulose, glucose, sorbitol	ND	67	ND	ND	ND	ND	ND	ND	ND	ND	ND	Low	Koeck et al., 2013
M1570	Avicel (19.5 g/L)	MTC	55	7.0	5.61	0.16	0.11	ND	ND	ND	0.61	ND	Low	Argyros et al., 2011

ND, Not defined in original publication.

**Table 7.3:** Principal consolidated bioprocess for large-scale biofuel and bio – based chemicals using microorganism belonging to the *Clostridia* genus (Hannah Akinosho, 2014)

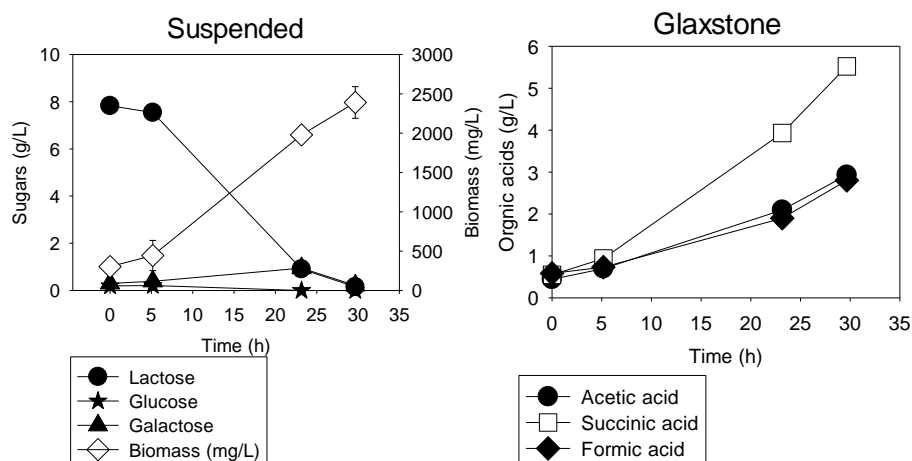


**Figure 7.3:** Suspended biomass tests for *S.A.* in microcosms scale. Sugars, biomass and acids concentration

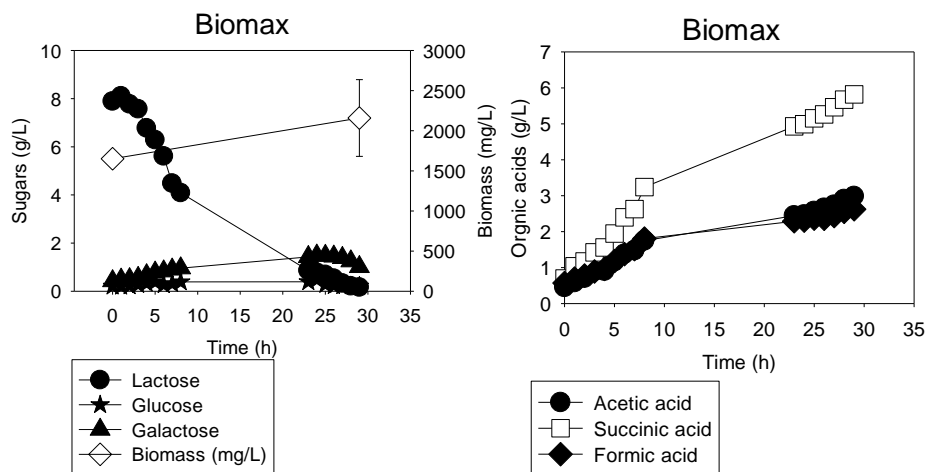


**Figure 7.4:** Biofilm fermentation tests – Biomax® initial screening with 7 g/L of lactose

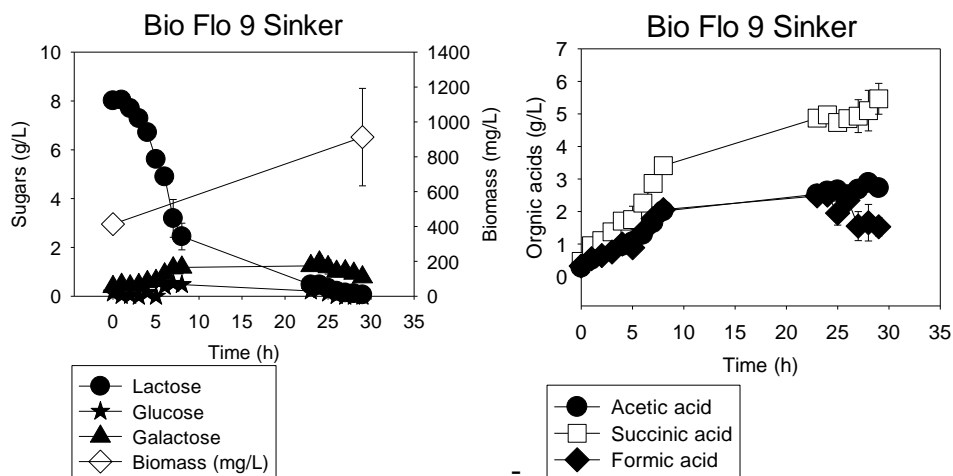


**Figure 7.5:** Biofilm fermentation tests – Bio Flo 9 Sinker® initial screening with 7 g/L of lactose

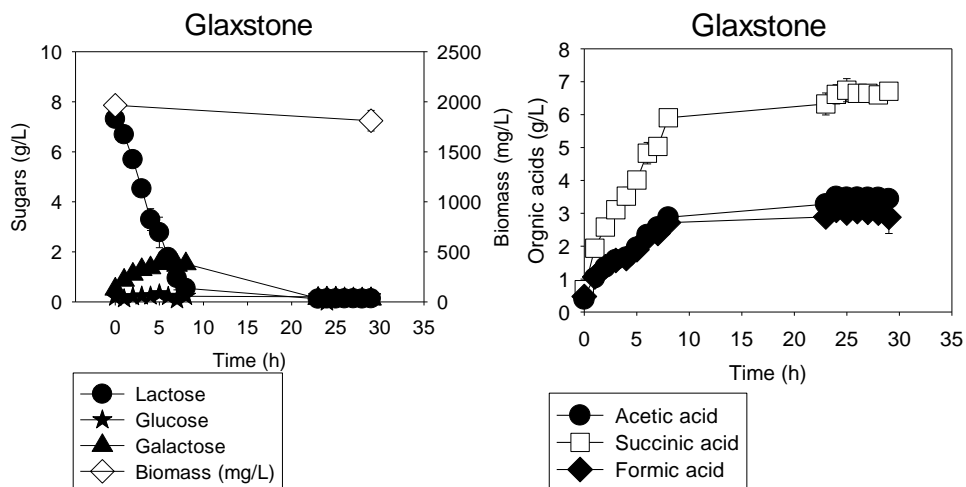


**Figure 7.6:** Biofilm fermentation tests – Glaxstone® initial screening with 7 g/L of lactose

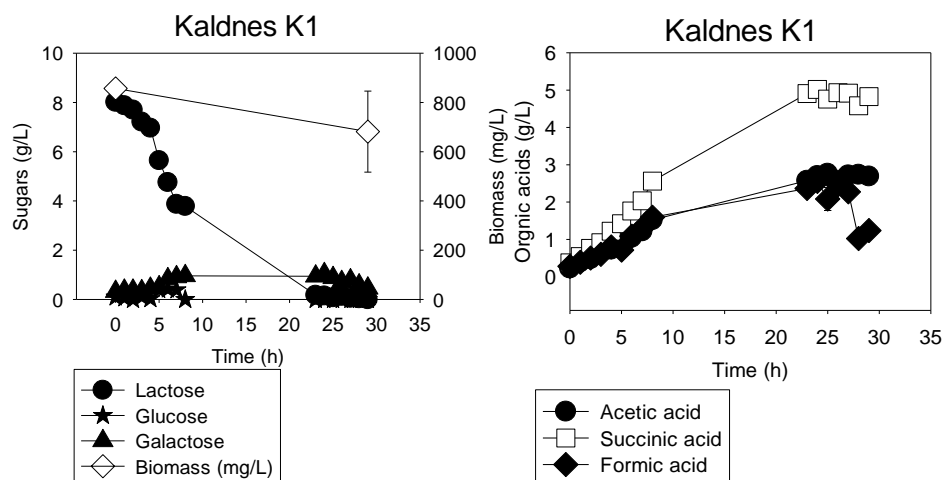


**Figure 7.7:** Biofilm fermentation tests – Kaldnes K1® initial screening with 7 g/L of lactose

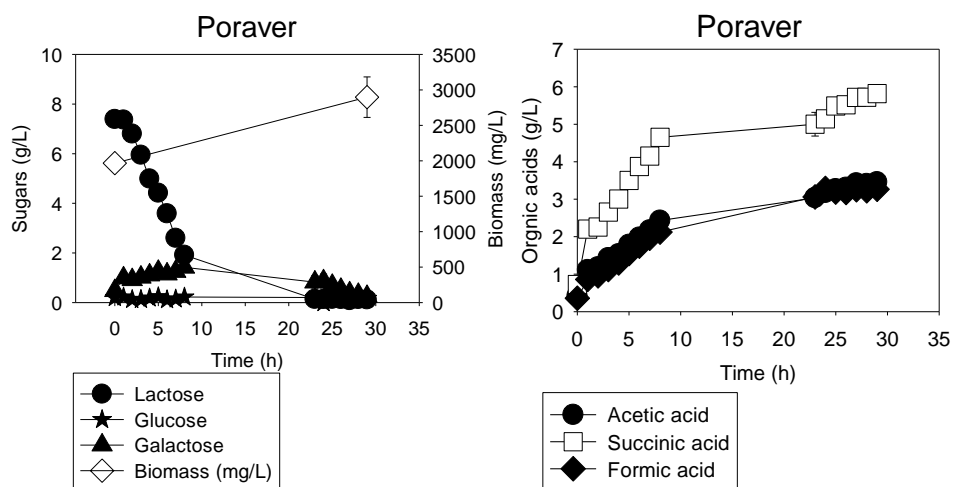


**Figure 7.8:** Biofilm fermentation tests – Poraver® initial screening with 7 g/L of lactose

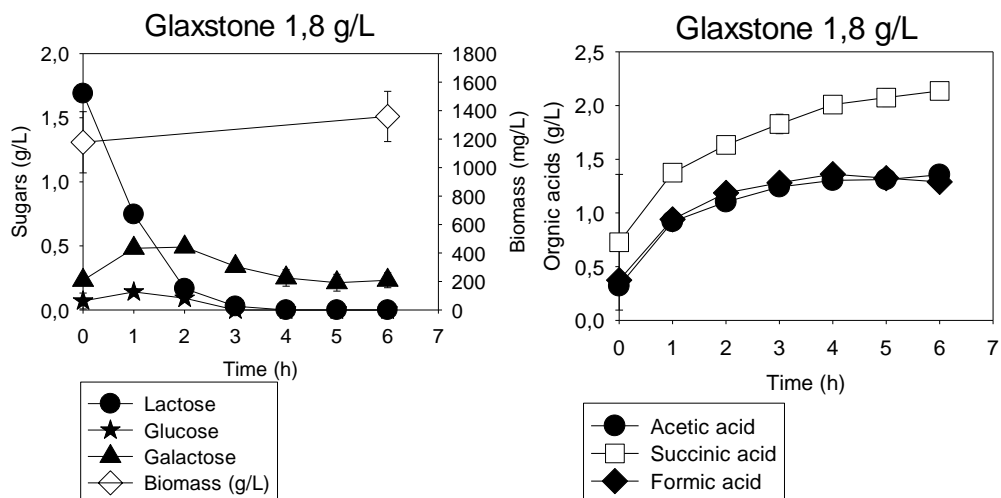


**Figure 7.9:** "Initial velocity method". Biofilm fermentation tests with Glaxstone® - 1,8 g/L of pure lactose

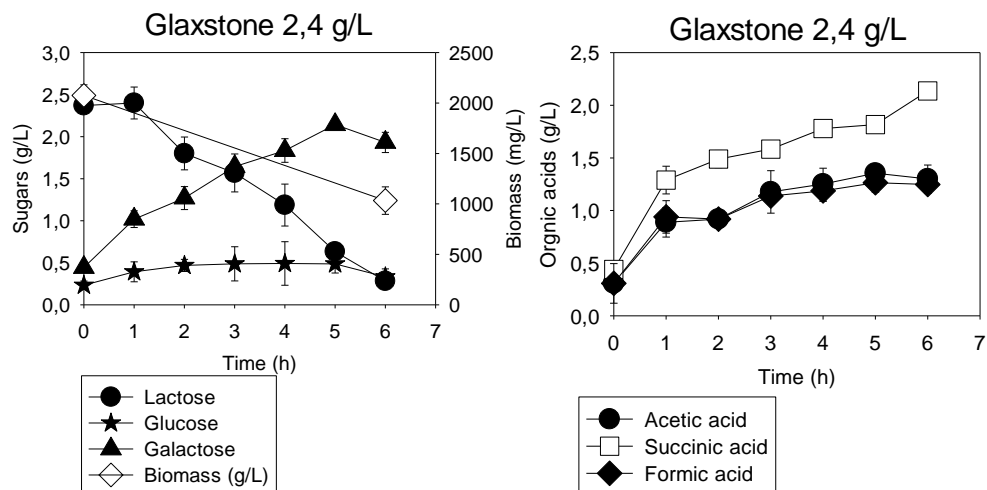


**Figure 7.10:** “Initial velocity method”. Biofilm fermentation tests with Glaxstone® - 2,4 g/L of pure lactose

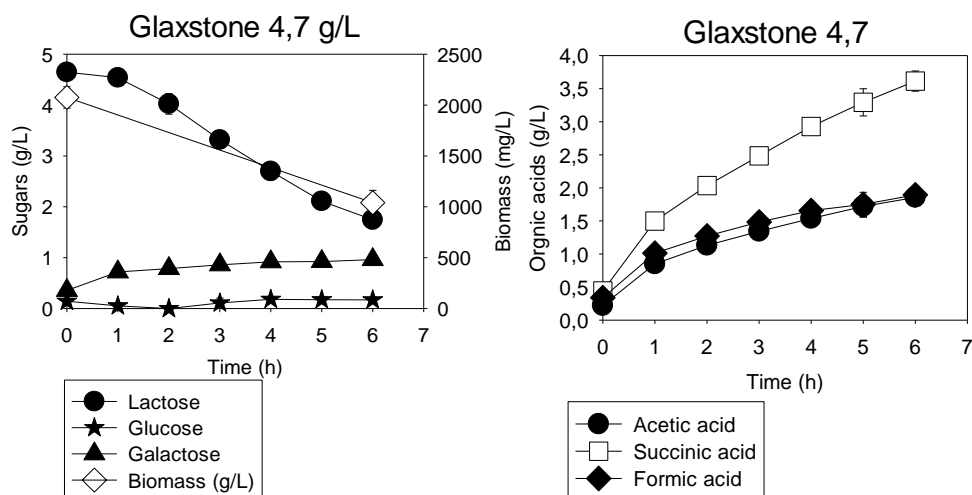


**Figure 7.11:** “Initial velocity method”. Biofilm fermentation tests with Glaxstone® - 4,7 g/L of pure lactose

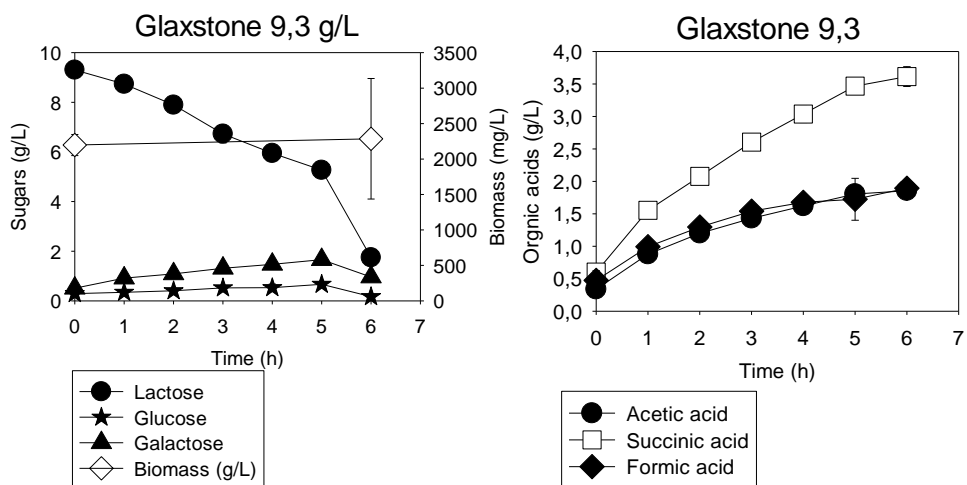


**Figure 7.11:** “Initial velocity method”. Biofilm fermentation tests with Glaxstone® - 9,3 g/L of pure lactose

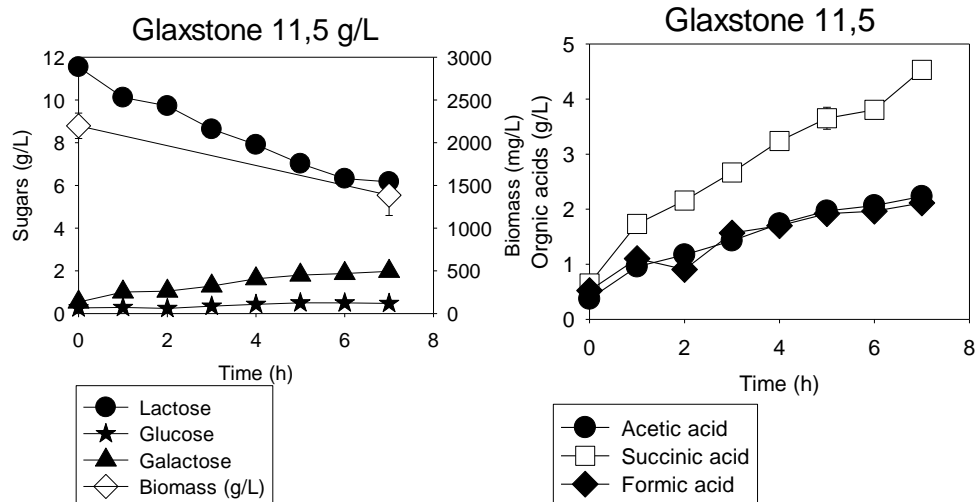


**Figure 7.12:** “Initial velocity method”. Biofilm fermentation tests with Glaxstone® - 11,5 g/L of pure lactose

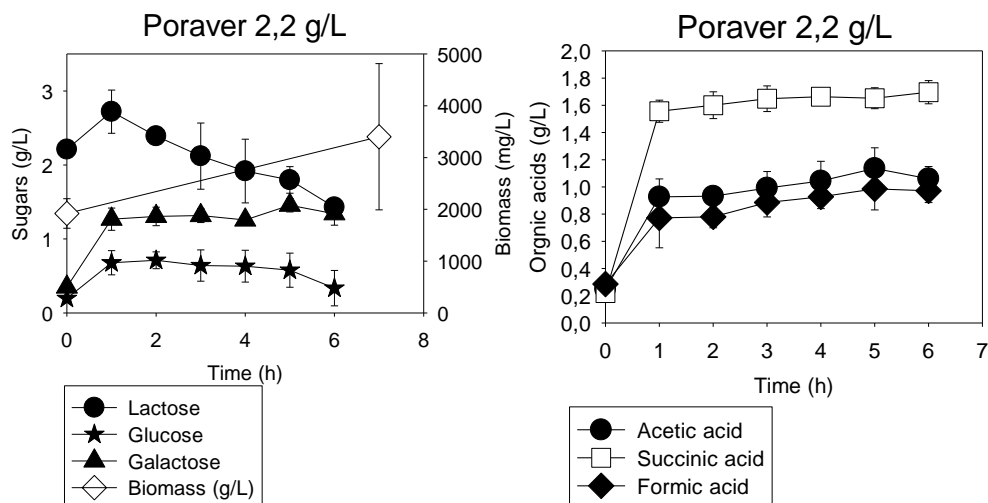


**Figure 7.13:** “Initial velocity method”. Biofilm fermentation tests with Poraver® - 2,2 g/L of pure lactose

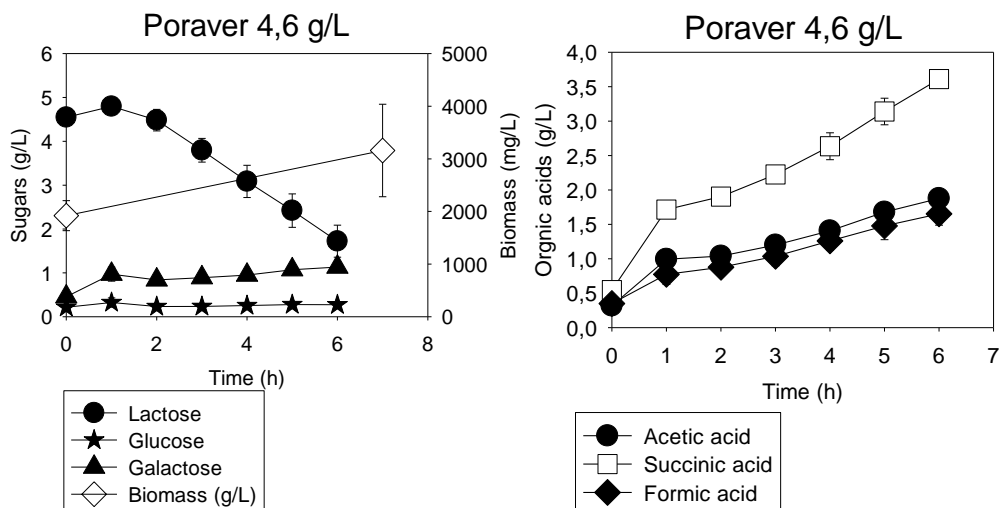


**Figure 7.14:** “Initial velocity method”. Biofilm fermentation tests with Poraver® - 4,6 g/L of pure lactose

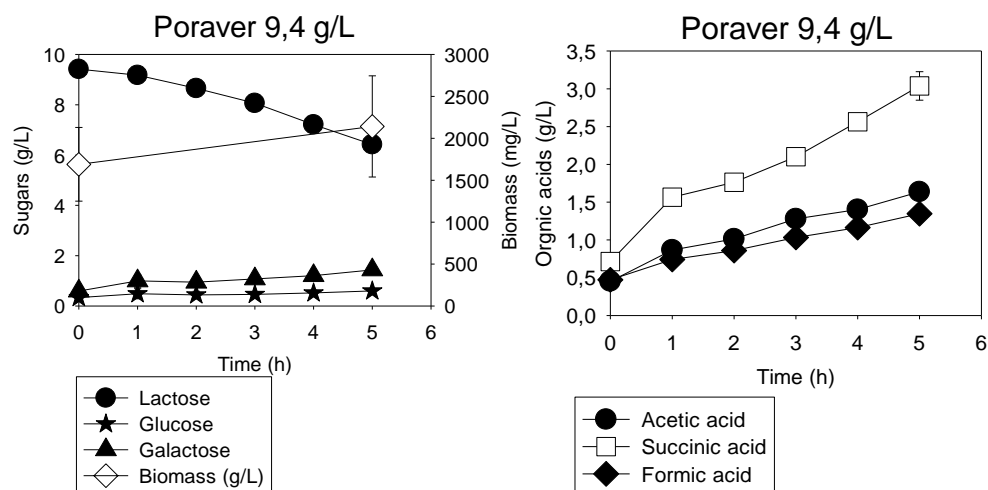


**Figure 7.15:** “Initial velocity method”. Biofilm fermentation tests with Poraver® - 9,4 g/L of pure lactose

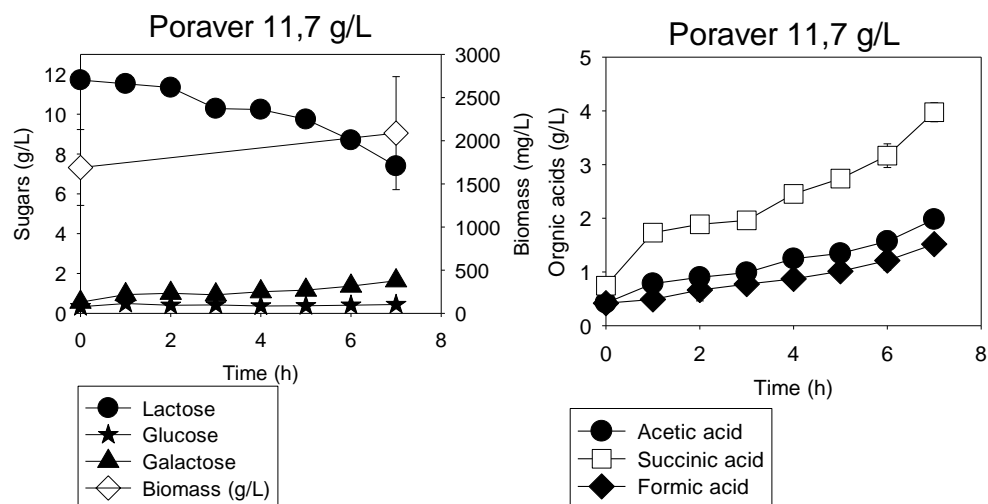


**Figure 7.16:** “Initial velocity method”. Biofilm fermentation tests with Poraver® - 11,7 g/L of pure lactose

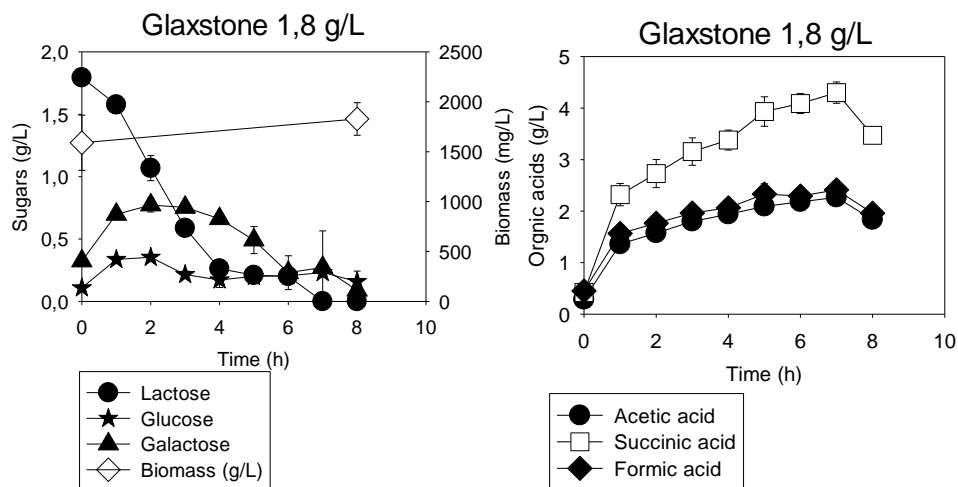


**Figure 7.17:** “Initial velocity method”. Biofilm fermentation tests with Glaxstone® - 1,8 g/L of equivalent lactose in milk whey

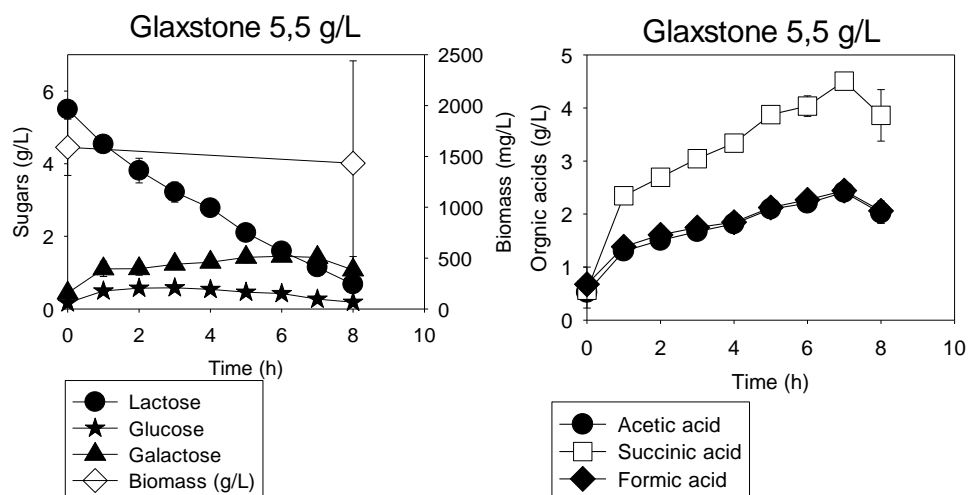


**Figure 7.18:** “Initial velocity method”. Biofilm fermentation tests with Glaxstone® - 5,5 g/L of equivalent lactose in milk whey

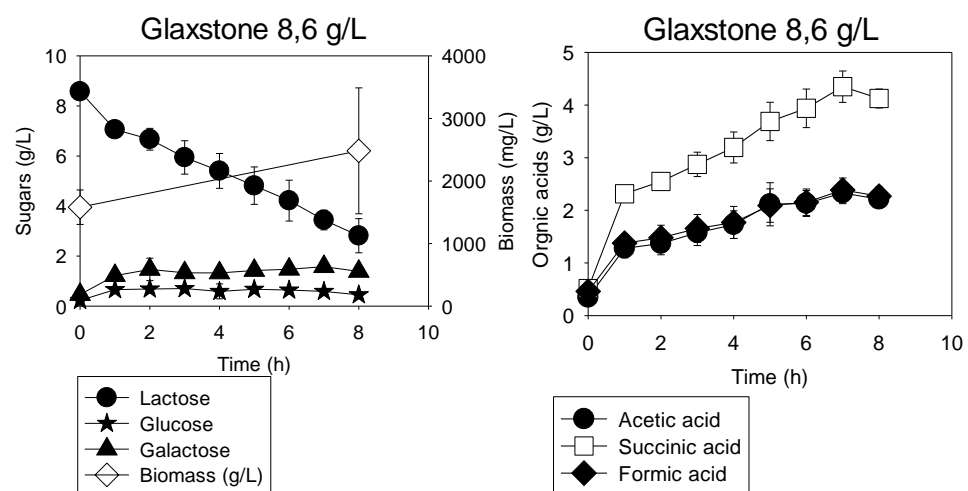


**Figure 7.19:** “Initial velocity method”. Biofilm fermentation tests with Glaxstone® - 8,6 g/L of equivalent lactose in milk whey

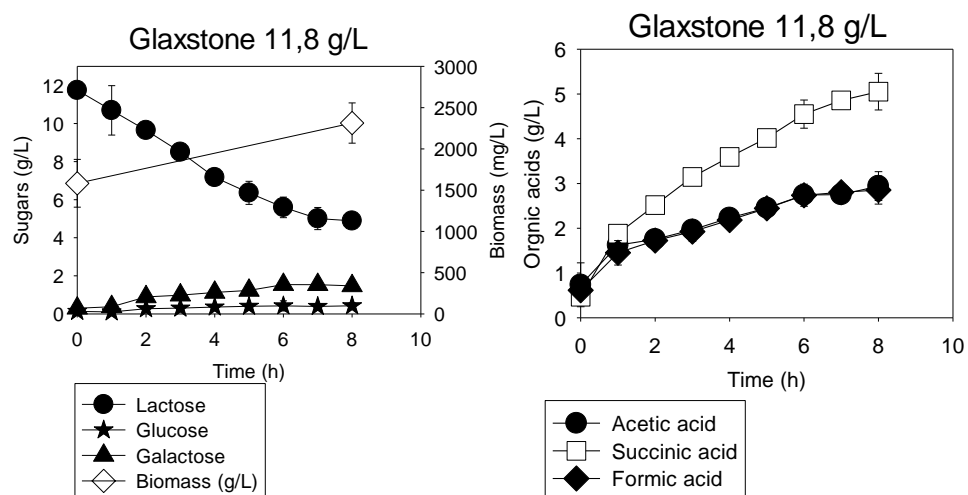


**Figure 7.20:** “Initial velocity method”. Biofilm fermentation tests with Glaxstone® - 11,8 g/L of equivalent lactose in milk whey

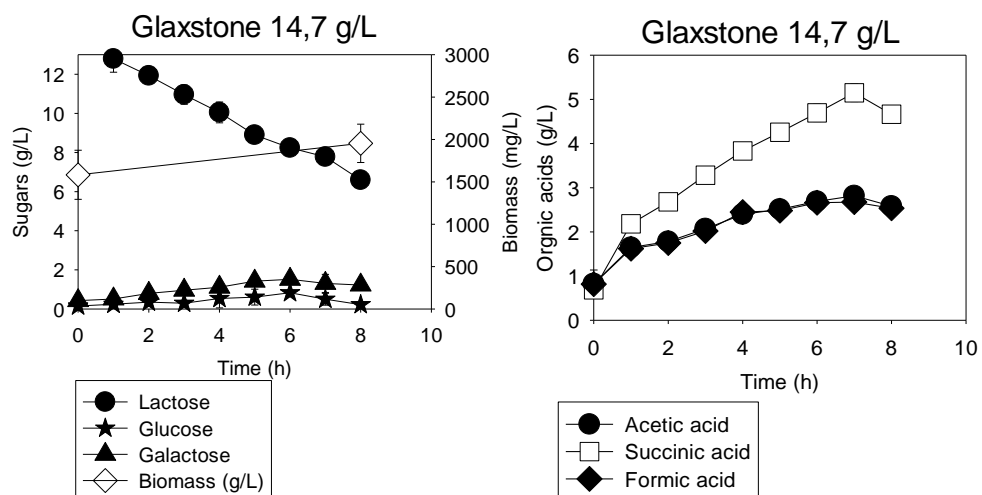


**Figure 7.21:** “Initial velocity method”. Biofilm fermentation tests with Glaxstone ® - 14,7 g/L of equivalent lactose in milk whey



## 8 REFERENCES

---

- A. Gianico, C. B. (2013). Ultrasonic and thermal pretreatments to enhance the anaerobic bioconversion of olive husks. *Bioresource Technology*, 147:623–626.
- A. Sluiter, B. H. (2008). *Determination of Total Solids in Biomass and Total Dissolved Solids in Liquid Process Samples - Laboratory Analytical Procedure (LAP)*. National Renewable Energy Laboratory.
- Aguilar, C. L. (1995). Degradation of volatile fatty acids by differently enriched methanogenic cultures: kinetics and Inhibition. *Water Research*, 29:505-509.
- Ahring, B. K. (1995). Volatile fatty acids as indicators of process imbalance in anaerobic digestors. *Applied Microbiology and Biotechnology*, 43:559-565.
- Akshat Tanksale, J. N. (2010). A review of catalytic hydrogen production processes from biomass. *Renewable and Sustainable Energy Reviews*, 14:166-182.
- Alastair J. Ward, P. J. (2008). Optimisation of the anaerobic digestion of agricultural resources. *Bioresource Technology*, 17:7928-7940.
- Alberto Vertova, G. A. (2009). Electrodialytic recovery of light carboxylic acids from industrial aqueous wastes. *J Appl Electrochem*, 39:2051-2059.
- Alén R. (2011). *Biorefining of forest resources*.
- Alexander Schiffer, G. F. (2010). *Handbook of Metalloproteins*. John Wiley & Sons.
- Alfons J. M. Stams, C. M. (2009). Electron transfer in syntrophic communities of anaerobic bacteria and archaea. *Nature Reviews Microbiology*, 7:568-577.
- Allen SA, C. W. (2010). Furfural induces reactive oxygen species accumulation and cellular damage in *Saccharomyces cerevisiae*. *Biotechnology for Biofuel*, 3-2.
- Amalendu Chakraverty, R. P. (2014). *Postharvest Technology and Food Process Engineering*. CRC Press.
- Amir Hussain, M. K.-L. (2015). Operational parameters and their influence on particle-side mass transfer resistance in a packed bed bioreactor. *AMB Express*, 5:51.
- Amlan K. Patra, Z. Y. (2014). Effects of vanillin, quillaja saponin, and essential oils on in vitro fermentation and protein-degrading microorganisms of the rumen. *Applied Microbiology and Biotechnology*, 2:897-905.
- Ana R.C. Morais, R. B.-L. (2013). Green Chemistry and the biorefinery concept. *Sustainable chemical processes*, 1: 18-21.
- Andersen, M. S. (2006). An introductory note on the environmental economics of the circular economy. *Sustainability Science*, 1-133-140.
- Ando, S. A. (1986). Identification of aromatic monomers in steam-exploded poplar and their influence on ethanol fermentation. *J. Ferment. Technol*, 64:546-570.
- Andrew D. Maynard, E. D. (2005). Airborne Nanostructured Particles and Occupational Health. *Journal of Nanoparticle Research*, Volume 7, Issue 6, pp 587-614.
- Angelidaki, M. et.al. (2009). Defining the biomethane potential (BMP) of solid organic wastes and energy crops: a proposed protocol for batch assays. *Water Science & Technology*, 59:927-934.
- Arantes V, S. J. (2010). Access to cellulose limits the efficiency of enzymatic hydrolysis: the role of amorphogenesis. *Biotechnol Biofuels*, 4:1-11.
- Arpiainen V. (2001). Production of light fuel oil from tall oil soap liquids by fast pyrolysis techniques. University of Jyväskylä.
- Ashok Pandey, R. H. (2015). *Industrial Biorefineries And White Biotechnology*. Elsevier.
- Astrup, T., & Bilitewski, B. (2011). *Pyrolysis and Gasification*. West Sussex, UK.

- Avery G. B., M. C. (1999). Controls on the stable carbon isotopic composition of biogenic methane produced in a tidal freshwater estuarine sediment. *Geochim. Cosmochim. Acta*, 63:1075–1082.
- AWWA. (1995). *Electrodialysis and Electrodialysis Reversal*. Denver: American Water Works Association.
- Axe, D. B. (1995). Transport of lactate and acetate through the energized cytoplasmic membrane of *Escherichia coli*. *Biotechnol Bioeng*, 47:8-19.
- Azhar, A. B. (1981). Factors affecting alcohol fermentation of wood acid hydrolysate. *Biotechnol. Bioeng. Symp.*, 293-300.
- B Bartolome, C. F. (1997). Enzymic release of ferulic acid from barley spent grain. *Journal of Cereal Science*, 1997, 3: 285-288.
- B. Kamm, M. K. (2004). Principle of biorefineries. *Applied Microbiology and Biotechnology*, 64:137-145.
- B.P. Tissot, D. W. (1985). *Petroleum Formation and Occurrence*. Tokio: Springer-Verlag.
- Banasiak, L. J. (2007). Desalination using electrodialysis as a function of voltage and salt concentration. *Desalination*, 205:38-46.
- Banasiak, L. J. (2007). Desalination using electrodialysis as a function of voltage and salt concentration. *Desalination*, 20:38-46.
- Banerjee S, M. S. (2010). Commercializing lignocellulosic bioethanol: technology bottlenecks and possible remedies. *Biofuels Bioprod Bioref*, 4:77-93.
- Barakat et.al. (2012). Effect of lignin-derived and furan compounds found in lignocellulosic hydrolysates on biomethane production. *Bioresource Technology*, 104:90-99.
- Bardet, M. R. (1985). On the reactions and degradation of the lignin during steam hydrolysis of aspen wood. *Sven. Papperstidn*, 6:61-67.
- Barelli, L. e. (2008). Hydrogen production through sorption-enhanced steam methane reforming and membrane technology: a review. *Energy*, 33:554-570.
- Bartl, A. (2014). Moving from recycling to waste prevention: A review of barriers and enables. *Waste Management & Research*, 32- 3:18 Supplement Data.
- Belkin, S., Wirsén, C., & Jannasch, H. (1986). A new sulfur-reducing, extremely thermophilic eubacterium from a submarine thermal vent. *Appl. Environ. Microbiol.*, 51:1180-1185.
- Benefits of Black Liquor Gasification*. (2003). Retrieved from The Center For Paper Business And Industries Studies:  
<http://www.paperstudies.org/research/projects/gasification/background.htm>
- Bertin, L., Bettini, C., Zanaroli, G., Fraraccio, S., Negroni, A., & Fava, F. (2012). Acclimation of an anaerobic consortium capable of an effective biomethanization of mechanically-sorted organic fraction of municipal solid waste through a semi-continuous enrichment procedure. *Journal Of Chemical Technology and Biotechnology*, 9:1312-1319.
- Bertin, L., Bettini, C., Zanaroli, G., Fraraccio, S., Negroni, A., & Fava, F. (2012). Acclimation of an anaerobic consortium capable of an effective biomethanization of mechanically-sorted organic fraction of municipal solid waste through a semi-continuous enrichment procedure. *Journal Of Chemical Technology And Biotechnology*, 87:1312-1319.
- Bertin, L., Lampis, S., Todaro, D., Scoma, A., Vallini, G., Marchetti, L., . . . Fava, F. (2010). Anaerobic acidogenic digestion of olive mill wastewaters in biofilm reactors packed with ceramic filters or granular activated carbon. *Water Research*, 15:4537-4549.
- Biely P. (2012). Microbial carbohydrate esterases deacetylating plant polysaccharides. *Biotechnol Adv.* 2012, 6:1575-1588.
- Biermann, Christopher J. (1993). *Essentials of Pulping and Papermaking*. San Diego: Academic Press.

- Biwei Sua, A. H. (2013). A review of the circular economy in China: moving from rhetoric to implementation. *Journal of Cleaner Production*, 42:215-227.
- Biwei Sua, A. H. (2013). A review of the circular economy in China: moving from rhetoric to implementation. *Journal of Cleaner Production*, 42:215-227.
- Bougrier C, B. A.-P. (2007). Combined ozone pretreatment and anaerobic digestion for the reduction of biological sludge production in wastewater treatment. *Ozone Sci Eng*, 29:201-206.
- Bougrier C, D. J. (2007). Impacts of thermal pre-treatments on the semicontinuous anaerobic digestion of waste activated sludge. *Biochem Eng J.*, 34:20-27.
- Boyaval, P. C. (1987). Continuous lactic acid fermentation with concentrated product recovery by ultrafiltration and electrodialysis. *Biotechnology Letters*, 9:207-212.
- Boyer, L. V. (1992). The effects of furfural on ethanol production by *S.cerevisiae*. *Biomass Bioeng*, 3:41-48.
- Braun, R. L., & Burnham, I. K. (1993). Chemical Reaction Model for Oil and Gas Generation from Type I and Type II Kerogen. *Lawrence Livermore National Laboratory Publication*.
- BRIDGES. (2013). *Bringing together Research and Industry for the Development of Glider Environmental Services*. Retrieved from Horizon 2020: <http://www.bridges-h2020.eu/>
- Brioukhanov, A. A. (2006). The catalase and superoxide dismutase genes are transcriptionally up-regulated upon oxidative stress in the strictly anaerobic archaeon *Methanosarcina bakeri*. *Microbiology*, 152:1671-1677.
- Burak Demirel, P. S. (2008). The roles of acetotrophic and hydrogenotrophic methanogens during anaerobic conversion of biomass to methane: a review. *Reviews in Environmental Science and Bio/Technology*, 2:173-190.
- C. Curtain. (2000). Plant biotechnology- the growth of Australia's algal  $\beta$ -carotene industry. *Australas Biotechnol*, 10-19.
- C.R. Shen, J. (2008). Metabolic engineering of *Escherichia coli* for 1-butanol and 1-propanol production via the keto-acid pathways. *Metabolic Engineering*, 10:312-320.
- Calli, B. M. (2005). Effects of high free ammonia concentrations on the performances of anaerobic bioreactors. *Process Biochemistry*, 40:1285–1292.
- Canfield, D. E. (2005). *Thermodynamics and Microbial Metabolism In Aquatic Geomicrobiology*. San Diego: Elsevier Academic Press.
- Cao Y, Z. R. (2013). Fermentative Succinate Production: An Emerging Technology to Replace the Traditional Petrochemical Processes. *Hindawi Publishing Corporation*, 147:5-12.
- Cappelletti et.al. (2012). Biohydrogen production from glucose, molasses and cheese whey by suspended and attached cells of four hyperthermophilic *Thermotoga* strains. *J Chem Technol Biotechnol*, 87:1291-1301.
- Carlier JP, B.-F. M. (2010). Proposal to unify *Clostridium orbiscindens* and *Eubacterium plautii* with description of *Flavonifractor plautii*, and reassignment of *Bacteroides capillosus* to *Pseudoflavonifractor capillosus*. *Int J Syst Evol Microbiol*, 60:585-590.
- Carmo, M. e. (2013). A comprehensive review on PEM water electrolysis. *International Journal of Hydrogen Energy*, 38:4901-4934.
- CC Pegels, C. W. (2005). Application of the theory of constraints to a bottleneck operation in a manufacturing plant. *Journal of Manufacturing Technology*, 16:302-311.
- Cedervall PE, D. M. (2010). Structural insight into methyl-coenzyme M reductase chemistry using coenzyme B analogues. *Biochemistry*, 49:7683–7693.
- Centre, N. N.-F. (2011). *NNFCC Renewable Fuels and Energy Factsheet: Anaerobic Digestion*".
- Chao Jin, M. Y.-f. (2011). Progress in the production and application of n-butanol as a biofuel. *Renewable and Sustainable Energy Reviews*, 8:4080-4106.

- Cheng K, Z. X. (2012). Biotechnological production of succinic acid: current state and perspectives. *Society of Chemical Industry*, 15:302-318.
- Cheng YS, Z. Y. (2010). Evaluation of high solids alkaline pretreatment of rice straw. *Appl Biochem Biotech*, 162:1768-1784.
- Chengjian Yang, J. A. (2016). Nitrate and Inhibition of Ruminant Methanogenesis: Microbial Ecology, Obstacles, and Opportunities for Lowering Methane Emissions from Ruminant Livestock. *Front. Microbiol*, DOI=10.3389/fmicb.2016.00132.
- Circle Economy. (2010). *About the circular economy*. Retrieved from <http://www.circle-economy.com/circular-economy/>
- Claassen PAM, L. C. (1999). Utilisation of biomass for the supply of energy carriers. *Applied Microbiology and Biotechnology*, 52:741-755.
- Clean Edge, Inc. (2013). *Clean Energy Trends*.
- Conrado, R. J. (2014). Envisioning the bioconversion of methane to liquid fuels. *Science*, 343-621:623.
- Corinna Bang, C. E.-V. (2014). Biofilm formation of mucosa-associated methanoarchaeal strains. *Frontiers in Microbiology*, 353:1-9.
- Corma A, I. S. (2007). Chemical routes for the transformation of biomass into chemicals. *Chem Rev*, 107:2411–502.
- D. Botheju, a. R. (2010). Bio-gasification under partially aerated conditions; Results from batch experiments. *Submitted Manuscript to the proceedings of the Linnaeus Eco-Tech'10, The 7th International Conference on the Establishment of Cooperation Between Companies and Institutions in the Nordic Countries, the Baltic Sea Region, and the World, Kalmar*.
- D. Botheju, B. L. (2010). Oxygen effects in Anaerobic Digestion – II. *Modeling, Identification and Control*, 2:55-65.
- D. Lagadic-Gossmann, L. H. (2004). Alterations of intracellular pH homeostasis in apoptosis: origins and roles. *Cell Death and Differentiation*, 11:953-961.
- D. Pleissner, J. V. (2014). Agricultural residues as feedstocks for lactic acid fermentation. In R. L. S.O. Obare, *Green Technologies for the Environment* (pp. 247-263). American Chemical Society.
- D. Vasudevan. (1995). Reduction of maleic-acid at a Ti ceramic at TiO<sub>2</sub> cathode. *Journal of applied electrochemical*, 14:176-178.
- D.R. Ranade, , A. (1999). Evaluation of the use of sodium molybdate to inhibit sulphate reduction during anaerobic digestion of distillery waste. *Bioresource Technology*, 3:287–291.
- D'Ippolito, G. D. (2010). Hydrogen metabolism in the extreme thermophile *Thermotoga neapolitana*. *Int. J. Hydrogen Energy*, 35:2290-2295.
- DA. Glassner, D. A. (1995). Purification process for succinic acid produced by fermentation. *Applied Biochemistry and Biotechnology*, 51:73-82.
- Daniel Pleissner, Q. Q. (2015 in press). Valorization of organic residues for the production of added value chemicals: A contribution to the bio-based economy. *Biochemical Engineering Journal*, doi:10.1016/j.bej.2015.12.016.
- Daniel Pleissner, Q. Q. (2015). Valorization of organic residues for the production of added value chemicals: A contribution to the bio-based economy. *Biochemical Engineering Journal*, <http://dx.doi.org/10.1016/j.bej.2015.12.016>.
- Dario Frascari, M. C. (2013). A kinetic study of biohydrogen production from glucose, molasses and cheese whey by suspended and attached cells of *Thermotoga neapolitana*. *Bioresource Technology*, 147:553-561.

- Day, J. I.-O. (1970). Enzymic reduction of long-chain acyl-CoA to fatty aldehyde and alcohol by extracts of *Clostridium butyricum*. *Biochimica et Biophysica Acta (BBA)-Lipids and Lipid Metabolism*, 218:179-182.
- De Vrije, T. B. (2009). Efficient hydrogen production from the lignocellulosic energy crop *Miscanthus* by the extreme thermophilic bacteria *Caldicellulosiruptor saccharolyticus* and *Thermotoga neapolitana*. *Biotechnol. Biofuels*, 2:12-27.
- Delbes, C. R.-J. (2000). Monitoring of activity dynamics of an anaerobic digester bacterial community using 16S rRNA polymerase chain reaction–single-strand conformation polymorphism analysis. *Environmental Microbiology*, 5:506-515.
- Demirel, B. a. (2011). Trace element requirements of agricultural biogas digesters during biological conversion of renewable biomass to methane. *Biomass and Bioenergy*, 35:992-998.
- Diaz de Villegas, M. V. (1992). Conversion of furfural into furfuryl alcohol by *Saccharomyces cerevisiae*. *Acta Biotechnol.*, 12:351-354.
- Diego AF, R. C. (2007). Can ionic liquids dissolve wood? processing and analysis of lignocellulosic materials with 1-n-butyl-3-methylimidazolium chloride. *Green chemistry*, 9:63-69.
- Digman MF, S. K.-J. (2010). Optimizing on-farm pretreatment of perennial grasses for fuel ethanol production. *Bioresour Technol*, 101:305-314.
- Dorado, M. P. (2009). Cereal-based biorefinery development: utilisation of wheat milling by-products for the production of succinic acid. *Journal of biotechnology*, 143:51-59.
- Dufour, A. e. (2015). Catalytic conversion of methane over a biomass char for hydrogen production: deactivation and regeneration by steam gasification. *Applied Catalysis A: General*, 490: 170-180.
- Dunlop, A. (1948). Furfural formation and behaviour. *Ind. Eng. Chem.*, 40:204-209.
- Dutta, S. (2014). A review on production, storage of hydrogen and its utilization as an energy resource. *Journal of Industrial and Engineering Chemistry*, 20:1148-1156.
- DW Pearce, R. T. (1990). *Economics of natural resources and the environment*. JHU Press.
- E. Dinuccio, . P. (2010). Evaluation of the biogas productivity potential of some Italian agro-industrial biomasses. *Bioresource Technology*, 10:3780–3783.
- Earle MJ, S. K. (2000). Ionic liquids - green solvents of future. *Pure Appl Chem*, 72:1391-1398.
- Ellen MacArthur Foundation. (2012). Towards the Circular Economy: an economic and business rationale for an accelerated transition., (pp. 1-60).
- EllenMcCarthur Foundation. (2013). Retrieved from Ellen MacArthur Foundation (2013) (<http://www.ellenmacarthurfoundation.org/circular-economy/circular-economy/interactive-system-diagram>).
- El-Mashad HM, Z. R. (2010). Biogas production from co-digestion of dairy manure and food waste. *Bioresour Technol*, 101:4021-4028.
- Emiliano Bruni, A. P. (2010). Anaerobic digestion of maize focusing on variety, harvest time and pretreatment. *Applied Energy*, 7:2212–2217.
- Environmental and Protection Agency, World Health Organization. (2012). *Provisional Assessment of Recent Studies on Health Effects of Particulate Matter Exposure*.
- Environmental Protection Agency. (1987). *EPA.gov*. Retrieved from Particulate Matter: <http://www3.epa.gov/pm/>
- Environmental Protection Agency. (2014). *Climate change indicators in the United States*. Washington: U.S. Environmental Protection Agency.
- European Biogas Association. (2013). *Biogas/Biomethane for use as a transport fuel*. Retrieved from European Biofuel Technology Platform.
- European Commission. (1994). *The Packaging and Packaging Waste Directive*.
- European Commission. (1999). *The Landfill Directive*.

- European Commission. (2000). *The End-of-life Vehicles Directive*.
- European Commission. (2006). *The Batteries Directive*.
- European Commission. (2008). *The Waste Framework Directive*.
- European Commission. (2012). *The Waste Electrical and Electronic Equipment Directive*.
- European Commission. (2015). *Action Plan for the Circular Economy*. Bruxelles.
- European Commission report. (2015, June). *HORIZON 2020 - The EU Framework Programme for Research and Innovation*. Retrieved from Horizon 2020 kick-starts Bio-based industries in Europe with €50 million: <https://ec.europa.eu/programmes/horizon2020/en/news/horizon-2020-kick-starts-bio-based-industries-europe-%E2%82%AC50-million>
- European Union. (2008). Directive 2008/98/EC of the European Parliament and of the Council of 19 november 2008 on waste and repealing certain directives. *Official Journal of EU*.
- European Union. (50 / 2008). *Air Quality Directive*.
- Eva Palmqvist, B. H.-H. (2000). Fermentation of lignocellulosic hydrolysates. II: inhibitors and mechanisms of inhibition. *Bioresource Technology* 74 (2000) 25±33, 4:25-33.
- FAO. (2012). *The state of food insecurity of the world: Undernourishment around the world in 2012*. Rome.
- FAO. (2014). *Food wastage footprint. Impacts on natural resources - Summary Report*.
- Fayyaz Ali Shah, Q. M. (2014). Microbial Ecology of Anaerobic Digesters: The Key Players of Anaerobiosis. *ScientificWorldJournal*, 183752.
- Feng Y, Z. Y. (2014). Enhanced anaerobic digestion of waste activated sludge digestion by the addition of zero valent iron. *Water Res*, 52:242-250.
- Fernández-Rodríguez J, P. M. (2014). Dry thermophilic anaerobic digestion of the organic fraction of municipal solid wastes: solid retention time optimization. *Chem Eng J*, 251:435-444.
- Field, J. A. (1987). The methanogenic toxicity and anaerobic degradability of a hydrolyzable tannin. *Water Research*, 21:367-374.
- Field, J. A. (1989). The tannin theory of methanogenic toxicity. *Biological Wastes*, 29:241-262.
- Fogler, H. S. (2014). *Essential Of Chemical Reactions Engineering*. Pearson Edu.
- Forster-Carneiro T, P. M. (2008). Thermophilic anaerobic digestion of source-sorted organic fraction of municipal solid waste. . *Bioresour Technol*, 99:6763-6760.
- Francesco Cherubini, G. J. (2009). Toward a common classification approach for biorefinery systems. *Biofuel, Bioproducts and Biorefineries*, 5: 534–546.
- Francisco, J. S. (1993). Specific adhesion and hydrolysis of cellulose by intact Escherichia coli expressing surface anchored cellulase or cellulose binding domains. *Biotechnology*, 11:491-495.
- G. Gottschalk, a. S. (1992). *The anaerobic life: A handbook on the biology of bacteria, vol. 1: ecophysiology, isolation, identification, application*. New York: Springer-Verlag, 2nd ed.
- G. Montante, A. P. (2012). Analysis of dilute solid-liquid suspensions in turbulent stirred tanks. *Chemical Engineering Research and Design*, 90:1448-1456.
- G. Montante, F. L. (2010). Two-phase flow and bubble size distribution in air-sparged and surface-aerated vessels stirred by a dual impeller. *Industrial and Engineering Chemistry Research*, 49:2613-2623.
- G. Montante, M. C. (2013). Computational analysis of a vortex ingesting bioreactor for hydrogen production. *Chemical Engineering Transactions*, 32: 721-726.
- Gallucci, F. e. (2013). Recent advances on membranes and membrane reactors for hydrogen production. *Chemical Engineering Science*, 92:40-66.
- Gerard Muyzer, A. J. (2008). The ecology and biotechnology of sulphate-reducing bacteria. *Nature reviews | microbiology*, 6:441-454.

- Ghezzaz H, P. L. (2012). Biorefinery implementation for recovery debottlenecking at existing pulp mills - Part I: potential for debottlenecking. *Tappi J*, 7:17-25.
- Ghirardi ML. (2006). Hydrogen production by photosynthetic green algae. *Indian J Biochem Biophys*, 43:201-210.
- Ghisellini, P. e. (2015). A review on circular economy: the expected transition to a balanced interplay of environmental and economic systems. *Journal of Cleaner Production*.
- GmbH. (n.d.). Retrieved from <http://www.pca-gmbh.com/membrane/datasht2.htm>
- Goldberg, E. (1997). *Handbook of Downstream Processing*. Chapman & Hall.
- Gollapalli LE, D. B. (2002). Predicting digestibility of ammonia fibre explosion (AFEX) treated rice straw. *Appl Biochem Biotechnol*, 100:23-25.
- Gottschalk, G. (2006). *Bacterial Metabolism*. Weinheim: WILEY-VCH Verlag GmbH & Co. KGaA.
- Gredmaier, L. (2013, April). *Notes on Bioenergy, Biofuels and Energy-from-waste*. Retrieved from Biofuel Lecture Notes: <http://www.southampton.ac.uk/~lg1e08/cenv6141/biofuellecturenotes.html>
- Gu Y, C. X. (2014). Effect of inoculum sources on the anaerobic digestion of rice straw. *Bioresour Technol*, 158:149-155.
- Guerrero, M. S. (2008). Extraction of polyphenols from white distilled grape pomace: Optimization and modelling. *Bioresour technol*, 99:1311-1318.
- Guettler MV, R. D. (1999). *Actinobacillus succinogenes* sp. nov., a novel succinic-acid-producing strain from the bovine rumen. *Int J Syst Bacteriol*, 1:207-216.
- Guettler MV, R. D. (1999). *Actinobacillus succinogenes* sp. nov., a novel succinic-acid-producing strain from the bovine rumen. *International Journal of Systematic Bacteriology*, 19:207-216.
- Guo, X. e. (2014). Direct, nonoxidative conversion of methane to ethylene, aromatics, and hydrogen. *Science*, 344:616-619.
- Gustavsson, J. e. (2011). *The methodology of the FAO study: "Global Food Losses and Food Waste—extent, causes and prevention*. SIK The Swedish Institute for Food and Biotechnology.
- H. Detlef Klüber, R. C. (1998). Effects of nitrate, nitrite, NO and N<sub>2</sub>O on methanogenesis and other redox processes in anoxic rice field soil. *FEMS Microbiology Ecology*, 3:301-318.
- Hafner, S. B. (2009). Modeling of ammonia speciation in anaerobic digesters. *Water Research*, 43:4105-4114.
- Hallac BB, R. A. (2011). Analyzing cellulose degree of polymerization and its relevancy to cellulosic ethanol. *Biofuels Bioprod Bioref*, 5:215-225.
- Hallenbeck, P. D. (2009). Advances in fermentative biohydrogen production: the way forward? *Trends Biotechnol*, 27:287-297.
- Hannah Akinosho, K. Y. (2014). The emergence of *Clostridium thermocellum* as a high utility candidate for consolidated bioprocessing applications. *Front. Chem.*, 26 August 2014, 2:1-18.
- Hansen, K. A. (1998). Anaerobic digestion of swine manure: inhibition by ammonia. *Water Research*, 35:5-12.
- Harada, H. S. (1994). Interaction between sulfate-reducing bacteria and methane-producing bacteria in UASB reactors fed with low strength wastes containing different levels of sulfate. *Water Research*, 28:355-367.
- Harris, J. R. (1986). Solvent production by *Clostridium pasteurianum* in media of high sugar content. *Biotechnol. Lett*, 8:889-892.
- Hartmann H, A. B. (2005). Anaerobic digestion of the organic fraction of municipal solid waste: influence of co-digestion with manure. *Water Res*, 39:1543-1552.

- Haryanto, A. e. (2005). Current status of hydrogen production techniques by steam reforming of ethanol: a review. *Energy & Fuels*, 19: 2098-2106.
- Hasegawa S, S. N. (2000). Solubilization of organic sludge by thermophilic aerobic bacteria as a pretreatment for anaerobic digestion. *Water Sci Technol*, 41:163-169.
- Hasunuma T, O. F. (2013). A review of enzymes and microbes for lignocellulosic biorefinery and the possibility of their application to consolidated bioprocessing technology. *Bioresour Technol*, 135:513-522.
- Hedin, L. O. (1998). Thermodynamic constraints of nitrogen transformation and other biogeochemical process at soil-stream interfaces. *Ecology*, 79:684-703.
- Heike Sträuber, M. S. (2012). Metabolic and microbial community dynamics during the hydrolytic and acidogenic fermentation in a leach-bed process. *Energy, Sustainability and Society*, 2:13-14.
- Heipieper, H. W. (1994). Mechanism of resistance of whole cells to toxic organic solvents . *TIBTECH*, 12:409-415.
- Helmut Rechberger, T. H. (2010). *Solid Waste Technology & Management*. Blackwell Publishing Ltd.
- Herbert Pobeheim, B. M. (2010). Influence of trace elements on methane formation from a synthetic model substrate for maize silage. *Bioresource Technology*, 2:836–839.
- Hill K, H. R. (2009). Natural fats and oils. In *Sustainable solutions for modern economies* (pp. 167-237). Cambridge: RSC Publ.
- Hiroshi Kaneda, K. S. (1985). *U.S.A. Patent No. US4539088 A*.
- Ho, L. H. (2012). Mitigating ammonia inhibition of thermophilic anaerobic treatment of digested piggery wastewater: use of pH reduction, zeolite, biomass and humic acid. *Water Research* , 46:4339–4350.
- Höfer R, Bigorra J. (2008). Biomass-based green chemistry: sustainable solutions for modern economies. *Green Chem Lett Rev*, 1:79.
- Hong SH, K. J. (2004). The genome sequence of the capnophilic rumen bacterium *M. succinoproducens*. *Nature Biotechnology*, 22:1275-1281.
- Hungate RE. (1969). A role tube method for cultivation of strict anaerobes. *Meth Enzymol*, 3B:117-132.
- Hyeok Choi, K. Z. (2005). Influence of cross-flow velocity on membrane performance during filtration of biological suspension. *Journal of Membrane Science*, 148:189-199.
- Hyne, N. J. (2001). Nontechnical Guide to Petroleum Geology, Exploration, Drilling and Production. In N. J. Hyne, *Nontechnical Guide to Petroleum Geology, Exploration, Drilling and Production* (pp. 1-4).
- IEA. (2014). *Task 42 Biorefinery*.
- IEA. (2014). *Task 42 for Biorefinery*.
- Ingram T, R. T. (2009). Semicontinuous liquid hot water pretreatment of rye straw. *J Supercrit Fluid*, 48:238-246.
- Ingrid H. Franke-Whittle, A. W. (2014). Investigation into the effect of high concentrations of volatile fatty acids in anaerobic digestion on methanogenic communities. *Waste Management*, 11:2080-2089.
- Intergovernmental Panel on Climate Change. (2014). *Climate Change 2014: Synthesis Report*. Geneva: Intergovernmental Panel On Climate Change.
- International Energy Agency. (2009). Retrieved from InterEnerStat Meeting: [http://www.iea.org/interenerstat\\_v2/meeting/2009/Coal.pdf](http://www.iea.org/interenerstat_v2/meeting/2009/Coal.pdf)
- International Energy Agency. (2013). *Resources to Reserves*. IEA.
- International Energy Agency. (2015). *CO2 Emissions from Fuel Combustion*. Paris: IEA Publishing.



- Isom, C. E. (2015). Improved conversion efficiencies for n-fatty acid reduction to primary alcohols by the solventogenic acetogen "Clostridium ragsdalei". *Journal of industrial microbiology & biotechnology*, 42:29-38.
- J. C. Akunna, N. B. (1998). Effect of Nitrate on Methanogenesis at Low Redox Potential. *Environmental Technology*, 12:1249-1254.
- J. Catalano, J. T. (2012). The effect of relative humidity on the gas permeability and swelling in PFSI membranes. *International Journal of Hydrogen Energy*, 37: 6308-6316.
- J. E. Johansen, a. R. (2006). Enhancing hydrolysis with microaeration. *Water Science and Technology*, 53:43-50.
- J. Gerritse, F. S. (1990). Mixed chemostat cultures of obligately aerobic and fermentative or methanogenic bacteria grown under oxygen-limiting conditions. *FEMS Microbiology Letters*, 66:87-94.
- J. Guendouz, P. B.-P. (2010). Dry anaerobic digestion in batch mode: Design and operation of a laboratory-scale, completely mixed reactor. *Waste Management*, 10:1768-1771.
- J. H. Martin, a. D. (1988). Degradation of DNA in cells and extracts of the obligate anaerobic bacterium Roseburia cecicola upon exposure to air. *Applied and Environmental Microbiology*, 6:1619-1621.
- J. P. Adams, C. M. (2013). Development of GSK's acid and base selection guides. *Green Chemistry*, 15: 1542-1549.
- James L. Unmack, M. C. (2011). *1 - propanol. Healt Base Assesment and Reccomendation for HEAC*.
- Jana SK, G. V. (1994). Production and hydrolytic potential of cellulase enzymes from a mutant strain of Trichoderma reesei. *Biotechnol Appl Bioc*, 20-233-239.
- Jannasch, H., Huber, R., Belkin, S., & Stetter, K. (1988). Thermotoga neapolitana sp. nov. of the extremely thermophilic, eubacterial genus Thermotoga. *Arch. Microbiol.* , 150:103-104.
- Jarrell, K. F. (1985). Extreme oxygen sensitivity in methanogenic archaeobacteria. *Bioscience*, 5:298-302.
- Jin, M. e. (2011). Consolidated bioprocessing (CBP) performance of Clostridium phytofermentans on AFEX-treated corn stover for ethanol production. *Biotechnology and Bioengineering*, 108:1290-1297.
- Jin-Young Jung, S.-M. L.-K.-C. (2000). Effect of pH on Phase Separated Anaerobic Digestion. *Biotechnol. Bioprocess Eng.*, 5:456-459.
- João C. Queiroz, M. V. (2010). Control of sulfate reducing bacteria through the application of sodium molybdate. *2nd Mercosur Congress on Chemical Engineering*.
- John A. Mathews, H. T. (2011). Towards a circular economy in China. *Journal of Industrial Ecology*, 3:435-457.
- Jonsson, L. P.-H. (1998). Detoxification of wood hydrolysates with laccase and peroxidase from the white-rot fungus Trametes versicolor. *Appl. Microbiol. Biotechnol.*, 49:691-697.
- Joseph G. Usack, C. M. (2012). Continuously-stirred Anaerobic Digester to Convert Organic Wastes into Biogas: System Setup and Basic Operation. *J Vis Exp*, 65:3978.
- Joseph J. Bozell, G. R. (2010). Technology development for the production of biobased products from biorefinery carbohydrates—the US Department of Energy’s “Top 10” revisited. *Green Chemistry*, 12:539-541.
- Juan E. Ramírez-Morales, E. T.-V.-A.-F. (2015). Simultaneous production and separation of biohydrogen in mixed culture systems by continuous dark fermentation. *Water Sci Tech*, 71:1271-1285.

- Jungmeier G, S. H. (2013). A biorefinery fact sheet for the sustainability assessment of energy driven biorefinery. *Conference Proceedings of the 21st European Biomass Conference*. Copenhagen: IEA.
- Jyri-Pekka Mikkola, E. S. (2010). *The Biorefinery and Green Chemistry*. Helsinki.
- K. Alfonsi, J. C. (2008). The Good, the Bad and the Ugly. A guide to solvent selection. *Green Chemistry*, 10: 31-36.
- Kail-Lai G. Ho, A. L. (1997). Optimization of L-(1)-Lactic Acid Production by Ring and Disc Plastic Composite Supports through Repeated-Batch Biofilm Fermentation. *Applied and Environmental Microbiology*, 63:2533–2542.
- Kajan Srirangan, e. a. (2013). Manipulating the sleeping beauty mutase operon for the production of 1- propanol in engineered Escherichia coli. *Biotechnology for Biofuels*, 6:139-145.
- Kalogirou, S. A. (2005). Seawater desalination using renewable energy sources. *Progress in energy and combustion science*, 31:242-281.
- Kamm B., K. M. (2005). Principles of biorefineries. *Appl Microbiol Biotechnol*, 64:137–145 .
- Kammerer, D. e. (2004). Polyphenol screening of pomace from red and white grape varieties (*Vitis vinifera* L.) by HPLC-DAD-MS/MS. *Journal of Agricultural and Food Chemistry*, 14:4360-4367.
- Kan Liu, H. K. (2014 a). Continuous syngas fermentation for the production of ethanol n-propanol and n-butanol. *Bioresource Technology*, 151:69-77.
- Kan Liu, H. K. (2014). Mixed culture syngas fermentation and conversion of carboxylic acids into alcohols . *Bioresource Technology* 152 (2014) 337-346, 152:337-346.
- Kayhanian, M. (1999). Ammonia inhibition in high-solids biogasification: an overview and practical solutions. *Environmental Technology*, 20:355-365.
- Ke-Ke Cheng, X.-B. Z.-A. (2012). Biotechnological production of succinic acid: current state and perspectives. *Biofuels, Bioprod. Bioref*, :6:302-318.
- Kim M, S. R. (2002). Reactor configuration-Part I. Comparative process stability and efficiency of mesophilic anaerobic digestion. *Environ Technol*, 6:631-642.
- Kim, M. I. (2009). Continuous Production of Succinic Acid Using an External Membrane Cell Recycle System. *J. Microbiol. Biotechnol.*, 19:1369-1373.
- Kim, Y. B. (2011). Series assembly of microbial desalination cells containing stacked electrodialysis cells for partial or complete seawater desalination. *Environmental science & technology*, 45:5840-5845.
- Kirsten J.J. Steinbusch, H. V. (2008). Alcohol production through volatile fatty acids reduction with hydrogen as electron donor by mixed cultures. *Water research*, 42:4059-4066.
- Kobayashi N, O. N. (2009). Characteristics of solid residues obtained from hot-compressed-water treatment of woody biomass. *Ind Eng Chem Res* , 48:373-379.
- Kouichi Izumi, Y.-k. O. (2010). Effects of particle size on anaerobic digestion of food waste. *International Biodeterioration & Biodegradation*, 7:601–608.
- Kubota, H. e. (2008). Biofilm formation by lactic acid bacteria and resistance to environmental stress. *Journal of bioscience and bioengineering*, 106:381-386.
- Kurzrock, T. D.-B. (2010). Recovery of succinic acid from fermentation broth. *Biotechnology letters*, 32:331-339.
- Kurzrock, T. D.-B. (2010). Recovery of succinic acid from fermentation broth. *Biotechnology letters*, 32:331-339.
- L. Bertin et.al. (2012 (a)). A continuous-flow approach for the development of an anaerobic consortium capable of an effective biomethanization of a mechanically sorted-organic fraction of municipal solid waste as the sole substrate. *Water Research*, 46:413-424.

- L. Hao, P. J. (2009). Regulating the hydrolysis of organic waste by micro-aeration and effluent recirculation. *Waste Management*, 29:2042-2050.
- Lapierre, C. R. (1983). Characterization of poplar lignins acidolysis products: capillary gas-liquid and liquid-liquid chromatography of monomeric compounds. *Holzforschung*, 37:189-198.
- Larsson S, P. E.-H.-O. (1999). The generation of fermentation inhibitors during dilute acid hydrolysis of softwood. *Enzyme Microb Tech*, 24:151-159.
- Larsson, S. Q.-S.-O. (2000). Influence of lignocellulose-derived aromatic compounds on oxygen-limited growth and ethanolic fermentation by *Saccharomyces cerevisiae*. *Appl. Biochem. Biotechnol*, 84:617-632.
- Lee, H.-J. e. (2002). Designing of an electrodialysis desalination plant. *Desalination*, 142:267-286.
- Lei Z, C. J. (2010). Methane production from rice straw with acclimated anaerobic sludge: effect of phosphate supplementation. *Bioresour Technol*, 101:4343-4348.
- Leif J Jönsson, B. A.-O. (2013). Bioconversion of lignocellulose: inhibitors and detoxification. *Biotechnology for Biofuels*, 6:16.
- Lett, L. A. (2014). Global threats, waste recycling and the circular economy concept. *Revista Argentina de Microbiología*, 1:1-2.
- Leung, C. C. (2012). Utilisation of waste bread for fermentative succinic acid production. *Biochemical Engineering Journal*, 65:10-15.
- Li KC, A. P. (2000). Relationship between activities of xylanases and xylan structures. *Enzym Microb Tech*, 27:89-94.
- Li Q, H. Y. (2009). Improving enzymatic hydrolysis of wheat straw using ionic liquid 1-ethyl-3-methyl imidazolium diethyl phosphate pretreatment. *Bioresour Technol*, 100:3570-3575.
- Li Y, Z. R. (2014). Anaerobic co-digestion of chicken manure and corn stover in batch and continuously stirred tank reactor (CSTR). *Bioresour Technol*, 156:342-347.
- Li, Q. e. (2010). Efficient conversion of crop stalk wastes into succinic acid production by *Actinobacillus succinogenes*. *Bioresource technology*, 101:3292-3294.
- Li, Y.-Y. S. (1996). Interactions between methanogenic, sulfate-reducing and syntrophic acetogenic bacteria in the anaerobic degradation of benzoate. *Water Research*, 30:1555-1562.
- Liam A. Royce, P. L. (2013). The damaging effects of short chain fatty acids on *Escherichia coli* membranes. *Appl Microbiol Biotechnol*, 97:8317-8327.
- Lin Y, G. X. (2014). Solid-state anaerobic co-digestion of spent mushroom substrate with yard trimmings and wheat straw for biogas production. *Bioresour Technol*, 169:468-474.
- Liu G, Z. R.-M. (2009). Effect of feed to inoculum ratios on biogas yields of food and green wastes. *Bioresour Technol*, 100:5103-5108.
- Liu LY, C. H. (2006). Enzymatic hydrolysis of cellulose materials treated with ionic liquid [BMIM]Cl. *Chin Sci Bull*, 51:2432-2436.
- Lowry, O. H. (1951). Protein measurement with the folin phenol reagent. *J. Biol. Chem.*, 265-275.
- M. Giacinti Baschetti, M. M. (2013). Gas permeation in perfluorosulfonated membranes: Influence of temperature and relative humidity. *International Journal of Hydrogen Energy*, 38: 11973-11982.
- M. Heyndrickx, P. D. (1991). Fermentation characteristics of *Clostridium pasteurianum* LMG 3285 grown on glucose and mannitol. *Journal of Applied Bacteriology*, 70:52-58.
- M. LL. Palops, S. V. (1989). Isolation and Characterization of an Anaerobic, Cellulolytic Bacterium, *Clostridium celerecrescens* sp. nov. *Int J Syst Evol Microbiol*, 36:68-71.
- M. Luna-del-Risco, A. N. (2011). Biochemical methane potential of different organic wastes and energy crops from Estonia. *Agronomy Research*, 9:331-342.
- M. Neureiter, J. T. (2011). Effect of silage preparation on methane yields from whole crop maize silages. *4th Int. Symposium Anaerobic Digestion of Solid Waste*. Copenhagen, Dänemark.

- M. T. Kato, J. A. (1997). Anaerobic tolerance to oxygen and the potentials of anaerobic and aerobic cocultures for wastewater treatment. *Brazilian Journal of Chemical Engineering*, 14:4-7.
- M.A. Bustamante, M. P.-M.-E.-C. (2007). Short-term carbon and nitrogen mineralisation in soil amended with winery and distillery organic wastes. *Bioresource Technology*, 17:3269-3277.
- M.F.A. Bradfield, W. N. (2014). Continuous succinic acid production by *Actinobacillus succinogenes* in a biofilm reactor: Steady-state metabolic flux variation. *Biochemical Engineering Journal*, 85:1-7.
- M.M. Bomgardner. (2011). BioBased Chemicals: myriant to build succinic acid plant in Louisiana. *Chem. Eng. News*, 89:2-7.
- Maedeh Mohammadi, G. D. (2011). Bioconversion of synthesis gas to second generation biofuels: A review. *Renewable and Sustainable Energy Reviews*, 15:4255-4273.
- Mairi Robinson, G. D. (1999). *Chambers 21st Century Dictionary*. Chambers.
- Makarova, K. e. (2006). Comparative genomics of the lactic acid bacteria. *Proceedings of the National Academy of Sciences*, 103:15611-15616.
- Maki M, L. K. (2009). The prospects of cellulase-producing bacteria for the bioconversion of lignocellulosic biomass. *Int J Biol Sci*, 5:500-516.
- Marion E. Cox, J. N. (2008). *U.S.A. Patent No. US20080311640 A1*.
- Martín B, C. L. (2009). Identification and tracing of *Enterococcus* spp. by RAPD-PCR in traditional fermented sausages and meat environment. *J Appl Microbiol.*, 106:66-77.
- Massé, D. M. (2003). The effect of temperature fluctuations on psychrophilic anaerobic sequencing batch reactors treating swine manure. *Bioresource Technology*, 89:57-62.
- Mata-Alvarez, J. M. (2000). Anaerobic digestion of organic solid wastes. An overview of research achievements and perspectives. *Bioresour Technol*, 74:3-16.
- Mbaneme-Smith V, C. M. (2014). Consolidated bioprocessing for biofuel production: recent advances. *Energy and Emission Control Technologies*, 3:23-44.
- McKinlay J B, L. M. (2010). A genomic perspective on the potential of *Actinobacillus succinogenes* for industrial succinate production. *BMC Genomics*, 680:56-65.
- McKinlay JB, S.-H. Y. (2007). Determining *Actinobacillus succinogenes* metabolic pathways and fluxes by NMR and GC-MS analyses of C-13-labeled metabolic product isotopomers. *Metabolic Engineering*, 9:177-192.
- Melbinger NR, D. J. (1971). Toxic effects of ammonia nitrogen in high-rate digestion. *J Water Pollut Control Fed*, 43:1658-1670.
- Melillo, J. M. (2014). *Climate Change Impacts in the United States: The Third National Climate Assessment*. U.S. Global Change Research Program.
- Michael J. McInerney, C. G. (2008). *Physiology, Ecology, Phylogeny, and Genomics of Microorganisms Capable of Syntrophic Metabolism*. New York: Annals of the New York Academy of Sciences.
- Mikael Hööka, X. T. (2013). Depletion of fossil fuels and anthropogenic climate change — A review. *Energy Policy*, 52: 797-809.
- Milledge JJ. (2011). Commercial application of microalgae other than as biofuels: a brief review. *Rev Environ Sci Bio/Technol*, 10:31.
- Ming-Der Bai, Y.-C. C.-H.-C.-T. (2008). Immobilized biofilm used as seeding source in batch biohydrogen fermentation. *IESCO - Science and technology vision*, 4:55-59.
- Mladenovska Z, H. H.-C. (2006). Thermal pretreatment of the solid fraction of manure: impact on the biogas reactor performance and microbial community. *Water Sci Technol*, 53:59-67.
- Modig T, L. G. (2002). Inhibition effects of furfural on alcohol dehydrogenase, aldehyde dehydrogenase and pyruvate dehydrogenase. *Biochemical Journal*, 363:769-776.

- Mohtada Sadrzadeh, T. M. (2008). Sea water desalination using electrodialysis. *Desalination*, 3:440–447.
- Müller, T. W. (2006). Ammonium toxicity in bacteria. *Current Microbiology*, 52:400–406.
- N. Abas, A. K. (2015). Review of fossil fuels and future energy technologies. *Futures*, 69: 31–49.
- N.S. Bentsen, C. F. (2014). Agricultural residue production and potentials for energy and materials services. *Prog. Energy Combust. Sci.*, 40:59–73.
- N.U., Y. (2005). Towards a Circular Economy: progress and challenges. *Greener Management International*, 50:11–24.
- Nagle DP Jr, W. R. (1983). Component A of the methyl coenzyme M methylreductase system of *Methanobacterium*: resolution into four components. *PNAS*, 80:2151–2155.
- Nakakubo, R. M. (2008). Ammonia inhibition of methanogenesis and identification of process indicators during anaerobic digestion. *Environmental Engineering Science*, 25:1487–1496.
- Nakas, J. P. (1983). System development for linked fermentation production of solvents from algal biomass. *Appl. Environ. Microbiol.*, 46:1017–1023.
- Natural Gas Supply Association. (n.d.). Retrieved from [www.NaturalGas.org](http://www.NaturalGas.org)
- Nel, L. H. (1985). The effect of trace elements on the performance efficiency of an anaerobic fixed film reactor treating a petrochemical effluent. *Water SA*, 11:107–110.
- Nelson, W. L. (1960). *Nelson's Complexity Factor*. Oil and Gas Journal.
- Neosepta Tokuyama Soda, J. (n.d.). Retrieved from [http://www.astom-corp.jp/en/product/images/astom\\_hyo.pdf](http://www.astom-corp.jp/en/product/images/astom_hyo.pdf)
- Ness, D. (2008). Sustainable urban infrastructure in China: Towards a Factor 10 improvement in resource productivity through integrated infrastructure systems. *International Journal of Sustainable Development and World Ecology*, 15: 288–301.
- Nick A. Owen, J. O. (2010). The status of conventional world oil reserves—Hype or cause for concern? *Energy Policy*, 38: 4743 – 4749.
- Nielsen, A. S. (2008). Calculating pH in pig manure taking into account ionic strength. *Water Science and Technology*, 57:1785–1790.
- Nirakar Pradhan, L. D. (2015). Hydrogen Production by the Thermophilic Bacterium *Thermotoga neapolitana*. *Int. J. Mol. Sci.*, 16: 12578–12600.
- Nuri Azbar, T. K. (2008). Enhancement of biogas production from olive mill effluent (OME) by co-digestion. *Biomass and Bioenergy*, 32:1195–1201.
- OE., A. (1961). Ammonia nitrogen and the anaerobic environment. *J Water Pollut Control Fed*, 33:978–95.
- Osuna, M. B. (2003). Effects of trace element addition on volatile fatty acid conversions in anaerobic granular sludge reactors. *Environmental technology*, 24:573–587.
- Overview of Natural Gas. (2012, 07 14). Retrieved from [www.NaturalGas.org](http://www.NaturalGas.org)
- P. Boyaval, C. C. (1987). Continuous lactic acid fermentation with concentrated product recovery by ultrafiltration and electrodialysis. *Biotechnol. Lett.*, 9:207–212.
- P. S. Jagadabhi, P. K. (2009). Effect of microaeration and leachate replacement on COD solubilization and VFA production during mono-digestion of grass-silage in one-stage leach-bed reactors. *Bioresource Technology*, 101:2818–2824.
- P.T. Anastas, J. W. (1998). Green Chemistry: Theory and Practice. In J. W. P.T. Anastas, *Green Chemistry: Theory and Practice*. Oxford: Oxford University Press.
- Palmqvist, E. A.-H. (1999). Influence of furfural on anaerobic glycolytic kinetics of *Saccharomyces cerevisiae* in batch culture. *Biotechnol. Bioeng.*, 62:447–454.
- Paolo S. Calabro', R. G. (2015). Anaerobic digestion of tomato processing waste: Effect of alkaline pretreatment. *Journal of Environmental Management*, 163:49–52.

- Papa, A. J. (2011). *Ullmann's Encyclopedia of Industrial Chemistry - Propanols*. Wiley-VCH Verlag GmbH & Co. KGaA.
- Papoutsakis ET. (2008). Engineering solventogenic clostridia. *Curr Opin Biotechnol*, 5:420-429.
- Parada, J. L., Caron, C. R., Medeiros, A. B., & Soccol, C. R. (2007). Bacteriocins from lactic acid bacteria: purification, properties and use as biopreservatives. *Braz. arch. biol. technol. vol.50 no.3 Curitiba May 2007*, 50:521-542.
- Paris Climate Conference. (2015). *United Nation Framework Convention On Climate Change*. Paris.
- Pavlostathis, S. G.-G. (1991). Kinetics of anaerobic treatment: A critical review. *Critical Reviews in Environmental Control*, 21:411-490.
- Peralta-Yahya, P. P. (2012). Microbial engineering for the production of advanced biofuels. *Nature*, 7411:320-328.
- Perez et.al. (2012). Biocatalytic Reduction of Short-Chain Carboxylic Acids Into Their Corresponding Alcohols With Syngas Fermentation. *Biotechnology and Bioengineering*, 110:1066-1077.
- Pooja Jambunathan, K. Z. (2014). Novel pathways and products from 2-keto acids. *Current Opinion in Biotechnology*, 29:1-7.
- Preston, F. (2012). A Global Redesign? Shaping the Circular Economy. Briefing Paper. *Royal Institute For International Affairs*.
- Prieto MB, H. A. (2002). Degradation of phenol by *Rhodococcus erythropolis* UPV-1 immobilized on Biolite® in a packed-bed reactor. *J. Biotechnology*, 97:1-11.
- Priscilla F. Fonseca Amaral, T. F. (2009). Glycerol valorization: New biotechnological routes. *Food and Bioproduct Processing*, 3:179-186.
- Procházka, J. D. (2012). Stability and inhibition of anaerobic processes caused by insufficiency or excess of ammonia nitrogen. *Applied Microbiology and Biotechnology*, 93:439-447.
- R. I. Scott, T. N. (1983). Oxygen sensitivity of methanogenesis in rumen and anaerobic digester populations using mass spectrometry. *Biotechnology Letters*, 6:375-380.
- R. Jain, Y. Y. (2011). Dehydratase mediated 1-propanol production in metabolically engineered *Escherichia coli*. *Microbial cell factories*, 10:97-105.
- R. Sarada, R. J. (1993). Biochemical changes during anaerobic digestion of tomato processing waste. *Process Biochem*, 28:461-466.
- Rajinikanth Rajagopal, D. I. (2013). A critical review on inhibition of anaerobic digestion process by excess ammonia. *Bioresource Technology*, 143:632-641.
- Rakopoulos, D. C. (2011). Combustion heat release analysis of ethanol or n-butanol diesel fuel blends in heavy-duty DI diesel engine. *Fuel*, 90:1855-1867.
- Raskin, L. B. (1996). Competition and coexistence of sulfate-reducing and methanogenic populations in anaerobic biofilms. *Applied and Environmental Microbiology*, 62:3847-3857.
- Ree van R, A. B. (2007). *Status Report Biorefinery*. Wageningen.
- REN 21 - Renewable Energy Policy Network for the 21st Century. (2015). *Renewable Global Status Report*.
- Renewable Fuels Association. (2015). *Ethanol Industry Outlook*. Los Angeles.
- Richa Kothari, V. T. (2010). Waste-to-energy: A way from renewable energy sources to sustainable development. *Renewable and Sustainable Energy Reviews*, 14: 3164-3170.
- Rigden, J. S. (2003). *Hydrogen: The Essential Element*. Harvard: Harvard University Press.
- Román-Leshkov, Y. M. (2010). Mechanism of glucose isomerization using a solid Lewis acid catalyst in water. *Angew. Chem. Int.*, 49:8954-8957.
- Rother, M. a. (2005). Genetic technologies for Archaea. *Current opinion in microbiology*, 6:745-751.

- Rottenberg, H. (1979). The measurement of membrane potential and DpH in cells, organelles, and vesicles. 55, 547. *Methods Enzymol*, 55:547-569.
- Rousseau, R. W. (1987). *Handbook of Separation Process Technology*. Wiley.
- S. H. Zinder, T. A. (1984). Effects of Temperature on Methanogenesis in a Thermophilic (58°C) Anaerobic Digester. *Appl Environ Microbiol*, 47: 808-813.
- S. J. Pirt, a. Y. (1983). Enhancement of methanogenesis by traces of oxygen in bacterial digestion of biomass. *FEMS Microbiology Letters*, 18:61-63.
- S. Matthias-Maser, R. J. (1995). The size distribution of primary biological aerosol particles with radii > 0.2  $\mu\text{m}$  in an urban/rural influenced region. *Atmospheric Research*, Volume 39, Issue 4, Pages 279–286.
- Sakai, S.-i. (2011). International comparative study of 3R and waste management policy developments. *Journal of Material Cycles and Waste Management*, 2, pp 86-102.
- Sambusiti C, M. F. (2013). A comparison of different pre-treatments to increase methane production from two agricultural substrates. *Appl Energy*, 104:62-70.
- Sarvari Horvath I, F. C. (2003). Effects of furfural on the respiratory metabolism of *Saccharomyces cerevisiae* in glucose-limited chemostats. *Applied and Environmental Microbiology*, 69:4076-4086.
- Sass AM, S. H. (2001). Microbial communities in the chemocline of a hypersaline deep-sea basin (Urania basin, Mediterranean Sea). *Appl. Environ. Microbiol.*, 67:5392–402.
- Scano EA, A. C. (2014). Biogas from anaerobic digestion of fruit and vegetable wastes: experimental results on pilot-scale and preliminary performance evaluation of a full-scale power plant. *Energy Convers Manage*, 77:22-30.
- Schink, B. (1997). Energetics of syntrophic cooperation in methanogenic degradation. *Microbiology and Molecular Biology Reviews*, 61:262-280.
- Schnürer, A. B. (1996). *Clostridium ultunense* sp. nov., a mesophilic bacterium oxidizing acetate in syntrophic association with a hydrogenotrophic methanogenic bacterium. *International Journal of Systematic and Evolutionary Microbiology* 46.4 (1996): 1145-1152., 46:1145-1152.
- Schoefer L1, M. R. (2003). Anaerobic degradation of flavonoids by *Clostridium orbiscindens*. *Appl Environ Microbiol*, 69:5849-5854.
- Senad Novalic, J. O. (1996). The characteristics of citric acid separation using electrodialysis with bipolar membranes. *Desalination*, 105:277–282.
- Sheldon, R. (2008). E factors, green chemistry and catalysis: an odyssey. *Chemical Communications*, 29: 3352-3365.
- Sheldon, R. A. (2014). Green and sustainable manufacture of chemicals from biomass: state of the art. *Green chemistry*, 16: 950-963.
- Shimshon Belkin, O. W. (1986). A New Sulfur-Reducing, Extremely Thermophilic Eubacterium from a Submarine Thermal Vent. *Appl Environ Microbiol*, 6:1180–1185.
- Shota Atsumi, J. C. (2008). Directed Evolution of *Methanococcus jannaschii* Citramalate Synthase for Biosynthesis of 1-Propanol and 1-Butanol by *Escherichia coli*. *Applied and Environmental Microbiology*, 15:7802-7808.
- Shu-Yuan Pan, Y. J.-W.-C. (2015). Development of Low-Carbon-Driven Bio-product Technology Using Lignocellulosic Substrates from Agriculture: Challenges and Perspectives. *Curr Sustainable Renewable Energy Rep*, 145-154.
- Somers, E. B. (2001). Biofilm formation and contamination of cheese by nonstarter lactic acid bacteria in the dairy environment. *Journal of Dairy Science*, 84:1926-1936.
- Song Z, L. X. (2014). Comparison of seven chemical pretreatments of corn straw for improving methane yield by anaerobic digestion. *PLoS One*, 9:e93801.

- Soto, M. M. (1991). Biodegradability and toxicity in the anaerobic treatment of fish canning wastewaters. *Environmental Technology*, 12:669-677.
- Southern pine prehydrolyzates: characterization of polysaccharides and lignin fragments. (1971). *J. Polym. Sci.*, 36:425-443.
- Stahel, W. (2010). *Stahel, W., 2010. The Performance Economy*. London: Second ed. Palgrave-MacMillan.
- Stams, A. J. (1994). Metabolic interactions between anaerobic bacteria in methanogenic environments. *Antonie van Leeuwenhoek*, 66:271-294.
- Stéphane Octave, D. T. (2009). Biorefinery: Toward an industrial metabolism. *Biochimie*, 91-659:664.
- Stern, S. (1968). The "Barrer" Permeability Unit . *Journal of Polymer Science Part A-2: Polymer Physics*, 11:1-3.
- Steve S.F. Yu, K. H.-C.-H.-S.-F.-J.-S. (2003). Production of High-Quality Particulate Methane Monooxygenase in High Yields from *Methylococcus capsulatus* (Bath) with a Hollow-Fiber Membrane Bioreactor. *J. Bacteriol.*, 20:5915-5924.
- Stieb, M. a. (1985). Anaerobic oxidation of fatty acids by *Clostridium bryantii* sp. nov., a sporeforming, obligately syntrophic bacterium. *Archives of microbiology*, 140:387-390.
- Stouthamer, A. (1979). The search for a correlation between theoretical and experimental growth yields. *Int. Rev. Biochem Microb. Biochem*, 3:21-28.
- Strathmann, H. (2001). Membrane separation processes: current relevance and future opportunities. *AIChE Journal*, 47:1077-1087.
- Sudip Chakraborty, V. A. (2012). Biomass to biofuel: a review on production technology. *Asia-Pac. J. Chem. Eng. 2012; 7 (Suppl. 3): S254–S262*, 7 (Suppl 3): 254-262.
- Sudip Chakraborty, V. A. (2012). Biomass to biofuel: a review on production technology. *Asia-Pacific Journal of Chemical Engineering*, 7:254-262.
- Sun Ye, C. J. (2002). Hydrolysis of lignocellulosic materials for ethanol production: a review. *Bioresour Technol*, 83:1-11.
- T. Scheper, B. A. (2003). *Biomethanization I*. New York: Springer.
- Taherzadeh MJ, G. L. (2000). Physiological effects of 5-hydroxymethylfurfural on *Saccharomyces cerevisiae*. *Appl Microbiol. Biotechnol*, 53:701-708.
- Taherzadeh, M. G. (1998). Conversion of furfural in aerobic and anaerobic batch fermentation of glucose by *Saccharomyces cerevisiae*. *J. Biosci. Bioeng*, 87:169-174.
- Takahata, Y. e. (2001). *Thermotoga petrophila* sp. nov. and *Thermotoga naphthophila* sp. nov., two hyperthermophilic bacteria from the Kubiki oil reservoir in Niigata, Japan. *Int J Syst Evol Microbiol*, 51:1901-1909.
- Taylor, T. N., & Taylor, E. L. (n.d.).
- Taylor, T. N., Taylor, E. L., & Krings, M. (2009). *Paleobotany: The biology and evolution of fossil plants*. APME - Associated Press Media Editors.
- Tilche A., M. F. (1998). Biogas production in Europe: an overview. *European Conference "Biomass for energy and industry"*.
- Tornabene TG, Benemann JR. (1985). *Chemical profiles on microalgae with emphasis on lipids*. Springfield.
- Tran, A. C. (1985). Red oak derived inhibitors in the ethanol fermentation of xylose by *Pichia stipitis* CBS 5776. *Biotechnol. Lett.*, 7:841-846.
- Tyrrell GJ, T. L. (2002). *Enterococcus gilvus* sp. nov. and *Enterococcus pallens* sp. nov. isolated from human clinical specimens. *J Clin Microbiol.*, 40:1140-1145.
- U.S. Census Bureau. (2012). *Historic Global Energy Consumption and Worldwide Population Growth*. Suitland.



- U.S. Department of Energy. (2014). *Energy Efficiency and Renewable Energy - Top Value Added Chemicals from Biomass*. T. Werpy and G. Petersen, Editors.
- U.S. Energy Information Administration. (2015). *The Annual Energy Outlook 2015*.
- Ulbricht, R. S. (1984). A review of 5-hydroxymethylfurfural HMF in parental solutions. *Fundam. Appl Toxicol.*, 4:843-853.
- Ungerfeld, E. M. (2015). Shifts in metabolic hydrogen sinks in the methanogenesis-inhibited ruminal fermentation: a meta-analysis. *Front. Microbiol.*, 6:37.
- United Nation. (1992). Rio declaration on environmet and development. Brazil, Rio de Janeiro: United Nation.
- United Nation. (2011). *Global Food Losses and Food Waste*. ROME: Food And Agriculture Organization Of The United Nations.
- United Nation Environment Program. (2015). *Global Trends in Renewable Energy Investment Report (GTR)*.
- United Nations. (1987). *""Sustainable Development". Our Common Future"*. United Nations Report of the World Commission on Environment and Development.
- United Nations Environment Programme. (2015). *Global Waste Management Outlook*.
- United Nations, Department of Economic and Social Affairs, Population Division. (2015). *World Population Prospects: The 2015 Revision, Key Findings and Advance*.
- United States Energy Information Administration. (2001). *Global Annual Energy Outlook 2015*.
- Van der Bruggen, B. C. (2002). Distillation vs. membrane filtration: overview of process evolutions in seawater desalination. *Desalination*, 3:207-218.
- Van der Werf MJ, G. M. (1997). Environmental and physiological factors affecting the succinate product ratio during carbohydrate fermentation by *Actinobacillus* sp. 130Z. *Archives Microbiology*, 167:332-342.
- Van Donkelaar, A. R. (2015). Global Annual PM2.5 Grids from MODIS, MISR and SeaWiFS Aerosol Optical Depth (AOD). *NASA Socioeconomic Data and Applications Center (SEDAC)*.
- Van Zyl WH, L. L. (2007). Consolidated bioprocessing for bioethanol production using *Saccharomyces cerevisiae*. *Adv Biochem Eng Biotechnol*, 108:205-235.
- Vandenbergh, P. A. (1993). Lactic acid bacteria, their metabolic products and interference with microbial growth. *FEMS Microbiology Reviews*, 12:2219237.
- Varga E, R. K. (2004). Optimization of steam pretreatment of corn stover to enhance the enzymatic digestibility. *Appl Biochem Biotechnol*, 113:509-523.
- Venessa Eeckhaut, F. V. (2011). Butyrate production in phylogenetically diverse Firmicutes isolated from the chicken caecum. *Microb Biotechnol*, 4:503-512.
- Věra Hábová, K. M. (2004). Electrodialysis as a useful technique for lactic acid separation from a model solution and a fermentation broth. *Desalination*, 162:361–372.
- Verduyn, C. P. (1990). Energetics of *Saccharomyces cerevisiae* in anaerobic glucose-limited chemostat cultures. *J. Gen. Microbiol*, 136:405-412.
- Verduyn, C. P. (1992). Effect of benzoic acid on metabolic fluxes in yeasts: a continous-culture study on the regulation of respiration and alcoholic fermentation. *Yeast*, 8:501-517.
- Vilis Dubrovskis, I. P. (2009). manure, Investigation of biogas production from mink and cow manure. *Engineering for rural development* , 5:28-29.
- Vinuselvi Parisuthama, T. H. (2014). Feasibilities of consolidated bioprocessing microbes: From pretreatment to biofuel production. *Bioresource Technology*, 161:431-440.
- Vishnu Menon, M. R. (2012). Trends in bioconversion of lignocellulose: Biofuels, platform chemicals & biorefinery concept. *Progress in Energy and Combustion Science*, 38:522-550.

- W.-W. Yang, E. C.-W. (2009). Production and characterization of pure Clostridium spore. *Journal of Applied Microbiology*, 106:27-33.
- Wallace, P. S. (2015). *U.S.A. Patent No. US8999171 B2*.
- Wan C, L. Y. (2008). Succinic acid production from cheese whey using *Actinobacillus succinogenes* 130 Z. *Appl Biochem Biotechnol*, 145:111-119.
- Ward A, S. H. (1998). Effect of autothermal treatment on anaerobic digestion in the dual digestion process. *Water Sci Technol*, 38:435-442.
- Weigert, B. K. (1998). Influence of furfural on the aerobic growth of the yeast *Pichia stipitis*. *Biotechnol. Lett.*, 12:895-900.
- William F. Loomis, B. M. (1967). Glucose-Lactose Diauxie in *Escherichia coli*. *J Bacteriol*, 93:1397-1401.
- Wingren, A. M. (2003). Techno-economic evaluation of producing ethanol from softwood: Comparison of SSF and SHF and identification of bottlenecks. *Biotechnology progress*, 19:1109-1117.
- World Coal Institute. (2013). *The Coal Resource: A Comprehensive Overview Of Coal*. London: Cambridge Press.
- www.siadeb.org. (n.d.). *The Ibero-American Society for the Development of Biorefineries*. Retrieved from The Ibero-American Society for the Development of Biorefineries: www.siadeb.org
- Xiao K, G. C. (2016). Acetic acid effects on methanogens in the second stage of a two-stage anaerobic system. *Chemosphere*, doi: 10.1016/j.chemosphere.2015.10.035.
- Xiu, Z.-L. A.-P. (2008). Present state and perspective of downstream processing of biologically produced 1, 3-propanediol and 2, 3-butanediol. *Applied Microbiology and Biotechnology*, 78:917-926.
- Xu J, T. M. (2009). Pretreatment on corn stover with low concentration of formic acid. *J Microbiol Biotechnol*, 19:845-850.
- Xu Tongwen, Y. W. (2002). Citric acid production by electrodialysis with bipolar membranes. *Chemical Engineering and Processing*, 41:519-524.
- Y. Wang, Y. Z. (2009). Effects of volatile fatty acid concentrations on methane yield and methanogenic bacteria. *Biomass Bioenergy*, 33:848-853.
- Y.H Kim, S.-H. M. (2001). Lactic acid recovery from fermentation broth using one-stage electrodialysis. *J. Chem. Technol. Biotechnol.*, 76:169-178.
- Yan Gong, Y. T.-l.-x.-h. (2004). The possibility of the desalination of actual 1,3-propanediol fermentation broth by electrodialysis. *Desalination*, 20:169-178.
- Ye Chen, J. J. (2008). Inhibition of anaerobic digestion process: A review. *Bioresource Technology*, 99:4044-4064.
- Ye Chen, J. J. (2008). Inhibition of anaerobic digestion process: A review. *Bioresource Technology*, 99:4044-4064.
- Yong Geng, B. D. (2008). Developing the circular economy in China: Challenges and opportunities for achieving 'leapfrog development'. *International Journal of Sustainable Development & World Ecology*, 3:231-239.
- Yu G, Y. S. (2010). Pretreatment of rice straw by a hot-compressed water process for enzymatic hydrolysis. *Appl Biochem Biotech*, 160:539-551.
- Yuan Y., R. C. (2011). Transcriptional response of methanogen *mcrA* genes to oxygen exposure of rice field soil. *Applied Microbiology*, 3:320-328.
- Yuan, W. J. (2012). Consolidated bioprocessing strategy for ethanol production from Jerusalem artichoke tubers by *Kluyveromyces marxianus* under high gravity conditions. *Journal of applied microbiology*, 112:38-44.

- Zanaroli G., e. (2010). Characterization of the microbial community from the marine sediment of the Venice lagoon capable of reductive dechlorination of coplanar polychlorinated biphenyls (PCBs). *Journal of Hazardous Materials*, 178:417-426.
- Zanaroli G., e. (2012). Enhancement of microbial reductive dechlorination of polychlorinated biphenyls (PCBs) in a marine sediment by nanoscale zerovalent iron (NZVI) particles. *J. Chem. Technol. Biotechnol*, 87:1246–1253.
- Zdravko Dragovic, M. M. (2014). *Germany Patent No. WO2014135633 A1*.
- Zeikus JG, J. M. (1999). Biotechnology of succinic acid production and markets for derived industrial products. *Appl Microbiol Biotechnol*, 10:545-552.
- Zhang C, X. G. (2013). The anaerobic co-digestion of food waste and cattle manure. *Bioresour Technol*, 129:170-176.
- Zhao H, B. G. (2009). Fast enzymatic saccharification of switchgrass after pretreatment with ionic liquids. *Biotechnol Prog*, 26:127-133.
- Zhenle Yuana, J. W. (2010). Biodiesel derived glycerol hydrogenolysis to 1,2-propanediol on Cu/MgO catalysts. *Bioresource Technology*, 18:7088–7092.
- Zhenming Zhou, Q. M. (2011). Effects of Methanogenic Inhibitors on Methane Production and Abundances of Methanogens and Cellulolytic Bacteria in In Vitro Ruminal Cultures. *Appl Environ Microbiol*, 77:2634-2639.
- Zhijun, F. (2007). Putting a circular economy into practice in China. *Sustainability Science*, 1:95-101.
- Zhu J, W. C. (2010). Enhanced solid-state anaerobic digestion of corn stover by alkaline pretreatment. *Bioresour Technol*, 101:7523-7528.
- Zhu S, W. Y. (2006). Comparison of three microwave/chemical pretreatment processes for enzymatic hydrolysis of rice straw. *Biosyst Eng*, 93:279-283.

## 9 LIST OF ABBREVIATIONS

---

The following project-specific and general technical abbreviations are used in this dissertation:

<b>AD</b>	Anaerobic digestion
<b>AFEX</b>	Ammonia fiber explosion
<b>ANOVA</b>	Analysis of variance
<b>APS</b>	Adenosine 5 – phosphosulphate
<b>AS</b>	Ashes
<b>ATP</b>	Adenosine triphosphate
<b>BCI</b>	Biorefinery complexity index
<b>BGL</b>	$\beta$ - glucanase
<b>BMP</b>	Biomethane potential
<b>bn bbl</b>	Billions of barrels
<b>BTUs</b>	British thermal units
<b>C/N</b>	Carbon-to-nitrogen ratio
<b>CE</b>	Circular economy
<b>CE</b>	Current efficiency
<b>CEs</b>	Carbohydrate esterases
<b>CFCs</b>	Chlorofluorocarbons
<b>CH<sub>4</sub></b>	Methane
<b>CHP</b>	Co-digestion heat and power
<b>CO<sub>2</sub></b>	Carbon dioxide
<b>COD</b>	Chemical oxygen demand
<b>CPB</b>	Consolidated bioprocess
<b>CSTR</b>	Continuous stirred tank reactor
<b>CV</b>	Coefficient of variation
<b>DMSO</b>	Dimethyl sulfoxide
<b>DOE</b>	Department of energy
<b>DP</b>	Degree of polymerization
<b>DSMZ</b>	German collection of microorganisms and cell cultures
<b>ED</b>	Electrodialysis
<b>EPA</b>	Environmental protection agency
<b>EU</b>	European Union
<b>EXG</b>	Exoglucanase
<b>ExoI</b>	Exonuclease I
<b>FAN</b>	Free ammonia nitrogen
<b>FAO</b>	Food and agriculture organization
<b>FastAP</b>	Alkaline phosphate
<b>GC</b>	Gas chromatography
<b>GHGs</b>	Greenhouse gases
<b>GHs</b>	Glycoside hydrolases
<b>GJ</b>	GigaJoule
<b>GP</b>	Grape pomace

<b>GSR</b>	Renewable global status report
<b>GTP</b>	Global trends in renewable energy investment report
<b>GWP</b>	Global warming potential
<b>H<sub>2</sub></b>	Hydrogen
<b>HFCs</b>	Hydrofluorocarbons
<b>HMF</b>	Hydroxymethylfurfural
<b>HPLC</b>	High performance liquid chromatography
<b>HRT</b>	Hydraulic retention time
<b>IEA</b>	International energy agency
<b>IPCC</b>	International panel on climate change
<b>ISPR</b>	In situ product recovery
<b>KDC</b>	2 – Ketoacid decarboxylase
<b>LAB</b>	Lactic acid bacteria
<b>LCD</b>	Limiting current density
<b>LHW</b>	Liquid hot water
<b>MiPAFF</b>	Ministry of Agriculture, Food and Forestry
<b>MS</b>	Maize silage
<b>MSW</b>	Municipal solid waste
<b>MT<sub>oe</sub></b>	Megatons of oil equivalent
<b>N<sub>2</sub></b>	Nitrogen
<b>N<sub>2</sub>O</b>	Nitrous oxide
<b>NASA</b>	National American space agency
<b>O<sub>2</sub></b>	Oxygen
<b>OECD</b>	Organization for economic cooperation and development
<b>OFMSW</b>	Organic fraction of municipal solid waste
<b>OLR</b>	Organic loading rate
<b>OMW</b>	Olive mill wastewater
<b>OPEC</b>	Organization of the Petroleum Exporting Countries
<b>PCR - DGGE</b>	Polymerase chain reaction – Denaturing gradient gel electrophoresis
<b>PEP</b>	Phosphoenolpyruvate
<b>PEP - K</b>	Phosphoenolpyruvate decarboxylase
<b>PFCs</b>	Perfluorocarbons
<b>PFR</b>	Plug flow reactor
<b>PHA</b>	Polyhydroxyalkanoate
<b>PLA</b>	Poly lactic acid
<b>PM</b>	Particulate matter
<b>Q</b>	Volumetric flow rate
<b>REN21</b>	Renewable energy policy network for the 21 <sup>st</sup> century
<b>S.A.</b>	Succinic acid
<b>S.M.</b>	Sodium molybdate
<b>SF<sub>6</sub></b>	Sulphur hexafluoride
<b>SHF</b>	Separate hydrolysis and fermentation
<b>SOD</b>	Superoxide dismutase
<b>SPCSTR</b>	Structure packing continuous stirred tank reactor
<b>SRB</b>	Sulphate reducing bacteria

<b>SSCF</b>	Simultaneous saccharification and co-fermentation
<b>SSF</b>	Simultaneous saccharification and fermentation
<b>TAN</b>	Total ammonia nitrogen
<b>TP</b>	Tomato peel
<b>TRL</b>	Technology readiness level
<b>TS</b>	Total solid
<b>TW</b>	Water transport
<b>UNEP</b>	United nation environment program
<b>USD</b>	United states dollar
<b>VFAs</b>	Volatile fatty acids
<b>VITO</b>	Flemish Institute For Technological Research
<b>VS</b>	Volatile solid
<b>WCED</b>	World commission for the environment and development
<b>WHO</b>	World health organization
<b>WTE</b>	Waste-to-energy

## 10 ACKNOWLEDGEMENTS

---

This Ph.D. dissertation was supported by the actions of numerous companies and research centers. On behalf of Prof. Davide Pinelli and Dr. Dario Frascari, I would like to sincerely thank “*La Glicine*” winery and “*Eridania – SADAM S.p.A.*” for the supply of the grape pomaces, “*CO.PAD.OR.*” company for the tomato peels, *Olio Terra Nostra*” oil mill for the wastewaters, and “*Sebigas S.p.A.*” for the maize silage. Thanks to Dr. Giacomo Bucchi (Sebigas) and Prof. Lorenzo Bertin (Bologna University) for the gently concession of “OMW” – “MAIS” and “SEBIGAS” consortia, and to Dr. Giulio Zanaroli with the collaboration of Dr. Antonella Rosato (Bologna University) for the constant assistance in the sequencing procedures. Thanks to Dr. De Wever Heleen, Dr. Wouter Van Hecke and Dr. Garcia-Gonzalez Linsey, of the Separation and Conversion Technologies Unit - Flemish Institute For Technological Research, for the contribution, hospitality, and the disponibility in establish a collaboration for the succinic acid project in the framework of the “ReNew” project. I would like also to thank for the teamwork the Diffusion in Polymers and Membrane Separation Group of Prof. M. G. Baschetti and G. C. Sarti (Bologna University), for the preliminary studies on the bio – H<sub>2</sub> separation module within the “Bio-Hydro” project, and the Applied Fluid Dynamics and Mixing Group of Prof. A. Paglianti and Prof.ssa G. Montante (Bologna University), for the CFD fluidodynamic analysis of the bioreactors used in this study. Thanks also to Askoll Due S.p.A. and Poraver S.p.A. for the free samples of Biomax ® and Poraver ®, and to all the master thesis students (Angelica Chimienti, Matteo Cerullo, Luca Lazzarini, Cecilia Spagni and Rubertelli Giorgia) for the participation in everyday lab duties.

Thanks to my parents, my brother, my relatives. Thanks to the Prof. Davide Pinelli, Dr. Dario Frascari, and to all the DICAM company (you’re magic!). Thanks to the Flemish Institute For Technological Research, and to the Boeretang (long live to the Kingdom!).

Thanks to all of my friends, and finally, thanks to me.

*“The science of today is the technology of tomorrow”*

Edward Teller